

# Investigations into the Manipulation of 1,2,3-Triazoles and Towards an Asymmetric ‘Click’ Reaction of *Meso* *Bis-Alkynes*

---

James Martin Harvey

This thesis is submitted in partial fulfilment of the requirements  
for the degree of Doctor of Philosophy



University of East Anglia, Norwich

Department of Chemistry

September 2015

© This copy of the thesis has been supplied on condition that anyone who consults it is understood to recognise that its copyright rests with the author and that use of any information derived there from must be in accordance with current UK Copyright Law. In addition, any quotation or extract must include full attribution.

# Preface

The work described within the 176 pages of this thesis is, to the best of my knowledge, original and my own work, except where due reference has been made.

James Martin Harvey

September 2015

## Abstract

This thesis describes the synthetic approaches undertaken to generate various substituted 1,2,3-triazoles and a small group of *bis* alkyne-containing compounds, followed by their attempted application in an asymmetric ‘click’ reaction. The first chapter gives an outline to the importance of desymmetrization within organic synthesis, providing examples of the types of stereoselective reactions found within the literature. Attention is then focused on the field of ‘click’ chemistry, specifically the copper-catalysed azide-alkyne cycloaddition (CuAAC), its mechanistic studies and recent applications.

Chapter two contains the results and discussion of the project and begins with the application of the CuAAC reaction to produce a simple 1,4-disubstituted 1,2,3-triazole from its two coupling partners, an azide and an alkyne, in near quantitative yields. The 1,4-disubstituted triazole is then transformed to its corresponding triazolium salt, with the longer alkyl chains only giving 40-45% product. They are then reacted with potassium *tert*-butoxide to generate the 1,5-disubstituted 1,2,3-triazole in yields of 83% or above. The reaction steps were optimised to give a standard procedure for the conversion of 1,4- to 1,5-triazoles, with a small series of test reactions giving overall yields of up to 90%.

The second section of the results and discussion chapter centres on the development of *meso bis*-alkynes which were to be used in the evaluation of an asymmetric ‘click’ reaction. A number of synthetic approaches to these compounds are described, with most falling short of their final target compound, and either needing further work or a redesign of the target compound itself. One target compound, *meso*-1,2-*bis*-(prop2-yn-1-ol)benzene **29**, was synthesised and a series of further *meso bis*-alkynes produced by various additions to the propargylic alcohol. Evaluation of the asymmetric ‘click’ reaction using this group of compounds under a wide selection of reaction conditions gave no successful results, all returning only starting material. Chapter two concludes with a brief summary of future work.

Finally, chapter 3 contains full experimental details for the synthetic studies carried out in the preceding chapters.

## Acknowledgments

First of all, I would like to thank Dr G. Richard Stephenson & Prof Phil Page for their supervision, support and guidance, and for giving me the opportunity to study my PhD at UEA.

Secondly, I would like to thank Dr Yohan Chan for all of his support in the lab. Always willing to help, his frequent ~~moaning~~ advice has kept the lab running.

I would also like to thank the friends and colleagues that I have worked alongside at UEA. The past and present members of the Page & Stephenson groups, who have been great to work with. All of whom helped create an extremely fun and enjoyable working environment, providing numerous, hilarious memoires that never fail to bring a smile to my face when I think back.

A special thanks goes to Ryan Tinson and Alix Horton. They have been there with me from the start and I can only hope we will remain true friends long into the future. Our Fridays lunch trips and support of each other has proven invaluable through our respective 'lows'. I am certain that if not for knowing the two of them, my experience would not have been anywhere near as smooth or enjoyable.

Thanks also goes to all my friends from UEA Baseball & Softball, whom I see as my second family. Without all of the great times, on and off of the field, I'm not sure I would have been capable of keeping my sanity through these last 4 years. To each of them I send my heartfelt appreciation and wish them all the success and happiness they deserve. Go Blue Sox!

Finally I would like to thank my parents for their unconditional support throughout the years. I am enormously grateful of it all, and can only hope that I have done them proud.

Thank you,

James 'Mini Eggs' Harvey

# Contents

## Chapter 1: Introduction

<b>1.0</b>	Desymmetrization .....	2
<b>1.1</b>	Compounds containing one reactive functional group with two enantiotopic centres.....	3
<b>1.1.1</b>	Ring-opening of epoxides and aziridines.....	3
<b>1.1.2</b>	Heck reaction.....	6
<b>1.1.3</b>	Ring-opening of bridged systems.....	8
<b>1.2</b>	Compounds containing two reactive enantiotopic groups .....	9
<b>1.2.1</b>	Desymmetrization and kinetic resolution .....	9
<b>1.2.2</b>	Monoprotection of <i>meso</i> -compounds .....	11
<b>1.2.2.1</b>	Acylation of prochiral diols.....	11
<b>1.2.2.2</b>	Allylation of <i>meso</i> -diamides.....	13
<b>1.2.2.3</b>	Silylation of <i>meso</i> -diols.....	14
<b>1.2.3</b>	Reduction of <i>meso</i> -compounds .....	15
<b>1.3</b>	Desymmetrization in total synthesis .....	17
<b>2.0</b>	'Click' chemistry.....	20
<b>2.1</b>	Olefin-based additions .....	22
<b>2.2</b>	Nucleophilic ring-opening .....	24
<b>2.3</b>	Non-aldol carbonyl chemistry .....	25
<b>2.4</b>	Cycloaddition reactions .....	27
<b>2.4.1</b>	Stereoselectivity of Diels-Alder reactions .....	27
<b>2.4.2</b>	Regioselectivity of Diels-Alder reactions .....	28
<b>2.5</b>	Copper-catalysed Huisgen 1,3-cycloaddition - The 'Click reaction' .....	29
<b>2.5.1</b>	Mechanism of the CuAAC.....	30
<b>2.5.2</b>	Applications of the CuAAC.....	35

2.5.2.1	'Click' chemistry in bioconjugation .....	35
2.5.2.2	'Click' chemistry in materials science .....	39
2.5.2.3	'Click' chemistry in drug discovery and natural product synthesis ...	44
2.6	Ruthenium-catalysed Huisgen 1,3-cycloaddition.....	49
3.0	Aim of the project .....	51
3.1	Current work .....	52

## Chapter 2: Results & Discussion

1.0	Manipulation of triazoles.....	55
1.1	Synthesis of 1-benzyl-4-phenyl-1,2,3-triazole .....	56
1.2	Attempts to 'unclick' a triazole .....	58
1.3	Developing the 1,3- to 1,5-triazole interconversion pathway .....	60
1.3.1	<i>N</i> -alkylation step.....	60
1.3.2	Debenzylation step .....	62
1.4	Testing of the 1,3 to 1,5-triazole interconversion pathway.....	64
1.5	Testing the new pathway for the synthesis of 1,4,5-trisubstituted triazoles .....	67
1.6	Application of the 1,3- to 1,5-triazole interconversion to asymmetric 'click' systems.....	71
2.0	Synthesis of <i>meso</i> compounds .....	75
2.1	<i>Meso bis</i> -alkyne <b>26</b> .....	76
2.2	<i>Meso bis</i> -alkyne <b>27</b> .....	84
2.3	<i>Meso bis</i> -alkyne <b>28</b> .....	89
2.4	<i>Meso bis</i> -alkynes <b>29, 30, 31 &amp; 32</b> .....	93
2.4.1	<i>Meso bis</i> -alkyne <b>29</b> .....	93
2.4.1.1	Assignment of configuration of chiral propargylic alcohols using Mosher's ester .....	95

2.4.2	<i>Meso bis-alkyne 30</i> .....	98
2.4.3	<i>Meso bis-alkyne 31</i> .....	99
2.4.4	<i>Meso bis-alkyne 32</i> .....	99
2.4.5	<i>Meso bis-alkyne 60</i> .....	100
2.4.6	Synthesis of <i>meso</i> -compounds using <i>meta</i> - & <i>para</i> -phthalaldehyde .....	102
3.0	The asymmetric ‘click’ reaction with <i>meso bis-alkynes</i> .....	104
4.0	Future work.....	110
4.1	Manipulation of triazoles .....	110
4.2	Synthesis of <i>meso bis-alkynes</i> .....	111
4.3	Asymmetric ‘click’ reaction.....	113
5.0	Conclusion .....	113

## Chapter 3: Experimental

General Experimental .....	116
1-Benzyl-4-phenyl-1 <i>H</i> -1,2,3-triazole <b>2</b> .....	117
Original synthetic method: .....	117
One-pot procedure:.....	117
Microwave-assisted one-pot method:.....	118
1-Benzyl-3-methyl-4-phenyl-1 <i>H</i> -1,2,3-triazolium iodide <b>3</b> .....	119
Original synthetic method: .....	119
Microwave-assisted method: .....	119
Optimised microwave-assisted method:.....	119
1-Benzyl-3-methyl-4-phenyl-1 <i>H</i> -1,2,3-triazolium iodide <b>3</b> with sodium alkoxide .....	121
With sodium methoxide: .....	121
With sodium ethoxide: .....	121

1-Methyl-5-phenyl-1 <i>H</i> -1,2,3-triazole <b>4</b> .....	122
Reduction using LiAlH <sub>4</sub> : .....	122
Reduction using <i>t</i> BuOK: .....	122
1-Benzyl-3-ethyl-4-phenyl-1 <i>H</i> -1,2,3-triazolium iodide <b>5</b> .....	124
1-Benzyl-3- <i>n</i> -propyl-4-phenyl-1 <i>H</i> -1,2,3-triazolium iodide <b>6</b> .....	125
1-Benzyl-3- <i>n</i> -butyl-4-phenyl-1 <i>H</i> -1,2,3-triazolium iodide <b>7</b> .....	126
1-Ethyl-5-phenyl-1 <i>H</i> -1,2,3-triazole <b>8</b> .....	127
1- <i>n</i> -propyl-5-phenyl-1 <i>H</i> -1,2,3-triazole <b>9</b> .....	128
1- <i>n</i> -Butyl-5-phenyl-1 <i>H</i> -1,2,3-triazole <b>10</b> .....	129
1,3-Dimethyl-4-phenyl-1 <i>H</i> -1,2,3-triazolium iodide <b>11</b> .....	130
1,3-Diethyl-4-phenyl-1 <i>H</i> -1,2,3-triazole <b>12</b> .....	131
1,3-Di- <i>n</i> -propyl-4-phenyl-1 <i>H</i> -1,2,3-triazolium iodide <b>13</b> .....	132
1,3-Di- <i>n</i> -butyl-4-phenyl-1 <i>H</i> -1,2,3-triazolium iodide <b>14</b> .....	133
1,4-Di- <i>n</i> -butyl-5-phenyl-1 <i>H</i> -1,2,3-triazole <b>15</b> .....	134
Methyl 2-cyano-2-(prop-2-yn-1-yl)pent-4-ynoate <b>19</b> .....	135
Methyl 2-[(1-benzyl-1 <i>H</i> -1,2,3-triazol-4-yl)methyl]-2-cyanopent-4-ynoate <b>20</b> .....	136
Alkylation of methyl 3-(1-benzyl-1 <i>H</i> -1,2,3-triazol-4-yl)-2-[(1-benzyl-1 <i>H</i> -1,2,3-triazol-4-yl)methyl]-2-cyanopropanoate <b>20</b> with iodomethane .....	137
2-((1-Methyl-1 <i>H</i> -1,2,3-triazol-5-yl)methyl)pent-4-ynenitrile <b>23</b> .....	138
1-Benzyl-4-(2-cyano-2-(methoxycarbonyl)pent-4-yn-1-yl)-3-methyl-1 <i>H</i> -1,2,3-triazol-3-ium triflate <b>24</b> .....	139
Methyl 2-[(1-benzyl-1 <i>H</i> -1,2,3-triazol-4-yl)methyl]-2-cyanopent-4-ynoic acid <b>25</b> .....	140
(2 <i>R</i> ,3 <i>S</i> ,4 <i>R</i> ,5 <i>S</i> )-dimethyl 2,3,4,5-tetrahydroxyhexanedioate <b>35</b> .....	141
(4 <i>S</i> ,4' <i>S</i> ,5 <i>R</i> ,5' <i>R</i> )-Dimethyl-2,2,2',2'-tetramethyl-[4,4'-bi(1,3-dioxolane)]-5,5'-dicarboxylate <b>36</b> .....	142
((4 <i>R</i> ,4' <i>R</i> ,5 <i>S</i> ,5' <i>S</i> )-2,2,2',2'-Tetramethyl-[4,4'-bi(1,3-dioxolane)]-5,5'-diyl)dimethanol <b>38</b> .....	143
2-Iodoxybenzoic acid (IBX) <b>40</b> .....	144



1,1,1-Triacetoxy-1,1-dihydro-1,2-benziodoxol-3(1 <i>H</i> )-one (DMP) <b>39</b> .....	145
((4 <i>R</i> ,4' <i>R</i> ,5 <i>S</i> ,5' <i>S</i> )-2,2,2',2'-Tetramethyl-[4,4'-bi(1,3-dioxolane)]-5,5'-diyl)bis(methylene)bis(4-methylbenzenesulfonate) <b>44</b> .....	146
(4 <i>S</i> ,4' <i>S</i> ,5 <i>R</i> ,5' <i>R</i> )-5,5'-Bis(iodomethyl)-2,2,2',2'-tetramethyl-4,4'-bi(1,3-dioxolane) <b>45</b> .	147
1,9- <i>Bis</i> (trimethylsilyl)nona-1,8-diyne-3,7-dione <b>48</b> .....	148
Nona-1,8-diyne-3,7-dione <b>49</b> .....	149
Desilylation using potassium carbonate: .....	149
Desilylation using sodium borate:.....	149
Nona-2,8-diyne-3,5-diol <b>46</b> (mixture of diastereoisomers) .....	150
2,6-Diethynyltetrahydro-2 <i>H</i> -pyran <b>27</b> (mixture of diastereoisomers).....	151
2,6- <i>Bis</i> (1-benzyl-1 <i>H</i> -1,2,3-triazol-4-yl)tetrahydro-2 <i>H</i> -pyran <b>52</b> (mixture of diastereoisomers) .....	152
B-3-Pinanyl-9-borabicyclo[3.3.1]-nonane (Alpine-borane) <b>51</b> .....	153
<i>endo</i> -Norbornene-5,6-dicarboxylic anhydride <b>54</b> .....	154
<i>endo</i> -Norbornene-5,6-dimethanol <b>53</b> .....	155
<i>endo</i> -Norbornene-5,6-diyl <i>bis</i> (methylene)- <i>bis</i> (4-methylbenzenesulfonate) <b>56</b> .....	156
<i>endo</i> -Norbornene-5,6-dimethyl iodide <b>58</b> .....	157
From <i>bis</i> -tosyl <b>56</b> : .....	157
From diol <b>53</b> :.....	158
1,2- <i>bis</i> -(Prop-2-yn-1-ol)benzene <b>29</b> .....	159
<i>meso</i> -(1 <i>S</i> ,1' <i>R</i> )-1,2- <i>bis</i> -(Prop-2-yn-1-ol)benzene <b>29</b> : .....	160
(±)-1,2- <i>bis</i> -(Prop-2-yn-1-ol)benzene (±) <b>29</b> : .....	160
General method for the esterification of compounds using Mosher's acid for the assessment of stereochemistry.....	161
1,1'-(1,2-Phenylene)- <i>bis</i> -(prop-2-yn-1-one) <b>59</b> .....	162
(1 <i>S</i> ,1' <i>R</i> )-1,2- <i>bis</i> -(1-(Acetyl)prop-2-yn-1-yl)benzene <b>30</b> .....	163
(1 <i>S</i> ,1' <i>R</i> )-1,2- <i>bis</i> -(1-(Benzyloxy)prop-2-yn-1-yl)benzene <b>31</b> .....	164
(1 <i>S</i> ,1' <i>R</i> )-1,2- <i>bis</i> -(1-(Benzoyloxy)prop-2-yn-1-yl)benzene <b>32</b> .....	165

(1 <i>S</i> ,1' <i>R</i> )-1,2-bis-(1-((Methylsulfonyl)oxy)prop-2-yn-1-yl))benzene <b>62</b> .....	166
1,3- <i>bis</i> -(Prop-2-yn-1-ol)benzene <b>63</b> .....	167
1,4- <i>bis</i> -(Prop-2-yn-1-ol)benzene <b>64</b> .....	168
General method used for the attempted ‘click’ reaction of <b>29</b> shown in Table 5 .....	169

## List of figures for Chapter 1: Introduction

Figure 1: Classification of desymmetrization substrates .....	2
Figure 2: Interaction between the metal-salen complex and the epoxide .....	4
Figure 3: Examples of organocatalysts used in enantioselective aziridine ring-opening .	5
Figure 4: Enantioselective insertion of the two different catalysts (the backbone of the ligands has been omitted for clarity).....	7
Figure 5: Example of a <i>meso</i> 1,2- <i>bis</i> -(Trs)-amide used by the group .....	13
Figure 6: Several Trost ligands.....	14
Figure 7: Proposed transition state model for catalytic enantioselective silylation of <i>meso</i> -diols.....	15
Figure 8: Model for the selectivity observed in the reduction of <i>meso</i> -imides .....	16
Figure 9: Structure of desymmetrization catalysts <b>27</b> & <b>29</b> .....	17
Figure 10: Suggested reaction transition state.....	18
Figure 11: Possible structures of mosin B.....	19
Figure 12: Possible chelation intermediates of base-promoted acetal fission.....	20
Figure 13: Common transfection lipids .....	26
Figure 14: Drugs containing hydrazine and pyrazole moieties .....	26
Figure 15: Comparison of orbitals of conjugated systems.....	28
Figure 16: Regioselectivity observed in Diels-Alder reactions.....	29
Figure 17: CPMV coated in azides or alkynes .....	36
Figure 18: Azide/alkyne-dyes that were attached to the azide/alkyne-coated CPMV ...	37
Figure 19: Schematic illustration of test substrates immobilized onto the glass slide ...	39
Figure 20: Dendrimer synthesized using click chemistry .....	40
Figure 21: Selection of azides and polyacetylene cores used in the synthesis of chain-end-functionalized dendrimers .....	42

Figure 22: Asymmetrical dendrimer containing 16 mannose units and 2 coumarin chromophores .....	42
Figure 23: Example of a water-soluble calixarene .....	44
Figure 24: Azide and acetylene building blocks .....	45
Figure 25: Inhibitor found directly by the azide-alkyne cycloaddition in the presence of AChE.....	46
Figure 26: Inhibitor of Fuc-T synthesized using CuAAC.....	47
Figure 27: Antitumour agent cryptophycin-52 and triazole analogue "clicktophycin-52" .....	48
Figure 28: Structure of antibiotic vancomycin.....	48
Figure 29: <i>Meso bis</i> -alkynes that will be synthesized for testing.....	52

## List of schemes for Chapter 1: Introduction

Scheme 1: Desymmetrization of <i>meso</i> -epoxides.....	3
Scheme 2: Enantioselective ring-opening of <i>meso</i> -epoxides with ( <i>R,R</i> )- <b>1</b> .....	3
Scheme 3: Enantioselective desymmetrization of <i>meso</i> -aziridines.....	5
Scheme 4: Proposed mechanism for the organocatalytic desymmetrization of aziridines	6
Scheme 5: Desymmetrization of a cyclic olefin using the Heck reaction .....	6
Scheme 6: Bond rotation and dissociation of olefin .....	8
Scheme 7: Rhodium-catalysed asymmetric ring opening .....	9
Scheme 8: Proposed catalytic cycle of the rhodium catalysed asymmetric ring opening	9
Scheme 9: Desymmetrization of a <i>meso</i> -diol with a planar catalyst .....	10
Scheme 10: Desymmetrization and kinetic resolution of <i>meso</i> -diols.....	11
Scheme 11: Formation of dinuclear zinc complex <b>14</b> from <b>15</b> .....	11
Scheme 12: Enantioselective acylation of a 1,3-propanediol.....	12
Scheme 13: Proposed catalytic cycle for the desymmetrization of 2-substituted-1,3-propanediols .....	12
Scheme 14: Asymmetric desymmetrization of <i>meso</i> -diamides through catalytic enantioselective <i>N</i> -allylation .....	13
Scheme 15: Substituent effect of the sulfonyl group on the nitrogen atom.....	14
Scheme 16: Catalytic enantioselective silylation of a <i>meso</i> -diol .....	15
Scheme 17: Use of an anthracene template for the desymmetrization of an <i>N</i> -substituted maleimide .....	16

Scheme 18: Synthetic route to (+)-biotin <b>25</b> .....	17
Scheme 19: Desymmetrization using an enantioselective intramolecular aza-Michael reaction.....	18
Scheme 20: Stereodivergent synthesis to give both candidate structures .....	19
Scheme 21: Asymmetric desymmetrization protocol for cyclic <i>meso</i> 1,2-diols .....	20
Scheme 22: Some examples of 'click' reactions .....	22
Scheme 23: Mechanism for dihydroxylation using osmium tetroxide .....	23
Scheme 24: Proposed mechanisms for the hydrothiolation of an unsaturated hydrocarbon.....	23
Scheme 25: Solvent effect on regioselectivity reactions of amines with a diepoxide ....	24
Scheme 26: Influence of the nitrogen substituent on the regioselectivity of aziridine ring-opening .....	25
Scheme 27: Synthesis of oxime ethers.....	25
Scheme 28: Synthesis of hydrophobic oxime ether.....	26
Scheme 29: General Diels-Alder reaction of a diene and a dienophile .....	27
Scheme 30: Example Diels-Alder reaction giving the <i>endo</i> and <i>exo</i> adducts.....	28
Scheme 31: Azide-alkyne Huisgen cycloaddition .....	29
Scheme 32: Proposed catalytic cycle for the Cu(I)-catalysed ligation .....	31
Scheme 33: Catalytic cycle proposed by Bock .....	32
Scheme 34: Observed isotopic enrichment of triazolide <b>46</b> .....	33
Scheme 35: Control reactions showing no isotopic enrichment .....	33
Scheme 36: Mechanistic rationale for the isotopic enrichment of triazolide <b>52</b> .....	34
Scheme 37: Proposed catalytic model for the CuAAC with two copper atoms.....	35
Scheme 38: Biotinylated surface produced by sequential Diels-Alder and azide-alkyne cycloadditions.....	38
Scheme 39: Convergent approach toward triazole dendrimers.....	41
Scheme 40: Synthesis of neoglycopolymers using alkyne-derived polymer and azido-derived sugars.....	43
Scheme 41: Structural mimics of vancomycin comprising 1,4- and 1,5-disubstituted triazole-containing cyclic tripeptides.....	49
Scheme 42: Ru-catalysed synthesis of triazoles from internal alkynes .....	50
Scheme 43: Proposed catalytic cycle of the RuAAC reaction .....	50
Scheme 44: Bis-alkyne reactivity under CuAAC conditions.....	51
Scheme 45: Proposed reaction to give a selective version of the CuAAC .....	51

Scheme 46: Attempted kinetic resolution using CuAAC .....	52
Scheme 47: Desymmetrization of <i>bis</i> -alkynes by CuAAC.....	53
Scheme 48: Asymmetric 'click' reaction with a <i>bis</i> -alkyne.....	53

## List of figures for Chapter 2: Results & Discussion

Figure 1: Optimization of <i>N</i> -alkylation step showing yield as a function of reaction time and temperature .....	61
Figure 2: <sup>1</sup> H-NMR of unknown compound, believed to be <b>14</b> .....	65
Figure 3: Products of the <i>N</i> -alkylation reactions .....	68
Figure 4: <i>Meso bis</i> -alkynes to be synthesized for testing .....	76
Figure 5: Structure of new target <i>meso bis</i> -alkyne .....	82
Figure 6: A - <sup>1</sup> H NMR spectrum of the diastereoisomer mixture; B - <sup>1</sup> H NMR spectrum of the crystal collected from the mixture .....	94
Figure 7: ORTEP drawing showing 2 units of <i>meso bis</i> -alkyne <b>29</b> .....	94
Figure 8: ( <i>R</i> )-Mosher's acid.....	95
Figure 9: A - <sup>1</sup> H NMR spectrum of the mixture of diols; B - <sup>1</sup> H NMR spectrum of the mixture of Mosher diesters.....	96
Figure 10: Target compound <b>60</b> .....	100
Figure 11: Synthesised <i>meso bis</i> -alkynes for testing .....	104
Figure 12: Possible structures of <i>bis</i> -copper-alkyne complexes .....	107
Figure 13: Structure of L1 .....	108
Figure 14: Structures of chiral ligands used.....	109
Figure 15: Synthesised <i>meso bis</i> -alkynes for testing .....	114

## List of schemes for Chapter 2: Results & Discussion

Scheme 1: Separation of a triazole into its original components .....	55
Scheme 2: Application of ultrasound to a triazole embedded within a poly(methyl acrylate) chain .....	56
Scheme 3: Synthesis of triazole <b>2</b> .....	56
Scheme 4: Synthesis of triazole <b>2</b> using a one-pot procedure.....	57

Scheme 5: Synthesis of triazole <b>2</b> using a microwave-assisted one-pot procedure.....	57
Scheme 6: Conversion of a triazole into the corresponding triazolium salt .....	58
Scheme 7: Conversion of a triazole to its triazolium salt using the original procedure .	58
Scheme 8: Reduction of triazolium salt <b>3</b> using LiAlH <sub>4</sub> .....	59
Scheme 9: The synthesis of 1,5-disubstituted 1,2,3-triazoles as proposed by Koguchi .	59
Scheme 10: Microwave-assisted conversion of a triazole to its triazolium salt.....	60
Scheme 11: Standard procedure for the <i>N</i> -alkylation of <b>2</b> with different alkyl groups..	62
Scheme 12: Attempted debenzoylation of <b>3</b> using NaOMe & NaOEt .....	62
Scheme 13: Possible mechanisms for the displacement of the benzyl group .....	63
Scheme 14: Debonylation of <b>3</b> using <i>t</i> BuOK .....	63
Scheme 15: Optimized reaction plan for the 1,3- to 1,5-triazole interconversion .....	64
Scheme 16: Excess <i>N</i> -alkylation of triazole <b>2</b> .....	65
Scheme 17: Synthesis of 1,4,5-trisubstituted triazole <b>15</b> .....	66
Scheme 18: Regioselectivity in the RuAAC .....	66
Scheme 19: New possible pathway for the regioselective copper-catalysed synthesis of 1,4,5-trisubstituted triazoles .....	67
Scheme 20: General scheme for the <i>N</i> -alkylation of triazole <b>2</b> .....	67
Scheme 21: General scheme for the reaction of triazolium salts with <i>t</i> BuOK .....	68
Scheme 22: Reaction of triazolium salts with <i>t</i> BuOK.....	69
Scheme 23: Alternative possible mechanism for the 1,3,4- to 1,4,5-triazole interconversion .....	69
Scheme 24: Products from the inter- and intra-molecular reaction.....	70
Scheme 25: Synthesis of the cyanoacetate-derived mono-triazole <b>20</b> .....	71
Scheme 26: Attempted 1,3 to 1,5-triazole interconversion of mono-triazole <b>20</b> .....	72
Scheme 27: Krapcho decarboxylation of <b>20</b> .....	73
Scheme 28: <i>N</i> -alkylation of mono-triazole <b>20</b> using MeOTf.....	73
Scheme 29: Attempted reduction of the methyl ester in <b>20</b> .....	74
Scheme 30: Saponification of <b>20</b> .....	75
Scheme 31: Retrosynthetic route for the synthesis of <b>26</b> .....	76
Scheme 32: Synthesis of <i>meso</i> -diester <b>36</b> .....	77
Scheme 33: Attempted synthesis of di-aldehyde <b>37</b> .....	77
Scheme 34: Reduction of ester <b>36</b> to primary alcohol <b>38</b> .....	78
Scheme 35: Attempted Swern oxidation of <b>38</b> .....	78
Scheme 36: Attempted Parikh-Doering oxidation of <b>38</b> .....	79

Scheme 37: Synthesis of DMP <b>39</b> .....	79
Scheme 38: Attempted Dess-Martin oxidation of <b>38</b> .....	80
Scheme 39: Synthetic route to avoid the intramolecular reaction .....	80
Scheme 40: Synthesis to avoid the intramolecular reaction.....	81
Scheme 41: Conversion of the alcohol to a better leaving group .....	82
Scheme 42: Tosylation of <b>38</b> .....	82
Scheme 43: Alkynylation of <b>44</b> using the Grignard reaction.....	83
Scheme 44: Alkynylation of <b>44</b> using TMSA and <i>n</i> BuLi.....	83
Scheme 45: Iodination of <b>38</b> using Garegg's conditions.....	84
Scheme 46: Alkynylation of <b>45</b> using TMSA and <i>n</i> BuLi.....	84
Scheme 47: Pt(II)-catalyzed synthesis of a cycloparryl ether .....	84
Scheme 48: Retrosynthetic approach for the synthesis of <b>27</b> .....	85
Scheme 49: Alkyne addition to glutaryl chloride .....	85
Scheme 50: Acylation mechanism.....	85
Scheme 51: Removal of TMS protecting groups .....	86
Scheme 52: Propargylic ketone reduction using NaBH <sub>4</sub> .....	87
Scheme 53: Propargylic alcohol reduction using LiAlH <sub>4</sub> .....	87
Scheme 54: Mechanism of the reduction of propargylic ketones to ( <i>E</i> )-allylic alcohols mechanism.....	87
Scheme 55: Cyclization of diol mixture .....	88
Scheme 56: 'Click' reaction performed on the mixture of <i>meso</i> and <i>racemic bis</i> -alkyne .....	88
Scheme 57: Synthesis of alpine-borane <b>51</b> .....	89
Scheme 58: Reduction of dione <b>49</b> using alpine-borane <b>51</b> .....	89
Scheme 59: Retrosynthetic approach for the synthesis of <b>28</b> .....	89
Scheme 60: Synthesis of diol <b>53</b> .....	90
Scheme 61: Attempted Swern oxidation of <b>53</b> .....	90
Scheme 62: Conversion of an alcohol to a tosyl group .....	91
Scheme 63: Attempted insertion of alkyne groups into <b>56</b> .....	91
Scheme 64: Conversion of <b>56</b> to <b>58</b> .....	92
Scheme 65: Conversion of <b>53</b> to <b>58</b> .....	92
Scheme 66: Attempted incorporation of alkyne groups into <b>58</b> .....	92
Scheme 67: Reaction of <i>o</i> -phthalaldehyde with ethynyl magnesium bromide .....	93

Scheme 68: Reaction of diol <b>29</b> mixture with Mosher's acid (ME representing Mosher's ester).....	96
Scheme 69: Synthesis of <b>29</b> .....	97
Scheme 70: Diastereoselective reduction of tetralin-1,4-dione.....	97
Scheme 71: Synthesis of <b>59</b> from ( $\pm$ ) <b>29</b> .....	97
Scheme 72: Reduction of <b>59</b> using L-selectride.....	98
Scheme 73: Structures of <i>meso</i> -compounds <b>30</b> , <b>31</b> & <b>32</b> .....	98
Scheme 74: Synthesis of <b>30</b> from <b>29</b> .....	99
Scheme 75: Synthesis of <b>31</b> from <b>29</b> .....	99
Scheme 76: Synthesis of <b>32</b> from <b>29</b> .....	100
Scheme 77: Retrosynthetic plan for the synthesis of <b>60</b> .....	101
Scheme 78: Synthesis of <b>62</b> from <b>29</b> .....	101
Scheme 79: Synthesis of target compound <b>60</b> from <b>62</b> .....	102
Scheme 80: Reaction of <i>meta</i> -diol mixture with Mosher's acid (ME representing Mosher's ester).....	103
Scheme 81: Grignard addition to <i>meta</i> - and <i>para</i> -phthalaldehyde.....	103
Scheme 82: CuAAC reaction with <i>meso bis</i> -alkynes .....	105
Scheme 83: CuAAC reaction with <b>29</b> .....	105
Scheme 84: Synthesis of 1-phenylprop-2-yn-1-ol.....	106
Scheme 85: CuAAC reaction with <b>69</b> .....	107
Scheme 86: Asymmetric 'click' reactions of <i>meso bis</i> -alkynes <b>29-32</b> .....	108
Scheme 87: Asymmetric click of <i>meso bis</i> -alkynes <b>29</b> .....	109
Scheme 88: Ruthenium-free synthesis of 1,5-triazoles.....	110
Scheme 89: 1,3,4- to 1,4,5-trisubstituted triazole interconversion.....	111
Scheme 90: Stereoselective synthesis of 1,4,5-trisubstituted triazoles.....	111
Scheme 91: Staudinger reaction .....	111
Scheme 92: Conversion of a primary alcohol to a primary amine .....	112
Scheme 93: <i>Bis</i> -ketone candidates for the synthesis of new <i>meso bis</i> -alkynes.....	112
Scheme 94: New pathway for the synthesis of 1,5-triazoles using the CuAAC reaction .....	114
Scheme 95: Reaction of <i>o</i> -phthalaldehyde with ethynyl magnesium bromide .....	114



## List of tables for Chapter 2: Results & Discussion

Table 1: Optimization of the <i>N</i> -alkylation reaction step.....	60
Table 2: 1,3- to 1,5-triazole interconversion reactions .....	64
Table 3: Excess <i>N</i> -alkylation of triazole <b>2</b> .....	67
Table 4: Reaction of triazolium salts with <i>t</i> BuOK .....	68
Table 5: Attempts to perform the CuAAC reaction on <b>29</b> .....	105
Table 6: Asymmetric click of <i>meso bis</i> -alkynes <b>29-32</b> .....	108
Table 7: Asymmetric click of <i>meso bis</i> -alkynes <b>29</b> .....	109

# Abbreviations

Ac	acetyl
aq.	aqueous
Ar	aryl
atm	atmosphere
B:	base
br.	broad
Bu	butyl
cat.	catalytic
CAN	ceric ammonium nitrate
DCM	CH <sub>2</sub> Cl <sub>2</sub>
δ	chemical shift
DFT	density functional theory
DMP	Dess-Martin periodinane
de	diastereoisomeric excess
dr	diastereoisomeric ratio
DOTAP	<i>N</i> -[1-(2,3-dioleoyloxy)propyl]- <i>N,N,N</i> -trimethylammonium
DOTMA	<i>N</i> -[1-(2,3-dioleoyloxy)propyl]- <i>N,N,N</i> -trimethylammonium
VAPOL	2,2'-diphenyl-(4-biphenanthrol)
d	doublet
dd	doublet of doublet
EDAC	1-ethyl-3-(3-dimethylaminopropyl) carbodiimide
TMSA	ethynyltrimethylsilane
ee	enantiomeric excess
EPR	electron paramagnetic resonance
er	enantiomeric ratio
Et	ethyl
FT-IR	fourier transformed infra red spectroscopy
HPLC	high performance liquid chromatography
hr(s)	hour(s)
HRMS	high resolution mass spectrometry
<i>i</i>	iso

IR	infrared
<i>J</i>	coupling constant
lit.	literature
LHMDS	lithium bis(trimethylsilyl)amide
L-Selectride	lithium tri- <i>sec</i> -butylborohydride
m	multiplet
M	molar
<i>m</i>	meta
min	minute(s)
MW	microwave irradiation
Me	methyl
mol	mole(s)
Mp.	melting point
NMR	nuclear magnetic resonance
Nu	nucleophile
<i>p</i>	para
Ph	phenyl
ppm	parts per million
PMA	poly(methyl acrylate)
<i>t</i> BuOK	potassium <i>tert</i> -butoxide
<i>n</i>	normal
pyr.	pyridine
q	quartet
<i>rac</i>	racemic
RBF	round-bottomed flask
RT	room temperature
s	singlet
<i>s</i> -	secondary
sat.	saturated
Red-Al	sodium- <i>bis</i> (2-methoxyethoxy)aluminium hydride
SM	starting material
<i>t</i> -	tertiary
TBAF	tetra- <i>n</i> -butylammonium fluoride
t	triplet

TEA	triethylamine
Temp.	temperature
THF	tetrahydrofuran
TLC	thin layer chromatography
TMS	trimethylsilyl
TMSA	trimethylsilylacetylene
Tol	tolyl
Trs	2,4,6-triisopropylbenzenesulfonyl
Ts	<i>p</i> -toluenesulfonyl
UV	ultraviolet
v	volume

*Ever tried. Ever failed. No matter.*

*Try again. Fail again. Fail better*

- Samuel Beckett

# **Chapter 1: Introduction**

## 1.0 Desymmetrization

The production of enantioenriched compounds has been a challenge for the organic synthetic chemist for many years. Taking symmetrical compounds and introducing one or more aspects of chirality is a task which has been researched by many different groups. The desymmetrization of *meso* or achiral substrates is most commonly achieved by the use of an asymmetric catalyst. Areas of interest for chemists include researching how to improve the selectivity of these reactions, their application as key steps in the total synthesis of natural products, and the possibility of introducing selectivity into reactions that currently act indiscriminately. It is this final aspect my research focuses on.

This strategy of stereoselective synthesis uses a chiral reagent or catalyst which distinguishes between two enantiotopic groups or atoms within the same compound. The two reactive centres may be in the form of a single reactive enantiotopic group (such as that of an epoxide) or as two separate enantiotopic groups (such as a symmetrical diol). This distinguishing feature allows desymmetrization substrates to be classified as those that undergo a single transformation (ring opening of an epoxide) or able to perform multiple transformations (acylation of a diol, Figure 1).

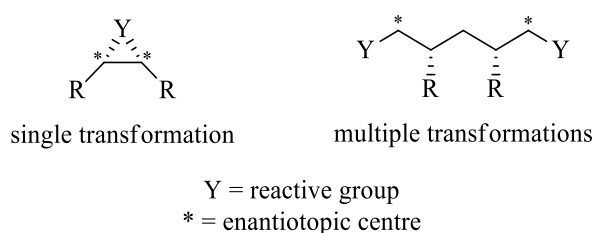


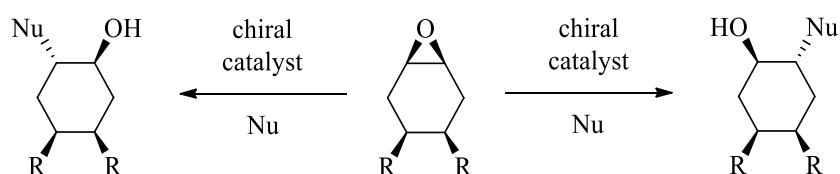
**Figure 1:** Classification of desymmetrization substrates

In some cases, the desymmetrization reaction is similar to a kinetic resolution. Unlike kinetic resolutions, which distinguish between two enantiomers of a substrate, the catalyst chooses between asymmetric centres of units. This means that the compounds that are successful kinetic resolution catalysts are often efficient at desymmetrization reactions.

## 1.1 Compounds containing one reactive functional group with two enantiotopic centres

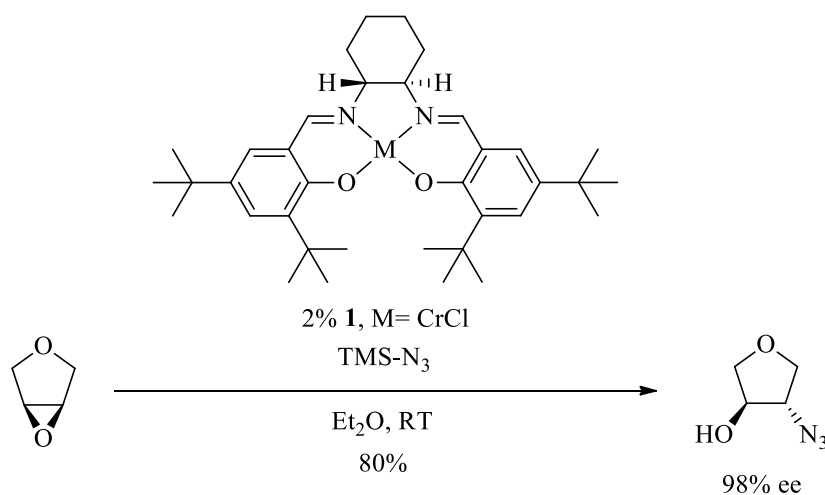
### 1.1.1 Ring-opening of epoxides and aziridines

Symmetrically substituted *meso*-epoxides and aziridines are examples of compounds with only one reactive functional group, where a reaction at each of the enantiotopic carbons leads to a different enantiomer of the product (Scheme 1).<sup>1</sup>



**Scheme 1:** Desymmetrization of *meso*-epoxides

An example of this desymmetrization was published by Jacobsen in which he used TMS-azide as the nucleophile to perform the ring-opening in 98% ee (Scheme 2).<sup>2</sup> As with most of the desymmetrization substrates that contain just a single reactive group, once the transformation has taken place it is inert to a further reaction; this means that the ee should remain constant provided that the catalyst remains unchanged.



**Scheme 2:** Enantioselective ring-opening of *meso*-epoxides with (*R,R*)-**1**

The selectivity-determining step of this reaction occurs at the point of insertion of the nucleophile once the epoxide has coordinated to the metal centre, so it is the orientation



of the epoxide within the metal-ligand system that induces the product stereochemistry. An in-depth study of the binding was carried out by Murphy and Fallis, in which they used several techniques, including pulsed EPR and DFT, to show the binding of an epoxide in a vanadyl salen complex.<sup>3</sup> They concluded that it is a combination of steric properties, H-bonds and weak electrostatic contributions that determines how the epoxide interacted. It is specifically the H-bond between the epoxide oxygen atom ( $O^{\text{epoxide}}$ ) and the methine proton ( $H_{\text{exo}}$ ) of the vanadyl salen complex that provides the pathway for the stereochemical communication (Figure 2).

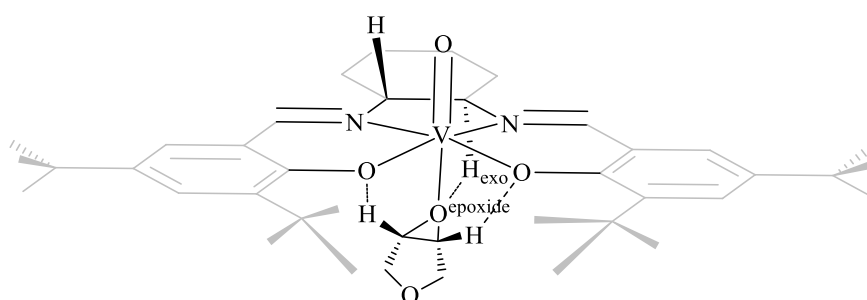


**Figure 2:** Interaction between the metal-salen complex and the epoxide

Like epoxides, aziridines are extremely reactive due to the high ring strain of the three-membered ring and will undergo similar reactions yielding various chiral amines. Although the enantioselective catalytic desymmetrization of *meso*-aziridines has been known for some time now, these generally also employ metal-based Lewis acids with chiral ligands.<sup>4-7</sup> Aziridines can mimic the interactions between the metal-salen complex and the ring that is observed with epoxides, above. It is only in recent years that the use of small organocatalysts has emerged, such as the cinchona alkaloid derivative **2**, the chiral phosphoric acid derived from VAPOL **3** and the chiral thiourea **4** (Figure 3).<sup>8</sup>

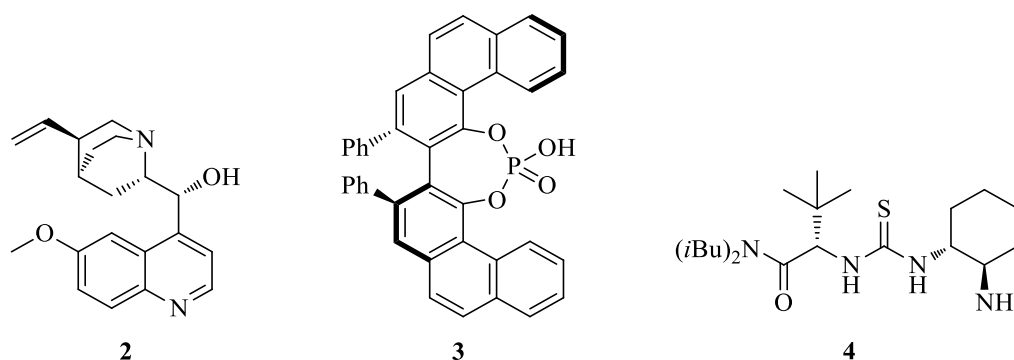
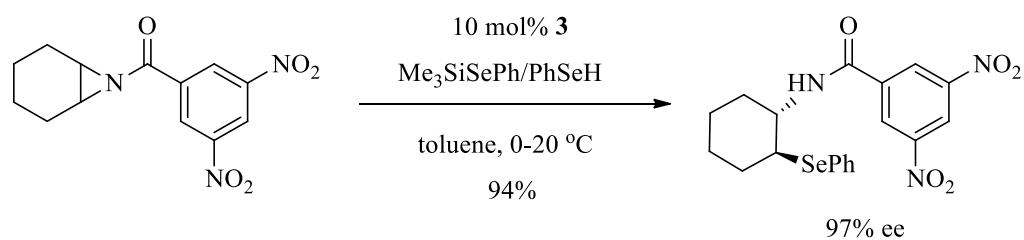


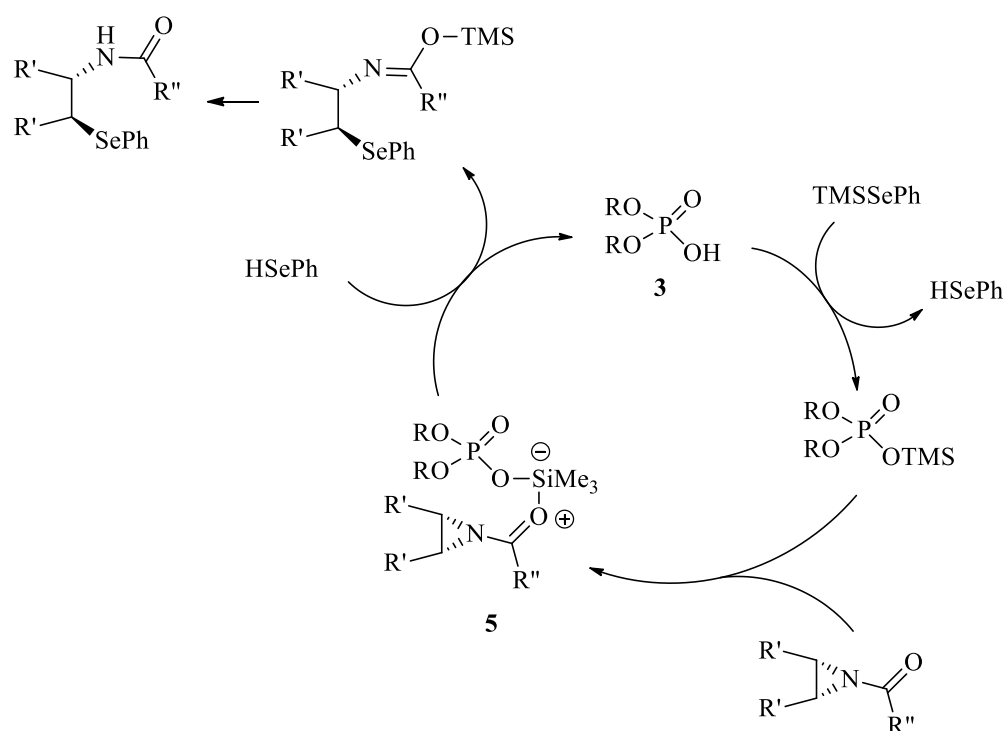
**Figure 3:** Examples of organocatalysts used in enantioselective aziridine ring-opening

A review by Wang described the enantioselectivity obtained when the organocatalysts shown in Figure 3 were used with different aziridines.<sup>8</sup> One of the more selective reactions used (*R*)-VAPOL phosphoric acid **3** as the catalyst and a silylated reagent (Scheme 3).<sup>9</sup>



**Scheme 3:** Enantioselective desymmetrization of meso-aziridines

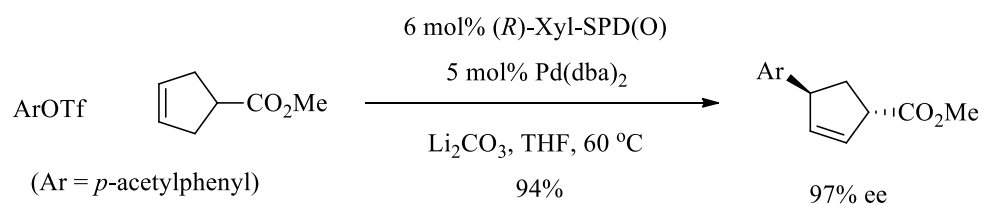
Unlike transition metal catalysis, it is the steric hindrance of the chiral pocket created by the VAPOL phosphoric acid **3** that prevents the attack to one side of the aziridine, controlling the stereochemistry.<sup>10</sup> In this example, the aziridine is not bound directly to the phosphoric acid; instead phenyl trimethylsilyl selenide reacts with **3** to generate the chiral catalyst. First the catalyst undergoes proton exchange with the phenyl TMS selenide; the silicon forms a complex with the carbonyl of the aziridine to form **5**. It is at this stage that the sterics of the VAPOL group directs which side of the aziridine is attacked. Finally, the protonation of the catalyst releases the amide product (Scheme 4).



**Scheme 4:** Proposed mechanism for the organocatalytic desymmetrization of aziridines

### 1.1.2 Heck reaction

Since its discovery in 1972, the Heck reaction has proven to be an extremely useful reaction for carbon-carbon bond formation, especially as it allows substitution at planar  $sp^2$ -hybridized carbon centres.<sup>11</sup> The first intramolecular version of the reaction was reported by Mori in 1977,<sup>12</sup> but it was not until over a decade later that chiral ligands were employed to give asymmetric versions of both the inter- and intramolecular reaction.<sup>13,14</sup> A recent example of a desymmetrization using the intermolecular Heck reaction was reported by Zhou, where cyclic substituted olefins were desymmetrized in high dr and ee (Scheme 5).<sup>15</sup>



**Scheme 5:** Desymmetrization of a cyclic olefin using the Heck reaction

In this reaction the stereochemical discrimination occurs from the enantioselective insertion of the alkene starting material into either the *si* or the *re* face to give the olefin-coordinated complex. This is then followed by a  $\beta$ -hydride elimination reaction, where a direct interaction between this hydrogen and the vacant site on the palladium centre is required. The mechanism of the palladium-catalysed asymmetric arylation was studied by Hayashi,<sup>16</sup> with their results helping to explain the ee seen in Scheme 5. In their example (**6**) the steric repulsion between the olefin and the equatorial phenyl group lead to an initial insertion through the *re* face, however when (*R*)-Xyl-SPD(O) is used (**7**) this is no longer a consideration (Figure 4).

Once the aryl group has been inserted a rotation around the Pd-C bond is required so that the  $\beta$ -hydride is in direct interaction with the vacant orbital. If the compound inserts onto the *re* face then the rotation required for the hydride elimination creates steric repulsion between the new aryl group and the equatorial phenyl group. Insertion on the *si* face does not result in any steric issues in the elimination step and the product in Scheme 5 is obtained in good ee (Scheme 6).

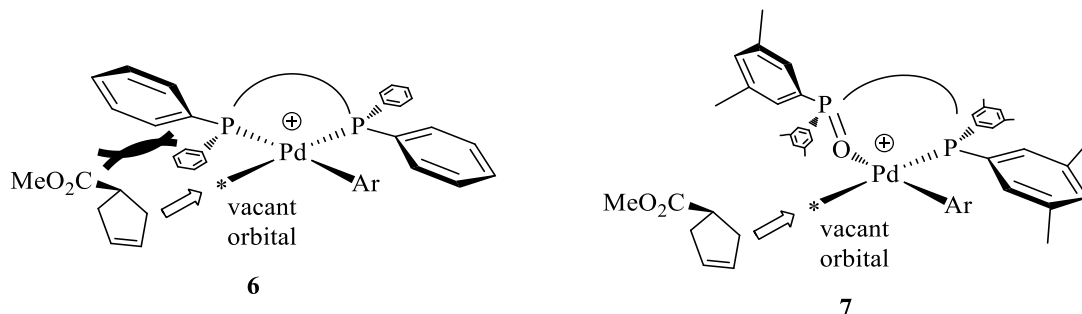
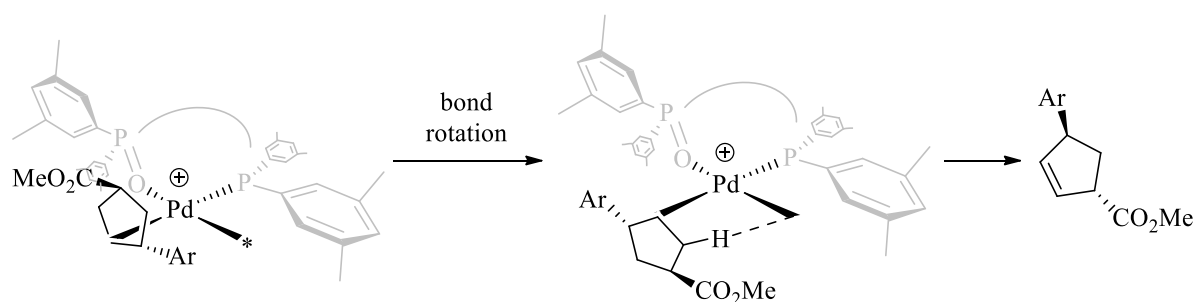


**Figure 4:** Enantioselective insertion of the two different catalysts (the backbone of the ligands has been omitted for clarity)



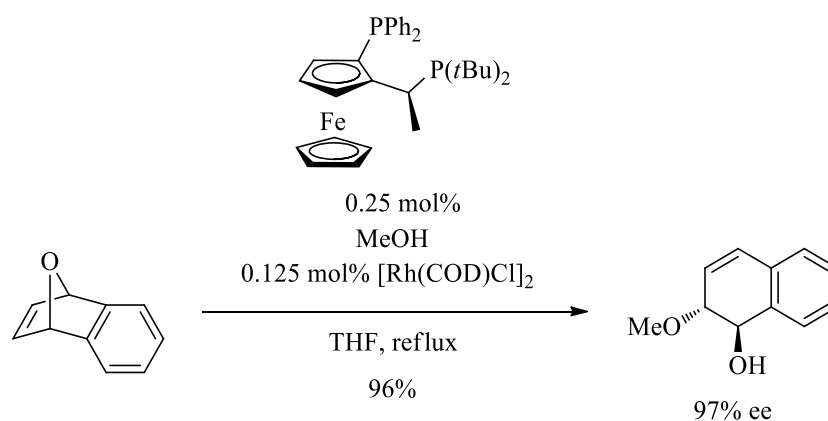
**Scheme 6:** Bond rotation and dissociation of olefin

### 1.1.3 Ring-opening of bridged systems

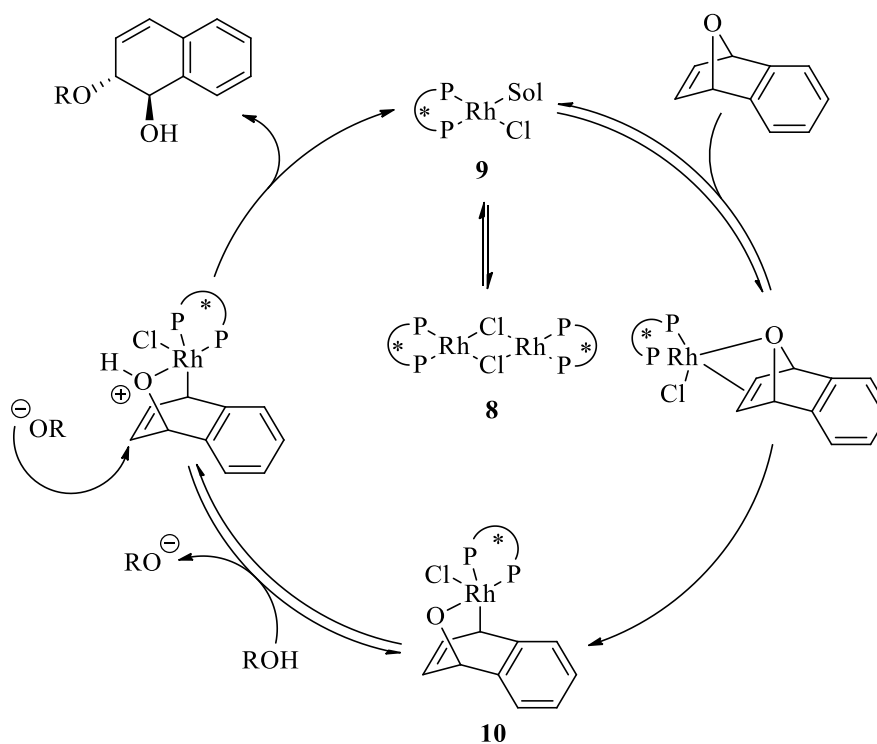
Much like the ring-opening of epoxides and aziridines, extensive research has been carried out regarding the enantioselective synthesis of new carbon-carbon and carbon-nitrogen bonds through the displacement of reactive bridged systems. Various nucleophiles and bridgehead atoms were tested, using rhodium as the metal catalyst.<sup>17</sup> Lautens studied the reaction between oxabenzonorbornadienes and various alcohol and nitrogen nucleophiles to form new carbon-oxygen and carbon-nitrogen bonds, respectively. The rhodium catalyst utilizing the cyclooctadiene ligand ( $[\text{Rh}(\text{COD})\text{Cl}]_2$ ) was used in every example giving enantioselectivities above 90% ee in most cases (Scheme 7).<sup>17</sup>

The reaction starts with the solvation of the dimeric complex **8**, resulting in the formation of the active rhodium catalyst **9**. The *exo*-coordination of the substrate is followed by an oxidative insertion into the bridgehead carbon-oxygen bond, retaining its stereochemistry to give the rhodium-alkoxide complex **10**.

It was proposed by Lautens that the formation of the complex is irreversible due to the release of the ring strain, and that this step is the enantiodiscriminating step of the catalytic cycle.<sup>18</sup> The final step consists of the protonation of the rhodium alkoxide and nucleophilic  $\text{S}_{\text{N}}2'$  attack with inversion of configuration to afford the *trans*-product as well as regeneration of the catalyst (Scheme 8).



**Scheme 7:** Rhodium-catalysed asymmetric ring opening



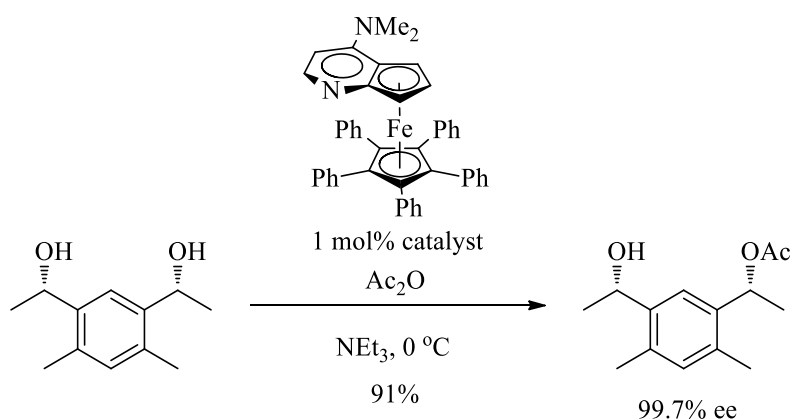
**Scheme 8:** Proposed catalytic cycle of the rhodium catalysed asymmetric ring opening

## 1.2 Compounds containing two reactive enantiotopic groups

### 1.2.1 Desymmetrization and kinetic resolution

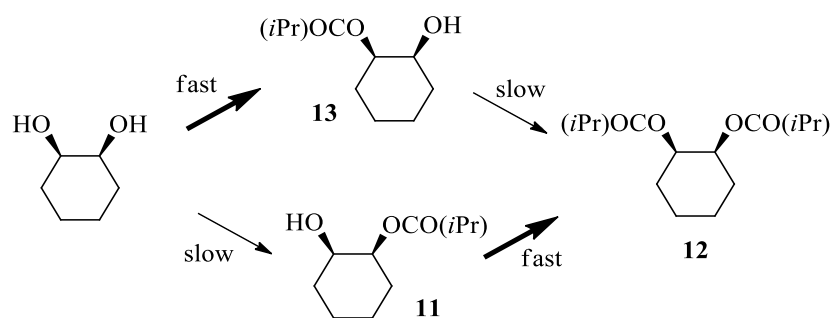
When a compound has a system containing two enantiotopic groups there is the potential for the reaction to occur twice on the single substrate. This means that *meso* substrates can be involved in an initial desymmetrization, followed by a kinetic

resolution step, which can lead to an increased enantiomeric purity of the product. A good example of this can be seen in the desymmetrization of diols.<sup>19</sup> However, this concept can be applied to many other desymmetrization reactions. In the reaction between a *meso*-diol and acetic anhydride using a planar chiral catalyst, matched and mismatched combinations with the catalyst may be observed. The matched pair will lead to a more rapid formation of the major enantiomer, while the mismatched pair will react slower to give the minor enantiomer (Scheme 9).



**Scheme 9:** Desymmetrization of a *meso*-diol with a planar catalyst

As both these products contain another reactive site, they can undergo a further transformation, which will give rise to a kinetic resolution. The kinetic resolution may lead to an increase in ee of the desired enantiomer because of the second reaction. Once the mismatched pair has done the initial reaction, the remaining reactive site is a matched pair and will react quickly. The opposite occurs if they start as a matched pair, with the first reaction being quick, followed by a slower second reaction between the mismatched pairs of the remaining reactive site. In practice this means that any of the minor enantiomer **11** that is formed will react quickly to give the diacylate **12**, leaving the major enantiomer **13**, as it reacts slowly with the second acyl unit (Scheme 10).<sup>20</sup>



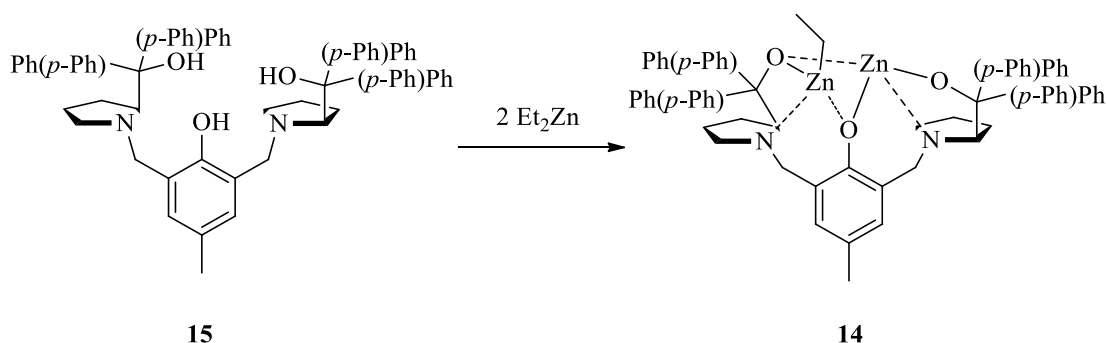
**Scheme 10:** Desymmetrization and kinetic resolution of *meso*-diols

### 1.2.2 Monoprotection of *meso*-compounds

Using *meso*-compounds, different functional groups can be reacted with various protecting groups to give monoprotected products in an enantioselective manner. The allylation of diamide derivatives, acylation and silylation of diols are the selected cases that are covered in this section.

#### 1.2.2.1 Acylation of prochiral diols

The examples shown above rely on the fact that the hydroxyl groups are adjacent to the pro-stereogenic centres. However, in systems where the hydroxyl groups are more remote, it proved more difficult to reach high enantioselectivity without the use of kinetic resolution.<sup>21</sup>

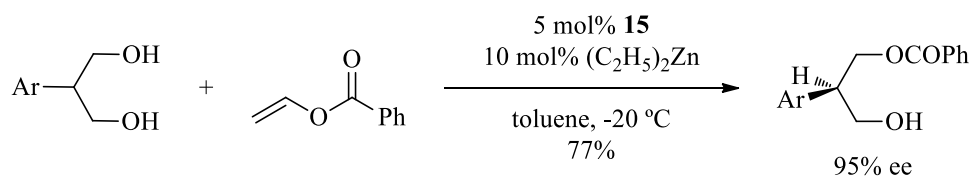


**Scheme 11:** Formation of dinuclear zinc complex **14** from **15**

Trost developed the novel dinuclear zinc complex **14** from **15** and diethyl zinc for asymmetric aldol reactions (Scheme 11),<sup>22</sup> and hoped that its ability to act both as an acid and a base would enable it to catalyse the asymmetric acylation of 1,3-diols. The

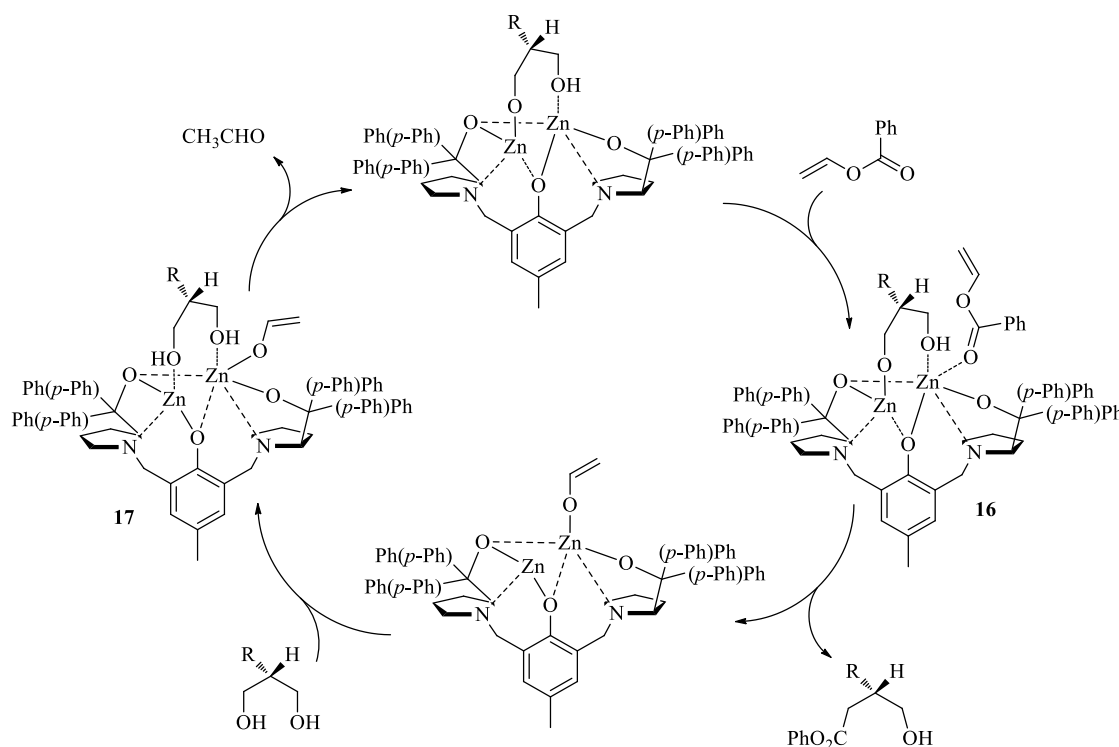


group was able to successfully produce the monoprotected products in up to 95% ee (Scheme 12).



**Scheme 12:** Enantioselective acylation of a 1,3-propanediol

The group proposed a catalytic cycle (Scheme 13) which starts with the coordination of the vinyl benzoate to the zinc centre with it pointing away from the diarylcarbinol unit of the prolinol group to give complex **16**.

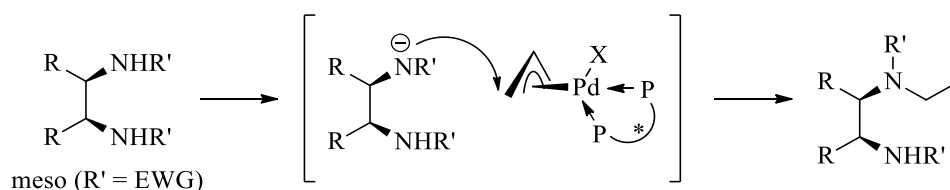


**Scheme 13:** Proposed catalytic cycle for the desymmetrization of 2-substituted-1,3-propanediols

According to Trost, the enantioselectivity occurs when the aryl group shifts to the oxygen of the alkoxide, with the two diarylcarbinol moieties defining the chiral space. The monoprotected product is then released, another diol unit inserts to give complex **17** and the vinyl alkoxide is released as acetaldehyde, continuing the cycle.

### 1.2.2.2 Alkylation of *meso*-diamides

Vicinal diamides and their derivatives have received great attention from synthetic and medicinal chemists, with various optically active diamine derivatives being employed as chemotherapeutic agents.<sup>23</sup> The first example of the asymmetric desymmetrization of *meso*-diamine derivatives was described in 2006 using a chiral allyl palladium catalyst.<sup>24</sup> In the area of transition metal catalysed N-C bond-forming reactions, this is a rare example of asymmetric induction at the nitrogen nucleophilic site. The reason why there are so few examples of this type of reaction may be the high nucleophilic reactivity of the amino groups, and their affinity to form a complex with transition metals, resulting in the dissociation of the chiral ligand and the deactivation of the catalyst. By using less reactive amide groups, Taguchi hoped that the nitrogen nucleophile would not form a complex and enantioselectivity could be achieved through the spatial arrangement of the chiral ligand around the metal centre (Scheme 14).



**Scheme 14:** Asymmetric desymmetrization of *meso*-diamides through catalytic enantioselective *N*-allylation

The group used Trost ligands **18-20** with palladium for the *N*-monoallylation of *meso*-1,2-*bis*-(Trs)-amides to get good to excellent enantioselectivity (85-96%).<sup>25</sup>

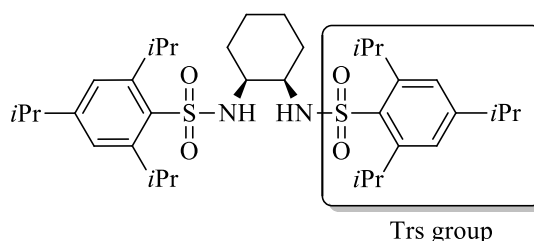


**Figure 5:** Example of a *meso* 1,2-*bis*-(Trs)-amide used by the group

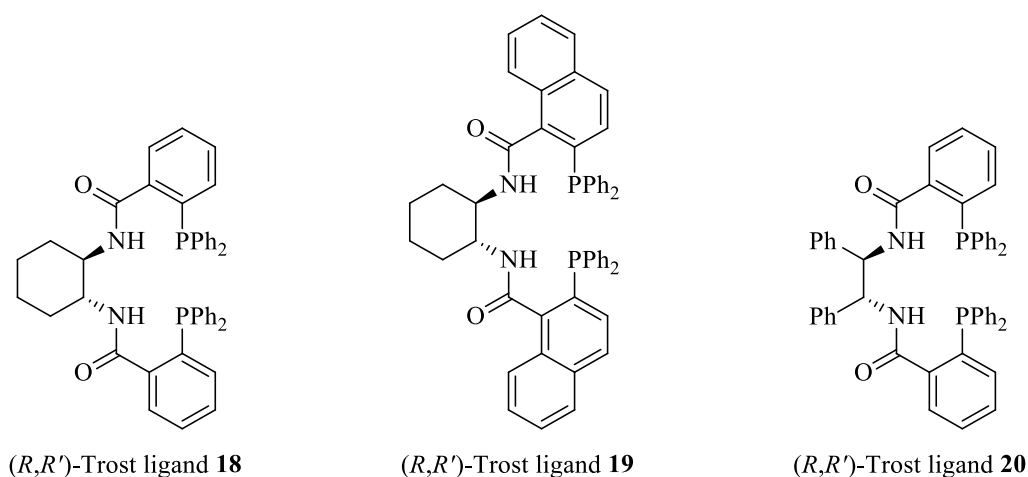
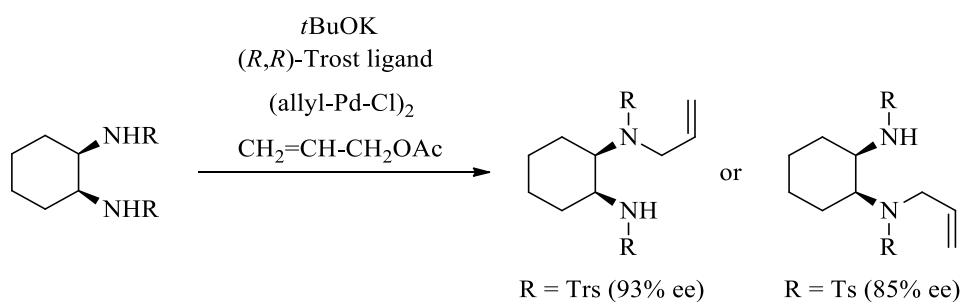


**Figure 6:** Several Trost ligands

They discovered that the presence of the Trs sulfonyl substituent on the nitrogen atom was essential for achieving such high enantioselectivity. When the reaction was carried out under the same conditions using a toluenesulfonyl group as the substituent, the other enantiomer was obtained (Scheme 15). Further reactions with different sulfonamide derivatives indicated the importance of an *o*-alkyl substituent for  $(1R,2S)$ -selectivity.

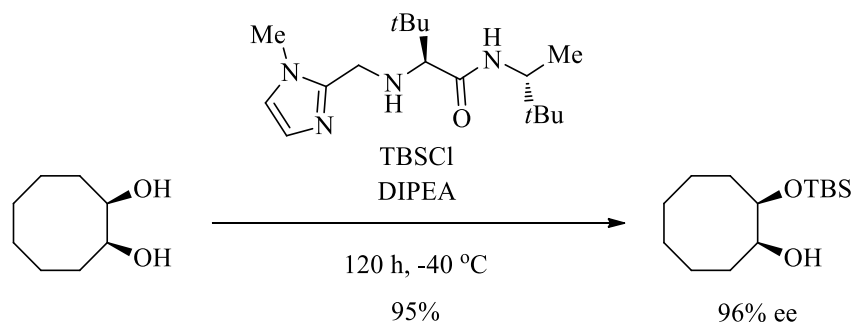


**Scheme 15:** Substituent effect of the sulfonyl group on the nitrogen atom

### 1.2.2.3 Silylation of *meso*-diols

Silyl groups are among the most commonly used protecting groups for alcohols; hence, the enantioselective protection of *meso*-diols using commercial silyl chlorides would prove extremely valuable in the development of complex synthesis. Hoveyda & Snapper used small amino acid-based molecules as catalysts to achieve exactly that (Scheme 16).<sup>26</sup> The substrate-catalyst association occurs through hydrogen-bonding, with the main bulk of the substrate pointing away from the catalyst due to steric

hindrance. The imidazole moiety of the catalyst also promotes the redistribution of electron density and enhances the silicon electrophilicity. These factors combine to give a transition state model as proposed in Figure 7.



**Scheme 16:** Catalytic enantioselective silylation of a *meso*-diol

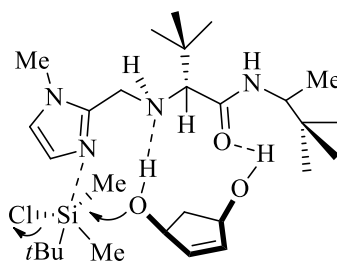
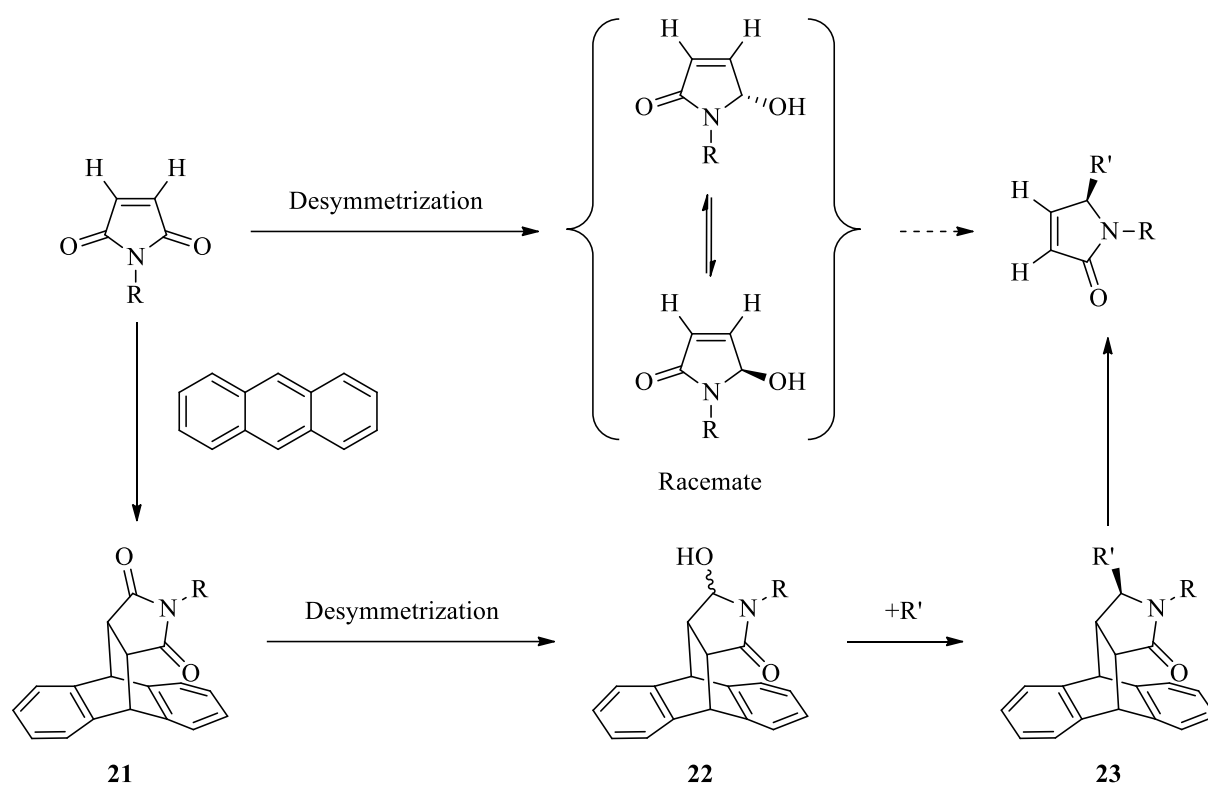


**Figure 7:** Proposed transition state model for catalytic enantioselective silylation of *meso*-diols

### 1.2.3 Reduction of *meso*-compounds

Although the reductive enantioselective desymmetrization of *meso*-imides is a known and effective strategy, researchers in the field believed it to be limited to 3,4-disubstituted saturated imides.<sup>27,28</sup> The direct desymmetrization of maleimides and succinimides by reduction cannot be performed selectively because of the second mirror plane of the molecule. One approach to avoid this difficulty is to temporarily remove the second mirror plane through a Diels-Alder reaction to give the substituted imide **21**.<sup>29</sup> The enantioselective reduction reaction can then proceed as described above, followed by the functionalization of the hydroxy lactam **22** and finally the retro Diels-Alder reaction of **23** to generate the desired product (Scheme 17).



**Scheme 17:** Use of an anthracene template for the desymmetrization of an *N*-substituted maleimide

The rigid framework of the installed anthracene group helps control the selectivity, with the reduction occurring from the more accessible face of the imide **24**, with the catalyst arranging to minimize the steric interaction (Figure 8).

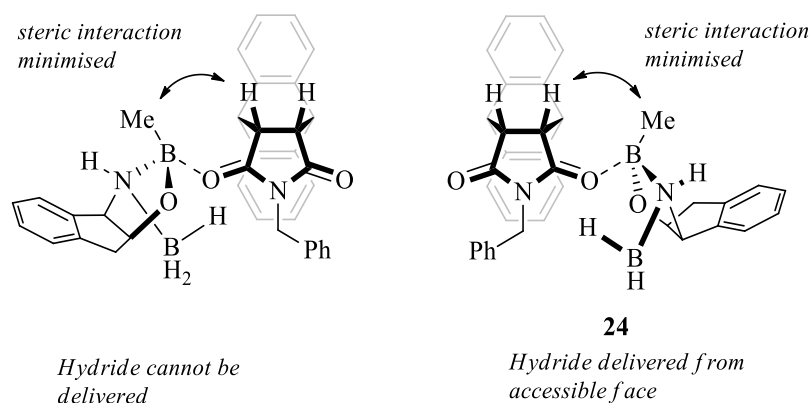
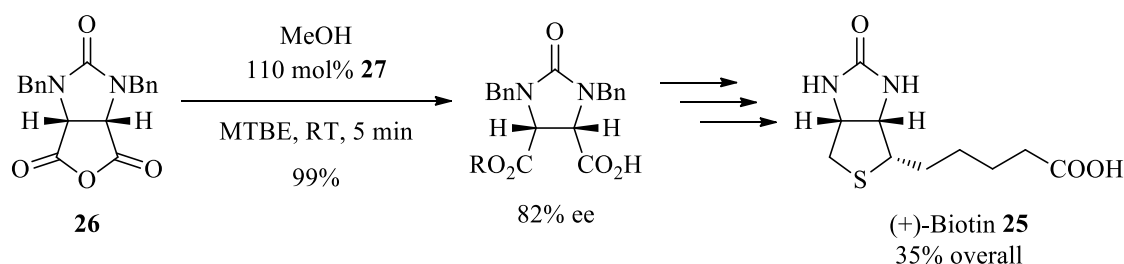


**Figure 8:** Model for the selectivity observed in the reduction of *meso*-imides

### 1.3 Desymmetrization in total synthesis

Desymmetrization reactions are a key tool that can be employed by synthetic organic chemists in the total synthesis of complicated natural products. A few examples of these applied methods are discussed below, with the desymmetrization occurring at different stages of the synthetic route, as well as being used to prove the absolute configuration of a natural compound.

(+)-Biotin **25**, also known as vitamin H, is a B-vitamin necessary for cell growth, the production of fatty acids and the successful metabolism of fats into amino acids. The first synthetic process for the synthesis of (+)-biotin was developed by Sternbach & Goldberg in the 1940s.<sup>30</sup> In 2010, Chen reported an improved synthesis involving the enantioselective desymmetrization of a *meso* cyclic-anhydride **26** at an early stage of the synthesis using catalyst **27** (Scheme 18).<sup>31</sup>



**Scheme 18:** Synthetic route to (+)-biotin **25**

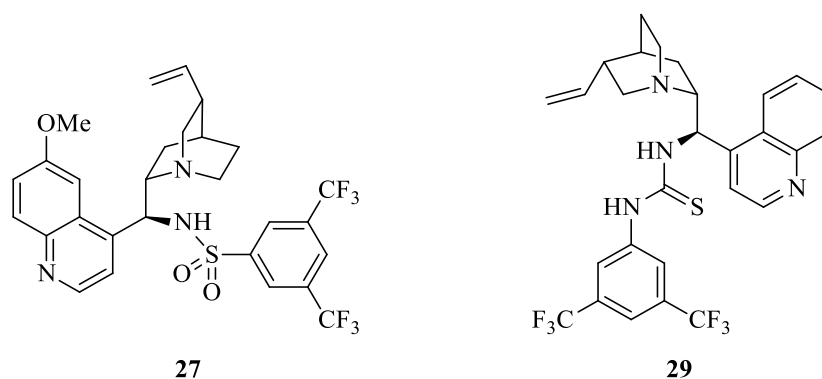
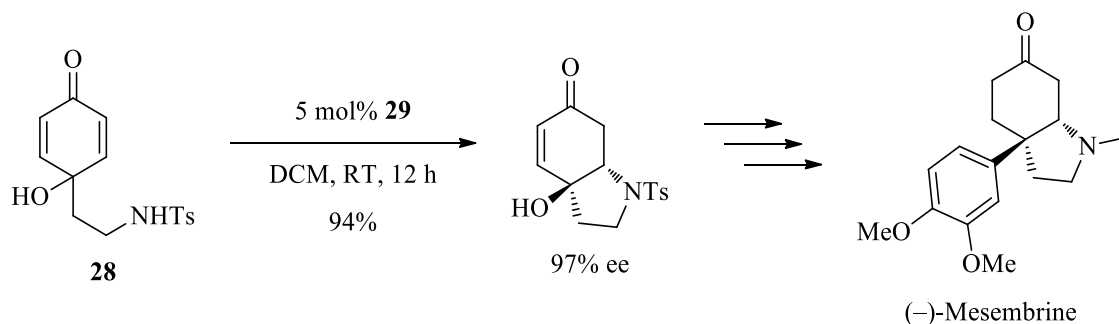


**Figure 9:** Structure of desymmetrization catalysts **27** & **29**

In 2011, You reported an enantioselective intramolecular aza-Michael reaction used to desymmetrize a molecule several steps into the synthesis of (–)-mesembrine.<sup>32</sup> Starting

from various *p*-substituted phenols, a sequence of reactions was performed to prepare **28**, followed by the aza-Michael reaction using catalyst **29** (Scheme 19).



**Scheme 19:** Desymmetrization using an enantioselective intramolecular aza-Michael reaction

The use of cinchona alkaloid-based catalysts such as **29** for the asymmetric aza-Michael reaction has been thoroughly researched to determine how the selectivity is achieved. The suggested reaction transition state can also be applied to the intramolecular version of the reaction, as seen above, with the model explaining how such high ee's are achieved.<sup>33</sup> The amino group of the catalyst establishes a hydrogen bond with the carbonyl, and the protected amino group on compound **28** approaches the double bond, with the lowest steric hindrance occurring from the aromatic group, as in **30** (Figure 10).

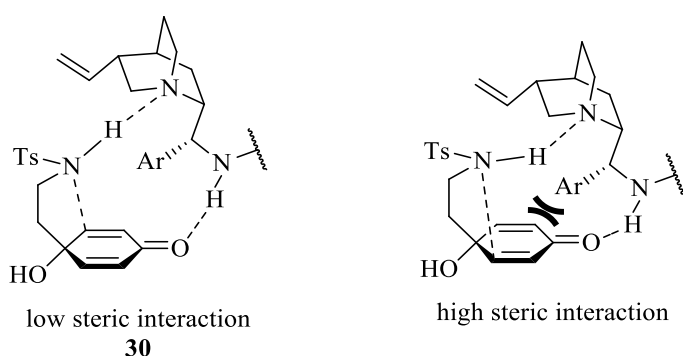


**Figure 10:** Suggested reaction transition state

A recent interesting example of a desymmetrization reaction used, not as a key step of a total synthesis, but instead to prove the absolute configuration of the antitumour acetogenin mosin B.<sup>34</sup> Mosin B is a *syn/trans/anti*-type mono-tetrahydrofuran

acetogenin that was isolated in 1997. Its structure **31** was assigned mainly on the basis of  $^1\text{H}$  and  $^{13}\text{C}$  NMR spectroscopy and MS data.<sup>35</sup> Although the relative stereochemistry of the tetrahydrofuran part was determined, the absolute configuration remained unknown, having **31a** and **31b** as the two possible structures.

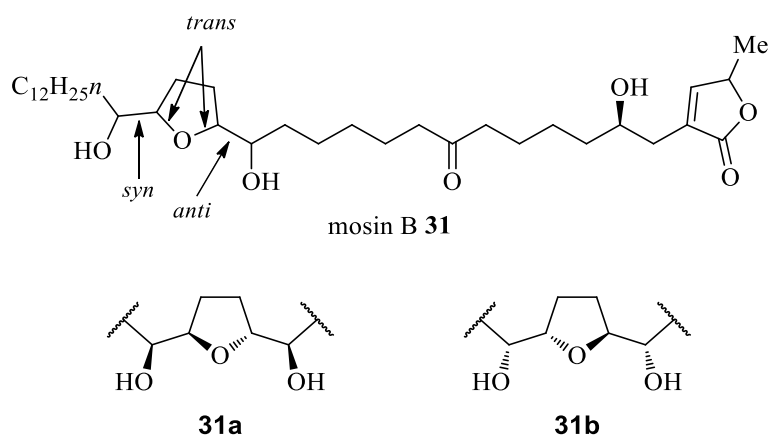
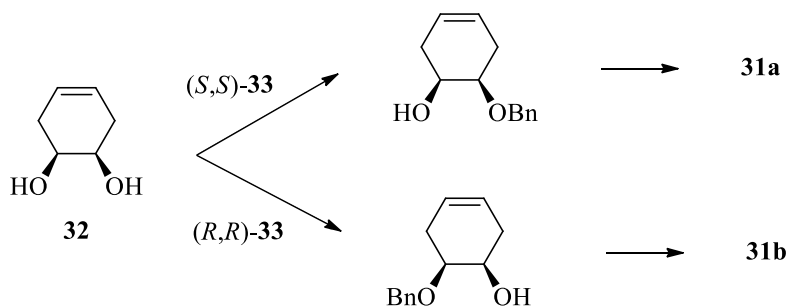


**Figure 11:** Possible structures of mosin B

The differentiation of the two possible structures using  $^1\text{H}$  and  $^{13}\text{C}$  NMR spectra analysis would be difficult because the two stereogenic regions are separated by a long carbon chain. X-ray analysis also proved to be difficult due to the waxy nature of the compound. It was therefore proposed that the group would establish the absolute configuration of mosin B by synthesising both candidate structures. This was achieved using stereodivergent synthesis, starting with the desymmetrization of the common intermediate 4-cyclohexene-1,2-diol **32** (Scheme 20).

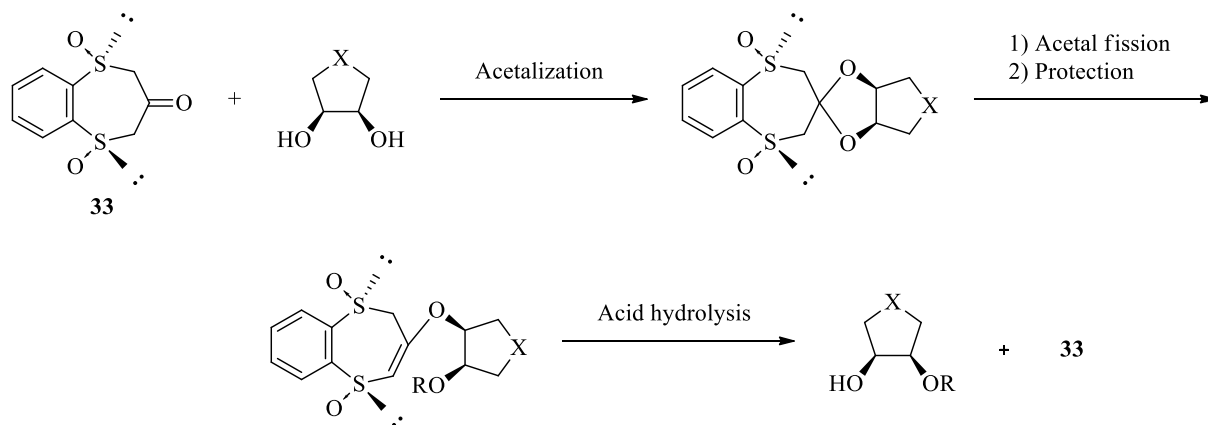


**Scheme 20:** Stereodivergent synthesis to give both candidate structures

The desymmetrization is catalysed by *bis*-sulfoxide **33**: the catalyst and the diol are condensed to form an acetal, the acetal moiety is rearranged to form a stabilised enol



and the resulting alkoxide is protected. Finally, an acid hydrolysis yields the desymmetrized diol (Scheme 21). The stereochemistry for both compounds was confirmed by a modified Mosher method.



**Scheme 21:** Asymmetric desymmetrization protocol for cyclic *meso* 1,2-diols

The selectivity occurs at the acetalization step with the cyclic part of the diol pointing up and away from the sulfinyl oxygen (see top view). The six-membered ring chelated intermediate then undergoes an *anti*-elimination (see side view), which after trapping of the released alkoxide and acid hydrolysis yields the product.<sup>36</sup>

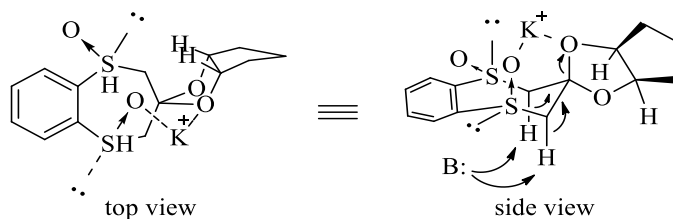


**Figure 12:** Possible chelation intermediates of base-promoted acetal fission

## 2.0 ‘Click’ chemistry

Synthetic chemists endeavour to prepare known and new substances similar to those found in Nature. This can be achieved by joining smaller subunits together with heteroatom linkers, developing a collection of building blocks that can be combined on both the large and small scale. The foundation of this approach is known today as ‘click’ chemistry and was introduced by Sharpless in 2001, when he, Finn & Kolb published a review describing this new strategy for organic synthesis.<sup>37</sup> Sharpless and

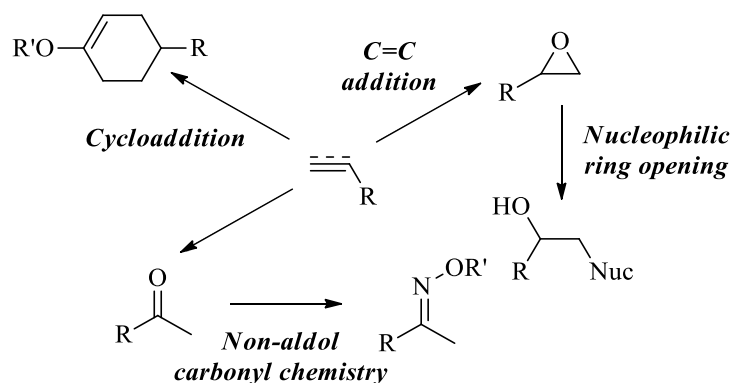
his colleagues note how Nature has a preference towards making carbon-heteroatom bonds over carbon-carbon bonds. Nucleic acids, proteins and polysaccharides are condensation polymers of small subunits that are connected by these carbon-heteroatom bonds. As a way of mimicking Nature's approach, they developed a set of powerful, highly reliable and selective reactions for the rapid synthesis of new compounds using heteroatom linkers. There are stringent criteria for a process to be classified as 'click' chemistry:

*“The reaction must be modular, wide in scope, give very high yields, generate only inoffensive by-products that can be removed by non-chromatographic methods, and be stereospecific (but not necessarily enantioselective).”*

The reaction conditions also need to meet specified criteria:

*“The required process characteristics include simple reaction conditions (ideally, the process should be insensitive to oxygen and water), readily available starting materials and reagents, the use of no solvent or a solvent that is benign (such as water) or easily removed, and simple product isolation. Purification must be by non-chromatographic methods such as crystallisation or distillation.”*

The click part of the name was coined by Sharpless and is meant to signify that following the outlined criteria, the joining of small molecular blocks should be as easy as clicking together the two pieces of a seat belt buckle. Certain aspects of the 'click' chemistry criteria are subjective, and although some of the more measurable and objective ones may be met, it is unlikely that any reactions will fit all of them perfectly. However, some reactions fit the concept more than others and can be classed as 'click' reactions. These reactions are classified into categories including cycloadditions to unsaturated species, additions to unsaturated carbon-carbon bonds, nucleophilic ring-opening reactions, and non-aldol type carbonyl chemistry (Scheme 22).

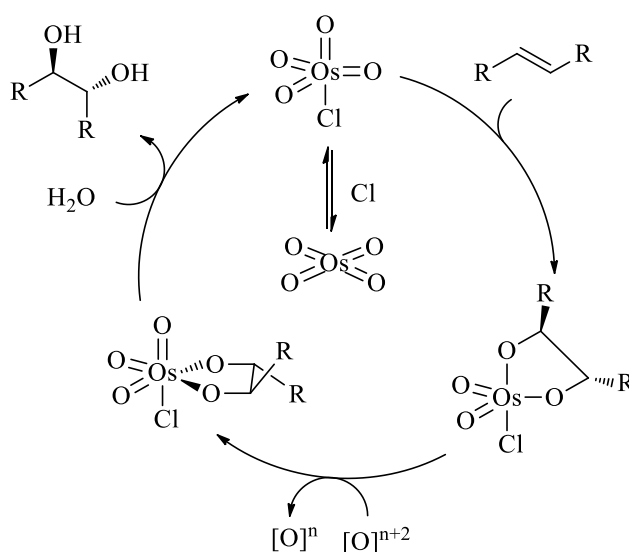


**Scheme 22:** Some examples of 'click' reactions

## 2.1 Olefin-based additions

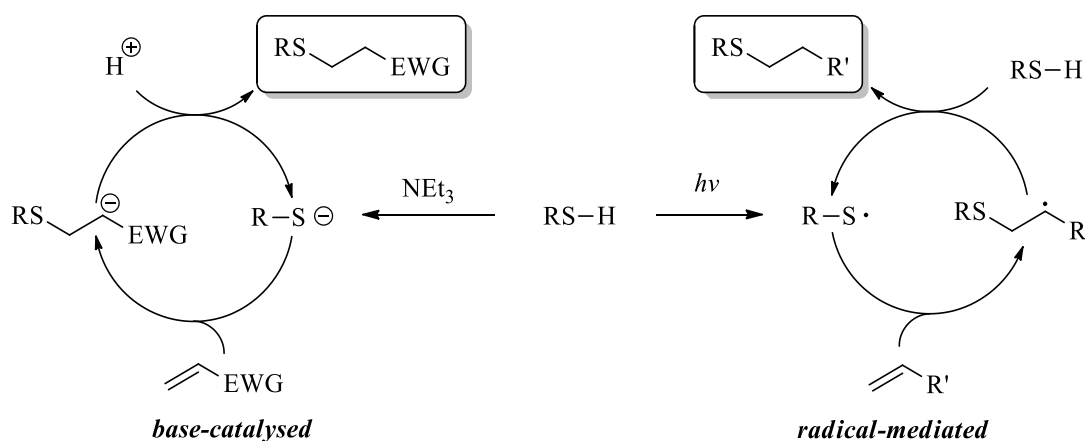
Olefins are one of the most attractive starting materials due to their availability, from Nature in the form of terpenes and fatty acids, or from the manipulation of petroleum-based hydrocarbons. Olefins become even more important given their role as precursors to higher energy intermediates such as epoxides and aziridines, which are perfect for click chemistry transformations. As well as being click chemistry precursors, olefins and alkynes are also able to react under click conditions in the thiol-ene/thiol-yne and dihydroxylation reactions.

A dihydroxylation is the transformation of an alkene to a vicinal diol using a high oxidation state transition metal, such as osmium or manganese, in the presence of an oxidant. There are several named methods that have been developed over the years, each with their own variation, the most recent and possibly the most useful being the Sharpless asymmetric dihydroxylation.<sup>38</sup> The mechanism of the dihydroxylation using the osmium catalyst remains the same as in other examples (Scheme 23). However it is Sharpless' use of a chiral auxiliary which positions the  $\text{OsO}_4$ , delivering the hydroxyl groups to either the  $\alpha$ - or  $\beta$ -face, inducing the selectivity.



**Scheme 23:** Mechanism for dihydroxylation using osmium tetroxide

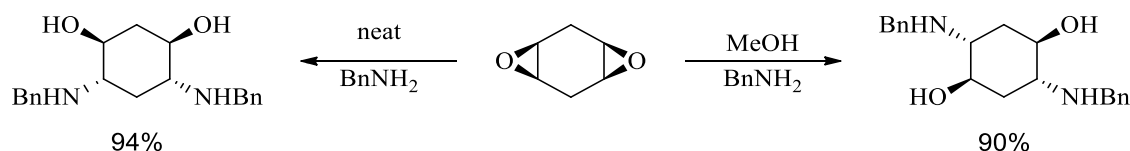
Both the thiol-ene and thiol-yne reactions involve the addition of a thiol across an unsaturated hydrocarbon system in an *anti*-Markovnikov manner by either a free radical or ionic mechanism (Scheme 24).<sup>39</sup> Historically, these reactions have been employed by the polymer and materials science fields in the preparation of large polymer networks and films.<sup>40</sup> Generally, these reactions are extremely rapid, tolerant to the presence of atmospheric air and moisture, and give the corresponding thioethers in near quantitative yields in a highly regioselective manner.



**Scheme 24:** Proposed mechanisms for the hydrothiolation of an unsaturated hydrocarbon

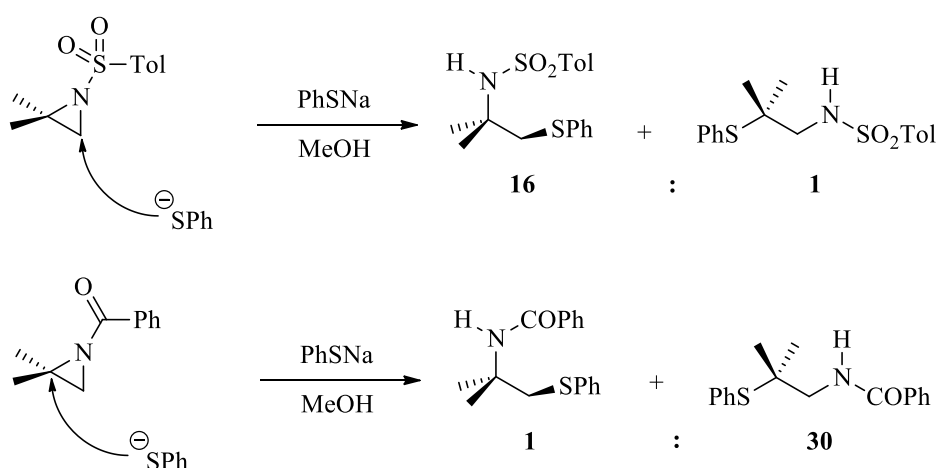
## 2.2 Nucleophilic ring-opening

Olefins are readily converted into three-membered ring heterocyclic electrophiles. These high-energy species, such as epoxides, aziridines, and cyclic sulphates can then easily undergo an  $S_N2$  ring-opening from various nucleophiles. An advantage of three-membered ring-opening reactions is that not only does the steric strain cause the substrates to be especially susceptible to nucleophilic attack, but also that the competing elimination process, which would further increase the steric strain on the ring, is stereoelectronically disfavoured, resulting in high yields. Most of these reactions can be attempted in the absence of solvents or in water, with the choice of solvent affecting the regioselectivity in some cases (Scheme 25).<sup>41,42</sup>



**Scheme 25:** Solvent effect on regioselectivity reactions of amines with a diepoxide

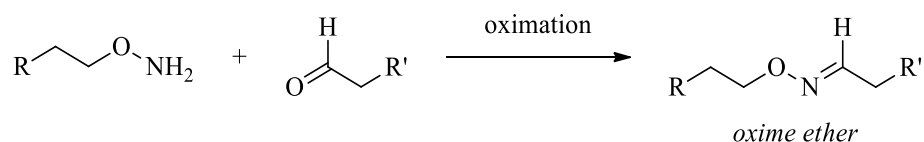
Aziridines are the nitrogen analogues of epoxides, but the presence of a substituent on the nitrogen atom allows an extra element which can be manipulated to alter its reactivity and give greater product diversity. An example of the effect of the N-substituent has been described by Stamm:<sup>43</sup> changing from a sulfonyl to an acyl group results in an attack on the other carbon of the aziridine (Scheme 26).



**Scheme 26:** Influence of the nitrogen substituent on the regioselectivity of aziridine ring-opening

### 2.3 Non-aldol carbonyl chemistry

The synthesis of oxime ethers occurs when the carbonyl group, from either a ketone or an aldehyde, is reacted with an aminoxy group (Scheme 27).



**Scheme 27:** Synthesis of oxime ethers

This reaction earns its place within the concept of click chemistry as a result of some of its applications within the biochemical field. Like most other ‘click’ reactions, its tolerance to a wide range of reaction conditions makes it ideal for use in biological systems. One such example was reported by Nantz when he applied the oximation reaction to link the polar DNA binding domain and hydrophobic domain of structurally manipulated lipids (Scheme 28).<sup>44</sup> The manipulation of lipids, such as DOTMA & DOTAP, would improve the polynucleotide binding and delivery properties. The reliability and efficiency of this reaction makes it ideal for use as the linking reaction.



**Scheme 28:** Synthesis of hydrophobic oxime ether

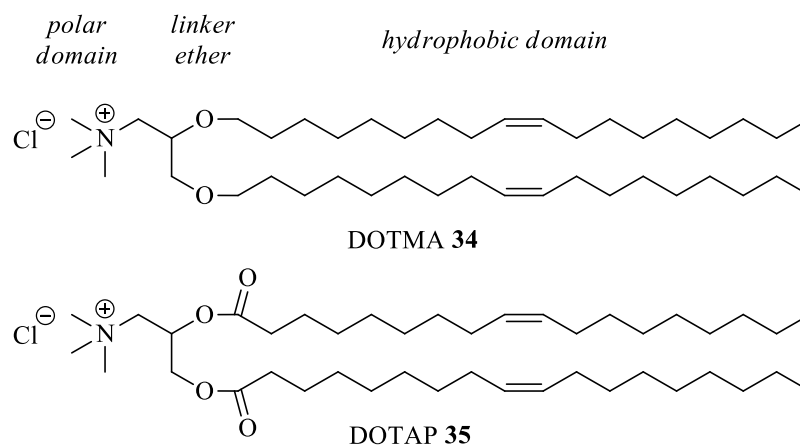


**Figure 13:** Common transfection lipids

The area of hydrazine formation is equally important in the field of chemical synthesis; for example, the hydrazine moiety is present in a number of drugs, such as Lodosyn® & Nardil®. The synthesis of hydrazines can be used in the preparation of amino acid analogues, such as cilengitide: replacing the  $\alpha$ -carbon of an amino acid in a peptide with a nitrogen atom to give an aza-peptide.<sup>45</sup> The condensation of hydrazines with carbonyl containing compounds can also lead to the formation of various aromatic heterocycles. Again, the ease and reliability of this ‘click’ reaction makes it ideal in the synthesis of pyrazole-containing drugs such as Celebrex® **38**.<sup>46</sup>

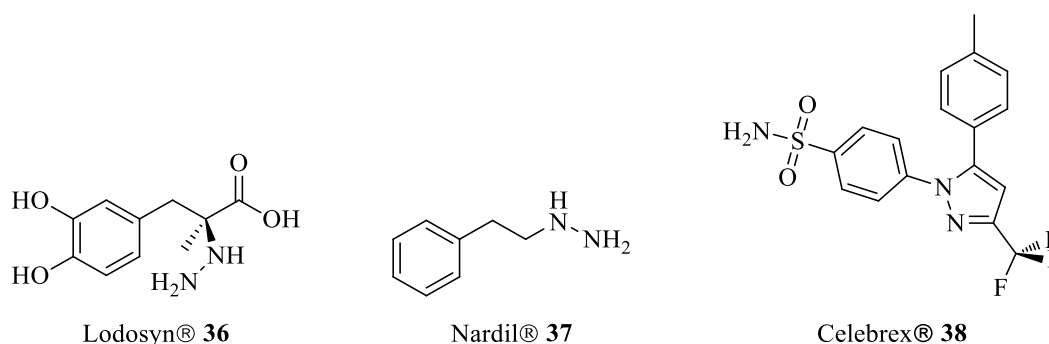
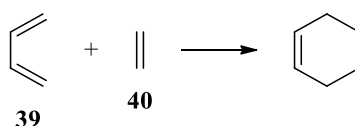


**Figure 14:** Drugs containing hydrazine and pyrazole moieties

## 2.4 Cycloaddition reactions

Some of the best examples of ‘click’ chemistry can be found in the area of cycloadditions. Indeed, the formation of cyclic compounds can require very little energy, and, in some cases, the reaction is exothermic. One of the most common click reactions used in organic synthesis is the Diels-Alder reaction, which involves a [4+2] cycloaddition reaction between a diene **39** and a dienophile **40** (Scheme 29). The reason that the reaction is so desirable is that by simple variation of the substituent groups on either the diene or dienophile, one can control the regio and stereochemical properties of the product. The selectivity of this reaction and other cycloadditions can be easily rationalized by examining the frontier molecular orbitals (FMO) of the reaction components.

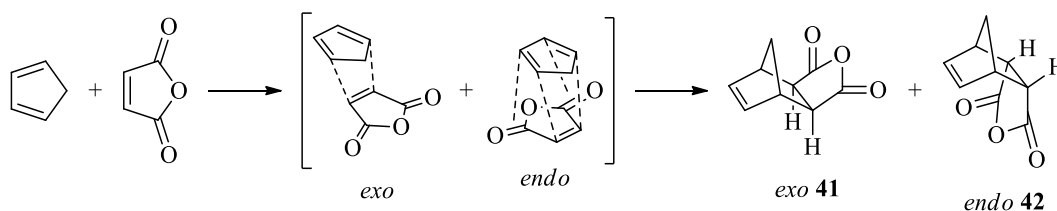


**Scheme 29:** General Diels-Alder reaction of a diene and a dienophile

### 2.4.1 Stereoselectivity of Diels-Alder reactions

When the dienophile is substituted, the reaction can give a product where the substituents are pointing either towards or away from the newly formed double bond. These two compounds are known as the *endo* and *exo* adducts, **42** and **41**, respectively. This can be seen more easily looking at an example where both the diene and dienophile are cyclic (Scheme 30). The selectivity occurs because of the dienophile substituent interaction with the  $\pi$ -system of the diene. The interaction may not be obvious just from looking at the products, however looking at the transition states of the reaction it becomes clearer. For normal Diels-Alder reactions, dienophiles with electron-withdrawing groups such as carbonyls, the *endo* transition state is preferred, despite the additional steric hindrance in the transition state.<sup>47</sup>





**Scheme 30:** Example Diels-Alder reaction giving the *endo* and *exo* adducts

### 2.4.2 Regioselectivity of Diels-Alder reactions

When looking at the regioselectivity of cycloaddition reactions, it can help to look at the relative energies and size of the frontier orbital coefficients as this can give a good approximation of reactivity. The frontier orbitals of a molecule are the highest occupied molecular orbital (HOMO) and the lowest unoccupied molecular orbital (LUMO). The occupied orbitals of one molecule (HOMO) and the unoccupied orbitals of another (LUMO) can interact with each other, causing an attraction. In compounds where conjugation can be observed, such as those with a carbonyl group, the conjugation lowers the energy of the LUMO, distorting the size of the coefficients on the  $\alpha$ - and  $\beta$ -carbon and affecting the level of interaction between the two frontier orbitals.

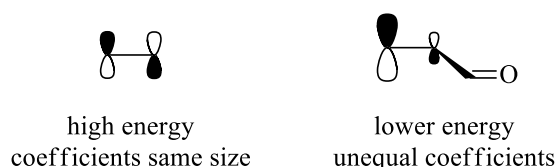


**Figure 15:** Comparison of orbitals of conjugated systems

The most important frontier molecular orbital interactions in the Diels-Alder reaction are between the HOMO of the diene and the LUMO of the dienophile, and so these will now be discussed. As the diene is a conjugated system, the same effect discussed above will be observed, with the two central carbons having the smaller coefficients. The reaction will therefore occur at the terminal carbons of the diene. The addition of different substituents onto the diene and dienophile will also affect the size of the coefficient. The compounds will arrange so that the largest coefficients will come together, giving the regioselectivity observed in Figure 16 between the HOMO of the diene and the LUMO of the dienophile (the central orbitals of the diene have been omitted).

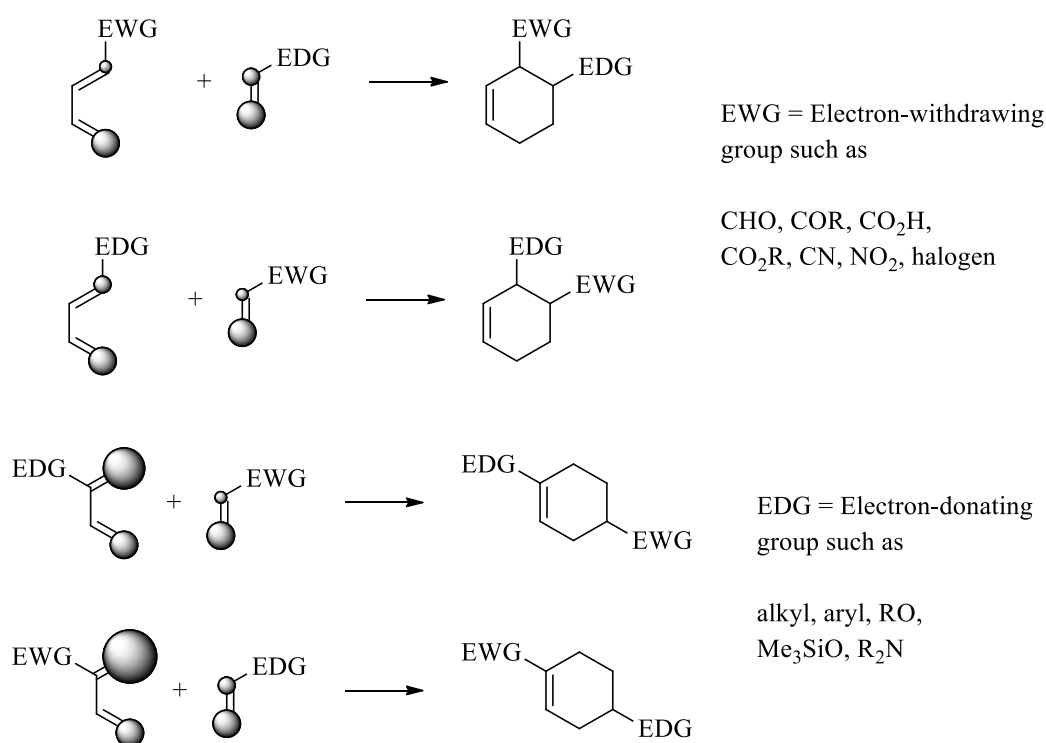
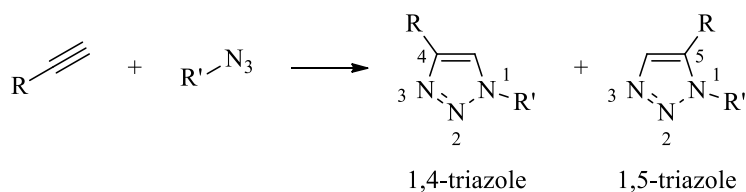


**Figure 16:** Regioselectivity observed in Diels-Alder reactions

## 2.5 Copper-catalysed Huisgen 1,3-cycloaddition - The ‘Click reaction’

Another excellent example of a cycloaddition click reaction is the Huisgen 1,3-dipolar cycloaddition between an azide and an alkyne to yield a 1,2,3-triazole (Scheme 31). The triazoles are afforded as a mixture of the 1,4- and 1,5-adduct in a 1:1 ratio. This reaction is so reliable and wide in scope that it has been referred to as the “cream of the crop” of ‘click’ reactions and a “premier example of a click reaction”.<sup>48,49</sup>



**Scheme 31:** Azide-alkyne Huisgen cycloaddition

In 2002, two independent reports were published by Sharpless and Meldal in which they reported an improved version of the Huisgen 1,3-cycloaddition with the use of a metal catalyst.<sup>50,51</sup> The copper(I)-catalysed variant gives the 1,4-triazole exclusively; however,

it can only be used between an azide and a terminal alkyne. This reaction is better known as the Copper(I)-catalysed Azide-Alkyne Cycloaddition (CuAAC). It is this variant on the Huisgen 1,3-cycloaddition that our group has been focusing its research on.

Many different sources of copper(I) can be used to catalyse the reaction such as cuprous bromide or iodide; however, the reaction works better when the Cu(I) is produced *in-situ*. A mixture of copper(II), such as copper(II) sulfate, and a reducing agent, such as sodium ascorbate, leads to the formation of the Cu(I) source. The benefits of producing the Cu(I) in this way means that there is no need to have a base in the reaction, which may lead to side reactions, and the presence of the reducing agent will make up for any oxygen in the system, which would otherwise oxidize the Cu(I) to Cu(II) and impede the reaction.

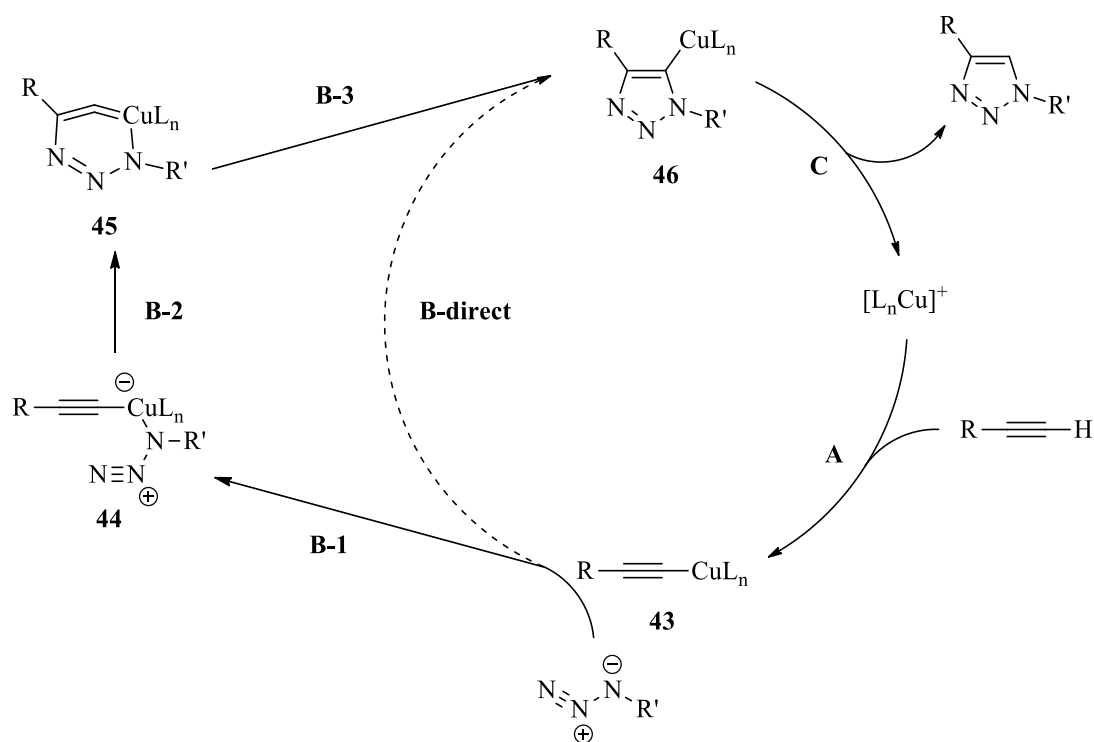
### 2.5.1 Mechanism of the CuAAC

There have been several proposed mechanisms reported for this reaction, all based on DFT calculations. In 2008 Meldal & Tornøe published a comprehensive review in which they discussed the role of the copper catalyst in the cycle, as well as the disputes and revisions since its discovery.<sup>52</sup> In 2002 Sharpless proposed a catalytic cycle involving a single Cu(I)-catalysed ligation (Scheme 32).<sup>50</sup>

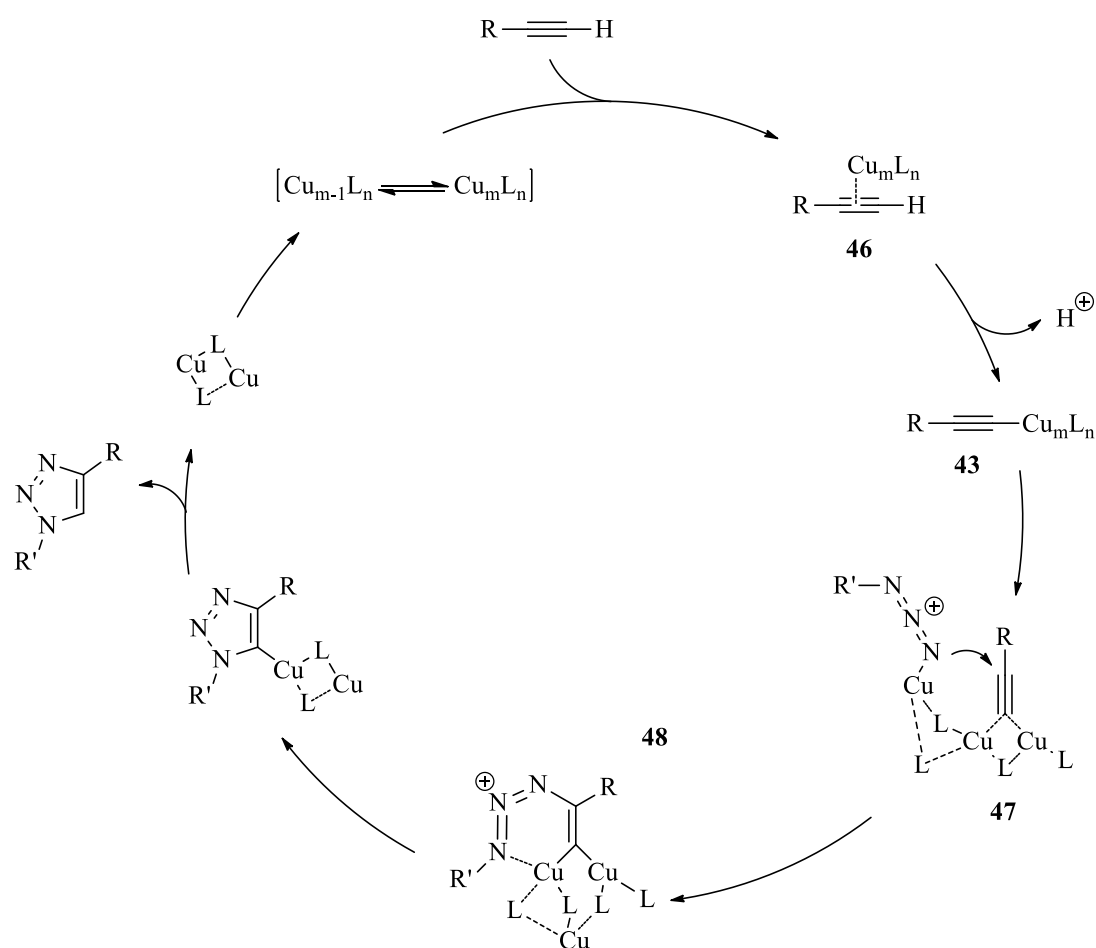
It begins with the formation of the linear copper(I)-acetylide **43**, followed by the azide species insertion. It was originally believed that the azide inserted through a concerted [2+3] cycloaddition (**B-direct**); however, DFT calculations have since suggested this path was disfavoured and instead a stepwise sequence, which proceeds through the six-membered copper-containing intermediate **45**, is involved (**B-1** → **B-2** → **B-3**).

In 2006, Bock improved our understanding of the mechanism when he suggested that multiple copper species are involved in the catalytic cycle.<sup>53</sup> Indeed, the first step in the catalytic cycle is now believed to be the formation of the  $\pi$ -complex **46**, followed by the Cu(I) insertion into the terminal alkyne (Scheme 33). The original DFT calculations assumed that the Cu<sup>+</sup> orientated itself linearly with the alkyne in the transition state.

Instead the  $\text{Cu}^+$  coordinates first with the acetylene  $\pi$ -electrons, lowering the  $\text{pK}_a$  of the acetylenic proton and leading to exothermic formation of the  $\text{Cu}^+$ -acetylide complex.



**Scheme 32:** Proposed catalytic cycle for the Cu(I)-catalysed ligation

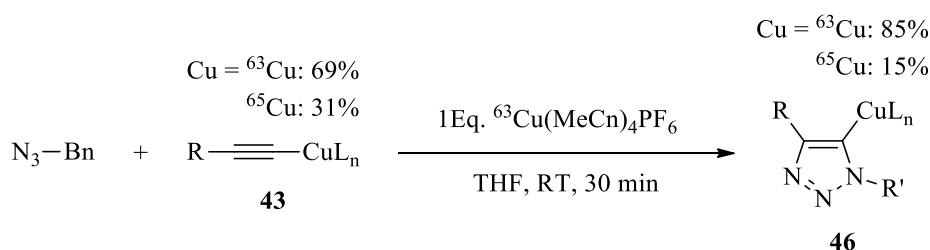


**Scheme 33:** Catalytic cycle proposed by Bock

Furthermore, considering the second order kinetics for the Cu(I) and the structural evidence, it is unlikely that a single Cu(I) atom is involved in the catalysis. It was instead suggested that the acetylide and azide are not necessarily coordinated to the same copper atom in the transition state **47**. The six-membered transition state **48** is then formed, allowing the subsequent formation of the triazole. Transition state **47** was suggested as having the two Cu(I) atoms involved is the only way to unambiguously explain the absolute regioselectivity of the reaction.

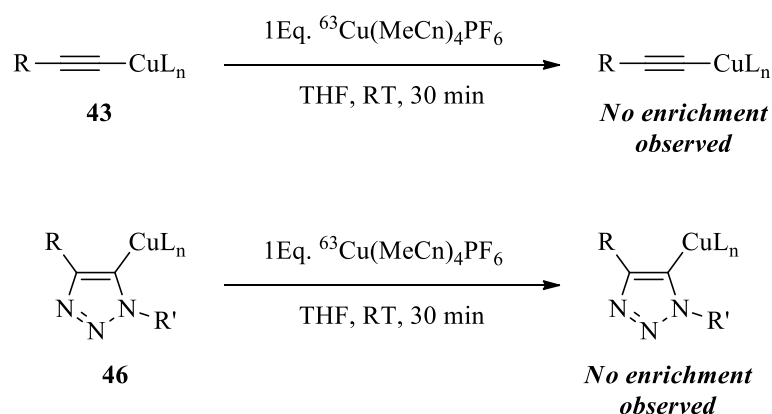
In 2013, Fokin reported further studies into the involvement of two copper atoms within the cycloaddition step.<sup>54</sup> After establishing the involvement of two copper centres, the two centres were then shown to act discretely, each with its own specialized role. Fokin hypothesized that the copper in the acetylide acts purely as a strongly  $\sigma$ -bound ligand, whereas the second copper bonds through weak  $\pi$ -complexation. Due to the stability of the copper-alkyne complex **46** and the acetylide **43**, the copper isotopes  $^{63}\text{Cu}$  and  $^{65}\text{Cu}$

can be used to observe their role in the mechanism. A stoichiometric crossover experiment was designed in which the isotopic enrichment of the resulting triazolide **46** would support the hypothesis (Scheme 34). The result of the experiment showed that there was a 50% isotopic enrichment during the cycloaddition.



**Scheme 34:** Observed isotopic enrichment of triazolide **46**

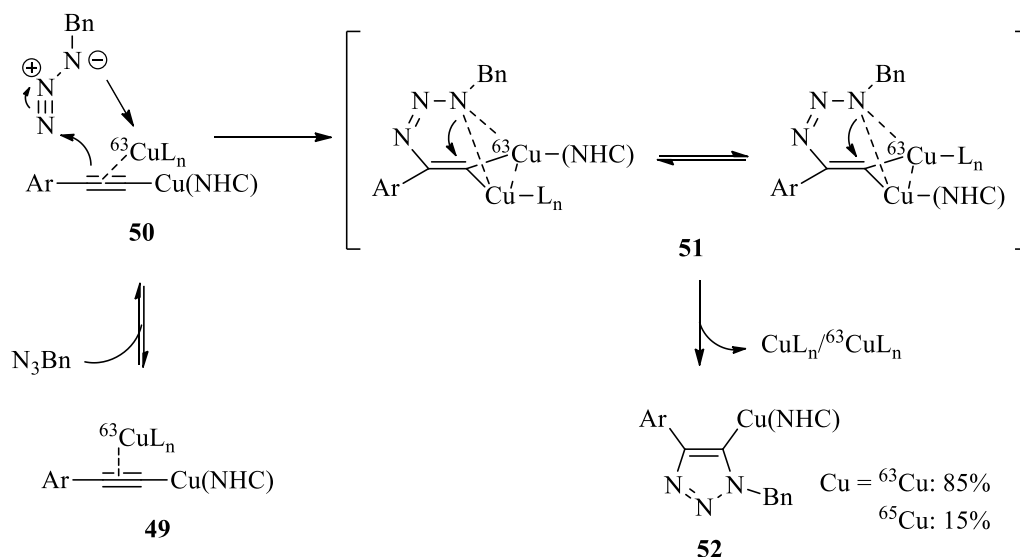
To show that the isotopic enrichment was not due to the exchange of copper independently of the reaction, two control reactions were carried out. In each reaction, **43** and **46** were heated with the isotopically pure  $^{63}\text{Cu}$  catalyst to show that no enrichment was observed, and therefore the results seen in Scheme 34 were due to the roles of the copper atoms in the mechanism (Scheme 35).



**Scheme 35:** Control reactions showing no isotopic enrichment

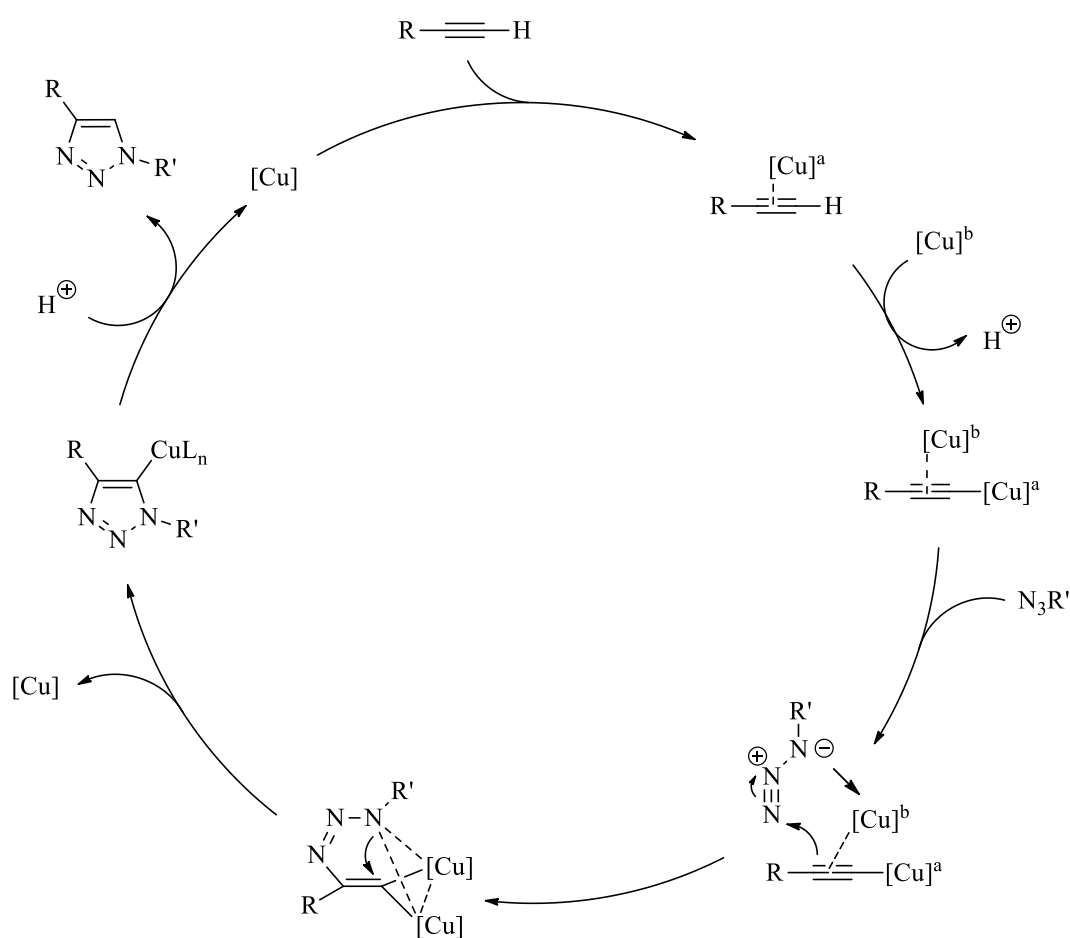
From the results of the experiments, a mechanism to account for the results was then proposed (Scheme 36). Firstly, the  $\sigma$ -bound copper acetylide bearing a  $\pi$ -bound enriched copper atom **49** coordinates with the organic azide to form complex **50**. Nucleophilic attack at the N-3 of the azide by the acetylide forms the first C-N bond, producing intermediate **51**. The ligand exchange of this intermediate is faster than the

ring closing C-N bond formation, explaining the statistical 50% isotopic enrichment of the triazolide **52**.



**Scheme 36:** Mechanistic rationale for the isotopic enrichment of triazolide **52**

These results, alongside the previous full catalytic cycle studies, support the mechanistic model featuring two chemically equivalent copper atoms working together to give the desired triazole (Scheme 37).



**Scheme 37:** Proposed catalytic model for the CuAAC with two copper atoms

### 2.5.2 Applications of the CuAAC

With the tolerance of CuAAC for many different conditions (e.g., temperature, solvent system and copper catalyst sources) it has become an extremely desirable reaction to apply to many different areas of research, particularly in the area of biochemistry.

#### 2.5.2.1 'Click' chemistry in bioconjugation

Bioconjugation is an area of science found between molecular biology and chemistry, whereby a stable covalent link is made between molecules in a biological environment. Current methods involve the introduction of labels into a biomolecular object; the incorporation of fluorophores,<sup>55</sup> isotopic labels<sup>56</sup> or ligands<sup>57</sup> into proteins and nucleic



acids. Bioconjugation is also used in the joining of two or more complicated systems, linking a biologically active carbohydrate or protein with a solid surface.<sup>58</sup>

Soon after his first publication reporting ‘click’ chemistry, Sharpless recognised that the ‘click’ reaction could be employed within biochemical environments and so began research into its use in the ligation of large protein structures.<sup>59</sup> The group chose the cowpea mosaic virus (CPMV) as the test protein because it has a structurally rigid assembly of 60 identical copies of a two-protein asymmetric unit around a single RNA genome, which was also readily available in gram quantities. The group covered the outside of the protein with the reactive azides or alkynes at the reactive lysine or cysteine sites, using 1-ethyl-3-(3-dimethylaminopropyl) carbodiimide (EDC) to activate the reaction between the surface amine group and the carboxylic acid group on the azide/alkyne fragment, giving particles **53-55** (Figure 17).

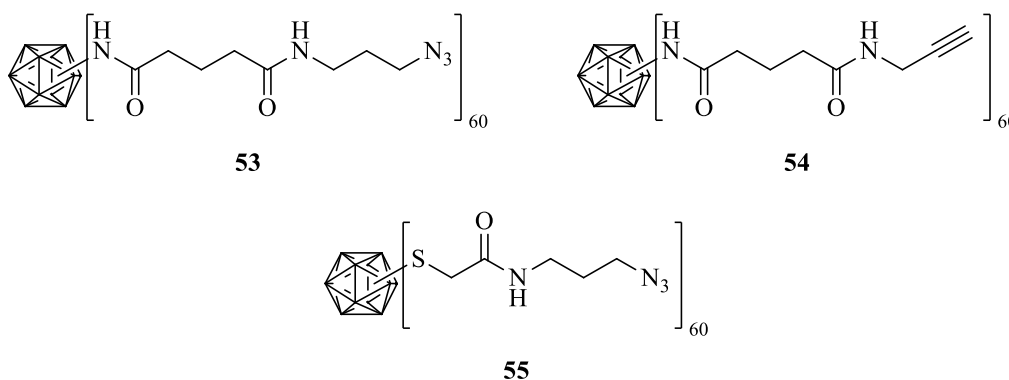


**Figure 17:** CPMV coated in azides or alkynes

To measure the efficiency of the reaction, the azide/alkyne-coated CPMV was reacted with the corresponding alkyne/azide-dye **56** & **57** (Figure 18), and the number of chromophores attached was determined by measurement of the absorbance. The results showed that they were able to successfully ligate the virus scaffold with a large number of attachments to each particle, with no damage occurring to the proteins. This led the group to correctly anticipate that this azide-alkyne ligation methodology would be applicable to a wide variety of biomolecules, scaffolds and cellular components.

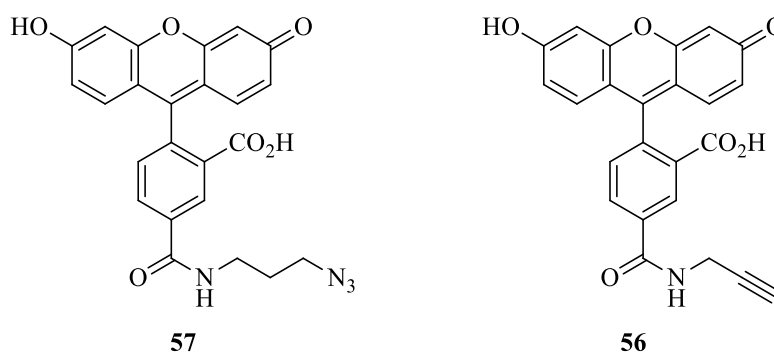


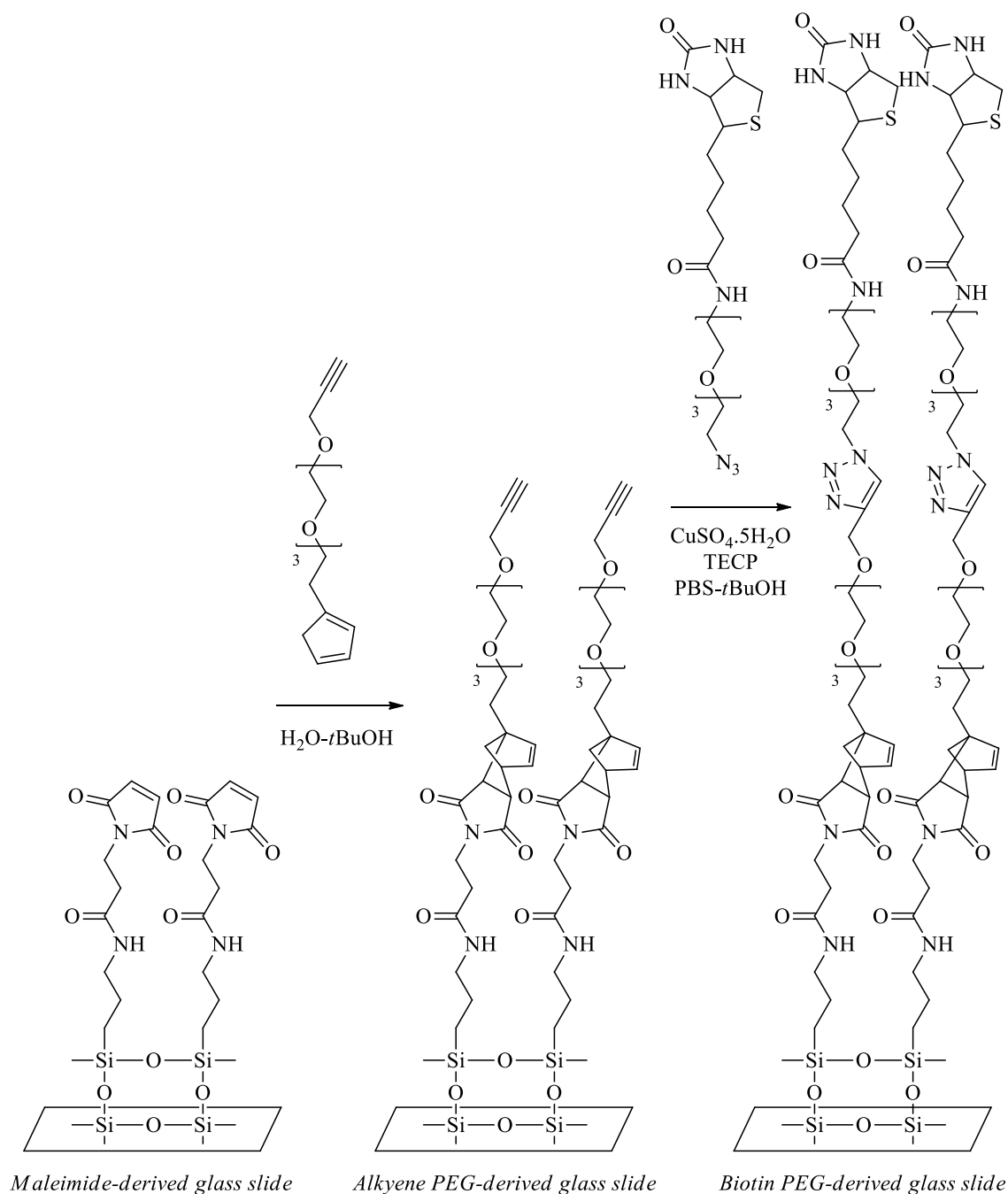
**Figure 18:** Azide/alkyne-dyes that were attached to the azide/alkyne-coated CPMV

In 2006, Gierlich used this tagging method to add small compounds such as **57** to different DNA strands, helping in the detection and sequencing of the strands.<sup>60</sup> Choosing different groups to incorporate into the DNA allow the group to either identify or isolate the strand depending on the nature of the probe.

Another interesting application of ‘click’ chemistry in biochemistry was reported by Chaikof,<sup>58</sup> in which the group demonstrated the ability to immobilize carbohydrates and proteins onto a solid surface. This was achieved through the sequential use of the Diels-Alder and CuAAC reactions, with neither reaction affecting the activity of the immobilized molecule or producing unwanted side products. The solid surface used was a maleimide-derivatized glass slide, allowing the connection of the alkyne-terminated PEG linker through the Diels-Alder reaction with the cyclopentadiene at the opposite end of the linker. The desired biotin substrate could then be immobilized using the CuAAC reaction between the alkyne-derived glass slide and the azide-derived biomolecule (Scheme 38).

As well as being able to immobilize biotin onto the glass surface using reliable ‘click’ reactions, the group also immobilized azide-containing sugars and recombinant proteins with C-terminal azide groups (Figure 19).

Immobilization of sugars is important as all cells bear many sugar containing entities formed by glycoproteins, proteoglycans and glycolipids, which is involved in specific events between cells and proteins, hormones, antibodies and toxins. Using immobilized carbohydrates allows the study of the mechanisms of these processes, which may lead to the development of new antimicrobial, anticancer and anti-inflammatory therapies.



**Scheme 38:** Biotinylated surface produced by sequential Diels-Alder and azide-alkyne cycloadditions

The use of ‘click’ reactions to immobilize proteins has proven to be invaluable as it is imperative that the protein has the correct orientation to achieve optimal interaction to form the functional complex. Previous reported surface conjugation methods offer only

a limited ability to control the three-dimensional orientation of the bound proteins, but the stereoselectivity of the ‘click’ reactions used makes them ideal for overcoming this problem.

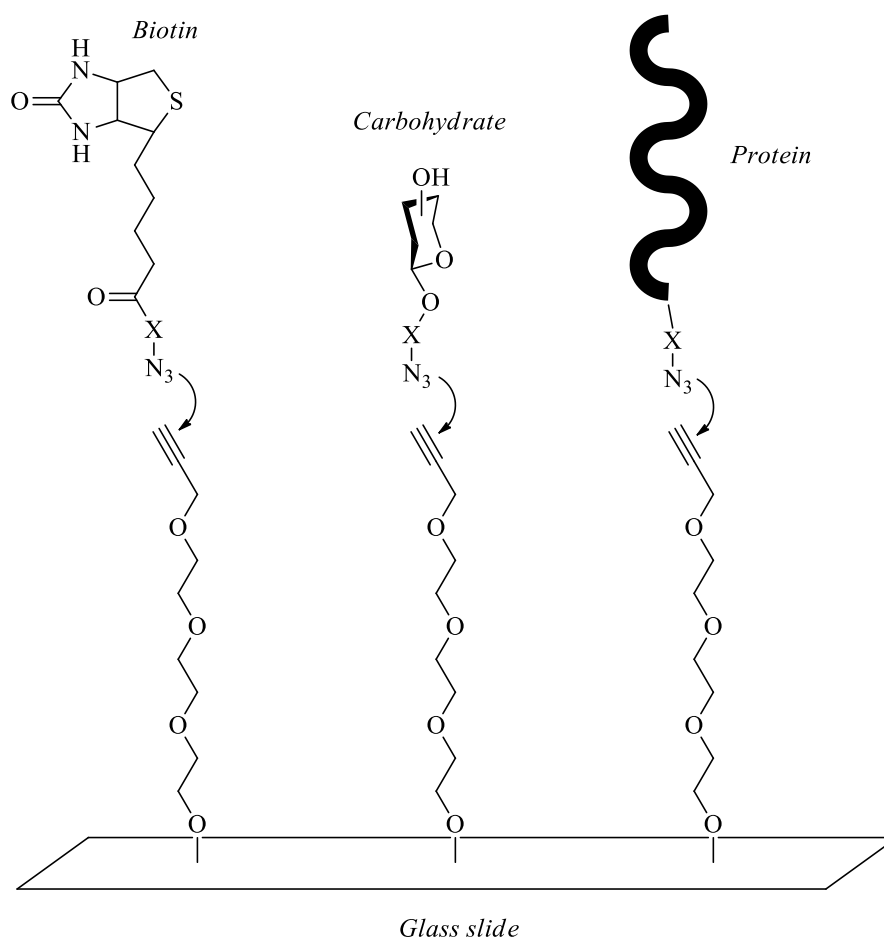
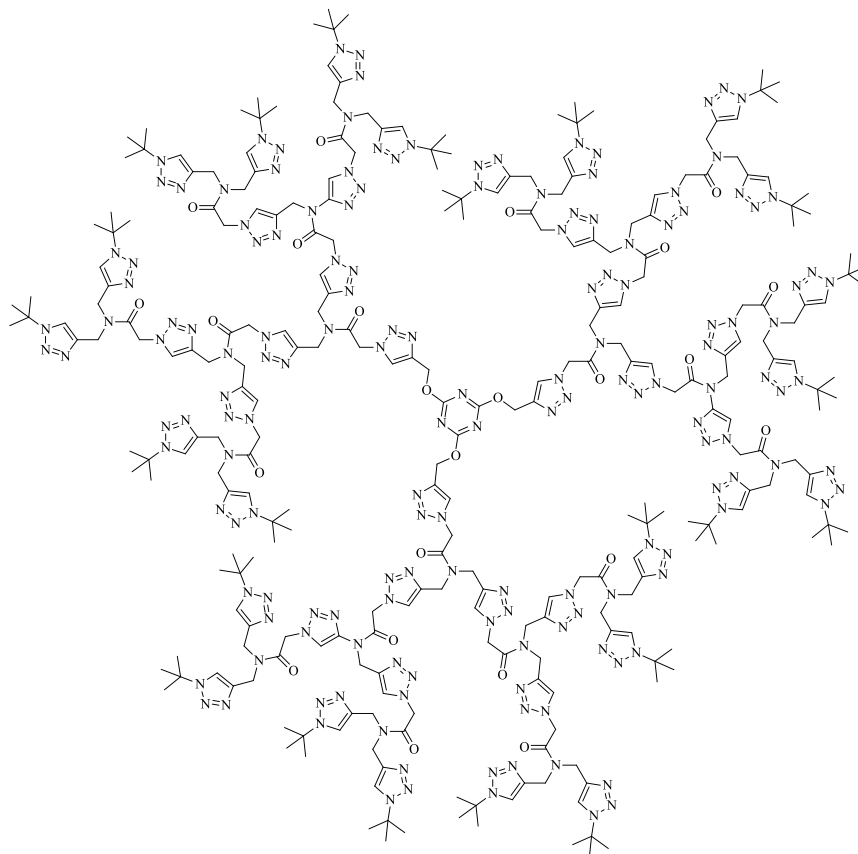


**Figure 19:** Schematic illustration of test substrates immobilized onto the glass slide

### 2.5.2.2 ‘Click’ chemistry in materials science

Dendrimers, such as **58** (Figure 20), are large repetitively branched molecules, which, due to their unique properties, make them ideal for applications in medicinal and materials science. Dendrimers are often symmetrical around the core, with each branched unit being called a dendron. Dendrimers have been synthesized for over 25 years, but there are still difficulties in the purification and separation of these compounds from closely related impurities. The fundamental ideas of ‘click’ chemistry,

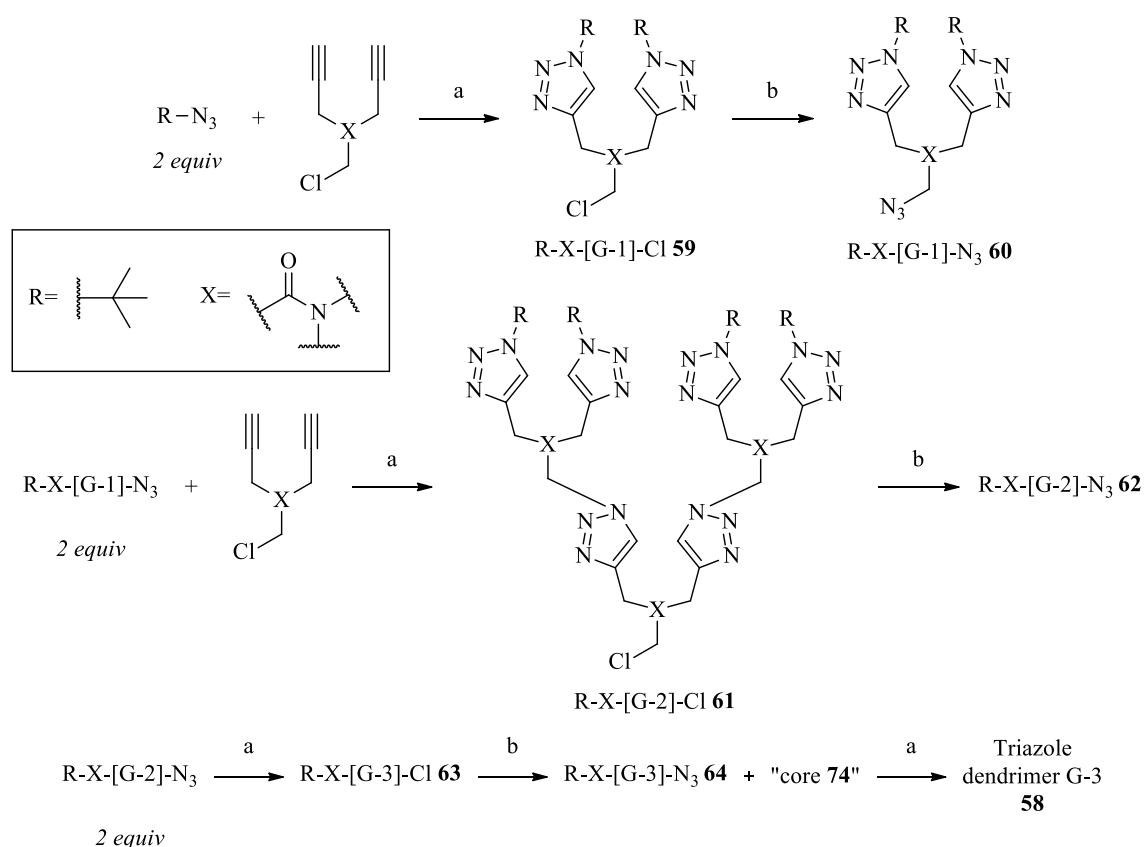
high efficiency and ease of work-up, make it an ideal system to use in the synthesis of these large complicated polymers.



58

**Figure 20:** Dendrimer synthesized using click chemistry

The first example of dendrimers synthesized using the click chemistry methodology was reported by Fokin in 2004.<sup>61</sup> The group were able to efficiently produce a catalogue of diverse dendritic structures in high purity and excellent yield. A key aspect of this route was the near perfect reliability of the CuAAC reaction, requiring only stoichiometric amounts of starting material and generating virtually no by-products. Fokin used a convergent approach in the synthesis, first building the individual dendrons, starting with the outer parts of the molecule. The branches were then coupled to the multivalent centre core piece, leading to a variety of dendrimers with different chain-end groups (R) and internal repeating units (X) (Scheme 39). The first branched level formed is known as a first generation dendron, with the following additions giving the second and third generation dendrons.



**Scheme 39:** Convergent approach toward triazole dendrimers (a)  $\text{CuSO}_4$ , sodium ascorbate,  $\text{H}_2\text{O}/t\text{BuOH}$  (1:1); b)  $\text{NaN}_3$ ,  $\text{CH}_3\text{COCH}_3/\text{H}_2\text{O}$  (4:1),  $60^\circ\text{C}$ , 1-3 h)

Based on this approach, Fokin was able to produce many dendrimers through the combination of different chain-end-functionalized azides **65-70** and polyacetylene cores **71-74** (Figure 21). This method was further adapted in the synthesis of bivalent dendrimers, large unsymmetrical molecules containing dual purpose recognition and detection agents.<sup>62</sup> To prepare the bivalent dendrimers, two sets of dendrons are synthesized independently and then joined together using ‘click’ chemistry. In the reported example, the bivalent dendrimer **75** contains one hydrophobic and one hydrophilic dendron (Figure 22).

For the inhibition of haem-agglutination, mannose and coumarin derivatives were used as this allowed for the simultaneous interaction with the biological receptor and the detection of this interaction, respectively.

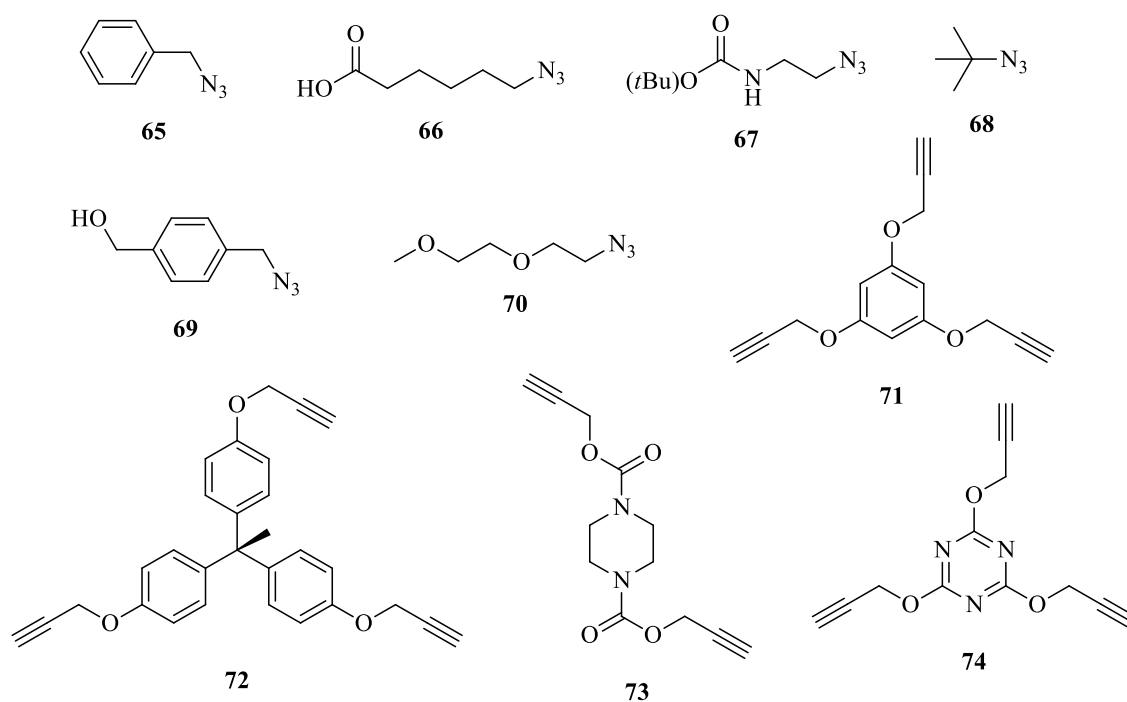


**Figure 21:** Selection of azides and polyacetylene cores used in the synthesis of chain-end-functionalized dendrimers

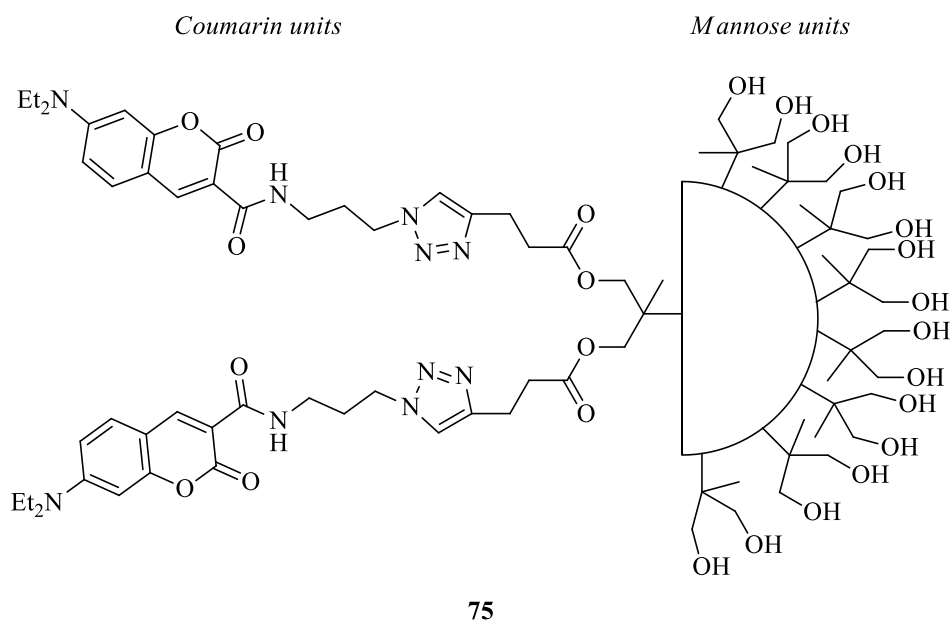
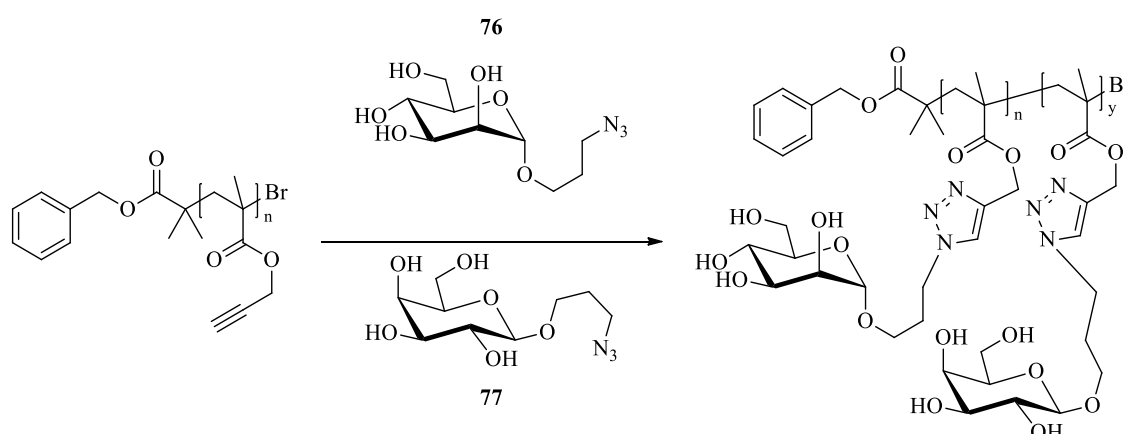


**Figure 22:** Asymmetrical dendrimer containing 16 mannose units and 2 coumarin chromophores

As well as ‘click’ chemistry being ideal for polymer synthesis applications due to its high efficiency and ease of purification/separation, it has also helped in overcoming an

issue in polymer science regarding incomplete reactions due to steric inaccessibility. Haddleton achieved the synthesis of sugar derived polymers, neoglycopolymers, in a close to 100% yield using the CuAAC reaction.<sup>63</sup> These compounds received attention due to their possible medicinal applications and interactions with protein receptors. A method was used by which the authors were able to react a mixture of azide-bearing sugar moieties,  $\alpha$ -mannoside **76** and  $\beta$ -galactoside **77**, with an alkyne-derived homopolymer chain using a CuAAC reaction (Scheme 40).



**Scheme 40:** Synthesis of neoglycopolymers using alkyne-derived polymer and azido-derived sugars

Supramolecular chemistry refers to an area of chemistry which focuses on the forces responsible for the spatial organization of compounds, examining the weaker and reversible non-covalent interactions between molecules. Calixarenes are some of the most useful compounds in the supramolecular field, especially water-soluble calixarenes such as **78**. Water-soluble calixarenes are extremely attractive because of their well-defined hydrophobic cavities, which make it possible to study molecular recognition in water. The introduction of such hydrophilic groups can be difficult due to functional group compatibility issues. Ryu and Zhao used ‘click’ chemistry to introduce these hydrophilic groups in high yields.<sup>64</sup> The group tested two systems in parallel, one in which alkynyl-derived calixarenes were reacted with water-soluble azides, and the other where azidocalixarenes were reacted with water-soluble alkynes. The results showed that azidocalixarenes performed better than alkynylcalixarenes as precursors; this was due to possible side reactions between the alkynes.



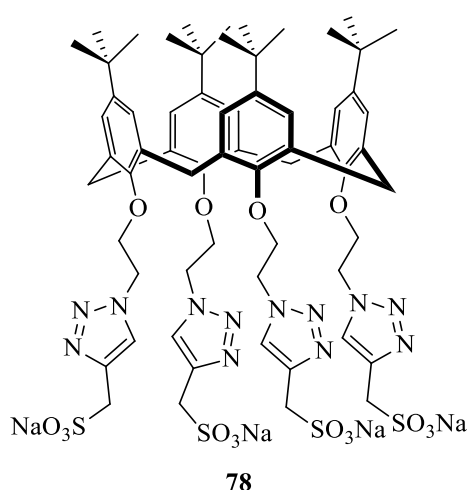


**Figure 23:** Example of a water-soluble calixarene

### 2.5.2.3 ‘Click’ chemistry in drug discovery and natural product synthesis

In the last decade there have been various target-guided synthesis (TGS) approaches developed for the synthesis of protein inhibitors from a large pool of smaller reactive fragments, using the target protein as a template. There are three major classes of TGS; (a) dynamic combinatorial chemistry (DCC), (b) catalyst-accelerated TGS, and (c) kinetic TGS. In dynamic TGS, a large pool of reactive fragments is mixed and the complementary reacting fragments are connected through a reversible covalent bond-forming reaction. Once all of the possible combinations have formed, the target is introduced into the mix. The combination that has the most effective ligation then inhibits the target, removing it from the reaction pool, and the equilibrium shifts towards the product showing the highest affinity. As the name suggests, catalysed-accelerated TGS requires a catalyst to promote the covalent bond formation between two fragments that are bound to the target protein.

In kinetic TGS, the fragments are joined by a covalent bond in an irreversible way. The target protein is introduced to the fragment pool from the start, each fragment binds to the individual sites and those with the highest affinity will form a covalent bond due to the close proximity of their reactive functionalities. Ideally, these reacting functionalities would combine slowly to form the covalent bond, with no or minor side products. The reaction should also work in aqueous media without affecting the

biological target. During the development of ‘click’ chemistry, Sharpless identified that the 1,3-dipolar cycloaddition between alkynes and azides has the ideal reaction profile for kinetic TGS.<sup>49</sup> Since then, *in-situ* ‘click’ chemistry has been successfully applied in numerous examples of kinetic TGS, for example in the discovery of an inhibitor of acetylcholine esterase (AChE).<sup>65</sup> Although these reactions proceed in the absence of copper, and therefore cannot be classed as CuAAC reactions, it is the target enzyme itself that acts as the catalyst, promoting a ‘pseudo-CuAAC’ reaction.

For the synthesis of the AChE bivalent inhibitor, a selection of site-specific inhibitors based on tacrine and phenanthridinium motifs were functionalized with alkyl azides and alkyl acetylenes of varying chain lengths (Figure 24). This small group of fragment molecules gave 98 potential bivalent inhibitors for AChE.

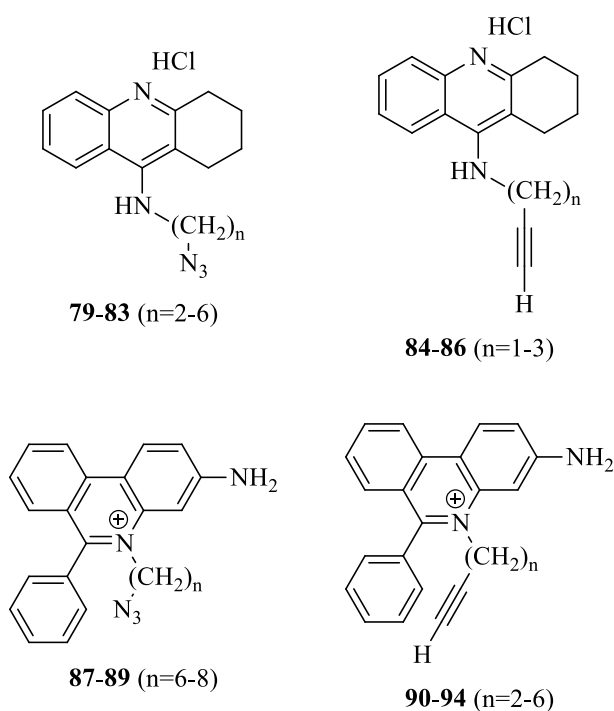


**Figure 24:** Azide and acetylene building blocks

The fragments were incubated at room temperature in the presence of *Electrophorus electricus* (electric eel) AChE. The rate of the reaction without the enzyme present was found to be negligible; hence it can be assumed that any formation of a triazole is due to the enzyme holding the fragments in close enough proximity to react. It can therefore be assumed that any product formation is an indication of successful binding. The

experiment showed that only one combination, **79** & **94**, showed a detectable amount of triazole present. Next, the group established which regioisomer had been formed using HPLC comparison, revealing triazole **95** as the produced inhibitor.

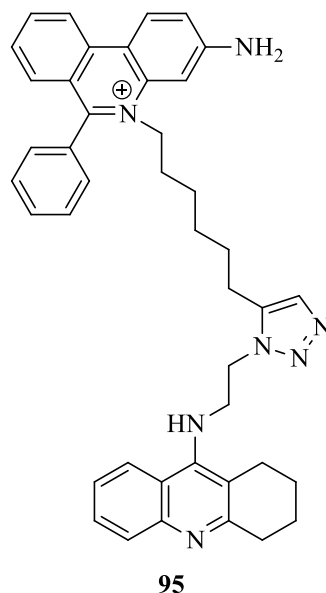


**Figure 25:** Inhibitor found directly by the azide-alkyne cycloaddition in the presence of AChE

This method of using *in-situ* ‘click’ chemistry has been applied to the synthesis of other inhibitors of important enzyme targets such as carbonic anhydrase (CA),<sup>66</sup> associated with the symptoms of glaucoma, and HIV-1 protease (HIV-1-Pr),<sup>67</sup> recognised as being involved in the replication of the HIV virus.

Thus far, the methods discussed for the synthesis of biological inhibitors have used the enzyme to catalyse the reaction; however, methods that utilize the CuAAC reaction *in-situ* have also been reported. In this screening process, a single functionalized moiety that shows affinity to the target is reacted with a large group of diverse possible binding fragments with the corresponding functionalization. Because the CuAAC reaction does not lead to the formation of side products, the synthesized triazole compounds can be screened directly with the target molecules, with no need for separation or purification. Although this method of screening produces a large number of compound ‘misses’ that are seemingly useless, the ability to quickly and easily produce these using CuAAC in such great numbers outweighs the low success rate.

One such example of this method was reported by Wong, in which he used this method to synthesize the inhibitor for fucosyltransferases (Fuc-T), an important catalyst in the biosynthesis and expression of many important saccharides.<sup>68</sup> The final step of this pathway involves the transfer of L-fucose from guanosine diphosphate  $\beta$ -L-fucose (GDP-fucose). It was found that the majority of the binding energy of Fuc-T lies at the GDP moiety and the hydrophobic pocket adjacent to the binding site. This led Wong to design a library of compounds that retained the important GDP core, while the attached hydrophobic group and linker length were varied. 85 Azide compounds were synthesized and reacted with the GDP-alkyne core to give 85 triazole candidates, from which three emerged as 'hits'. Further  $IC_{50}$  measurements of these three compounds showed that compound **96** had the highest affinity for Fuc-T.

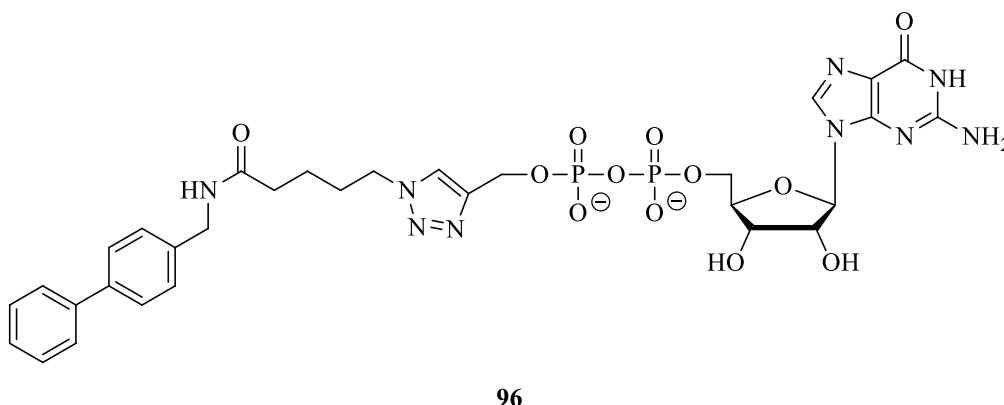


**Figure 26:** Inhibitor of Fuc-T synthesized using CuAAC

'Click' chemistry has also been used to synthesize analogues of natural products that show biological activity. It has been reported that triazoles can be used to replace several different functional groups within the structure of large natural compounds. Sewald reported that an endocyclic *trans*-amide linkage could be replaced by a 1,4-disubstituted 1,2,3-triazole ring.<sup>69</sup> They showed that although the size and dipole moment of the triazole ring are larger compared to a *trans*-amide, the physiochemical properties are similar enough that the triazoles act as *trans*-amide mimetics. This method was applied to the synthesis of cryptophycin-52 **97**, a macrocyclic antitumor agent, with its *trans*-amide linker replaced to give the analogue "clicktrophycin-52" **98** (Figure 27). Drug candidate **97** displayed high cytotoxicity against multidrug resistant cancer cells and solid tumours; however, it failed in phase II clinical trials because of

neurotoxicity. The group hoped that by replacing the amide linker with the triazole ring the high cytotoxicity would be maintained but the neurotoxicity issues would be overcome. In cytotoxicity assays against the multidrug resistant human cervix carcinoma cell line KB-V1, triazole analogue **98** showed results that were only slightly reduced compared to those of **97**.

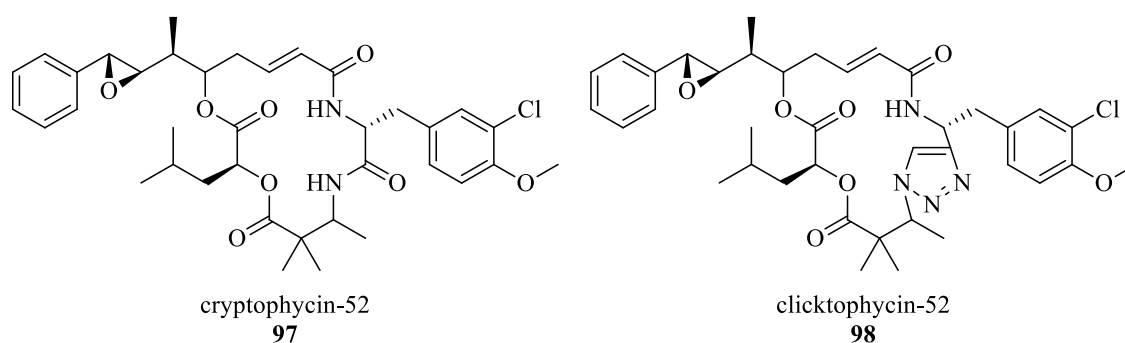


**Figure 27:** Antitumour agent cryptophycin-52 and triazole analogue "clicktrophycin-52"

Liskamp also reported a similar method by which the group replaced the biaryl ether bridge in vancomycin **99** with the triazole ring system.<sup>70</sup> The reduction of conformational flexibility is important to maximize the affinity of a peptide for its receptor. There are many covalent constraints used to reduce this flexibility, with some reducing flexibility further with the creation of cavity or shell-like structures.

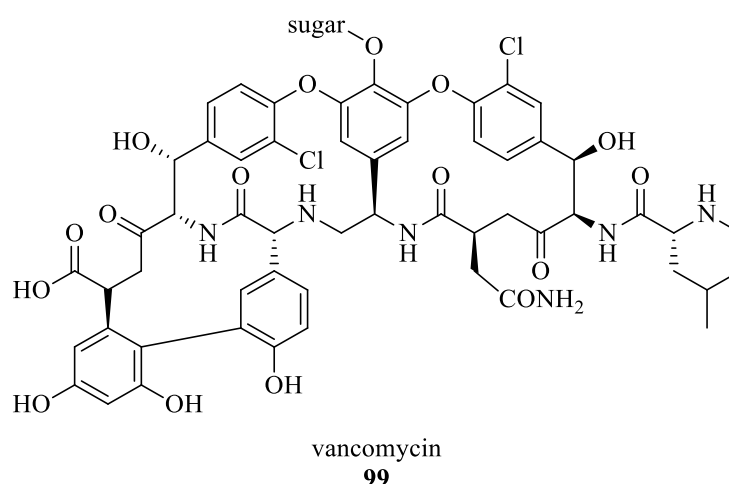
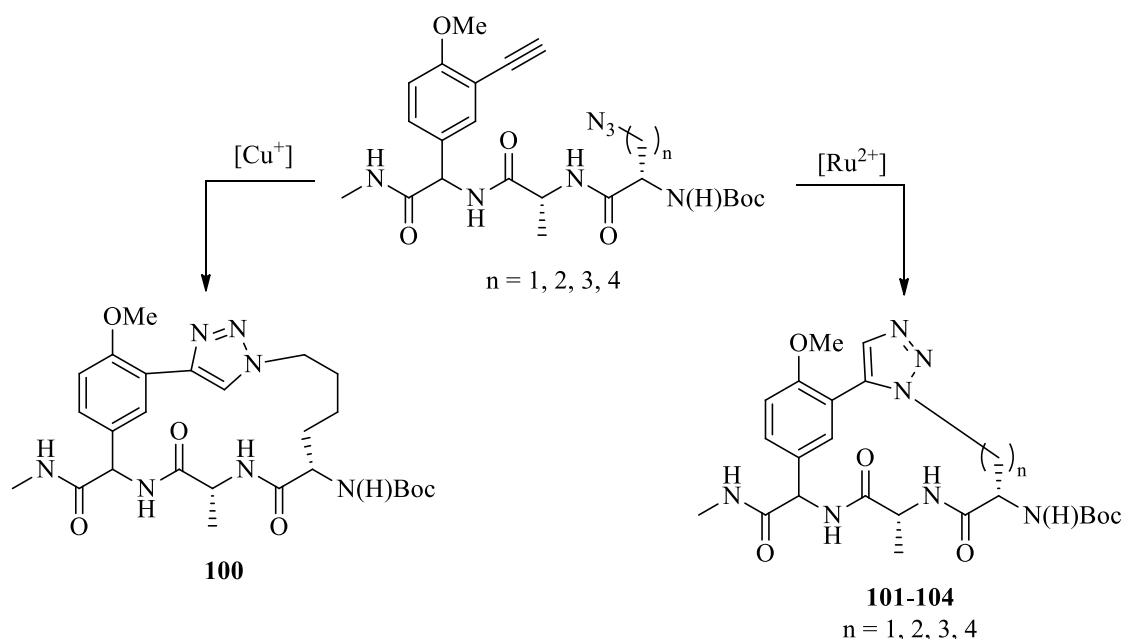


**Figure 28:** Structure of antibiotic vancomycin

The triazole ring can be introduced very conveniently by the CuAAC reaction either at the beginning of the synthesis or towards the end. These results showed that there is scope for the preparation of small cyclic peptides containing 1,4-disubstituted triazole ring systems. This method was expanded to the introduction of 1,5-disubstituted triazoles using the ruthenium-catalysed azide-alkyne cycloaddition (RuAAC), in which the substituents are positioned at a smaller angle relative to the 1,4-stereoisomer (Scheme 41).

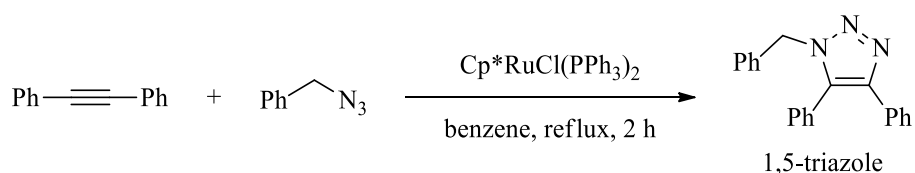


**Scheme 41:** Structural mimics of vancomycin comprising 1,4- and 1,5-disubstituted triazole-containing cyclic tripeptides

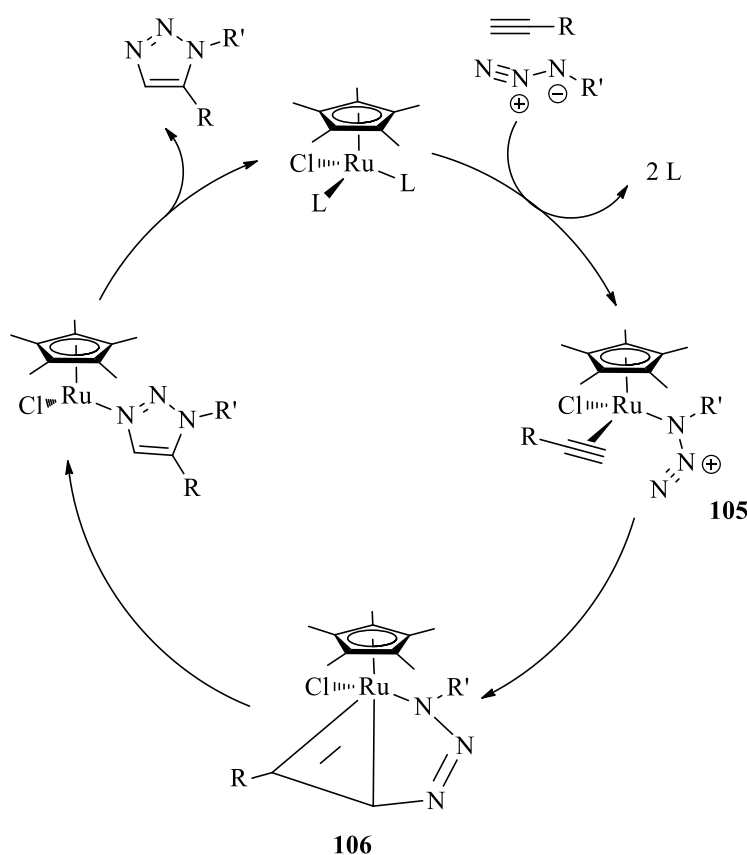
## 2.6 Ruthenium-catalysed Huisgen 1,3-cycloaddition

To this point, this section is focused on the copper-catalysed variant of the Huisgen 1,3-cycloaddition to give 1,4-disubstituted triazoles; however, it is also important to also indicate how to selectively synthesize 1,5-disubstituted triazoles. By using a ruthenium catalyst (RuAAC), the 1,5-triazole is selectively prepared (Scheme 42).<sup>71</sup> Unlike the CuAAC reaction, in the RuAAC both terminal and internal alkynes can participate in the reaction, suggesting there is a different metal-alkyne interaction in the catalytic cycle. Unlike in the CuAAC reaction where the alkyne interacts in an end-on linear fashion (Scheme 37), in the RuAAC, the metal coordinates perpendicularly to the

alkyne to give the activated complex **105** (Scheme 43). Next, the azide and alkyne are added using oxidative coupling to give the ruthenacycle **106**. It is this step that controls the regioselectivity of the reaction, with the new carbon-nitrogen bond forming between the more electronegative and less sterically-demanding carbon of the alkyne to the terminal nitrogen of the azide. Finally, the intermediate undergoes reductive elimination to release the triazole and regenerate the original catalyst.<sup>72</sup> This is different to that in the CuAAC process as the ruthenium catalyst does not coordinate to the alkyne in a linear fashion, instead coordinating across the triple bond. This allows the nitrogen containing the R'-group to form a new bond with the carbon of the alkyne with the R-group, giving the 1,5 regioisomer.



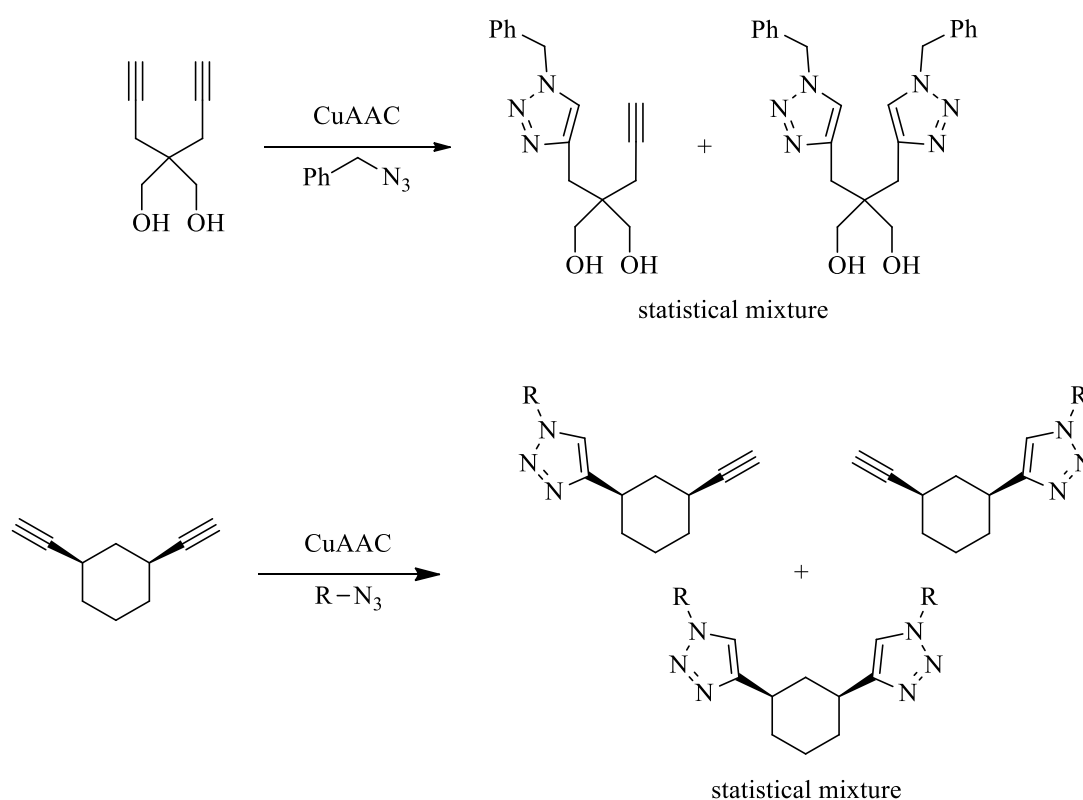
**Scheme 42:** Ru-catalysed synthesis of triazoles from internal alkynes



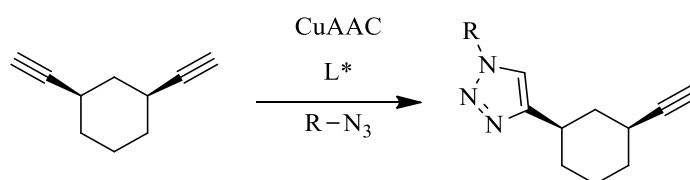
**Scheme 43:** Proposed catalytic cycle of the RuAAC reaction

### 3.0 Aim of the project

The aim of this project is to create a system where it is possible to selectively perform the CuAAC reaction on a single alkyne moiety of a *meso bis*-alkyne system. Under normal CuAAC conditions, reacting one equivalent of an azide with a *bis*-alkyne would yield a statistical mixture of the two mono-reacted products and the *bis*-triazole product (Scheme 44).<sup>73</sup> The proposal is that the introduction of a chiral ligand into the catalyst will allow the selective reaction of one alkyne over the other (Scheme 45).



**Scheme 44:** Bis-alkyne reactivity under CuAAC conditions



**Scheme 45:** Proposed reaction to give a selective version of the CuAAC



To show that the system would work and to explore the potential scope of the reaction, a series of *meso* bis-alkynes with different functional groups was synthesized (Figure 29).

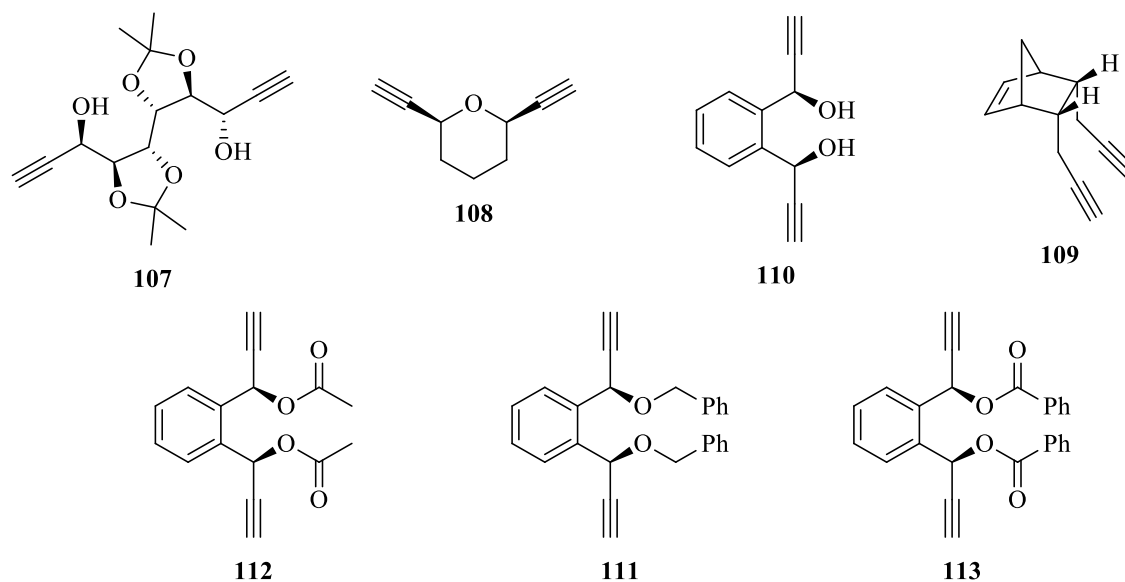
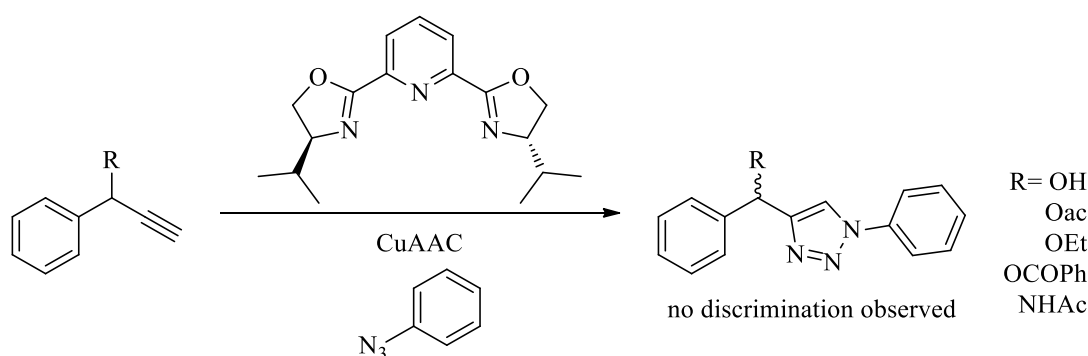


**Figure 29:** *Meso* bis-alkynes that will be synthesized for testing

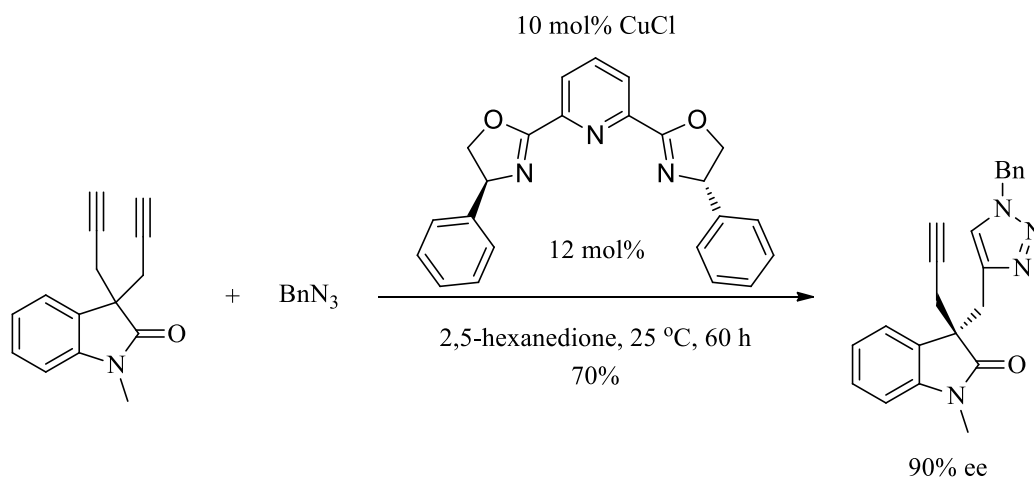
### 3.1 Current work

In 2005, Finn attempted to use the CuAAC reaction for kinetic resolution.<sup>74</sup> Different racemic 1-phenylpropargylic compounds were reacted with azides under CuAAC conditions in the presence of several chiral ligands. However, absolutely no enantiomeric discrimination was observed (Scheme 46).



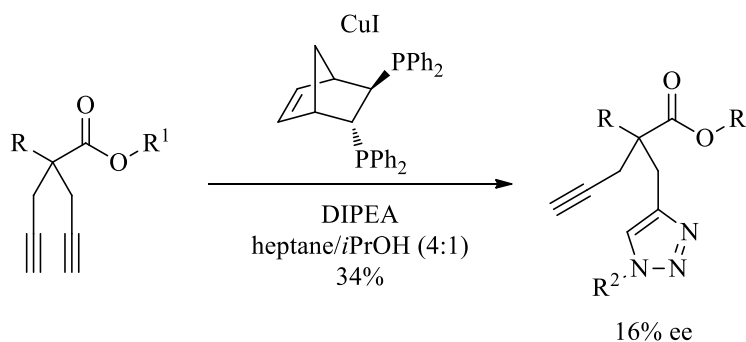
**Scheme 46:** Attempted kinetic resolution using CuAAC

More recently Zhou was able to achieve high yield and high enantioselectivity in the desymmetrization of oxindole-based 1,6-heptadiynes (Scheme 47).<sup>75</sup> Although this is not a *meso* system, like the one we wish to investigate, the ability of the group to desymmetrize the bis-alkyne with such high selectivity was extremely encouraging.



**Scheme 47:** Desymmetrization of *bis*-alkynes by CuAAC

Work within our own group also resulted in the desymmetrization of another bis-alkyne with a certain degree of enantioselectivity (Scheme 48).<sup>76</sup> We hoped that we could build on these results and those of Zhou, going forward and applying them to our synthesized *meso bis*-alkyne systems.



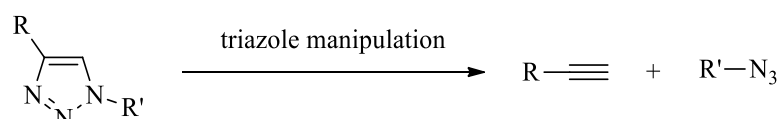
**Scheme 48:** Asymmetric 'click' reaction with a *bis*-alkyne

Once the *meso bis*-alkynes had been synthesized they would be tested using various chiral ligands under different CuAAC reaction conditions to try to create asymmetric 'click' reaction conditions.

## **Chapter 2: Results & Discussion**

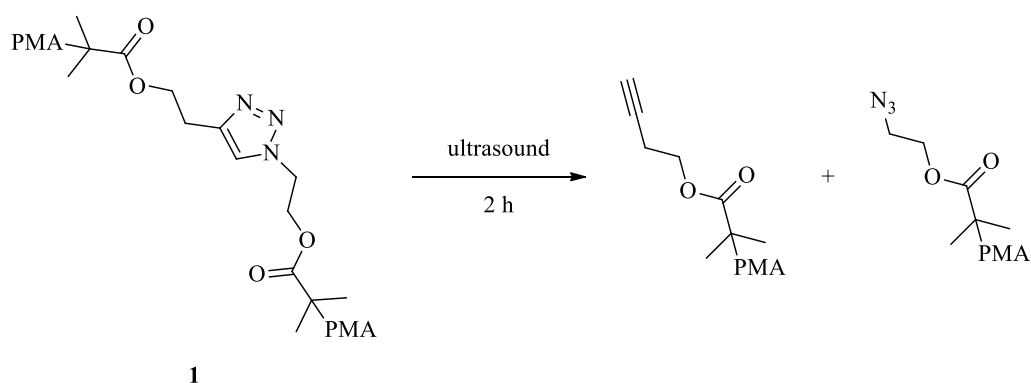
## 1.0 Manipulation of triazoles

At the beginning of the project, the group was interested in manipulating the triazole ring to allow it to break down into its original components: an alkyne and an azide (Scheme 1). The discovery of a reversible ‘click’ reaction would open up a wide variety of applications in the fields of biological chemistry and synthesis. One possible application would allow a biological tag to be easily added to a compound for testing using the CuAAC reaction, and, once the testing is complete, the tag would be removed, leaving the original target unaffected. Another possible application would be the use of triazoles as a delivery agent, transporting compounds to specific regions, allowing a process to occur, and finally ‘unclicking’ and departing.



**Scheme 1:** Separation of a triazole into its original components

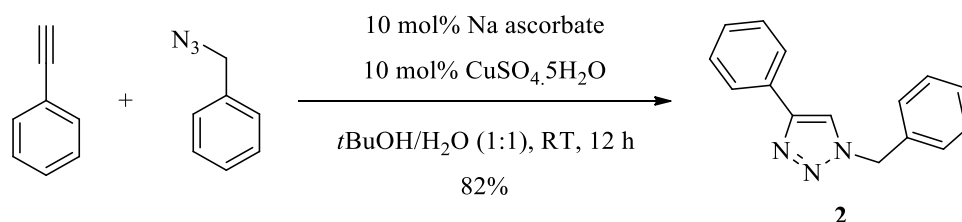
To date the only method that had successfully ‘unclicked’ a triazole moiety required extremely specific conditions that would not be practical for normal synthetic research applications.<sup>77</sup> The group hypothesized that triazoles, although inert toward chemical and thermal perturbation, could undergo cycloreversion through the application of a site-specific mechanical force. The desired pericyclic reaction is achieved through the application of ultrasound to polymer chains, which then direct the forces to the connected mechanophores or small molecules.<sup>78</sup> Using this as a foundation, the group first synthesized a triazole-centred poly(methyl acrylate) **1**, where the average molecular weight of the polymer was 96 kD, and split it into its respective alkyne and azide with the application of ultrasound for 2 h (Scheme 2). Although this method was successful in breaking down the triazole, its lack of versatility and limited application meant that a new, more practical, method was desirable.



**Scheme 2:** Application of ultrasound to a triazole embedded within a poly(methyl acrylate) chain

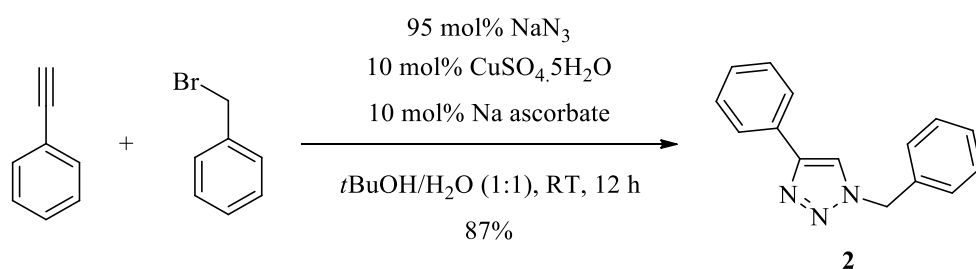
### 1.1 Synthesis of 1-benzyl-4-phenyl-1,2,3-triazole

Before the triazole cleavage could be attempted, a triazole had to be synthesized. 1-Benzyl-4-phenyl 1,2,3-triazole **2** was chosen as its successful synthesis has been reported multiple times using readily available starting materials. The original method reported by Fokin & Sharpless was repeated, giving triazole **2** in an 82% yield (Scheme 3).<sup>50</sup>



**Scheme 3:** Synthesis of triazole **2**

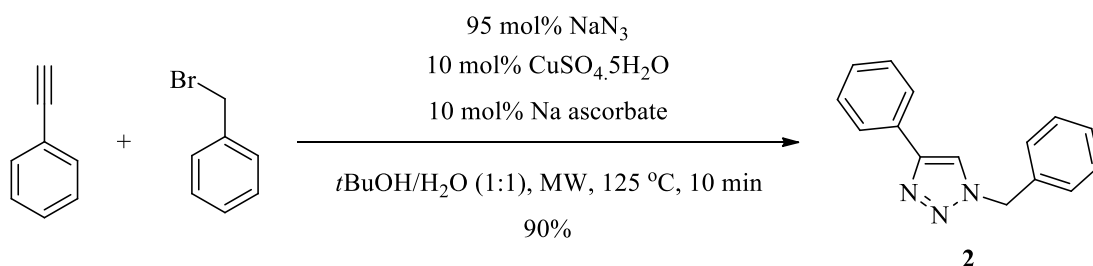
Although this method involved a simple work-up and was high yielding, the relatively high cost of the benzyl azide reagent, as well as the explosive properties associated with small azide compounds, led us to search for a cheaper and safer method. We found that benzyl azide can be formed *in-situ* from cheap reagents,<sup>79</sup> decreasing the cost and improving the safety, as the azide is never isolated and reacts with the alkyne reagent as soon as it is formed. We adapted Kacprzak's method,<sup>79</sup> using the same solvent system (*t*butanol/H<sub>2</sub>O) as in the previous procedure, without affecting the results and producing triazole **2** in 87% yield (Scheme 4).



**Scheme 4:** Synthesis of triazole **2** using a one-pot procedure

This method also has an easy work-up procedure and gives a higher yield; further, the lower cost of starting materials and increased safety aspect allows for the experiment to be repeated on a much larger scale, producing large quantities of **2**.

While researching into the possibility of a one-pot click reaction, we also found that Fokin & Eycken had reported a microwave-assisted synthesis where the organic azide was generated *in-situ*.<sup>80</sup> This method dramatically reduced the reaction time, from 12 h down to 10 min. We applied this method in the synthesis of triazole **2**, which was successfully produced in 90% yield (Scheme 5).

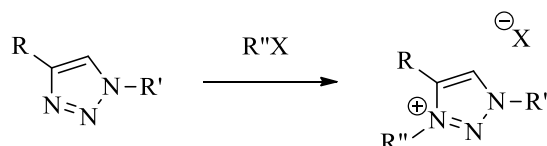


**Scheme 5:** Synthesis of triazole **2** using a microwave-assisted one-pot procedure

Although this method gave the highest yield, and produced a product of the highest purity, it was limited by its scalability. Indeed, when the reaction was carried out on a scale larger than 1 mmol, the yield and purity were lower. For this reason the one-pot and not the microwave-assisted procedure was employed for the production of **2** on a large enough scale for the next step, the cleavage part, of the research.

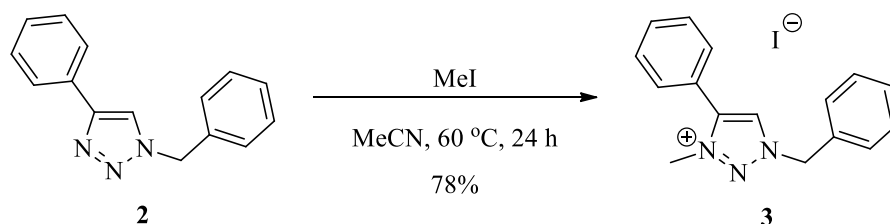
## 1.2 Attempts to ‘unclick’ a triazole

The group believed that to be able to break the triazole into the original azide and alkyne, it would be necessary to make the ring more reactive. We attempted to convert the triazole into the corresponding triazolium salt using various alkyl halides, to see if this would have any effect on the ring stability (Scheme 6).



**Scheme 6:** Conversion of a triazole into the corresponding triazolium salt

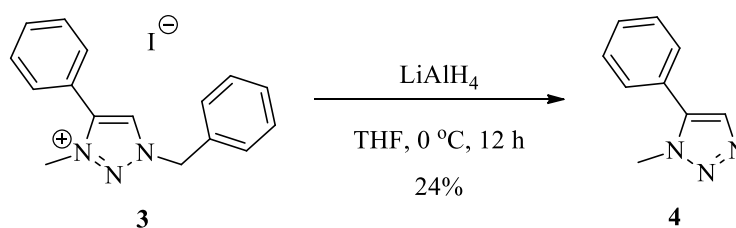
Firstly, the procedure described by Liebscher was used to synthesise a triazolium salt target.<sup>81</sup> The triazole **2** was heated under reflux in the presence of iodomethane for 24 h, yielding the triazolium salt **3** in 78% yield (Scheme 7).



**Scheme 7:** Conversion of a triazole to its triazolium salt using the original procedure

With 1-benzyl-3-methyl-4-phenyl triazolium iodide **3** in hand, we turned our attention to the reactivity of the substituted triazolium cation, in the hope that reduction of the cationic aromatic five-membered ring could be achieved, thus affording products that would be susceptible to hydrolysis. We chose to begin with a hydride reduction, and as we expected the reactivity of the aromatic cationic  $\pi$ -system to be low, the highly reactive lithium aluminium hydride was chosen as the reducing agent.

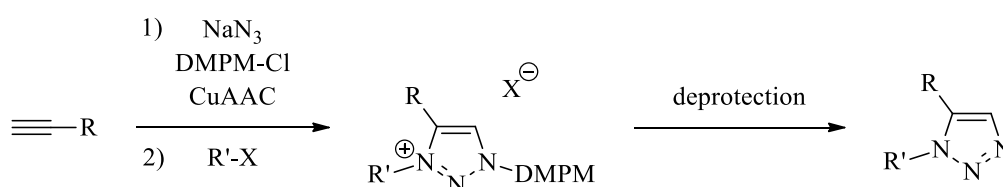
The cationic triazolium salt was reduced in THF at 0 °C to give a neutral product, however, to our surprise the product was proven to be the debenzylated 1,5-substituted 1,2,3-triazole **4** (Scheme 8).



**Scheme 8:** Reduction of triazolium salt **3** using  $\text{LiAlH}_4$

The structure of the product was determined using analysis of the  $^1\text{H-NMR}$  data, which showed signals corresponding to both the methyl and phenyl groups, and none corresponding to the benzyl group. The suggested structure of the product was confirmed to be **4** as the characterisation data was consistent with literature values.<sup>82</sup>

The unexpected formation of the 1,5 regioisomer is important as it represents a new pathway in the synthesis of 1,5-disubstituted triazoles without the need of expensive organo-ruthenium catalysts. A similar approach was reported by Koguchi, in which they use 1-(3,4-dimethoxybenzyl)-4-substituted 1,2,3-triazole substrates, install a selection of alkyl groups at N(3), and finally have the 3,4-dimethoxybenzyl (DMPM) protecting group removed using either ammonium nitrate or ceric ammonium nitrate (CAN) (Scheme 9).



**Scheme 9:** The synthesis of 1,5-disubstituted 1,2,3-triazoles as proposed by Koguchi

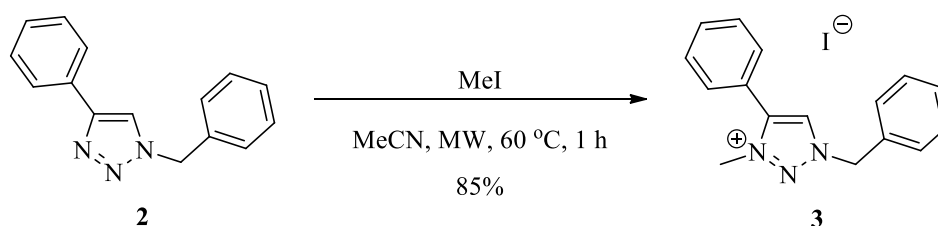
We believed that if developed into an efficient procedure, our debenzylation of **3** could provide a more general pathway to form 1,5-disubstituted triazoles using the cheaper copper catalyst, with an easier method of deprotection of the triazolium salt.



### 1.3 Developing the 1,3- to 1,5-triazole interconversion pathway

#### 1.3.1 *N*-alkylation step

To prove that our method could be applied more generally, the introduction of various groups at the N(3) position of the triazole was attempted. This could mean, however, that as we tried to introduce larger groups onto the triazole, yields would drop and reaction times would need to be increased. As seen above, using microwave-assisted synthesis improved yields and reduced reaction times in the synthesis of triazoles. We attempted to adapt the methodology to the *N*-alkylation step. The synthesis of **3** was attempted using microwave-assisted synthesis at the same temperature as the original procedure, to see if this had any effect on yield, with the results being extremely encouraging (Scheme 10).



**Scheme 10:** Microwave-assisted conversion of a triazole to its triazolium salt

The increased yield showed that the microwave-assisted synthesis was a more efficient method for this reaction. Hence, further optimisation of the reaction yield was attempted by altering the reaction time, equivalents of iodomethane and the reaction temperature (Table 1).

**Table 1:** Optimization of the *N*-alkylation reaction step

Entry	Time (Min)	Equiv. MeI	Temp (°C)	Yield (%) <sup>a</sup>
<b>1A</b>	120	2	100	50
<b>1B</b>	120	2	120	58
<b>1C</b>	120	2	140	54
<b>1D</b>	180	2	100	78
<b>1E</b>	180	2	120	91
<b>1F</b>	180	2	140	81

Entry	Time (Min)	Equiv. MeI	Temp (°C)	Yield (%) <sup>a</sup>
1G	210	2	100	69
1H	210	2	120	73
1I	210	2	140	68
1J	240	2	100	83
1K	240	2	120	71
1L	240	2	140	65
1M	180	1	120	63
1N	180	4	120	95
1O	180	5	120	97

<sup>a</sup>) yield determined from the mass of product collected after purification.

If this data is represented in a 3D graph, with the yield being shown as a function of reaction time and temperature (Figure 1), we can see that there are 2 areas of high yield (**A** & **B**).

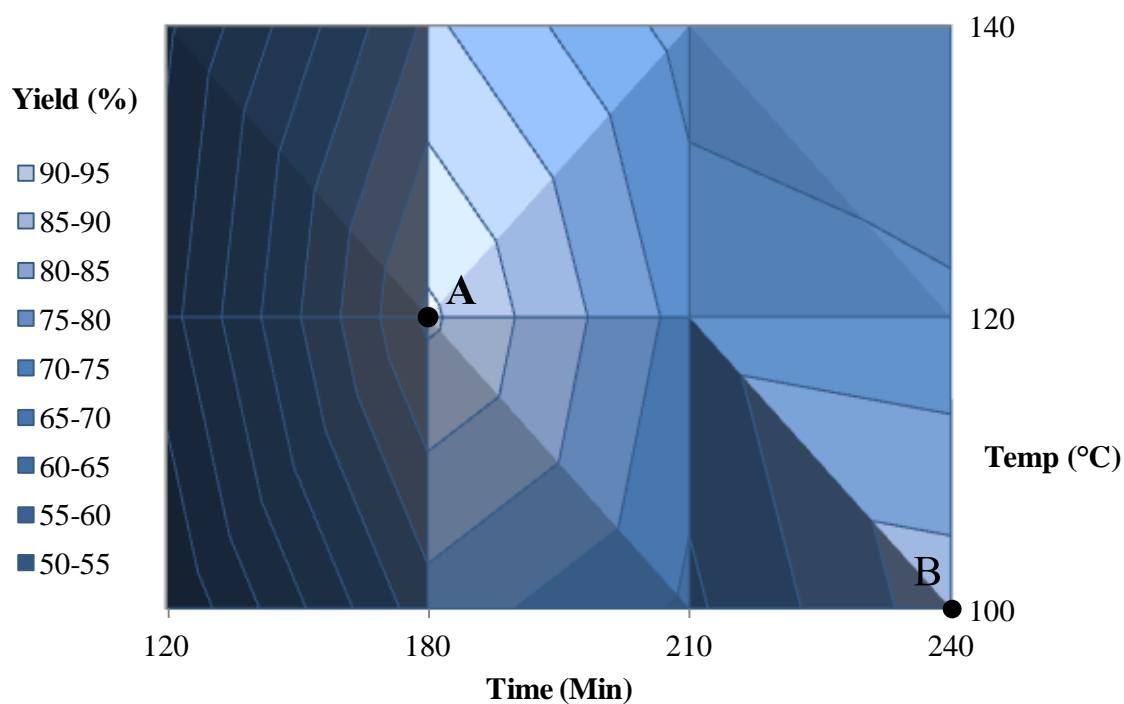
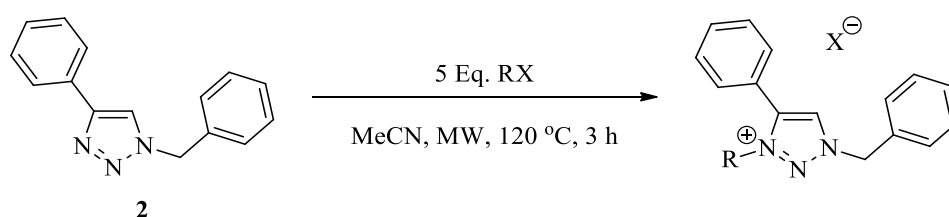


**Figure 1:** Optimization of *N*-alkylation step showing yield as a function of reaction time and temperature

From the two areas with the highest yield, **A** was chosen not only because it showed the highest yield but also that the reaction time was lower.

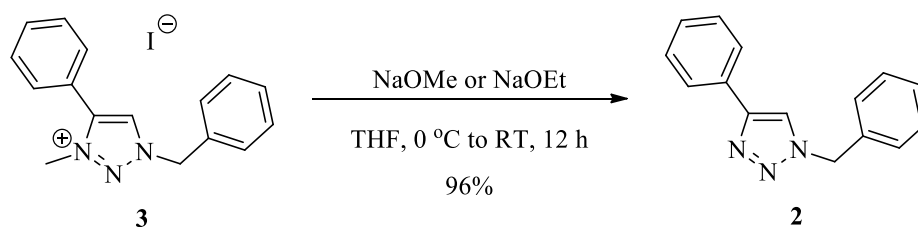
When the results from entry 1E, 1M, 1N & 1O are compared, the effect of the number of equivalents of the haloalkane on the yield is seen. From the optimization experiments we were able to design a procedure that could be used for the *N*-alkylation of triazole **2** with different alkyl groups (Scheme 11).



**Scheme 11:** Standard procedure for the *N*-alkylation of **2** with different alkyl groups

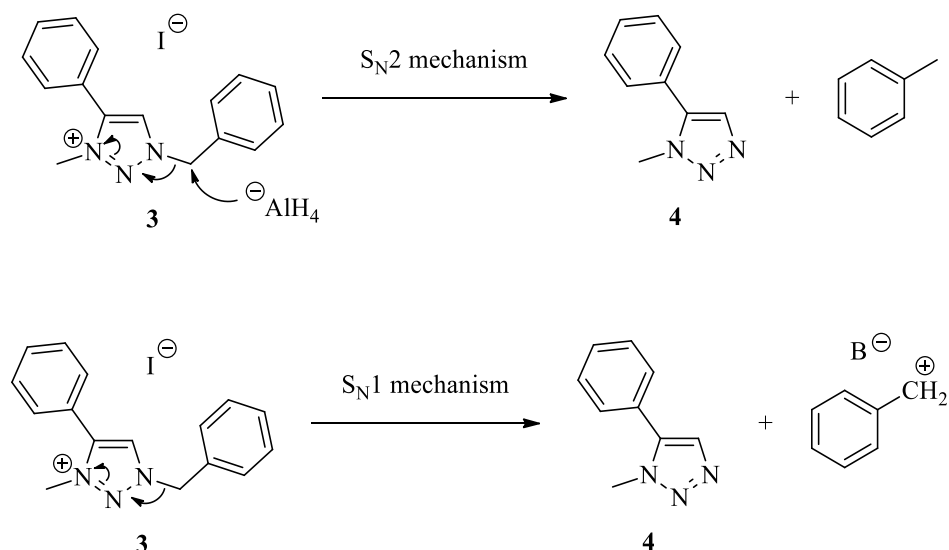
### 1.3.2 Debenzylation step

Next, we turned our attention to improving the removal of the benzyl group from the triazolium salt, giving the 1,5-triazole. When we used  $\text{LiAlH}_4$ , the 1,5-triazole was obtained in 24% yield. We believed that this low yield was due to the poor reactivity of the triazolium species, as the starting material was recovered in 66% yield. In an attempt to find a faster version of the debenzylation reaction, we switched from using the reducing agent  $\text{LiAlH}_4$  to the nucleophiles/bases NaOMe in methanol and NaOEt in ethanol. Under these conditions, the removal of the benzyl group was not observed, and instead the methyl group was removed, reforming **2** in up to 96% yield (Scheme 12).



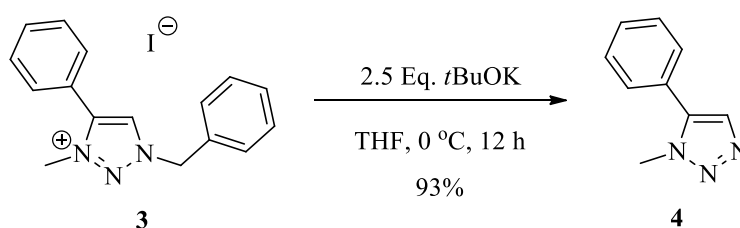
**Scheme 12:** Attempted debenzylation of **3** using NaOMe & NaOEt

This result led us to reason that  $\text{LiAlH}_4$  played a special role in the reaction, not acting as a hydride donor for the direct nucleophilic  $\text{S}_{\text{N}}2$  displacement of the triazole, but instead with the benzyl group leaving through an  $\text{S}_{\text{N}}1$  mechanism (Scheme 13).



**Scheme 13:** Possible mechanisms for the displacement of the benzyl group

To explore this possibility further, we chose to test the stronger non-nucleophilic base potassium *tert*-butoxide (*t*BuOK) in the reaction. When this was used in the debenzylation step, we immediately saw excellent results with the conversion of **3** to **4** taking place in 93% yield (Scheme 14).



**Scheme 14:** Debonylation of **3** using *t*BuOK

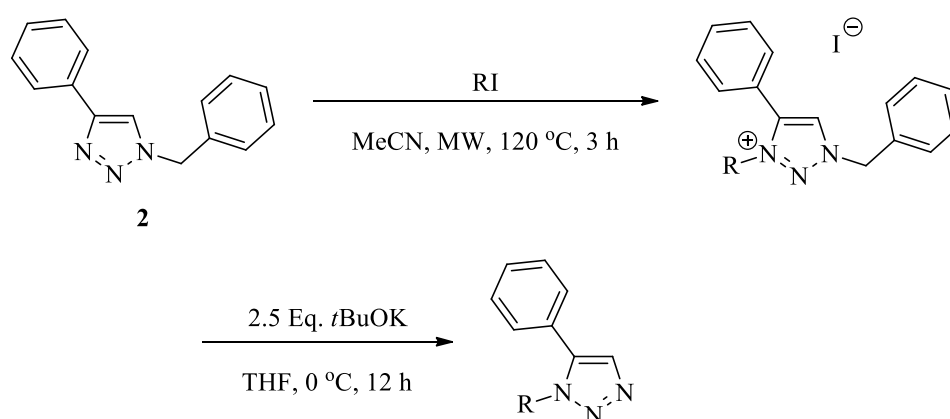
Combining these positive results and the optimised *N*-alkylation step, we began to test our interconversion pathway with various alkyl groups.

Another possible mechanism for the debenzylation of the triazolium salt may be by which the iodide anion attacks the benzyl carbon in an  $\text{S}_{\text{N}}2$  fashion, releasing the neutral triazole. With the isolated triazolium salts being extremely stable, it would appear that

the presence of compounds such as  $\text{LiAlH}_4$  or  $t\text{BuOK}$  is needed for the debenzoylation to occur, but this would need further investigation.

#### 1.4 Testing of the 1,3 to 1,5-triazole interconversion pathway

Armed with the reaction pathway and optimized conditions (Scheme 15), we began to study the efficiency of the method with increasing alkyl chain lengths.



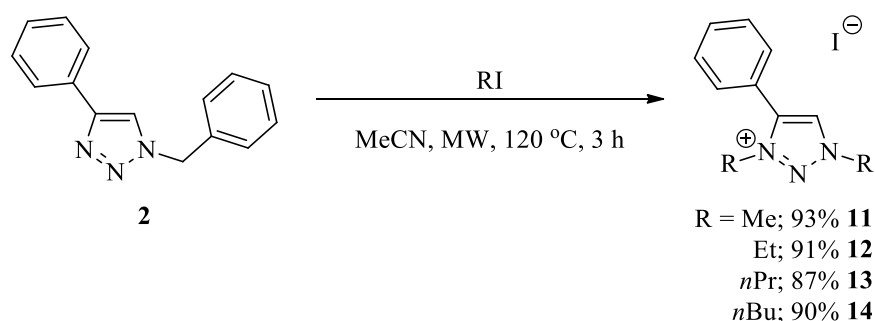
**Scheme 15:** Optimized reaction plan for the 1,3- to 1,5-triazole interconversion

**Table 2:** 1,3- to 1,5-triazole interconversion reactions

Entry	RX	N-alkylation Step Yield (%) [Product]	Debenzoylation Step Yield (%) [Product]
<b>2A</b>	MeI	97 [3]	93 [4]
<b>2B</b>	EtI	88 [5]	95 [8]
<b>2C</b>	<i>n</i> PrI	44 [6]	90 [9]
<b>2D</b>	<i>n</i> BuI	40 [7]	83 [10]

Initially the results were encouraging, with entry **2A** & **2B** giving high overall yields; 90% and 84% respectively, an improvement on those reported by Koguchi.<sup>83</sup> However, the remaining experiments showed a dramatic drop in yield, with yields from step A more than halving. With large amounts of starting material being recovered, it was believed that the low yields were a result of the decreasing reactivity of the haloalkanes as alkyl chain length increases. Therefore the synthesis of **6** & **7** was repeated with the reaction temperature increased to 160 °C resulting in full consumption of the starting material; however, compounds **6** & **7** were not isolated. Instead, analysis of the  $^1\text{H}$ -

NMR data showed a pair of identical peaks corresponding to those expected for an alkyl chain (see A-D, Figure 2). The data also indicated that the benzyl group was no longer present, with the aromatic protons integrating to 5, corresponding to the phenyl group on C(4), and the absence of the signal corresponding to the benzylic protons that would be expected around 5.5 ppm. This, along with the analysis of the  $^{13}\text{C}$ -NMR, COSY and HSQC spectra led us to believe that the *N*-alkylation of the triazole at the positions 1 and 3 was achieved alongside the displacement of benzyl group at the position 1 in a three-step one-pot procedure. The procedure was then repeated with the remaining alkyl chain lengths (Scheme 16).



**Scheme 16:** Excess *N*-alkylation of triazole **2**

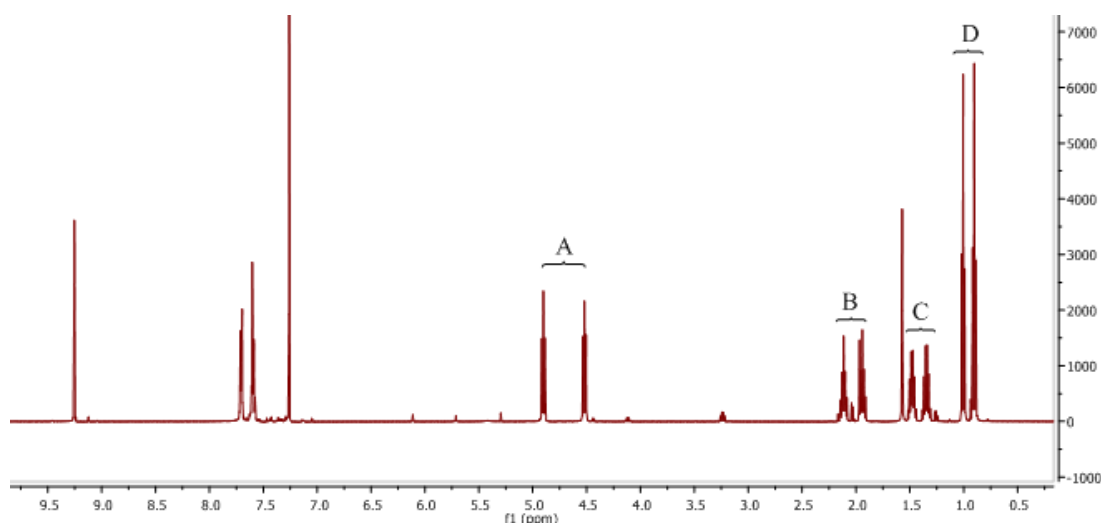
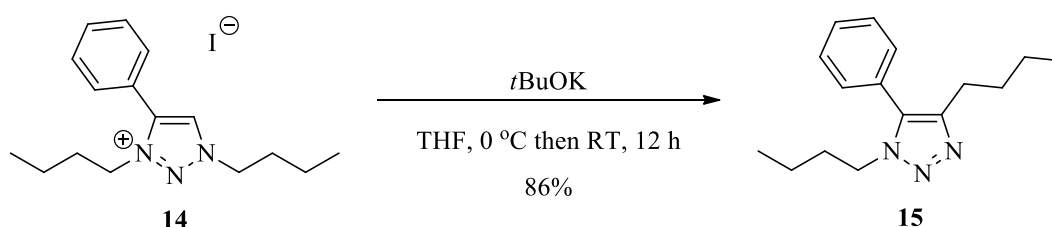


**Figure 2:**  $^1\text{H}$ -NMR of unknown compound, believed to be **14**

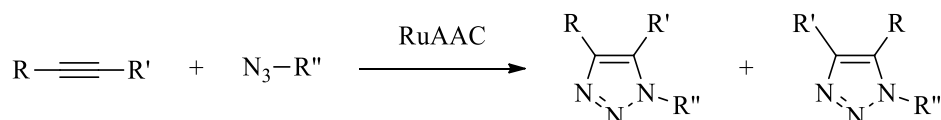
With the ‘over-alkylation’ observed with the different alkyl groups, we next proceeded with part (**2**) of the synthesis. Now that the triazoles no longer had a benzyl group that could be removed, we were intrigued to see if the use of *t*BuOK would still selectively promote the loss of one of the groups to give the corresponding neutral 1,4- or 1,5-

triazole. The reaction resulted in both groups still being present in the compound, as confirmed by the presence of signals in the  $^1\text{H-NMR}$  data corresponding to the two *n*-butyl groups. The low polarity of the compound also suggested that it was a neutral triazole, instead of the much more polar triazolium salt. In a triazolium salt, the peaks corresponding to the substituted groups are shifted further downfield compared to those of neutral triazoles; the substituted *n*-butyl peak of triazolium salt **7** is observed at 4.52 ppm, compared to the corresponding peak observed for the neutral triazole **10** at 4.35 ppm. The absence of the signal corresponding to the triazole proton, along with the information discussed, suggested the reaction proceeded to give a 1,4,5-trisubstituted triazole (Scheme 17).



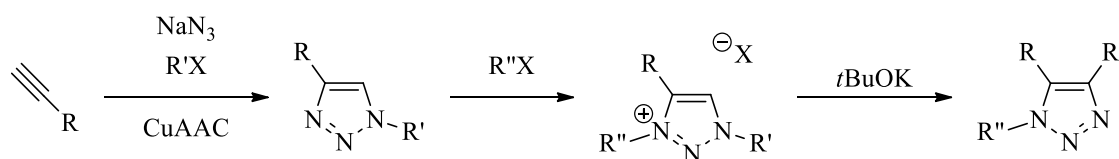
**Scheme 17:** Synthesis of 1,4,5-trisubstituted triazole **15**

One method for the synthesis of a 1,4,5-triazole is the ruthenium-catalysed azide-alkyne cycloaddition (RuAAC), used with an internal alkyne.<sup>84</sup> However, this method has the drawback that if the groups either side of the alkyne are not the same, then there can be an issue of regioselectivity in the reaction (Scheme 18).



**Scheme 18:** Regioselectivity in the RuAAC

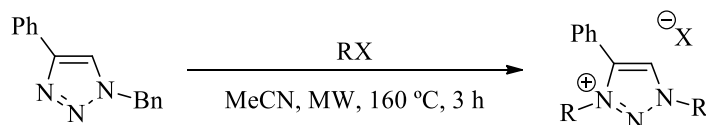
With the reaction in Scheme 17 we believe we have discovered a new pathway for the ruthenium-free synthesis of 1,4,5-trisubstituted triazoles with complete regioselective control (Scheme 19).



**Scheme 19:** New possible pathway for the regioselective copper-catalysed synthesis of 1,4,5-trisubstituted triazoles

### 1.5 Testing the new pathway for the synthesis of 1,4,5-trisubstituted triazoles

1-Benzyl-4-phenyl-1,2,3-triazole was chosen as the substrate for the testing sequence, applying the synthetic method discussed above. This consisted of alkylating the triazole at both the N1 and N3 positions, using various haloalkanes to displace the benzyl group and give a 1,3-dialkyl-4-phenyl triazolium halide (Scheme 20, Table 3). As the *N*-alkylation was first observed when the triazole was heated to 160 °C using microwave irradiation in the presence of the alkylating agent, these conditions were used.



**Scheme 20:** General scheme for the *N*-alkylation of triazole **2**

**Table 3:** Excess *N*-alkylation of triazole **2**

Experiment	RX	Yield (%) [Product]
<b>3A</b>	MeI	93 [ <b>11</b> ]
<b>3B</b>	EtI	91 [ <b>12</b> ]
<b>3C</b>	<i>n</i> PrI	87 [ <b>13</b> ]
<b>3D</b>	<i>n</i> BuI	90 [ <b>14</b> ]



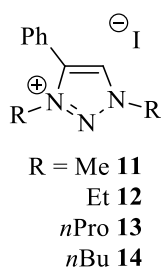
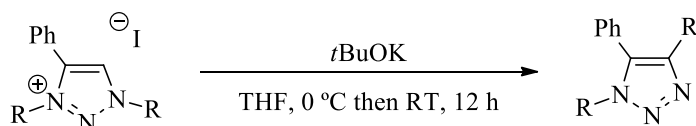


**Figure 3:** Products of the *N*-alkylation reactions

Once the alkylation step had been achieved, the rearrangement reaction was attempted on the triazolium salts using potassium *tert*-butoxide (Scheme 21, Table 4).

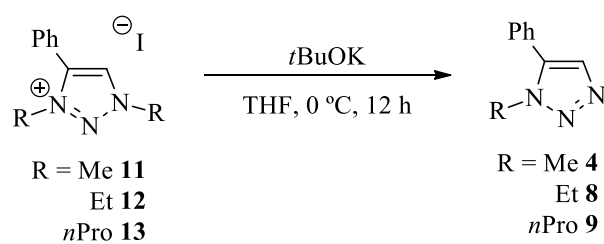


**Scheme 21:** General scheme for the reaction of triazolium salts with *t*BuOK

The results of the experiments showed that instead of the rearrangement observed for entry **4D**, only the triazoles **4**, **8** and **9** were isolated. It then appeared that for the triazolium salt systems where *n*-butyl was not the alkyl group, the group at the N1 position was removed, giving the corresponding 1-alkyl-5-phenyl-1,2,3-triazole (Scheme 22).

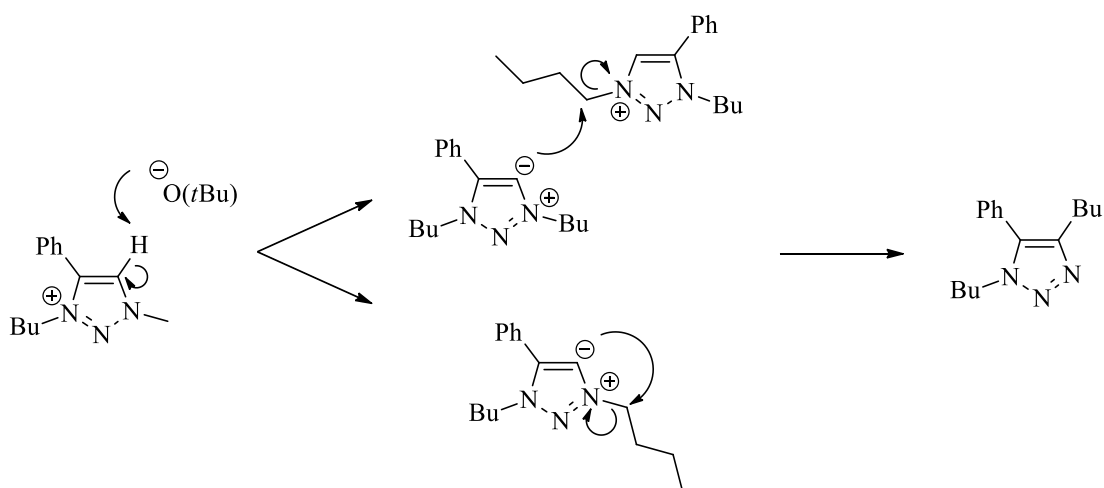
**Table 4:** Reaction of triazolium salts with *t*BuOK

Experiment	R	Yield (%) [Product]
<b>4A</b>	Me	Only <b>4</b> observed
<b>4B</b>	Et	Only <b>8</b> observed
<b>4C</b>	<i>n</i> Pr	Only <b>9</b> observed
<b>4D</b>	<i>n</i> Bu	86 [ <b>15</b> ]



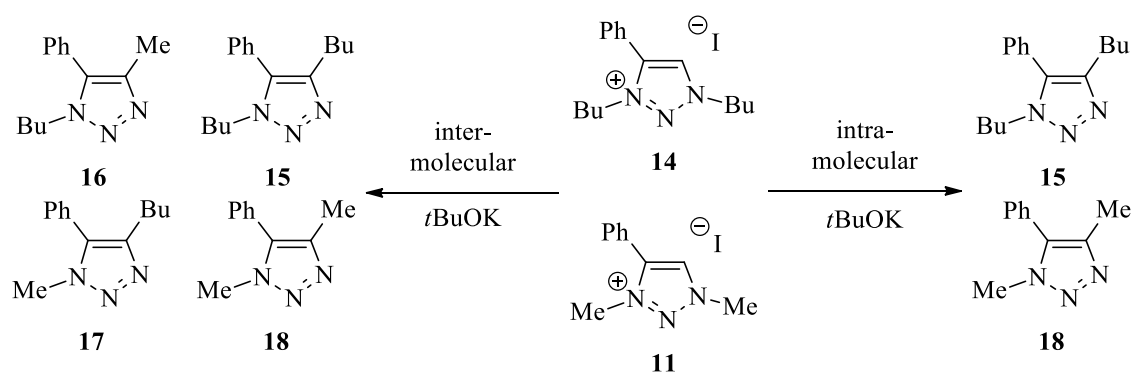
**Scheme 22:** Reaction of triazolium salts with *t*BuOK

In an attempt to explain why only experiment **4D** gave the 1,4,5-trisubstituted triazole, the mechanism behind the rearrangement was explored. One possibility is that first the triazole proton is removed by the *tert*-butoxide. The anion could then attack the alkyl group at the N1 position, either inter- or intramolecularly, to give the 1,4,5-triazole (Scheme 23).



**Scheme 23:** Alternative possible mechanism for the 1,3,4- to 1,4,5-triazole interconversion

An experiment was designed to help with the investigation of the mechanism. A mixture of the 1,3-dimethyl-4-phenyl and 1,3-dibutyl-4-phenyl triazolium salts were dissolved in THF in the presence of potassium *tert*-butoxide (Scheme 24).



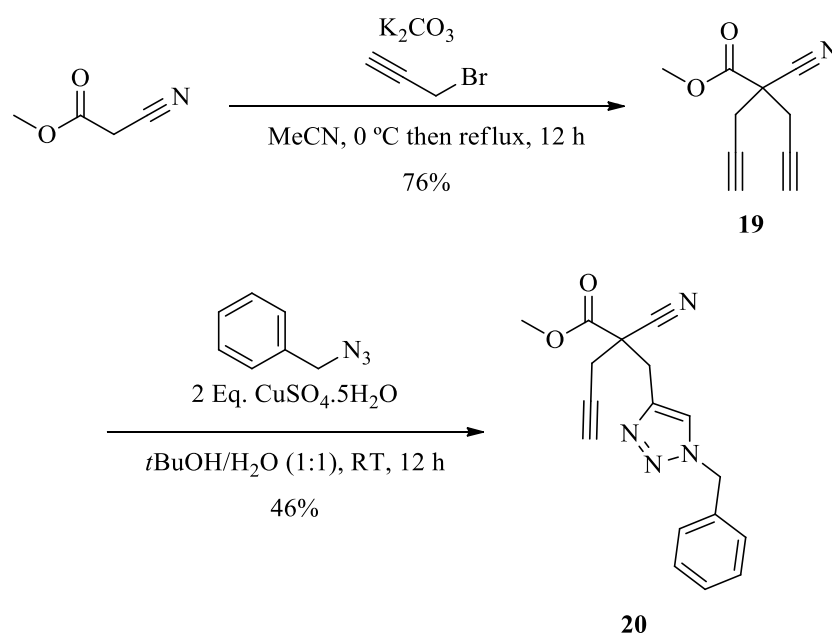
**Scheme 24:** Products from the inter- and intra-molecular reaction

Analysing the composition of the mixture of products produced would help determine the mechanistic pathway, and, in particular, whether the transfer of the alkyl group at the N1 position occurs through an inter- or intramolecular shift. If the reaction is intramolecular, only two triazoles should be obtained: 1,4-dibutyl-triazole **15** and 1,4-dimethyl-triazole **18**. If, on the other hand, the reaction is intermolecular, a statistical mixture of four products, 1-butyl-4-methyl- **16**, 1-methyl-4-butyl- **17**, 1,4-dibutyl- **15**, 1,4-dimethyl-triazoles **18**, would be obtained, resulting from all the possible combinations. There is also the possibility that both pathways can occur.

Our results only showed a mixture of products **4** & **10**, suggesting that instead of the expected rearrangement of the triazolium salts to the 1,4,5-trisubstituted triazoles, each salt had lost an alkyl group to yield the 1,5-disubstituted triazole. In an attempt to further explore the mechanism of the reaction, and reason why we had not seen the rearrangement in the above reaction, or in the reactions where the R-group chain length was shorter than *n*-butyl, we re-examined the original reaction that gave the 1,4-dibutyl-5-phenyl-triazole **15**. However, when the synthesis of **15** was repeated using our reported procedure, the reaction only yielded 1-butyl-5-phenyl-triazole **10**. We are currently attempting to repeat the synthesis of **15**, which we hope will help explain our previous findings.

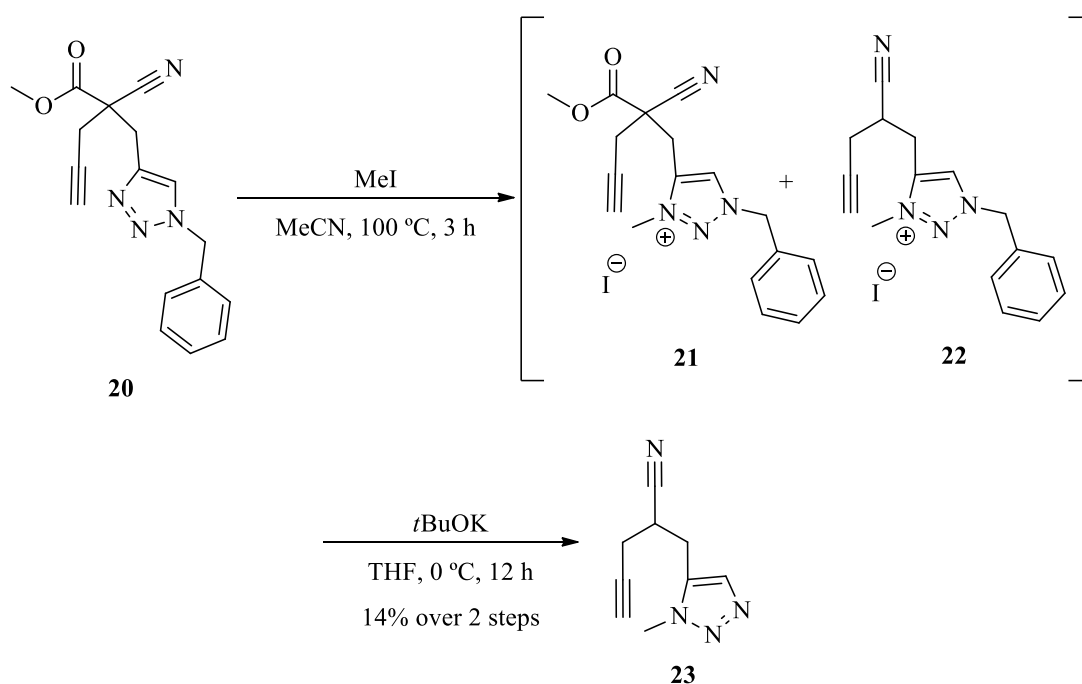
## 1.6 Application of the 1,3- to 1,5-triazole interconversion to asymmetric ‘click’ systems

Our group has reported the use of an asymmetric ‘click’ reaction to break the symmetry of *bis*-alkyne systems.<sup>76</sup> We believe that the application of the 1,3- to 1,5-triazole interconversion would provide the organic synthetic chemist with another tool for the diversification of a compound. Due to the limited amount of material produced from the asymmetric ‘click’ reactions, we decided that the tests would be run using a racemic mixture of the mono-triazole product **19**, from our cyanoacetate-derived series of prochiral bis-alkynes. First, the *bis*-alkyne **19** was synthesized using the method reported by the group, followed by the ‘click’ reaction to prepare the corresponding mono-‘click’ product (Scheme 25).



**Scheme 25:** Synthesis of the cyanoacetate-derived mono-triazole **20**

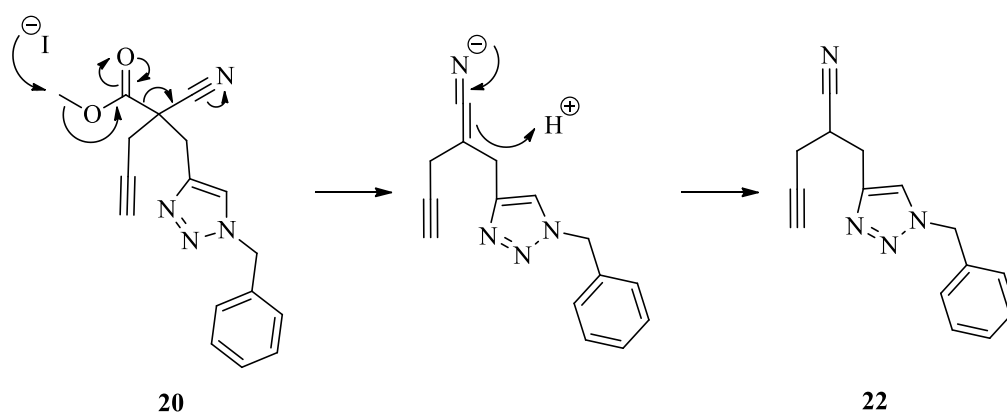
Once the mono-triazole compound was synthesized, the interconversion process was started with the *N*-alkylation of **20** using iodomethane (Scheme 26). The product was separated from the remaining starting material and isolated as a mixture of two inseparable compounds in a disappointingly low yield ( $\approx 15\%$ ).



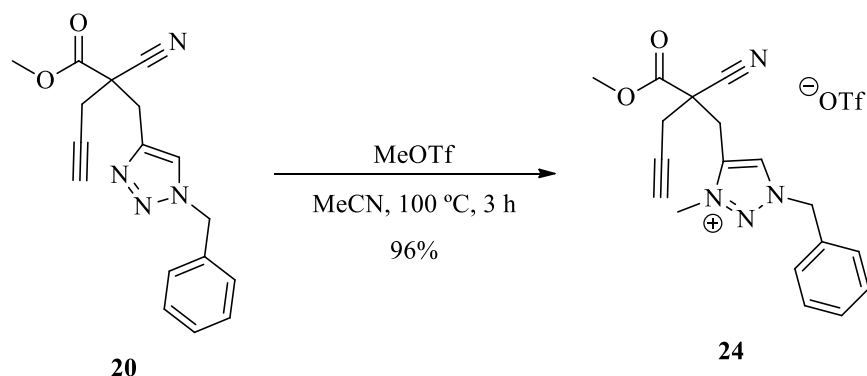
**Scheme 26:** Attempted 1,3 to 1,5-triazole interconversion of mono-triazole **20**

The spectroscopic data showed the presence of the expected *N*-alkylated triazolium salt **21**, but also that a second triazolium salt **22** was formed. Unlike the previous reactions, this was not a case of over alkylation, as the expected benzyl peaks were present for both compounds. Instead, when the  $^1\text{H-NMR}$  spectrum of the compound **22** was analysed, the signal corresponding to the methoxy group was not present and a new multiplet corresponding to a single proton was observed. This led us to believe that the methyl ester had been cleaved from the compound, giving triazolium salt **22**. The mixture of salts was taken forward to the debenylation step, which not only removed the benzyl groups but also the remaining ester group in salt **21**, to give a single neutral triazole **23**, in near quantitative yield.

We suspect that the presence of the iodine in the reaction causes the loss of the ester group through a Krapcho decarboxylation mechanism (Scheme 27). The issue was immediately overcome by using an alkylating agent that did not contain a halide, in this case methyl triflate, yielding the triazolium salt **24** in 96% yield (Scheme 28).



**Scheme 27:** Krapcho decarboxylation of **20**

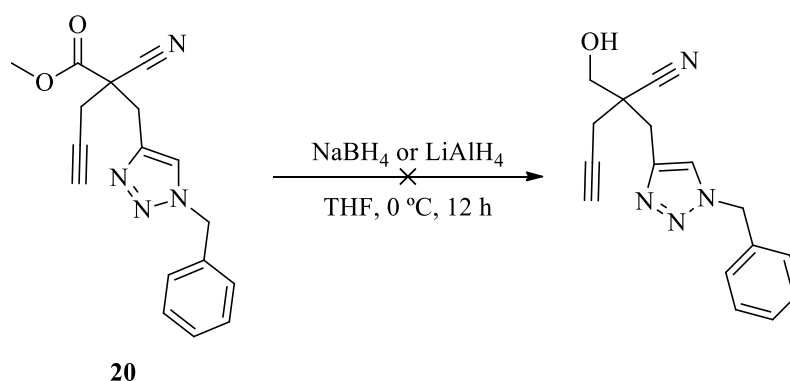


**Scheme 28:** *N*-alkylation of mono-triazole **20** using MeOTf

As the *N*-alkylation was successful, the removal of the benzyl group using potassium *tert*-butoxide was attempted. Unfortunately, the reaction was unsuccessful and only starting material was isolated. By altering the anion stabilizing the charge of the triazolium salt to the triflate, we conjectured that the ability of the *tert*-butoxide to act as a base and support the benzyl elimination was decreased. In an attempt to overcome this issue, we repeated the experiment using a non-nucleophilic base, lithium *bis*(trimethylsilyl)amide (LHMDS), but only starting material was observed.

After multiple attempts to remove the benzyl group, we decided that the results we had observed supported the theory discussed earlier, in which the iodide acts as a nucleophile to remove the benzyl group. Therefore a different approach would be taken to perform the 1,4- to 1,5-triazole interconversion while still retaining the original stereochemistry at the chiral centre.

The first new approach involved the reduction of the methyl ester to the corresponding alcohol, attempted using the common reducing agents sodium borohydride and lithium aluminium hydride (Scheme 29).

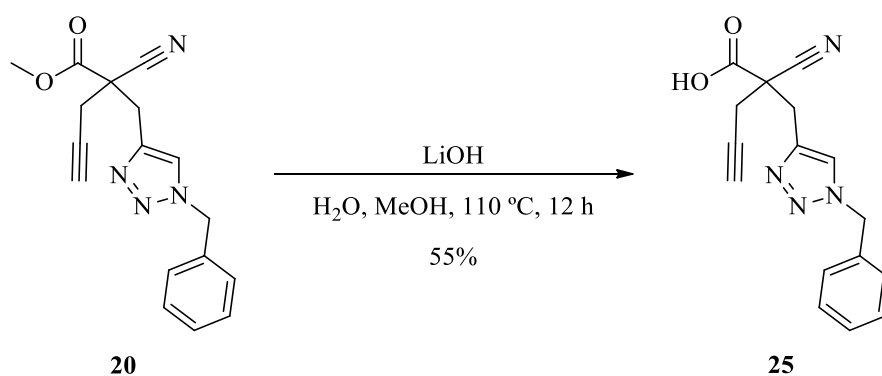


**Scheme 29:** Attempted reduction of the methyl ester in **20**

These reactions were unsuccessful: the sodium borohydride reduction only led to the recovery of the starting material as it was not reactive enough to reduce the ester moiety, and the lithium aluminium hydride reduction yielded a complicated mixture of products as both the ester and nitrile moieties reacted with the reducing agent.

Following a review of the literature, it appeared that there was no effective way to selectively reduce the methyl ester, so we once again attempted a different method to overcome the decarboxylation difficulties.

As discussed above, we believed that the compound was undergoing a Krapcho decarboxylation, initiated by the presence of the iodine. The initial attempts to replace the iodine were successful; however, further complications arose later in the synthesis. As the reduction attempts were unsuccessful, we planned to transform the methyl ester to the corresponding carboxylic acid using alkaline hydrolysis (Scheme 30).



**Scheme 30:** Saponification of **20**

With the successful conversion of **20** into **25**, we are now able to reattempt the *N*-alkylation reaction, in the hope that the decarboxylation, allowing us to achieve the 1,5-disubstituted triazole while retaining the stereochemistry at the chiral centre.

## 2.0 Synthesis of *meso* compounds

The second part of our research focuses on developing an asymmetric ‘click’ reaction which would be capable of selectively breaking the symmetry of *meso bis*-alkynes. Although *bis*-alkyne structures are common (our group has previously studied some of them<sup>76</sup>), the availability of natural *meso bis*-alkynes is extremely low. This means that before the asymmetric ‘click’ reaction could be tested, a number of test compounds had first to be synthesized (Figure 4).



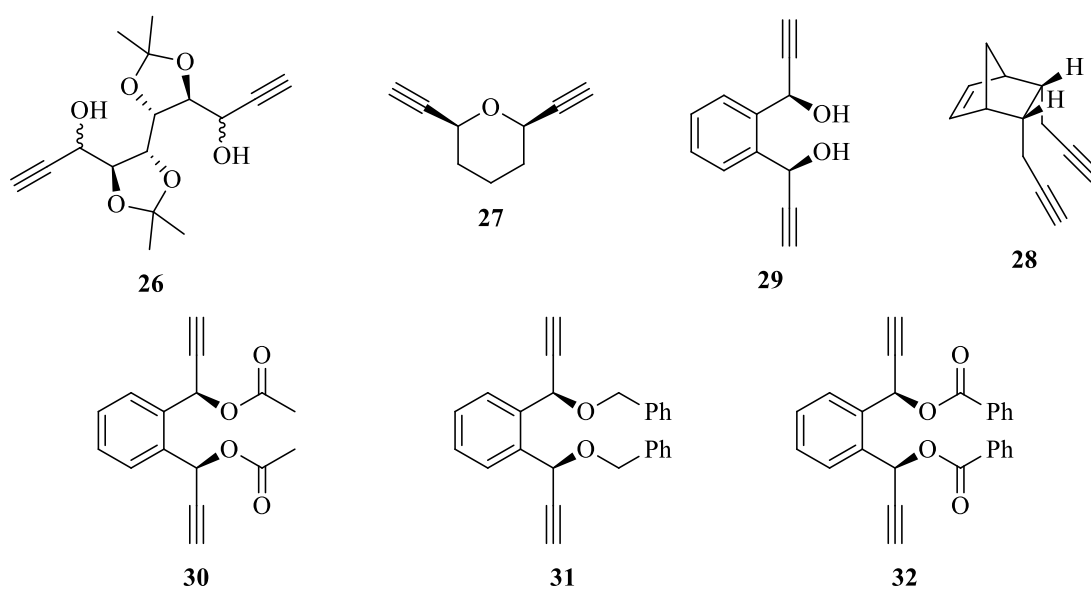
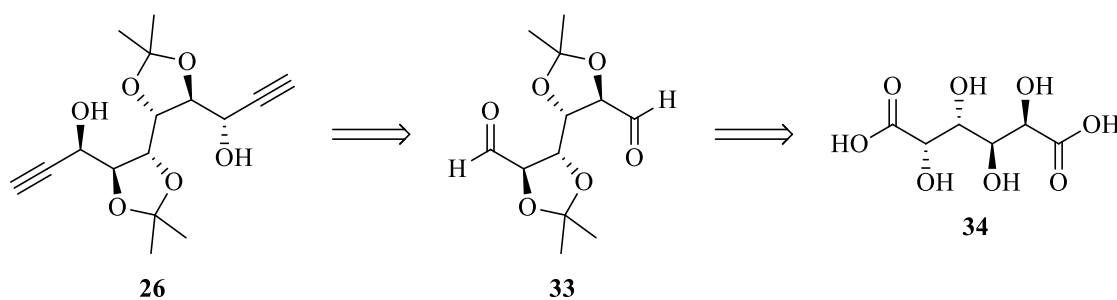


**Figure 4:** *Meso bis-alkynes* to be synthesized for testing

The synthetic paths investigated to synthesize *meso bis-alkynes* **26-32** are described below.

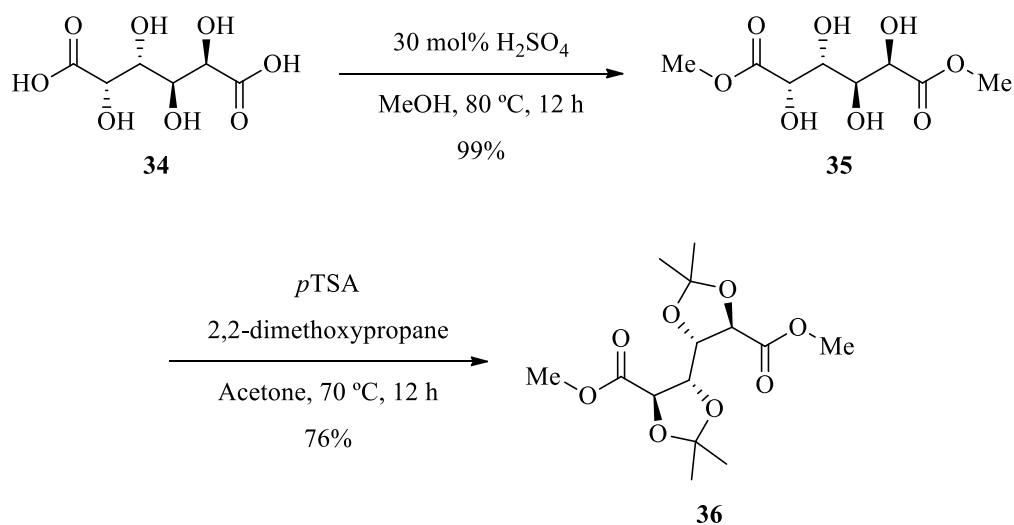
### 2.1 *Meso bis-alkyne* **26**

The synthetic plan for **26** involved a nucleophilic addition to the *bis*-aldehyde **33**, a key intermediate prepared from the commercially available *meso*-compound galactaric acid (mucic acid) **34** (Scheme 31).



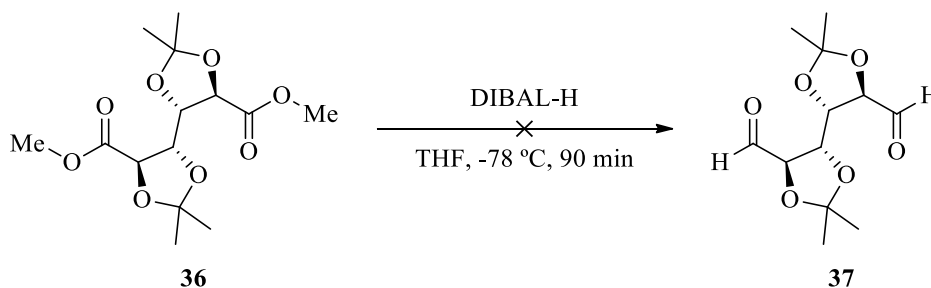
**Scheme 31:** Retrosynthetic route for the synthesis of **26**

The synthesis began with the acid-catalysed esterification of **34** using methanol to give **35**, followed by the protection of the two diol moieties with 2,2-dimethoxypropane (Scheme 32).



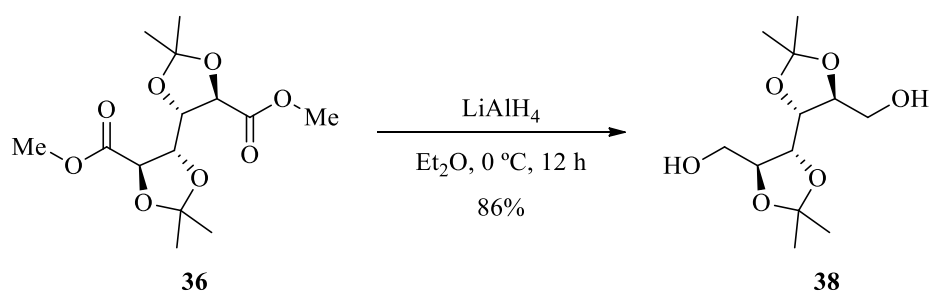
**Scheme 32:** Synthesis of *meso*-diester **36**

After the diol *bis*-protection, we next needed to reduce both ester moieties to prepare the novel *bis*-aldehyde **37**. Firstly, the direct conversion of the acid to the aldehyde was attempted using di-*iso*-butylaluminium hydride (DIBAL-H) and the method reported by Wu.<sup>85</sup> However, we were unable to isolate the desired *bis*-aldehyde **37** (Scheme 33).



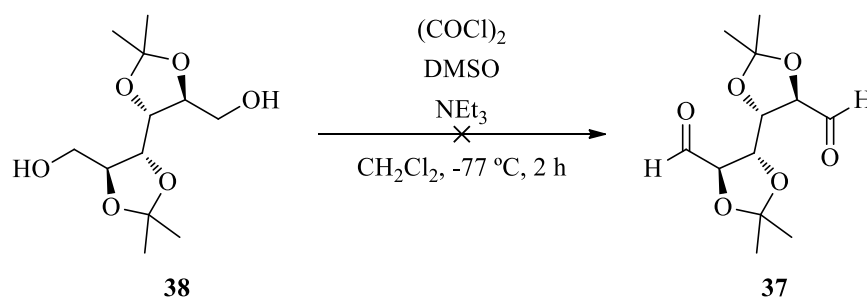
**Scheme 33:** Attempted synthesis of di-aldehyde **37**

After multiple unsuccessful attempts to achieve the direct conversion of **36** to **37**, we decided to synthesize **37** by reducing **36** to the primary alcohol **38** and then oxidizing the alcohol to the aldehyde (Scheme 34).



**Scheme 34:** Reduction of ester **36** to primary alcohol **38**

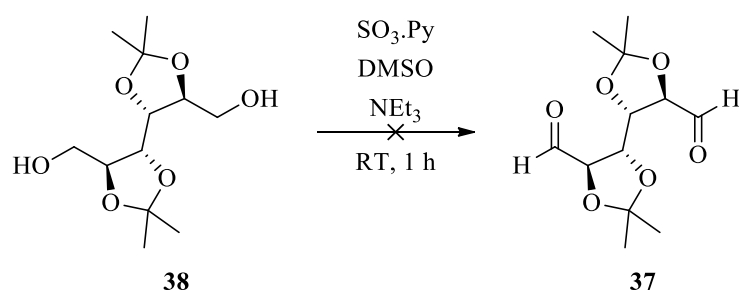
The ester was successfully reduced in high yield using  $\text{LiAlH}_4$ . The reduction proceeded smoothly, with the product easily purified by recrystallization. The next part of the synthesis was the oxidation: many methods for performing this transformation are available and we chose to begin with the Swern oxidation.<sup>86</sup>



**Scheme 35:** Attempted Swern oxidation of **38**

Analysis of the spectroscopic data suggested that the reaction was not successful as characteristic signals corresponding to an aldehyde moiety were not observed. The experiment was repeated several times, each time giving the same result, with TLC analysis showing a complex mixture of products.

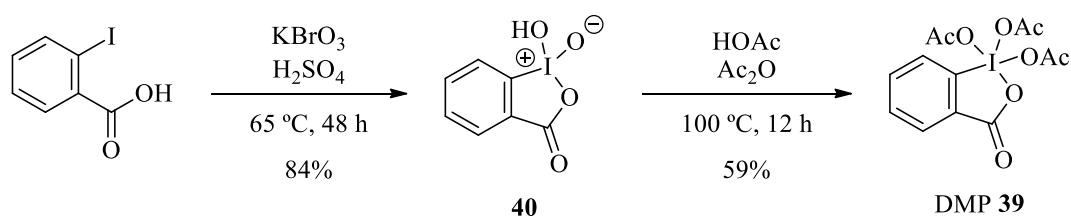
The success of the Swern oxidation is reliant on the reaction temperature being kept below  $-60\text{ }^\circ\text{C}$ , otherwise breakdown of the alkoxy-sulfonium ion can occur, giving a methylthiomethyl ether side product as a result. To try to overcome the issue of the temperature dependence, we attempted the Parikh-Doering oxidation,<sup>87</sup> which is similar to the Swern oxidation, except the use of a sulfur trioxide-pyridine complex allows the reaction to be carried out between  $0\text{ }^\circ\text{C}$  and room temperature (Scheme 36).



**Scheme 36:** Attempted Parikh-Doering oxidation of **38**

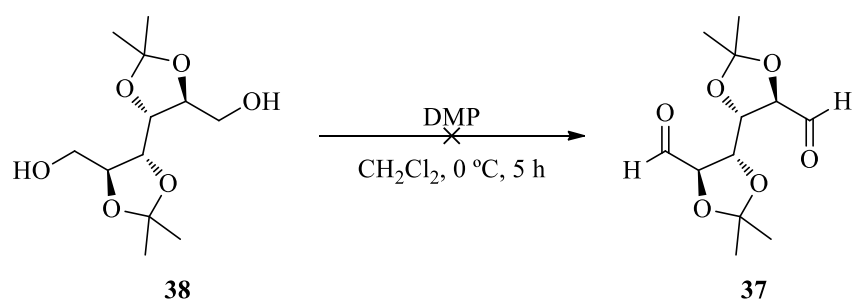
The Parikh-Doering oxidation of **38** led to similar results to the Swern oxidation, giving a complex mixture of products, and the presence of an aldehyde group was not observed using spectroscopic data analysis.

We next tried the Dess-Martin oxidation,<sup>88</sup> in the hope that using the Dess-Martin periodinane (DMP) instead of an activated dimethyl sulfoxide as the oxidizing reagent would lead to the successful oxidation of **38**. Firstly, we had to synthesize the DMP **39**, following the procedure reported by Martin (Scheme 37).<sup>88</sup>



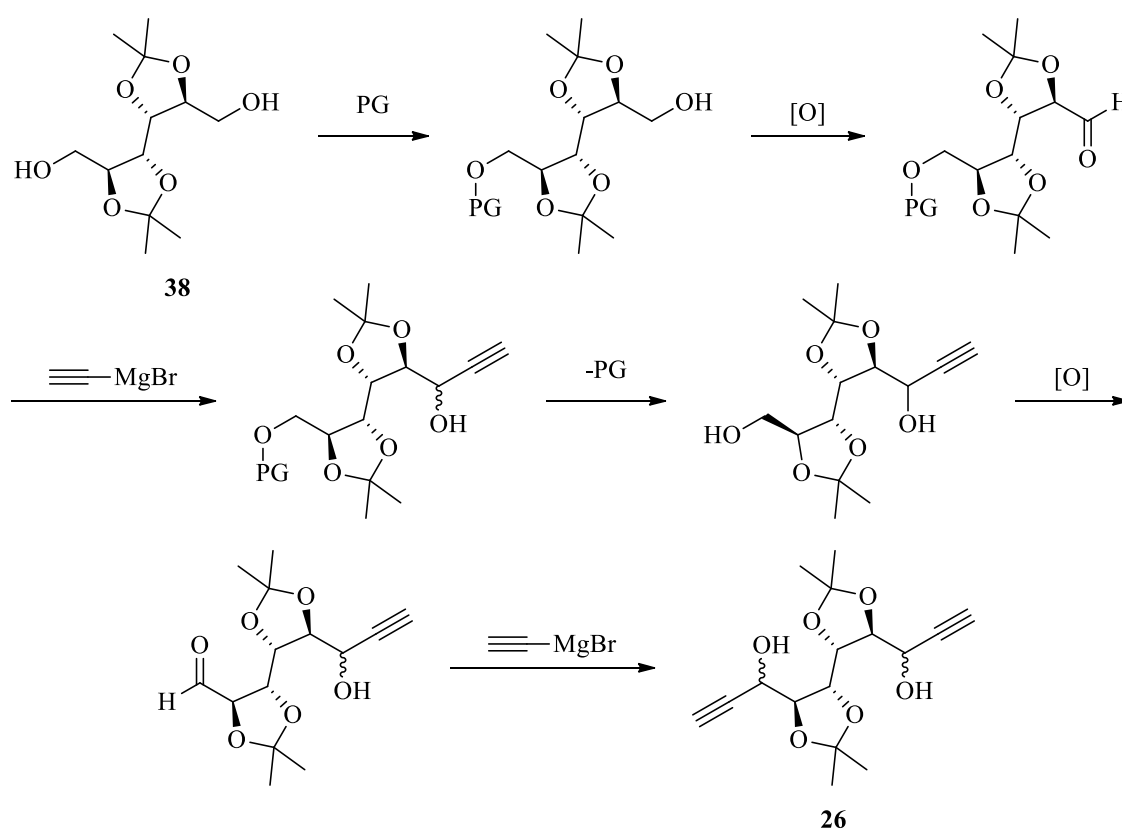
**Scheme 37:** Synthesis of DMP **39**

The oxidation was attempted using DMP **39**, but analysis of the <sup>1</sup>H NMR spectrum of the crude reaction mixture showed signals corresponding to the presence of several aldehyde functional groups in small amounts, and after column chromatography we were not able to isolate the desired product **37** (Scheme 38).



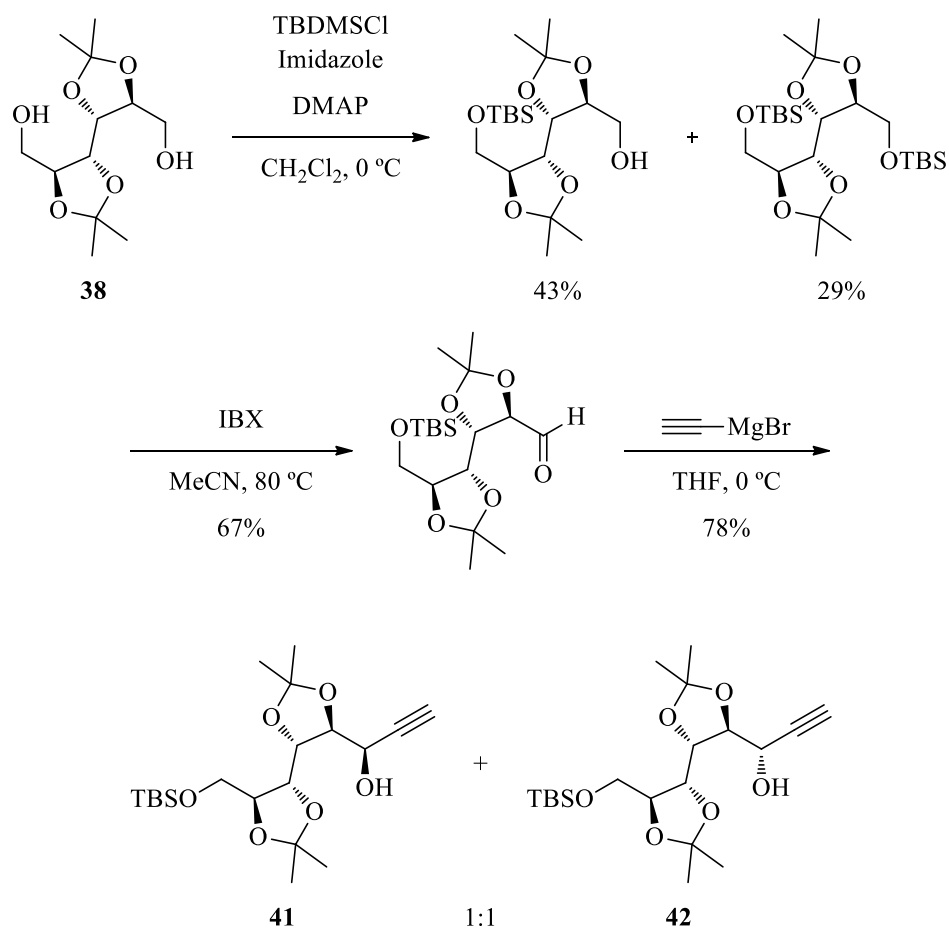
**Scheme 38:** Attempted Dess-Martin oxidation of **38**

After attempting several different oxidation methods, we were unable to obtain the desired *bis*-aldehyde **37**; hence, this synthetic route was abandoned. We believed that the possible issue with the oxidation is that once one aldehyde group has been oxidized, the alcohol group attacks the newly formed aldehyde intramolecularly. To see if this was a factor affecting the reaction, we investigated the possibility of mono-protecting the *bis*-alcohol, oxidizing the unprotected alcohol and inserting the alkyne, and then repeating the same sequence for the remaining alcohol moiety (Scheme 39).



**Scheme 39:** Synthetic route to avoid the intramolecular reaction

This research was carried out by another member of the group, with a successful outcome.<sup>89</sup> The group member was able to mono-protect the compound and oxidize the remaining alcohol group, and finally perform a Grignard reaction to insert the alkyne and give a racemic mixture of stereoisomers **41** & **42** (Scheme 40).



**Scheme 40:** Synthesis to avoid the intramolecular reaction

Although this synthetic route supported our theory about the intramolecular reaction, the low yielding step for the mono-protection, as well as the poor selectivity of the Grignard reaction, meant that this route was not pursued further. The mixture of stereoisomers **41** & **42** raised concerns that we would not be able to control the stereochemistry of the alkyne insertion to prepare **26**. To overcome this issue, we planned to insert the alkynes in the  $\beta$ -position with regards to the protected diols in an  $\text{S}_{\text{N}}2$  fashion, replacing the alcohol moieties: *bis*-alkyne **43** was targeted (Figure 5).

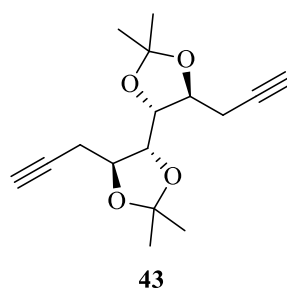
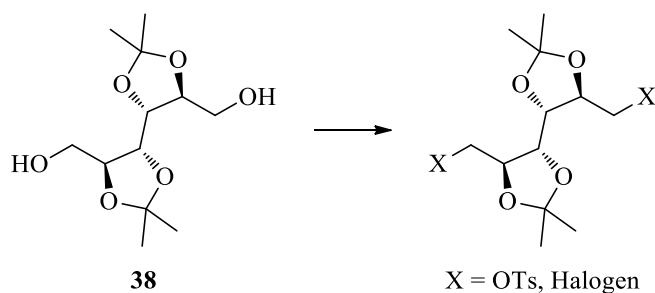


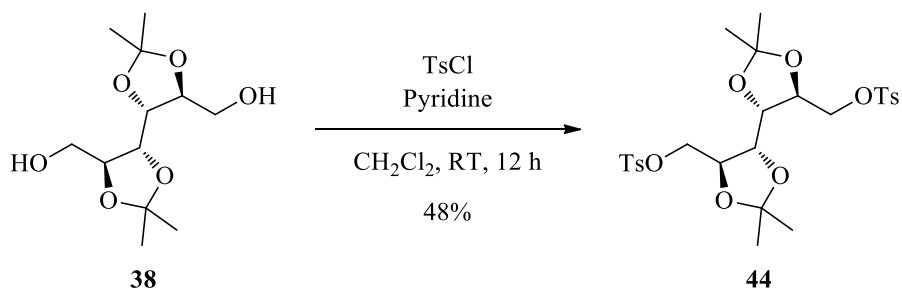
**Figure 5:** Structure of new target *meso* bis-alkyne

As the alkyne would be inserted as a nucleophilic acetylide ion, we planned to replace the alcohol moiety by a group that is a better leaving group, such as a halide or a tosylate (Scheme 41).



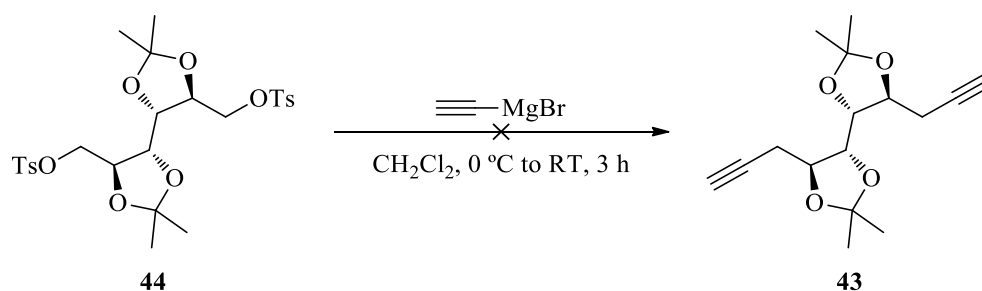
**Scheme 41:** Conversion of the alcohol to a better leaving group

We began by using *p*-toluenesulfonyl chloride (TsCl) to convert the alcohol moieties into the corresponding *bis*-tosyl derivative **44** (Scheme 42), as the reactants were readily available, and required conditions that were milder than those used for the substitution by a halide.



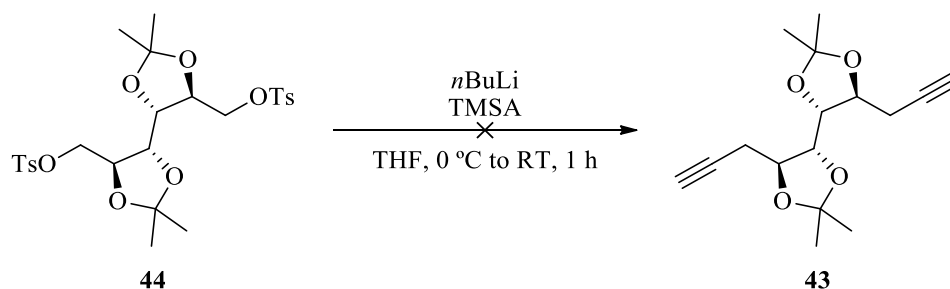
**Scheme 42:** Tosylation of **38**

We next attempted the insertion of the alkyne moieties, beginning with the use of the Grignard reagent ethynyl magnesium bromide (Scheme 43).



**Scheme 43:** Alkynylation of **44** using the Grignard reaction

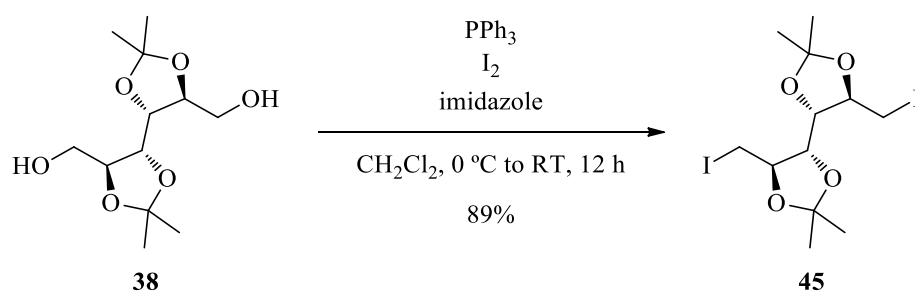
This reaction was unsuccessful, with  $^1\text{H}$  NMR spectra analysis showing only the presence of starting material. The reaction was repeated using ethynyltrimethylsilane (TMSA) and  $n\text{BuLi}$  as the acetylide source (Scheme 44).



**Scheme 44:** Alkynylation of **44** using TMSA and  $n\text{BuLi}$

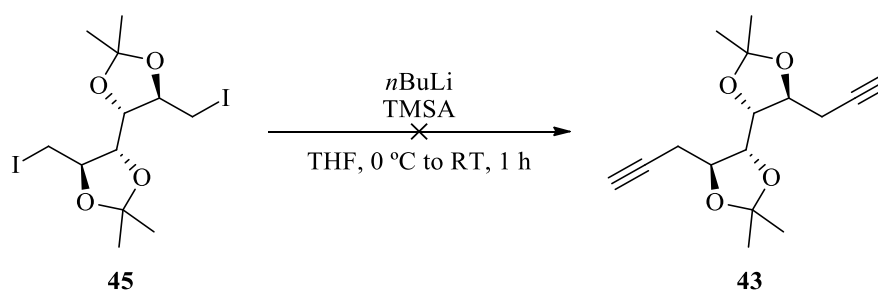
As observed with the addition of a Grignard reagent, only starting material was present. We therefore chose to exchange the alcohol group for a different leaving group, a halogen. One method for this transformation is the Appel reaction,<sup>90</sup> but its use of the hazardous carbon tetrabromide makes it undesirable. We instead chose to use the milder iodination method described by Garegg, which employs an iodine-triphenylphosphine-imidazole reagent combination.<sup>91</sup> The reaction using this milder method was successful, yielding the *bis*-iodide moiety in 89% yield (Scheme 45).





**Scheme 45:** Iodination of **38** using Garegg's conditions

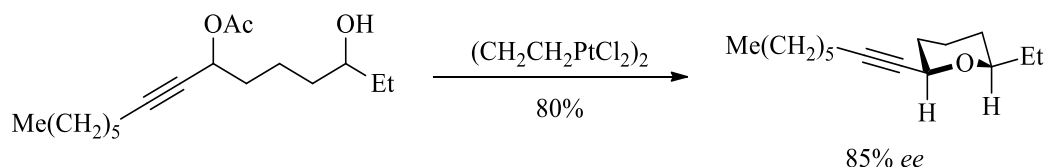
We repeated the alkylation reaction with the iodo group, however results proved to be unsuccessful (Scheme 46). This is currently as far as the synthesis has progressed.



**Scheme 46:** Alkylation of **45** using TMSA and  $n\text{BuLi}$

## 2.2 *Meso bis-alkyne 27*

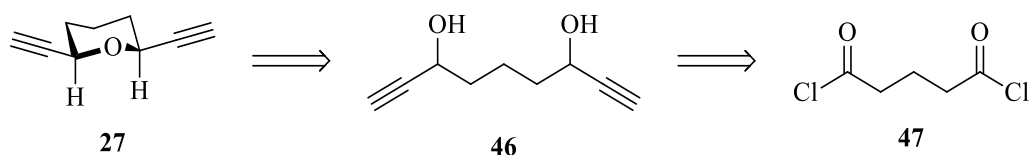
The synthesis of *meso bis-alkyne 27* was inspired by the work of Brabander that described cyclopropargyl ethers being produced with high stereoselectivity (Scheme 47).<sup>92</sup>



**Scheme 47:** Pt(II)-catalyzed synthesis of a cyclopropargyl ether

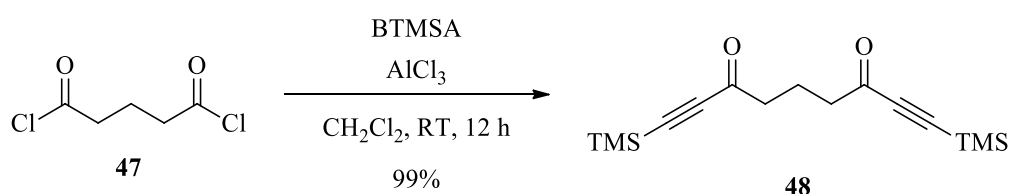
With these results suggesting that the *cis*-isomer is the preferred product, we attempted to synthesize a compound containing two propargylic alcohols which could then be cyclized to give the desired *meso bis-alkyne 27* (Scheme 48). Although introducing a

second alkyne would no longer allow the Pt(II) catalyst to direct the cyclization, a similar system was designed to afford a 2,6-*cis*-tetrahydropyran.



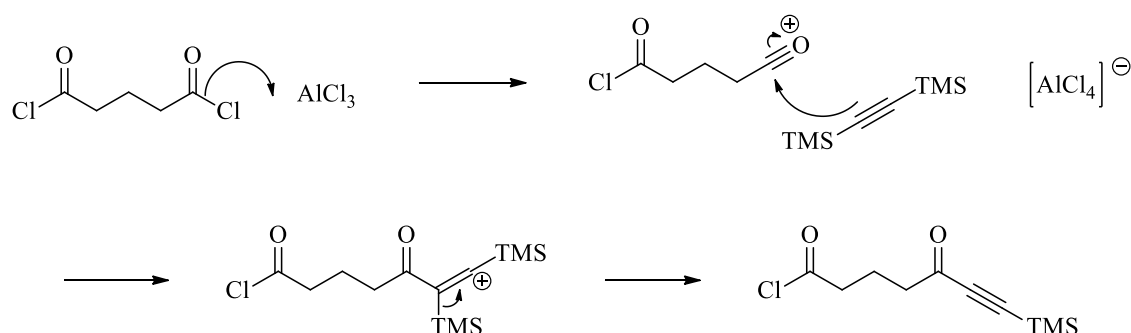
**Scheme 48:** Retrosynthetic approach for the synthesis of **27**

The synthesis began from the readily available starting material glutaryl dichloride **47**, which underwent incorporation of the alkyne groups by treatment with bis(trimethylsilyl)acetylene (BTMSA) in the presence of aluminium chloride (Scheme 49).



**Scheme 49:** Alkyne addition to glutaryl chloride

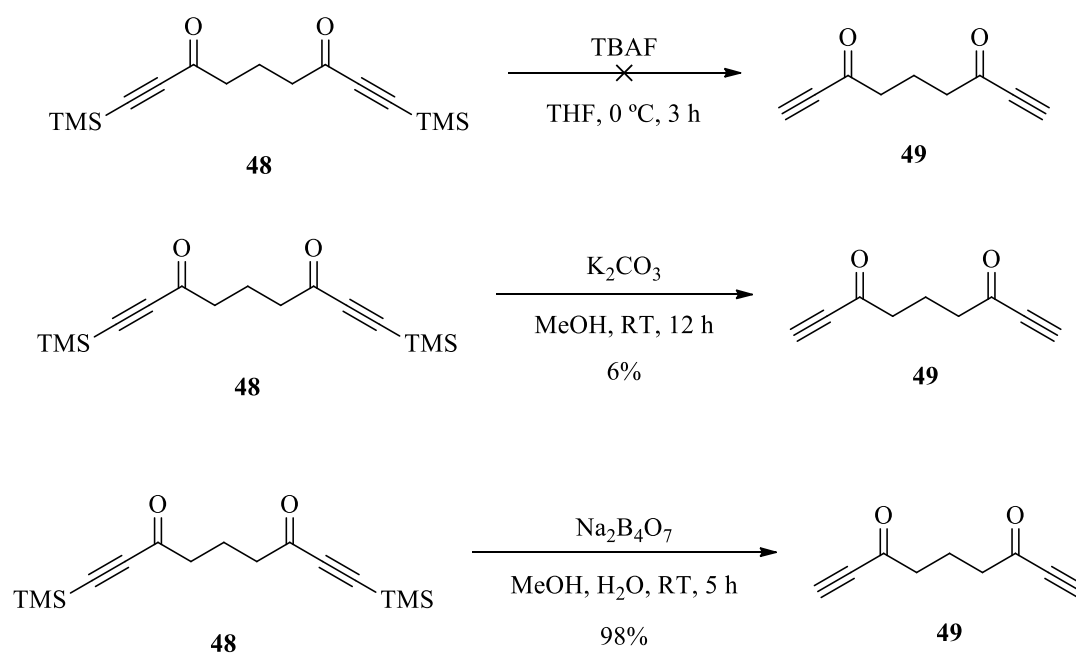
The mechanism of the reaction is reminiscent of the Friedel-Crafts acylation, where an acylium ion is produced upon interaction of an acyl chloride and aluminium chloride. The resulting ion is then trapped by BTMSA. Loss of a TMS group regenerates the alkyne moiety to give the desired product (Scheme 50)



**Scheme 50:** Acylation mechanism

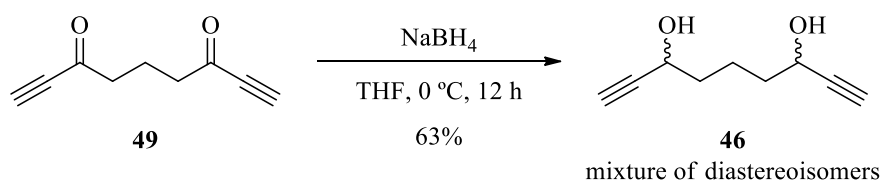
Once both of the TMS-protected alkynes were installed, giving the protected di-propargylic ketone, the TMS groups could be removed. Several different standard

methods for the removal of silyl protecting groups were investigated (Scheme 51). We began by using fluoride to remove the protecting group, with tetra-*n*-butylammonium fluoride (TBAF) as the fluoride anion source. These conditions appeared to be too harsh, and a mixture of decomposed materials was obtained. Next, a milder deprotection using potassium carbonate was attempted,<sup>93</sup> resulting in the product **49** being isolated in a very low yield (around 6%). Finally a method using borax (sodium tetraborate) was employed, yielding the product **49** in near quantitative yield (Scheme 51).<sup>94</sup>



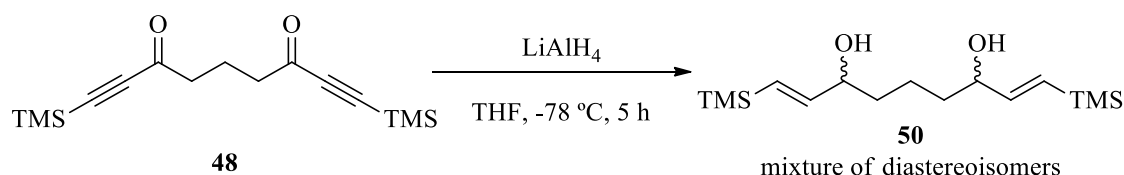
**Scheme 51:** Removal of TMS protecting groups

The next step was the reduction of the ketone moieties to give the diol **46** in an *anti*-arrangement, which we hoped would result in the *cis*-isomer after an acid-catalysed cyclization. To begin, a simple reduction was performed using the reducing agents  $\text{NaBH}_4$  and  $\text{LiAlH}_4$ . The reaction with the milder reducing agent  $\text{NaBH}_4$  was slow, and, although the starting material was nearly fully consumed, a mixture of inseparable diastereoisomers was isolated (Scheme 52).

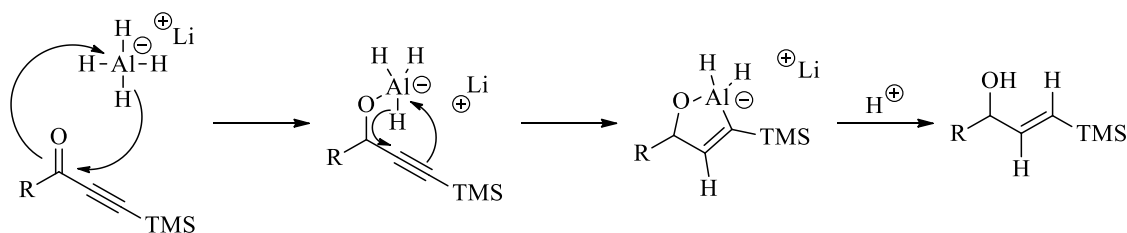


**Scheme 52:** Propargylic ketone reduction using  $\text{NaBH}_4$

When the more reactive  $\text{LiAlH}_4$  was used, full conversion of the starting material was observed; however, a complicated mixture of products was obtained.  $^1\text{H}$  NMR spectra analysis showed signals corresponding to the expected alcohols although the signal from the alkyne's terminal proton was not present. New multiplets were observed between 5.5-6.5 ppm, which suggested that the new compound contained an alkene, with the  $J$ -values being consistent with those of the *trans*-isomer. The newly formed propargylic alcohol has been reduced to the (*E*)-allylic alcohol **50** using  $\text{LiAlH}_4$  (Scheme 53). Once the hydride has added to the carbonyl group, the aluminium that is bound to the oxygen reacts through a *trans*-selective hydrometallation of the triple bond, releasing the alkene upon work-up (Scheme 54).<sup>95,96</sup>



**Scheme 53:** Propargylic alcohol reduction using  $\text{LiAlH}_4$

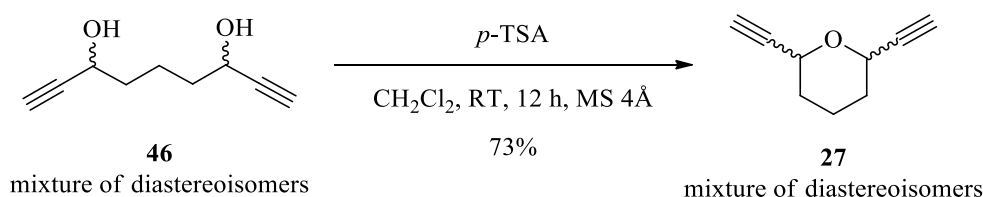


**Scheme 54:** Mechanism of the reduction of propargylic ketones to (*E*)-allylic alcohols mechanism

This reaction meant that  $\text{LiAlH}_4$  could not be used in the reduction of the dione. The problems encountered using both reducing agents led us to investigate the possibility of performing an asymmetric reduction of the propargylic ketone. The Midland reduction

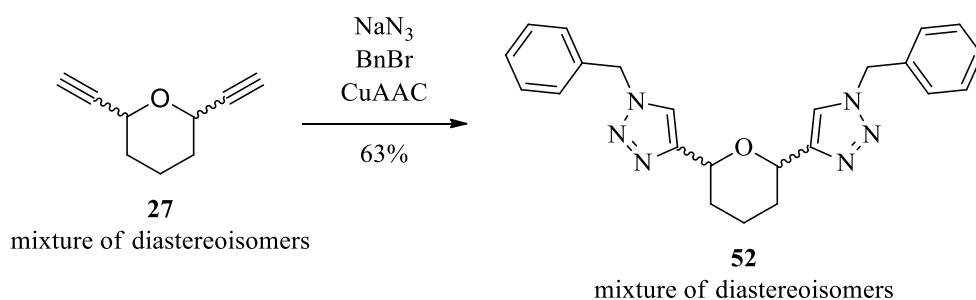
was chosen because of its reported high enantioselectivity in the reduction of propargyl ketones, utilising the asymmetric reducing agent B-3-pinanyl-9-borabicyclo[3.3.1]nonane **51** (alpine-borane).<sup>97</sup>

Before the enantioselective reduction was attempted, we wanted to ensure that the desired diol would cyclize to give the tetrahydropyran: the mixture of diols **46** was stirred with *p*-toluenesulfonic acid (*p*-TSA) at room temperature in the presence of 4 Å molecular sieve (Scheme 55).



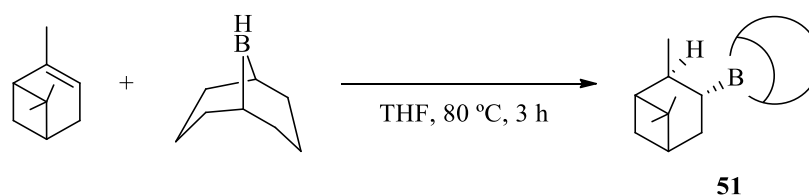
**Scheme 55:** Cyclization of diol mixture

2,6-Tetrahydropyran **27** was obtained in 73% yield and was then used to confirm that such *bis*-alkyne compounds would react under CuAAC reaction conditions to give the triazole product. The *bis*-alkyne **27**, as a mixture of the *meso* and the racemate, was submitted to standard CuAAC conditions with an excess of azide to give the expected mixture of bis-triazoles **52** (Scheme 56).<sup>79</sup>



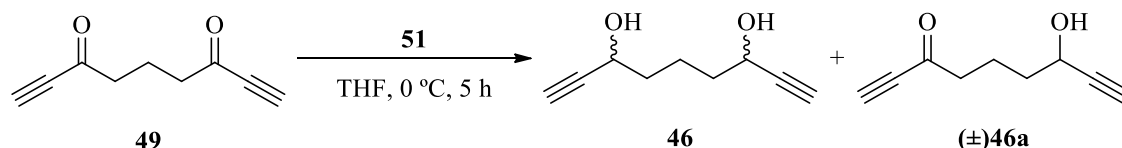
**Scheme 56:** ‘Click’ reaction performed on the mixture of *meso* and *racemic bis*-alkyne

The success of the cyclization and ‘click’ reactions were encouraging, and the enantioselective Midland reduction of dione **49** was then attempted. The alpine-borane reducing agent **51** was prepared using a method reported by Midland and used immediately without isolation (Scheme 57).<sup>97</sup>



**Scheme 57:** Synthesis of alpine-borane **51**

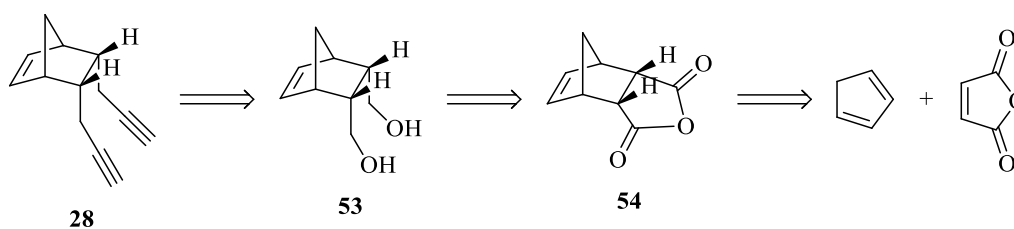
The dione **49** was then treated with the freshly prepared solution of alpine-borane **51**, to yield a complicated mixture of products (Scheme 58). Analysis of the  $^1\text{H}$  NMR spectrum suggested that a small amount of **46** as a mixture of diastereoisomers was present, along with the mono-reduced products ( $\pm$ )**46a**. Isolation of ( $\pm$ )**46** was attempted using column chromatography, however, the small quantity of ( $\pm$ )**46** and the presence of other by-products meant that isolation was not successful.



**Scheme 58:** Reduction of dione **49** using alpine-borane **51**

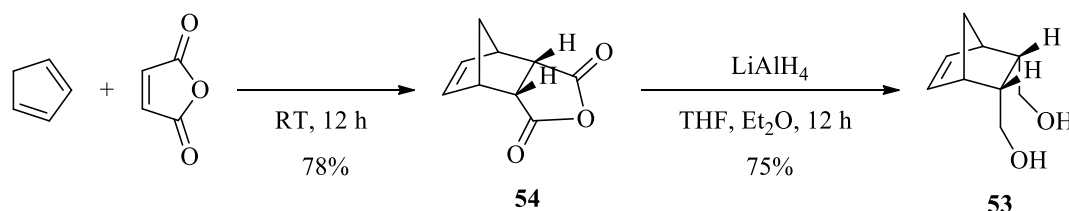
### 2.3 *Meso bis-alkyne 28*

The target compound **28** was chosen because it can be easily prepared as a single diastereoisomer using the stereospecific Diels-Alder reaction. The Diels-Alder reaction between cyclopentadiene and maleic anhydride, a standard reaction found in many undergraduate chemistry laboratories, was our starting point. The two carbonyl moieties would be reduced, and the corresponding hydroxyl groups used to introduce the alkynes, giving the *meso bis-alkyne 28* (Scheme 59).



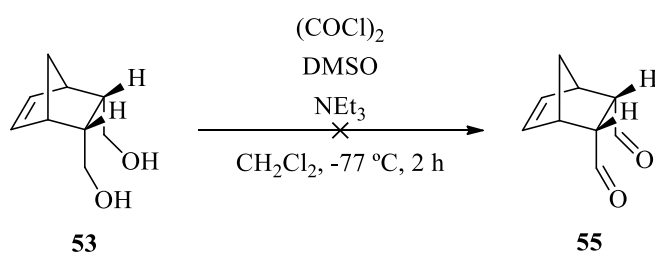
**Scheme 59:** Retrosynthetic approach for the synthesis of **28**

The Diels-Alder reaction was carried out to give anhydride **54** in high yield, after recrystallization from methanol. Reduction of the anhydride using lithium aluminium hydride afforded diol **53** in 75% yield, without further purification required after the work-up (Scheme 60).



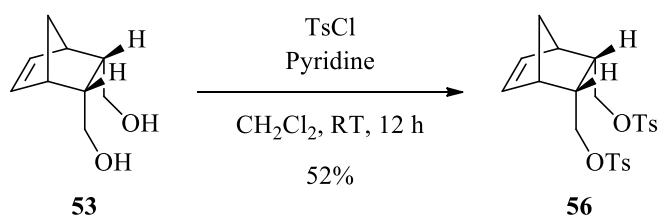
**Scheme 60:** Synthesis of diol **53**

As with the synthesis of *meso* bis-alkyne **26**, we next attempted to manipulate the alcohol groups so that alkynes could be introduced. With compound **26**, when the diol was oxidized in an attempt to form the dialdehyde product, we believe that a reaction intermediate cyclized. As the structure of **53** is more rigid, we hoped that the oxidation would be successful. However, we were cautious, as the close proximity of the diols may lead to a similar cyclisation. The Swern oxidation was the chosen method of oxidation. Analysis of the spectroscopic data showed that no aldehyde or alcohol was present in the crude product mixture (Scheme 61).



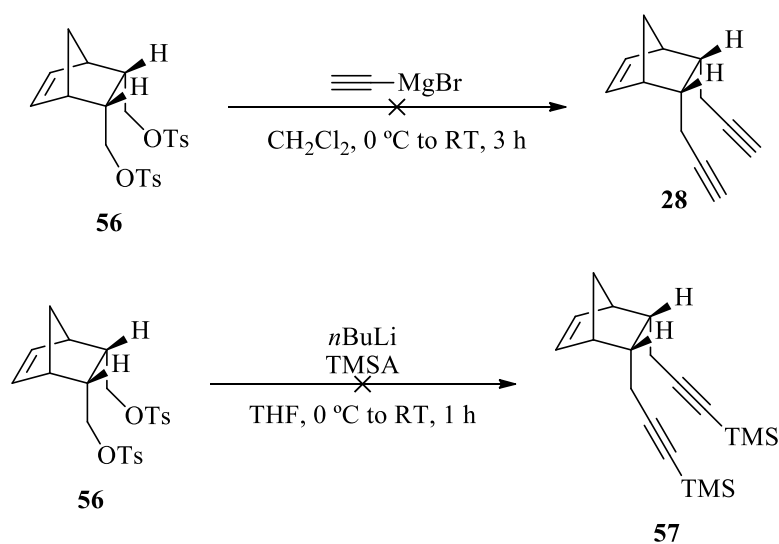
**Scheme 61:** Attempted Swern oxidation of **53**

As the oxidation route was unsuccessful, we attempted to convert the alcohol into a more effective leaving group to perform the alkyne introduction. We began with the transformation of the alcohol to the tosyl group, following the procedure used in the synthesis of **27**. This was successful, the ditosylate **56** being isolated in 52% yield (Scheme 62).



**Scheme 62:** Conversion of an alcohol to a tosyl group

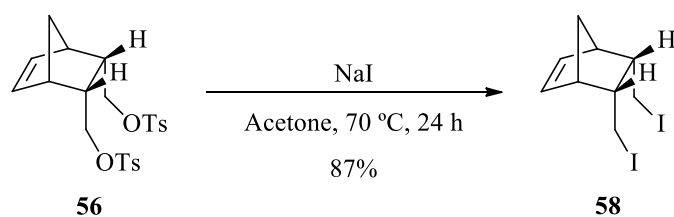
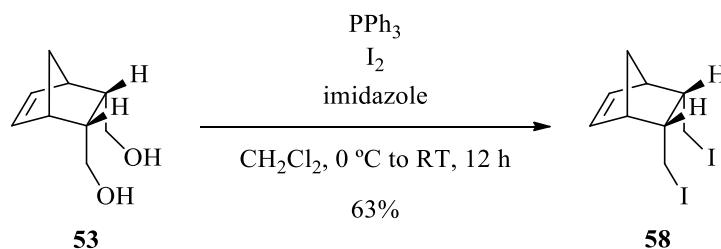
With the successful transformation to the tosyl groups, we next tried to install the alkyne groups using two different methods. Insertion of the alkyne moieties was attempted by using the Grignard reagent ethynyl magnesium bromide, and then trimethylsilylacetylene (TMSA) and *n*BuLi as the acetylide source, but neither method was successful (Scheme 63).



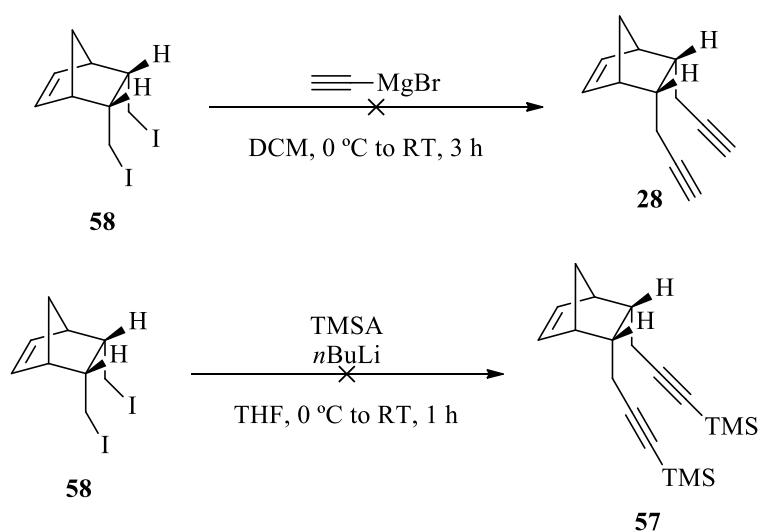
**Scheme 63:** Attempted insertion of alkyne groups into **56**

The same reactions were then repeated using an iodide as the leaving group. The iodo compound was synthesized first from the transformation of ditosylate **56** using sodium iodide (Scheme 64); this was then replaced by the more direct, one-step transformation of diol **53** using the method described by Garegg (Scheme 65).<sup>91</sup>



**Scheme 64:** Conversion of **56** to **58****Scheme 65:** Conversion of **53** to **58**

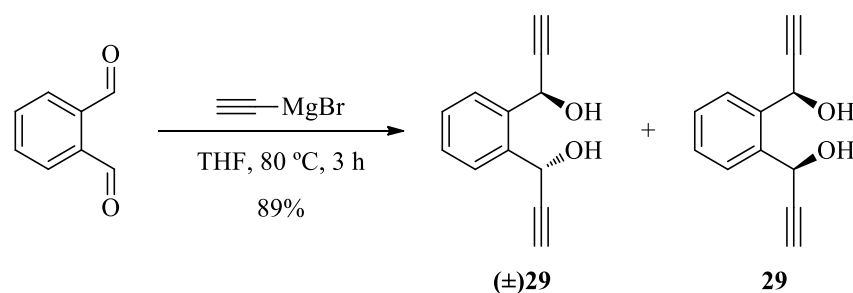
The incorporation of the alkyne groups was then attempted, but neither the reaction using ethynyl magnesium bromide, nor ethynyltrimethylsilane (TMSA) with *n*BuLi yielded the desired product (Scheme 66). Analysis of the <sup>1</sup>H NMR spectrum of the reaction mixture obtained using *bis*TMSA showed the presence of the desired product **28**, albeit in a negligible amount. This is currently as far as the synthesis has progressed.

**Scheme 66:** Attempted incorporation of alkyne groups into **58**

## 2.4 *Meso bis-alkynes 29, 30, 31 & 32*

### 2.4.1 *Meso bis-alkyne 29*

The preparation of compounds **30**, **31** & **32** began with the synthesis of the *meso bis-alkyne 29*, which involves the addition of ethynyl magnesium bromide to the dialdehyde *o*-phthalaldehyde. The addition reaction is not stereoselective, and gave a mixture of the *racemic* and *meso bis-alkynes*. It was attempted in the hope that the separation of the products could be achieved using chromatography. The reaction afforded the mixture of diastereoisomers as an orange oil in 89% yield in a 2:1 ratio (Scheme 67).



**Scheme 67:** Reaction of *o*-phthalaldehyde with ethynyl magnesium bromide

When the orange oil mixture was re-examined it was discovered that orange crystals had begun to form. These orange crystals were collected by filtration and washed with petroleum ether. Analysis of the  $^1\text{H}$  NMR spectrum of the crystals indicated that a single diastereoisomer had crystallised, specifically the one that was believed to be *meso* compound **29** (Figure 6).

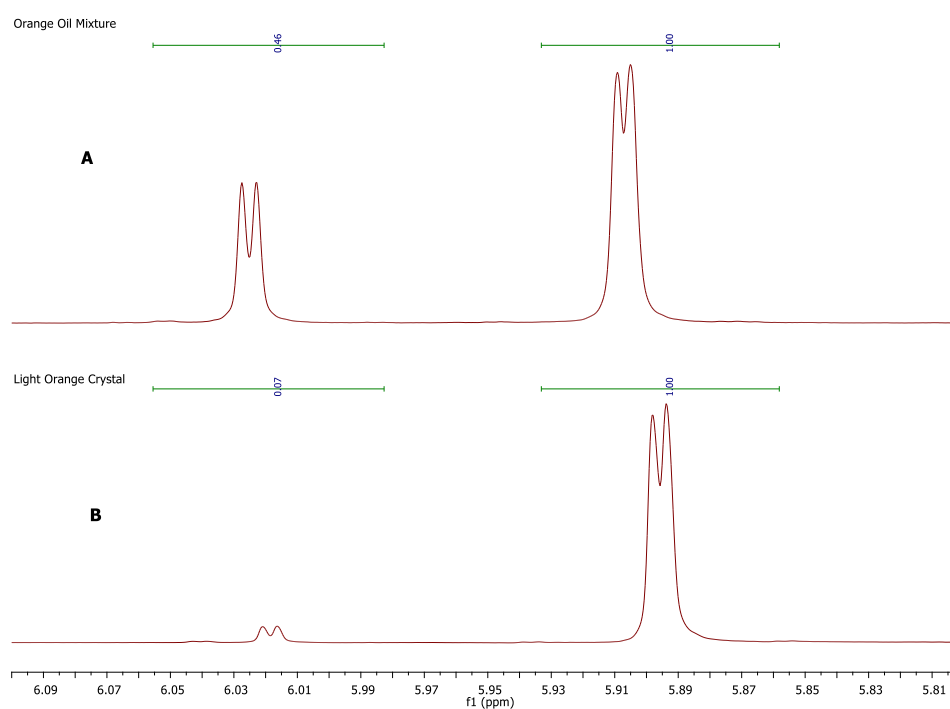


**Figure 6:** **A** -  $^1\text{H}$  NMR spectrum of the diastereoisomer mixture; **B** -  $^1\text{H}$  NMR spectrum of the crystal collected from the mixture

To separate the *meso* compound from the mixture, the mixture was dissolved in  $\text{CH}_2\text{Cl}_2$  and a small amount of petroleum ether was added. Small light orange crystals formed which were collected and dried. The light orange crystals were then recrystallized from hot ethanol giving colourless crystals, which were sent for X-ray analysis. The X-ray analysis of the crystal confirmed that it had the structure of the *meso bis*-alkyne **29** (Figure 7).

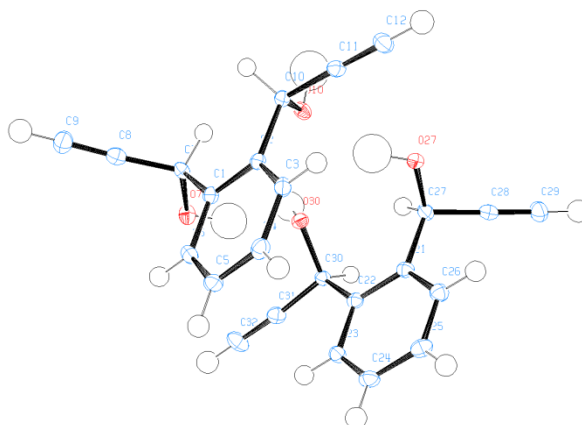


**Figure 7:** ORTEP drawing showing 2 units of *meso bis*-alkyne **29**

Inspection of the  $^1\text{H}$  NMR spectrum of the mixture of diols **29** and ( $\pm$ )**29** shows the expected pair of doublets for the alkyne protons of the two isomers (Figure 9A), at 2.73 and 2.75 ppm, corresponding to the racemic and *meso* forms. Conversion of the mixture of diols into the corresponding diesters using Mosher's acid (Figure 8) was also investigated to observe the effects on chemical shifts.<sup>98</sup>

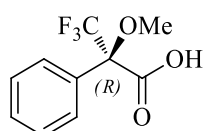
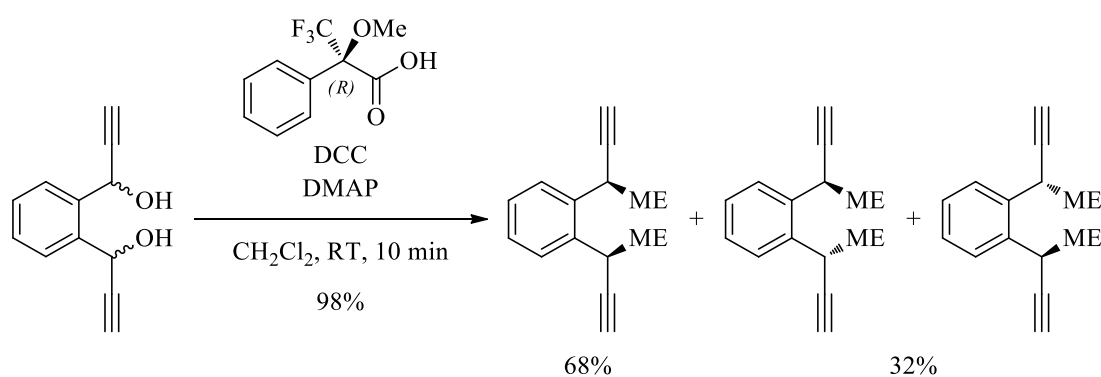


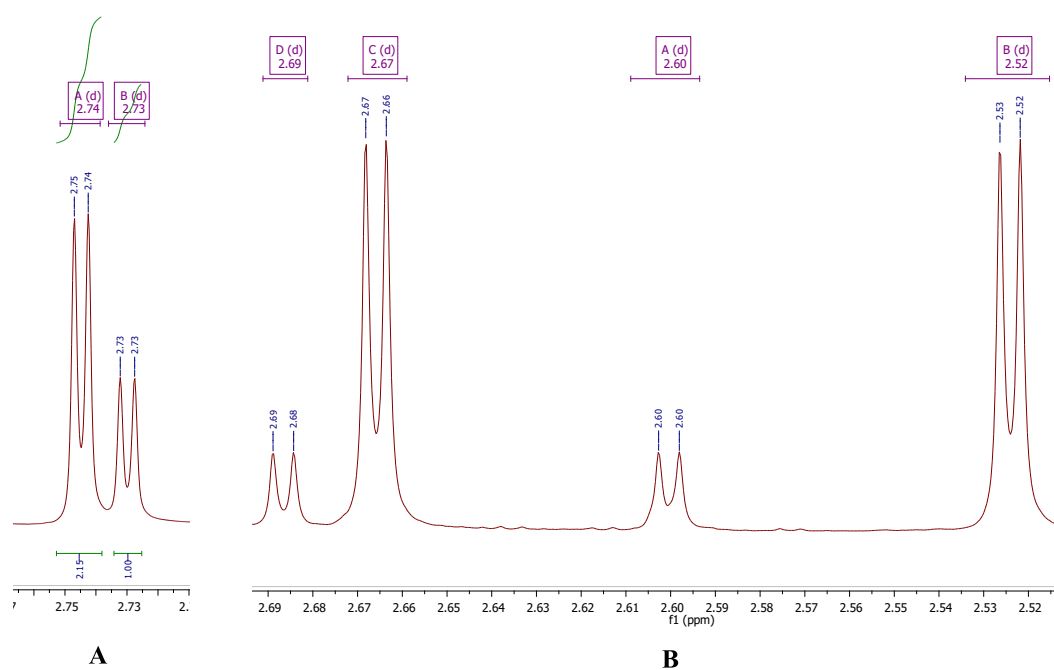
**Figure 8:** (*R*)-Mosher's acid

#### 2.4.1.1 Assignment of configuration of chiral propargylic alcohols using Mosher's ester

Conversion of the racemic form into the Mosher's diesters results in a pair of diastereoisomers, each of which produces one doublet in the  $^1\text{H}$  NMR spectrum. Similar derivatization of the *meso* compound provides a single compound in which the alkyne protons are in different environments (Scheme 68), and therefore also produces a pair of doublets in the  $^1\text{H}$  NMR spectrum (Figure 9B). It is interesting to note that the upfield chemical shift change is larger for the *meso* parent than the racemate; 0.18 & 0.32 ppm for the *meso* and 0.15 & 0.24 ppm for racemate. The larger upfield chemical shift observed for the *meso* parent is consistent with the guidelines described by Mosher. This observation may prove of use in the assignment of stereochemistry in further series of *bis*-alkynes.

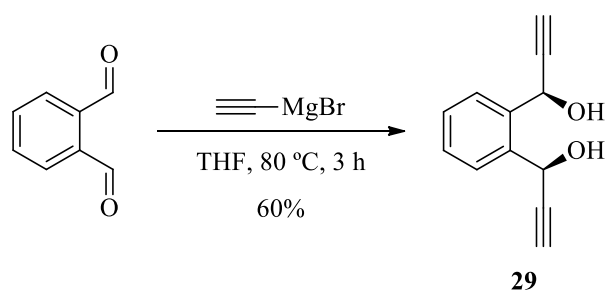


**Scheme 68:** Reaction of diol **29** mixture with Mosher's acid (ME representing Mosher's ester)

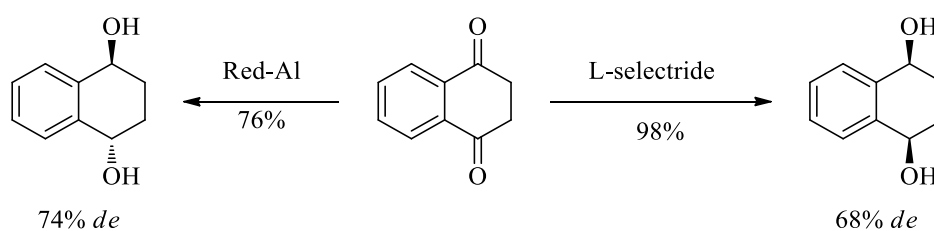


**Figure 9:** **A** -  $^1\text{H}$  NMR spectrum of the mixture of diols; **B** -  $^1\text{H}$  NMR spectrum of the mixture of Mosher diesters

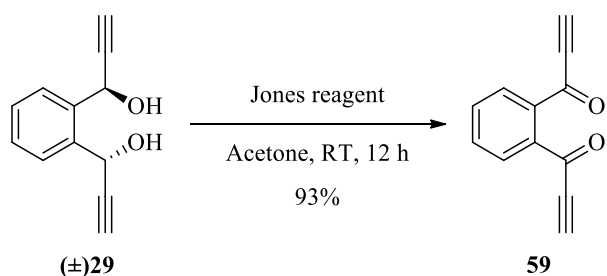
Now that we had a method for successfully synthesizing and isolating compound **29** (Scheme 69), we attempted to improve our synthesis and improve the yield of the desired product. Indeed, the racemic compound that remained, after isolation from the product mixture, can be recycled: oxidation to the ketone followed by a diastereoselective reduction should afford the diol.

**Scheme 69:** Synthesis of **29**

To achieve a diastereoselective reduction, a bulky reducing agent that acts as a single hydride source would be needed.<sup>99</sup> Kündig showed that the use of the reducing agents  $\text{LiAlH}_4$  and  $[\text{Al}(\text{H}_2)(\text{OCH}_2\text{CH}_2\text{OME})_2][\text{Na}]$  (Red-Al) on tetralin-1,4-dione gave the *trans*-diastereoisomer, whereas lithium tri-*sec*-butylborohydride (L-selectride) afforded product enriched with *cis*-diol (Scheme 70).

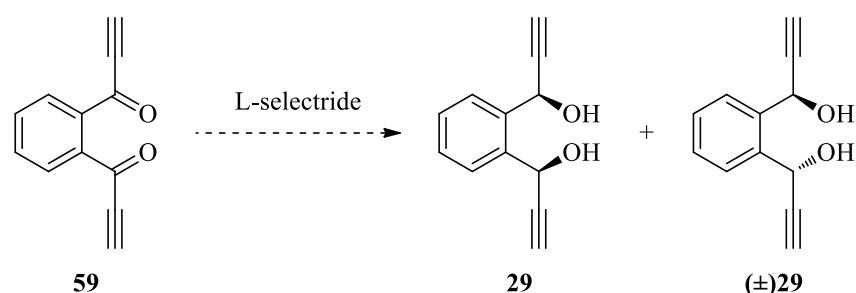
**Scheme 70:** Diastereoselective reduction of tetralin-1,4-dione

In the future, we hope that using L-selectride will give compound **29**, increasing its overall yield and allowing us to recycle by-products. The Jones oxidation of ( $\pm$ )**29** afforded the propargyl dione **59** in a high yield (Scheme 71).

**Scheme 71:** Synthesis of **59** from ( $\pm$ )**29**

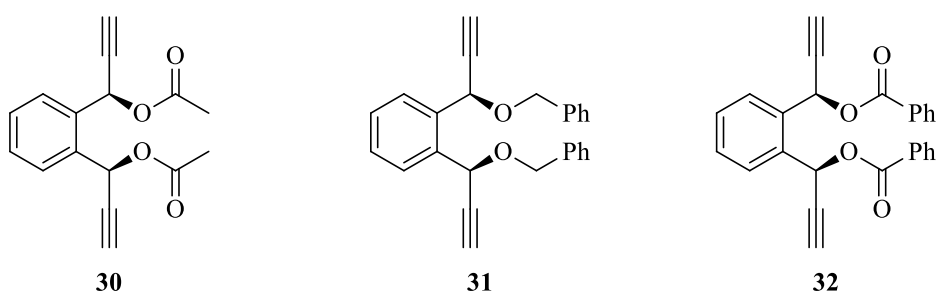
The oxidation of ( $\pm$ )**29** will be followed by the selective reduction of **59** using L-selectride to give the mixture of diols **29** & ( $\pm$ )**29** (Scheme 72). We hope that our results

will reflect those reported by Kündig, with the *meso*-diol **29** being isolated as the major diastereoisomer. A drawback to this synthetic route is the high cost of the reducing agent L-selectride. Although this pathway allows for the use of the reaction by-product ( $\pm$ )**29**, which would otherwise be discarded, the cost of the reducing agent against the amount of **29** returned would need to be evaluated.



**Scheme 72:** Reduction of **59** using L-selectride

Now that we had successfully synthesised *meso bis*-alkyne **29**, the testing of the selective mono-‘click’ reaction could start. In particular, we wanted to alter the  $\beta$ -substituents to see how this affected the selectivity of the mono-‘click’ reaction. Acyl, benzyl and benzoyl groups were targeted to give the *meso*-compounds **30**, **31** and **32** respectively (Scheme 73).

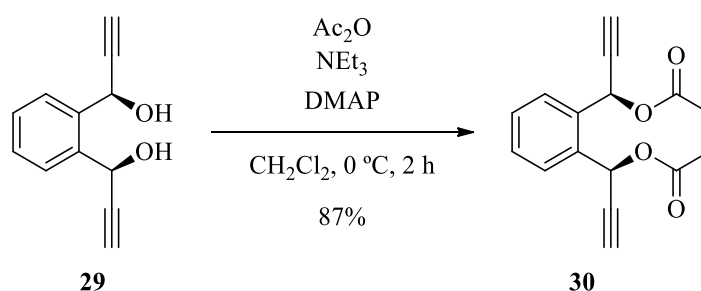


**Scheme 73:** Structures of *meso*-compounds **30**, **31** & **32**

#### 2.4.2 *Meso bis*-alkyne **30**

For further transformations, pure compound **29** was used to ensure that when the reaction was performed, as the relative stereochemistry should be retained, the final product should also be *meso* and remove any need for separation of diastereoisomers. The acylation was carried out using the method reported by Xiao, in which acetic

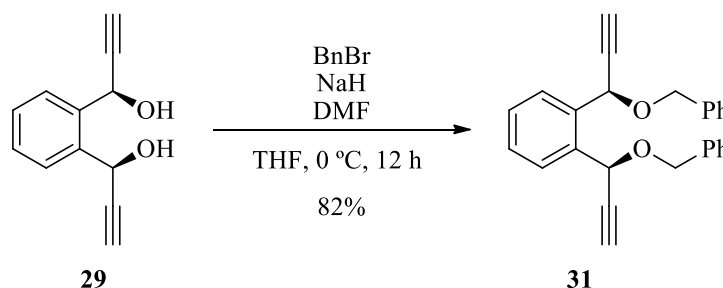
anhydride was used as the acyl source, giving the *bis*-acyl product **30** in high yield (Scheme 74).



**Scheme 74:** Synthesis of **30** from **29**

#### 2.4.3 *Meso bis*-alkyne **31**

For the transformation of alcohols in **29** to benzyl ethers, the method reported by Lee was employed, which utilized benzyl bromide and the strong base sodium hydride.<sup>100</sup> The reaction proved to be extremely efficient, giving the desired compound **31** in high yield (Scheme 75).

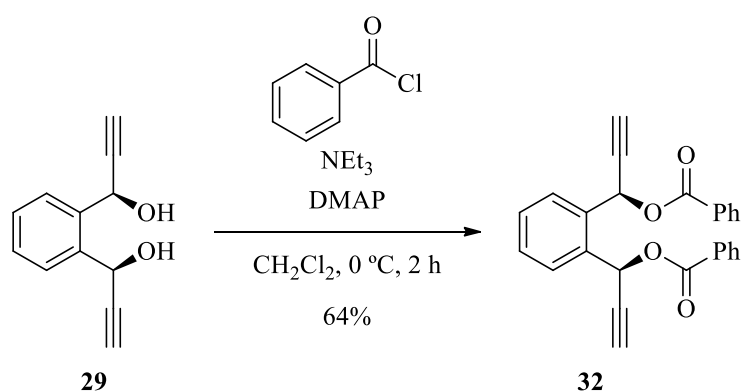


**Scheme 75:** Synthesis of **31** from **29**

#### 2.4.4 *Meso bis*-alkyne **32**

For the transformation of the alcohol to the benzoyl ester, a very similar method to that used for the synthesis of **30** was employed, replacing the acetic anhydride with benzoyl chloride. Although this method was not as high yielding, it still produced pure compound **32** (Scheme 76).





**Scheme 76:** Synthesis of **32** from **29**

#### 2.4.5 *Meso bis-alkyne 60*

So far all the compounds, **29-32**, contain an oxygen  $\beta$ - to the alkyne group. To further test the effects the  $\beta$ -group has on the selectivity of the mono-‘click’ reaction, exchanging the oxygen for another heteroatom such as nitrogen, may provide an interesting starting point. The amino group was chosen, giving new target compound *meso bis-alkyne 60* (Figure 10).

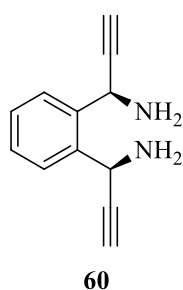
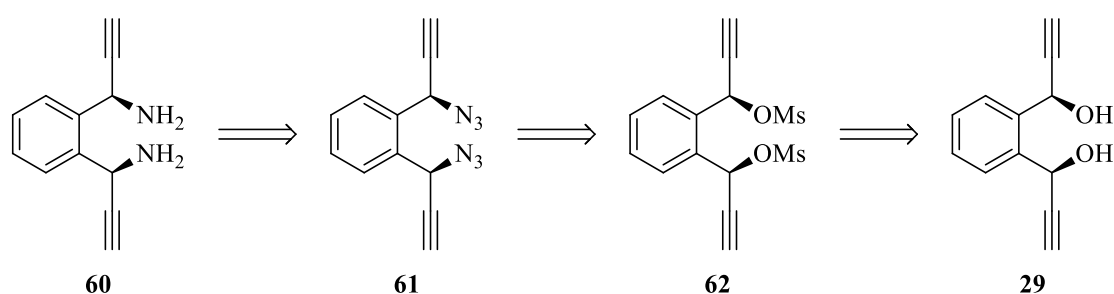


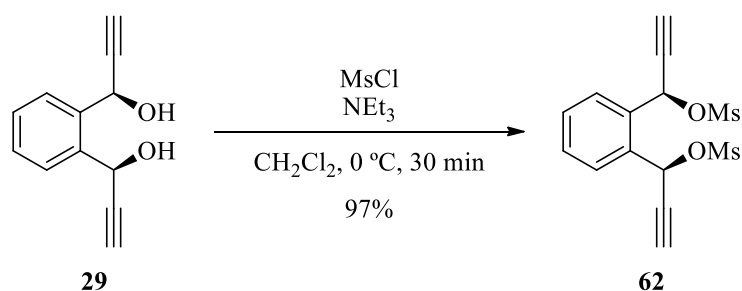
**Figure 10:** Target compound **60**

The conversion of an alcohol to an amine is generally a multistep process: first, the alcohol must be converted into a better leaving group such as a mesyl or tosyl group, which can then be displaced by an azide. Reduction of the azide should give the target compound **60**, while retaining the relative stereochemistry of **29** (Scheme 77).



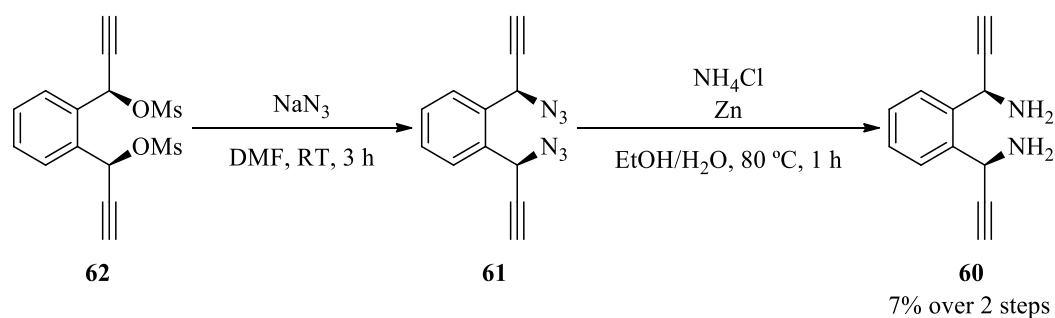
**Scheme 77:** Retrosynthetic plan for the synthesis of **60**

The mesylation reaction was carried out using methanesulfonyl chloride in the presence of an excess of triethylamine according to the method described by Baskaran.<sup>101</sup> The reaction was extremely efficient, with isolation giving near quantitative yields of **62** (Scheme 78). However, compound **62** was extremely air sensitive and unstable, and decomposed before spectral analysis could be performed; hence, in subsequent synthesis it was used immediately in the next reaction without complete isolation.



**Scheme 78:** Synthesis of **62** from **29**

Substitution of the mesyl group was attempted using an excess of sodium azide in DMF, stirred at room temperature, through a base-catalysed nucleophilic substitution.<sup>101</sup> The azide product **61** was not isolated due to the potential explosive properties associated with small azide compounds, and so was carried forward to the next step without further purification. The reduction of the azide to the amine was completed using the method described by Zhang, using zinc powder and ammonium chloride.<sup>102</sup> Analysis of the <sup>1</sup>H NMR spectrum of the crude reaction showed signals corresponding to a mixture of the fully converted *bis*-amine, as well as the mono-reacted and original starting diol. Purification of the mixture by column chromatography yielded the final product **60** in 7% yield over the two steps (Scheme 79).



**Scheme 79:** Synthesis of target compound **60** from **62**

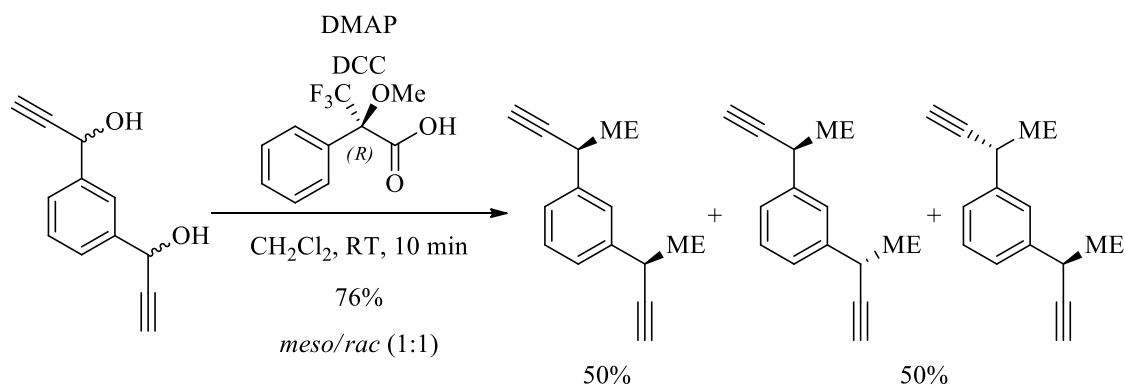
Although compound **60** was successfully synthesized, the poor yield obtained means that the synthesis needs to be improved before enough material can be produced to test the selective mono-‘click’ reaction.

#### 2.4.6 Synthesis of *meso*-compounds using *meta*- & *para*-phthalaldehyde

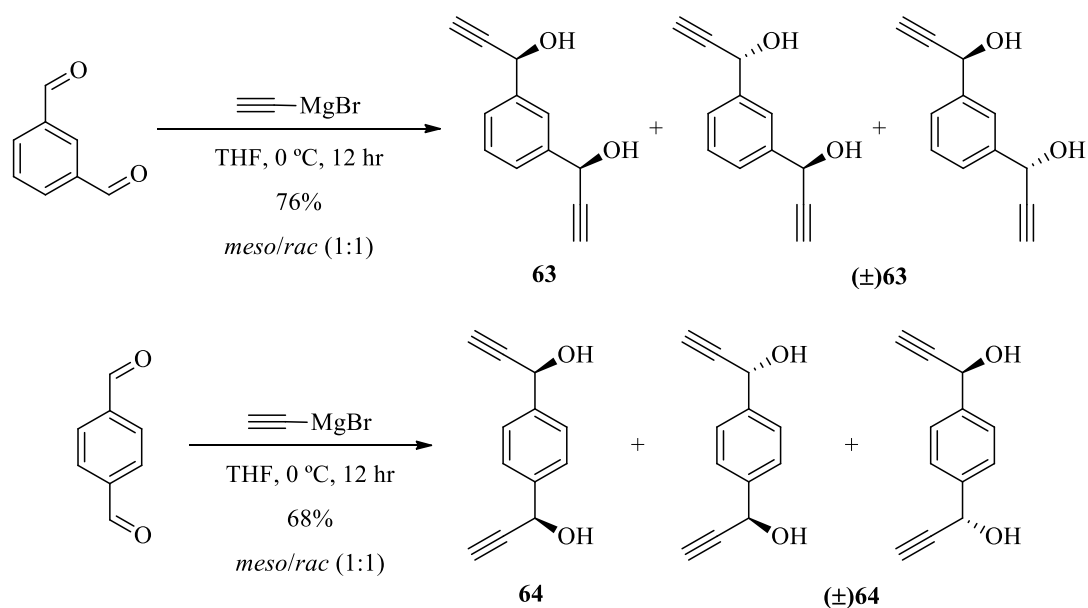
At this point, we had altered the group in the  $\beta$ -position to the alkyne moiety and attempted to change the heteroatom as a way to compare their effects on the mono-‘click’ reaction. Furthermore, we believed that it might be interesting to study the effect of the distance between the two alkyne groups on the selectivity of the ‘click’ reaction. In the examples reported for the mono-‘click’ reaction of achiral *bis*-alkynes, the two alkyne groups were in close proximity.<sup>15,76</sup> If the addition of the alkynyl Grignard reagent is applied to *meta*- and *p*-phthalaldehyde, *meso bis*-alkyne systems with increasing distances between the reactive alkyne sites would be produced. These systems would provide an interesting comparison and might help explore whether the relative position of the alkynes moiety is a factor in the selectivity.

Fortunately, the non-selective Grignard addition yielded the *meso*-diastereoisomer as the main product during the synthesis of **29**. We were fortunate again that the *meso*-product formed crystals, allowing for its easy separation from the mixture of diastereoisomers. When the reaction was performed on *meta*- and *para*-phthalaldehyde, neither of the reactions gave a product mixture containing a solid, and thick orange oils were obtained in both cases. Remarkably, in both of these examples, the signals in the <sup>1</sup>H NMR spectra for the *meso* and *racemic* forms of the diol products **63**/(±)**63** and **64**/(±)**64** are coincident. Again, Mosher’s esters were prepared using a sample of the

crude reaction mixtures, which after NMR spectra analysis, clearly showed the presence of both the *meso* and *racemic*-products in a near 1:1 ratio in both cases (Scheme 81).



**Scheme 80:** Reaction of *meta*-diol mixture with Mosher's acid (ME representing Mosher's ester)



**Scheme 81:** Grignard addition to *meta*- and *para*-phthalaldehyde

Unfortunately, the diastereoisomers were inseparable using column chromatography, and multiple recrystallization solvent systems also failed to yield either as a solid, returning only the mixture of diastereoisomers as an oil. Currently this is as far in the synthesis of *meso bis*-alkynes **63** & **64** that we have achieved.

Although the use of chiral auxiliaries for the enantioselective addition to phthalaldehyde has been reported,<sup>103,104</sup> the *racemic bis*-alkyl was the only compound targeted. A

possible route to prepare the *meso* structure as the main product could be obtained by applying the method used in the synthesis of **29**: the unwanted diastereoisomer was recycled by oxidation of the diol mixture followed by a selective reduction. Although this may not give a single diastereoisomer as the product, the presence of a larger proportion of one may help in the recrystallization and separation.

### 3.0 The asymmetric 'click' reaction with *meso bis*-alkynes

With a small pool of *meso bis*-alkynes in hand (Figure 11), we were able to begin the testing for the asymmetric 'click' reaction.

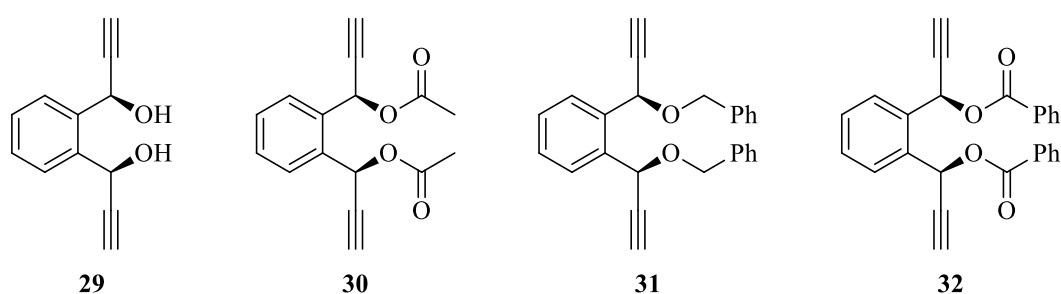
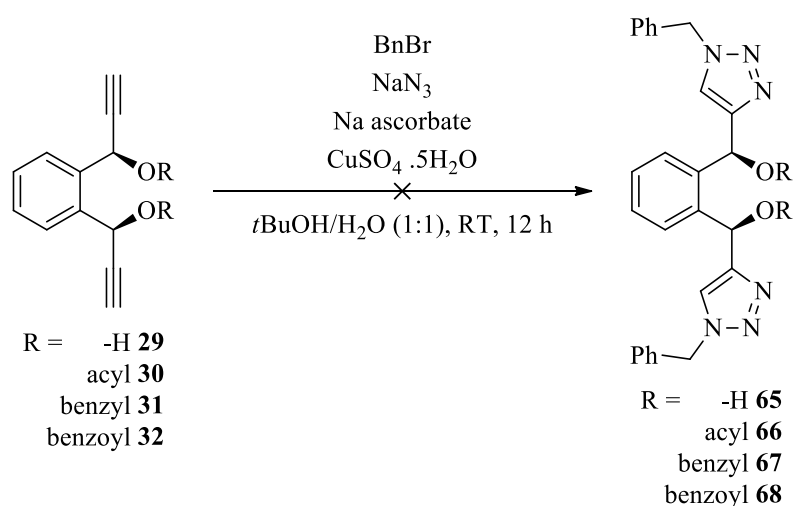


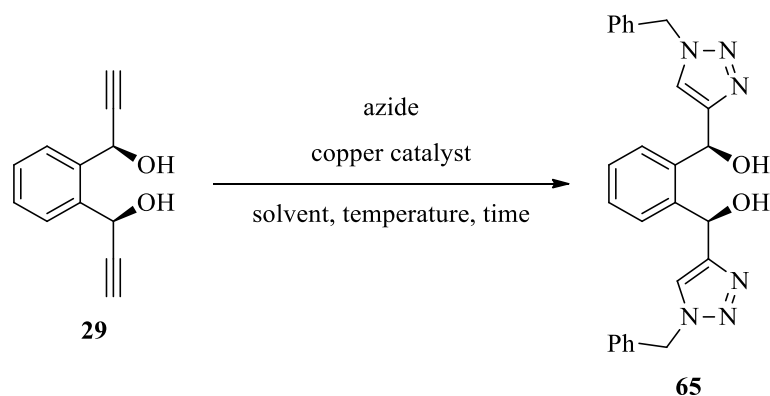
**Figure 11:** Synthesised *meso bis*-alkynes for testing

To begin, *meso* compounds **29**, **30**, **31** & **32** were submitted to standard CuAAC reaction conditions with an excess of azide reactant, to confirm that both alkynes are reactive and would give the corresponding *bis*-triazole product. When the CuAAC reaction was performed on these compounds, however, the starting material was the only compound observed (Scheme 82).



**Scheme 82:** CuAAC reaction with *meso bis*-alkynes

As the reaction using the standard CuAAC conditions was not successful, it was repeated on compound **29**, varying how the azide was introduced, the copper catalyst source, the solvent, as well as the reaction time and temperature (Scheme 83, Table 5).



**Scheme 83:** CuAAC reaction with **29**

**Table 5:** Attempts to perform the CuAAC reaction on **29**

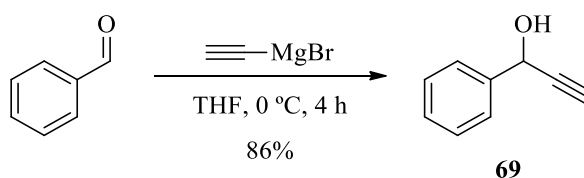
Experiment	Azide	Cu source	Solvent	Temp (°C)	Time	Yield
<b>5A</b>	BnBr + NaN <sub>3</sub>	CuSO <sub>4</sub> ·5H <sub>2</sub> O*	<i>t</i> BuOH/H <sub>2</sub> O <sup>†</sup>	RT	12 h	SM
<b>5B</b>	BnBr + NaN <sub>3</sub>	CuSO <sub>4</sub> ·5H <sub>2</sub> O*	<i>t</i> BuOH/H <sub>2</sub> O <sup>†</sup>	MW 100	1 h	SM
<b>5C</b>	BnN <sub>3</sub>	Cu powder	<i>t</i> BuOH/H <sub>2</sub> O <sup>†</sup>	RT	12 h	SM
<b>5D</b>	BnN <sub>3</sub>	Cu powder	<i>t</i> BuOH/H <sub>2</sub> O <sup>†</sup>	MW 120	1 h	SM
<b>5E</b>	BnN <sub>3</sub>	CuSO <sub>4</sub> ·5H <sub>2</sub> O*	<i>t</i> BuOH/H <sub>2</sub> O <sup>†</sup>	RT	12 h	SM

Experiment	Azide	Cu source	Solvent	Temp (°C)	Time	Yield
<b>5F</b>	BnN <sub>3</sub>	2 Eq. CuSO <sub>4</sub> ·5H <sub>2</sub> O*	<i>t</i> BuOH/H <sub>2</sub> O <sup>†</sup>	RT	12 h	SM
<b>5G</b>	BnN <sub>3</sub>	CuCl	2,5-hexadione	0	12 h	SM
<b>5H</b>	BnBr + NaN <sub>3</sub>	CuCl	2,5-hexadione	RT	12 h	SM
<b>5I</b>	BnBr + NaN <sub>3</sub>	CuCl	<i>t</i> BuOH/H <sub>2</sub> O <sup>†</sup>	RT	12 h	SM
<b>5J</b>	BnBr + NaN <sub>3</sub>	CuCl	<i>t</i> BuOH/H <sub>2</sub> O <sup>†</sup>	MW 120	1 h	SM

\* In the presence of sodium ascorbate; <sup>†</sup> 1:1 ratio of solvents

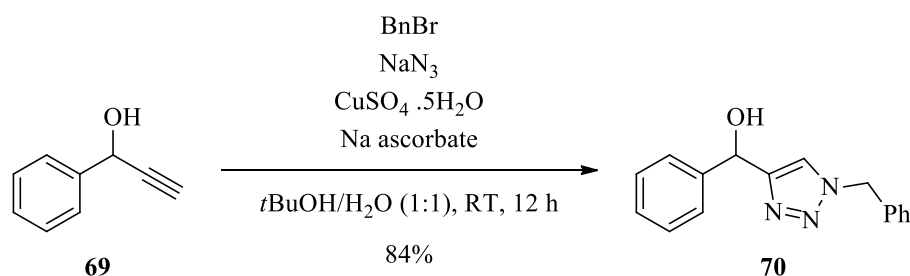
When the original experiment **5A** gave only starting material, we first hoped that an increase in the reaction temperature (**5B**) would afford the desired product. When this also failed, the azide source was altered. Instead of forming the azide *in-situ*, from sodium azide and benzyl bromide, benzyl azide was prepared prior to the reaction and then added to the reaction mixture (**5C-G**). Previously within the group, we have had success in performing the CuAAC reaction using a different source for the copper catalyst, and so copper powder (**5C-D**) and copper chloride (**5G-J**) were tested. So far, every modification of the reaction conditions failed to yield the desired product; in a final attempt to synthesize the *bis*-triazole product, the reaction solvent was changed. 2,5-Hexadione, an unusual solvent, has been reported to be the optimum solvent to achieve the successful mono-‘click’ of achiral *bis*-alkyne systems.<sup>75</sup>

As none of the reaction condition alterations improved the outcome, we began to investigate why the reaction was not proceeding as expected. To confirm that aromatic propargylic alcohols are capable of forming a triazole through the CuAAC reaction, 1-phenylprop-2-yn-1-ol was synthesised (Scheme 84).



**Scheme 84:** Synthesis of 1-phenylprop-2-yn-1-ol

For the test reaction, obtaining the product as a single enantiomer was not required; hence a non-selective Grignard addition was used. Once synthesized, the standard CuAAC conditions were used on compound **69** to form the triazole (Scheme 85).



**Scheme 85:** CuAAC reaction with **69**

The reaction showed that aromatic propargylic alcohols were able to form triazoles through the CuAAC reaction, so this was not the issue preventing the click reaction affording **29**.

Next, we looked at how the mechanism of this reaction would proceed, specifically if having the two alkyne groups in close proximity alters the standard mechanistic route, hindering the reaction. As discussed above, a large number of mechanistic studies of the CuAAC reaction have been undertaken. Initially, the monocopper species was believed to be the active catalyst; however, later, dicopper complexes were reported to act as the main reactive species. Indeed, Bertrand reported the isolation of one such *bis*-copper acetylide.<sup>105</sup> The group suggested that the *mono*- and *bis*-copper pathways are active in the CuAAC reaction but that the latter is the more kinetically favoured. If the *bis*-copper pathway is the preferred one, then having the two alkyne groups close to each other may be leading to a copper-alkyne complex system involving both alkynes, so sterically hindering the insertion of the azide and blocking the reaction (Figure 12).

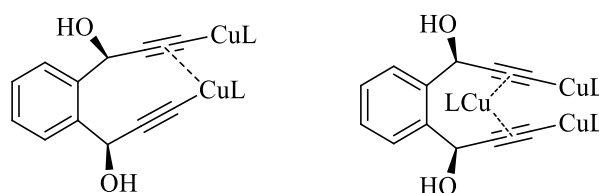


**Figure 12:** Possible structures of *bis*-copper-alkyne complexes

Zhou reported the highest selectivity in the asymmetric ‘click’ reaction of quaternary oxindoles when the ligand 2,6-bis[(4*S*)-4-phenyl-2-oxazolonyl]pyridine **L1** was used (Figure 13). In this copper-ligand species, the copper is coordinated to the three nitrogen



atoms of the ligand, so that its ability to coordinate the second alkyne is reduced, which may overcome the issue caused by the *bis*-copper pathway.

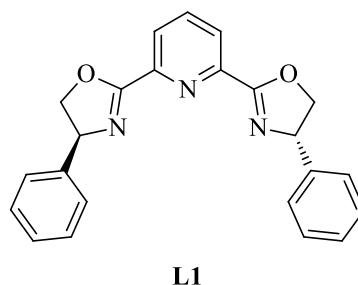
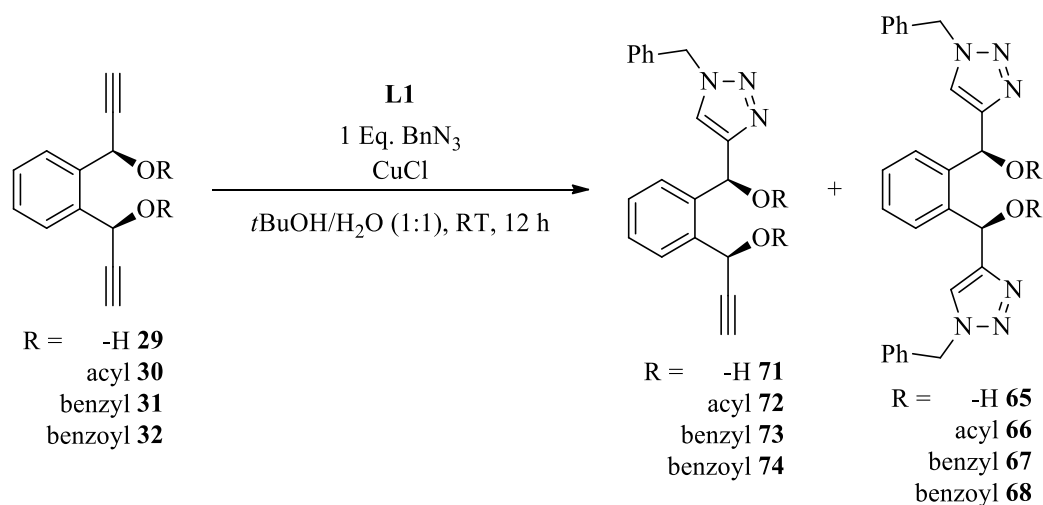


**Figure 13:** Structure of **L1**

Although we had not managed to synthesise the *bis*-triazole, we began to attempt the asymmetric ‘click’ reaction on the *meso bis*-alkyne compounds in the presence of commercially available **L1** (Scheme 86, Table 6). For these reactions, a single equivalent of pre-prepared azide was used.

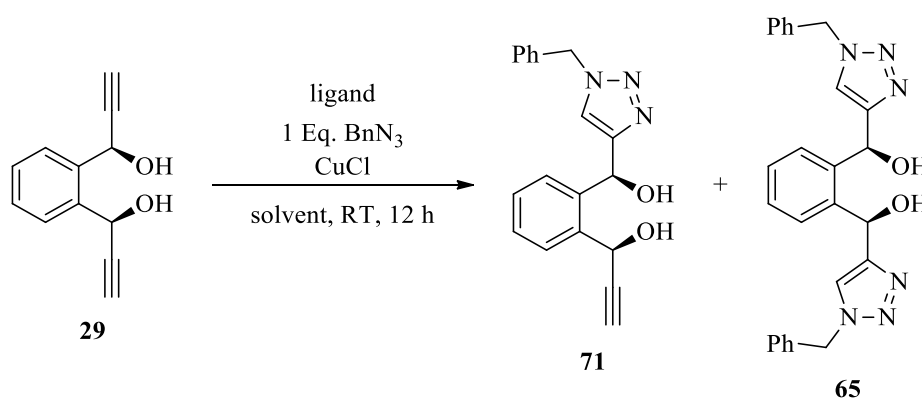


**Scheme 86:** Asymmetric ‘click’ reactions of *meso bis*-alkynes **29-32**

**Table 6:** Asymmetric click of *meso bis*-alkynes **29-32**

Experiment	<i>Meso bis</i> -alkyne	Yield (%)
<b>6A</b>	<b>29</b>	SM
<b>6B</b>	<b>30</b>	SM
<b>6C</b>	<b>31</b>	SM
<b>6D</b>	<b>32</b>	SM

With none of the reactions involving the *meso bis*-alkynes yielding the corresponding triazole product, the reaction was repeated on **29** using different chiral ligands (Figure 14) and in two different solvent systems (Scheme 87, Table 7). Zhou reported enantioselectivity of between 50-70% ee when the ligands **L2**, **L3** & **L4** were employed and we hoped to find a system that would reproduce these results.



**Scheme 87:** Asymmetric click of *meso bis*-alkynes **29**

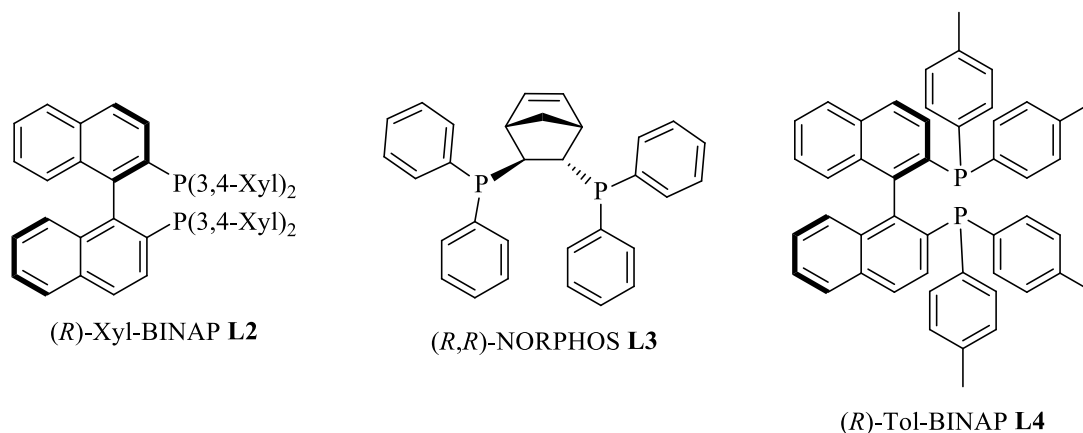


**Figure 14:** Structures of chiral ligands used

**Table 7:** Asymmetric click of *meso bis*-alkynes **29**

Experiment	Solvent	Ligand	Yield (%)
<b>7A</b>	<i>t</i> BuOH/H <sub>2</sub> O <sup>†</sup>	<b>L1</b>	SM
<b>7B</b>	<i>t</i> BuOH/H <sub>2</sub> O <sup>†</sup>	<b>L2</b>	SM
<b>7C</b>	<i>t</i> BuOH/H <sub>2</sub> O <sup>†</sup>	<b>L3</b>	SM
<b>7D</b>	<i>t</i> BuOH/H <sub>2</sub> O <sup>†</sup>	<b>L4</b>	SM

Experiment	Solvent	Ligand	Yield (%)
7E	2,5-hexadione	L1	SM
7F	2,5-hexadione	L2	SM
7G	2,5-hexadione	L3	SM
7H	2,5-hexadione	L4	SM

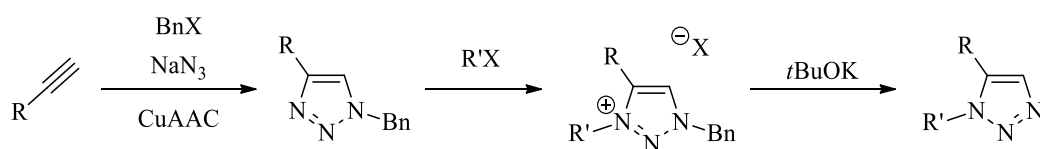
† 1:1 ratio of solvents

With all of the reactions only returning the starting compound **29**, further investigation into different reaction conditions is required.

#### 4.0 Future work

##### 4.1 Manipulation of triazoles

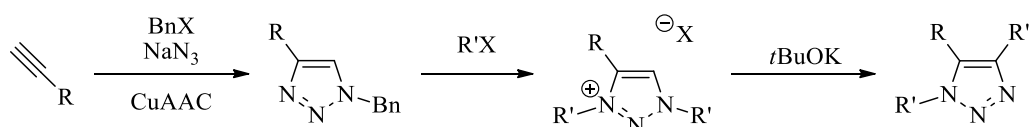
After producing an efficient pathway for the ruthenium-free synthesis of 1,5-triazoles by proceeding through the 1,3,4-triazolium salt intermediate, we would like to explore the scope of the route (Scheme 88).



**Scheme 88:** Ruthenium-free synthesis of 1,5-triazoles

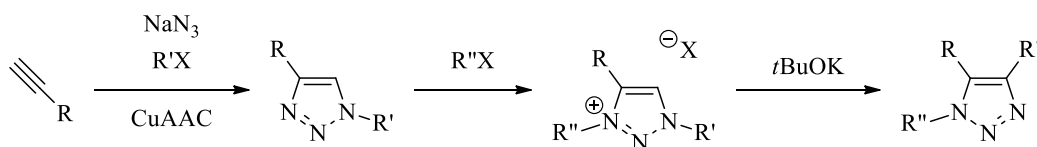
Apart from testing on the cyanoacetate-derived prochiral bis-alkyne **19**, we have only tested systems based on the 1-benzyl-4-phenyl-1,2,3-triazole, with the *N*-alkylation at the N3 position being performed using simple linear alkyl groups. If testing proves that the pathway can be applied to different groups, then we would wish to compare our results to those reported using the RuCAAC one. It may be possible to improve these reactions by applying our method, increasing the yield and reducing the cost of the reaction.

We would also perform further tests on the 1,3,4- to 1,4,5-trisubstituted triazole interconversion pathway to determine the scope and possible synthetic applications of the route (Scheme 89).



**Scheme 89:** 1,3,4- to 1,4,5-trisubstituted triazole interconversion

If this is successful then we would attempt to change the benzyl group for another alkyl group. If this is possible, then we would have a ruthenium-free pathway by which one is able to designate each group at the 1-, 4- and 5-position (Scheme 90).

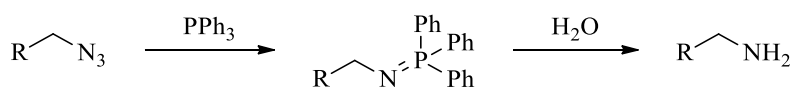


**Scheme 90:** Stereoselective synthesis of 1,4,5-trisubstituted triazoles

#### 4.2 Synthesis of *meso bis*-alkynes

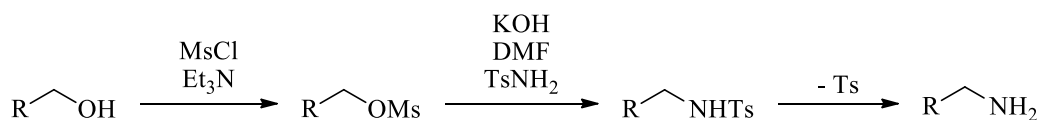
In the synthesis of the *meso bis*-alkynes, compounds **28** & **43** are both at a stage in the synthesis where the alkyne moiety has yet to be inserted. We have attempted to insert the alkyne group using a Grignard addition to replace various leaving groups, as well as using *n*BuLi to form an acetylide species. The reaction was repeated multiple times using different conditions; however, more time could be spent to discover a successful set of conditions. Finally, a different selection of leaving groups could be tested.

Although the synthesis of compound **60** was successful, the yield obtained was extremely poor and we were unable to isolate the compound from the crude product mixture. This reaction could perhaps be improved, specifically the transformation from the mesyl leaving group to the amine, as these are the low-yielding steps. One option is that once the azide has been installed, the Staudinger reaction could be performed to give the primary amine (Scheme 91).



**Scheme 91:** Staudinger reaction

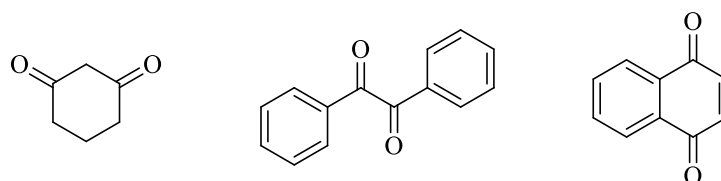
Another option is the transformation of the *bis*-alcohol **29** into a *bis*-tosylamide moiety, proceeding through a mesylate species, at which point the tosyl group may be removed (Scheme 92).<sup>106</sup>



**Scheme 92:** Conversion of a primary alcohol to a primary amine

For compounds **63** & **64**, the *meso* and *racemic*-compounds were obtained in a 1:1 ratio, but it was not possible to separate them using standard separation methods. We would like to attempt this separation, ideally using recrystallization as the method. As these are novel compounds, a large number of recrystallization systems would need to be tested, if it is even possible for either to form crystals.

The synthesis of compounds **29-32** began with the addition to the *bis*-aldehyde phthalaldehyde. Although these reactions are neither elegant nor very efficient, they are a quick path to reliably form propargylic alcohols. More *meso bis*-alkynes could be synthesized by using other compounds susceptible to Grignard reagent addition such as a *bis*-ketone species. Examples of such compounds are readily available commercially, some at low cost, which would be ideal because of the non-enantioselectivity of the reaction (Scheme 93).



**Scheme 93:** *Bis*-ketone candidates for the synthesis of new *meso bis*-alkynes

The successful synthesis of such *meso bis*-alkynes would provide a large pool of test compounds for the investigation of the asymmetric ‘click’ reaction.

### 4.3 Asymmetric ‘click’ reaction

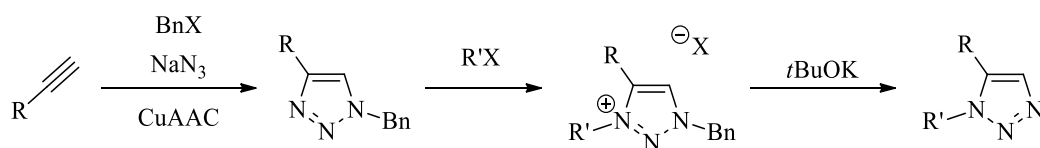
Due to the large amount of time taken in the synthesis of the *meso bis*-alkynes, we were not able to perform as many tests as we would have liked, to achieve the successful asymmetric ‘click’ reaction. In future we would wish to continue with these tests, employing various chiral ligands and reaction conditions to try to achieve a high yield and selectivity. The synthesis of a larger pool of compounds would allow for a greater number of test reactions to be performed, giving a scope for the reaction.

Currently there is an issue where the two alkynes are in close proximity, possibly caused by a laddering effect of a *bis*-copper-alkyne species hindering the reaction. If the synthesis of compounds **63** & **64** is successful then this may provide systems where the alkynes are further apart, allowing them to react more independently.

If the asymmetric click reaction is successful, then the absolute configuration of the product will need to be determined. This will be done using techniques such as X-ray crystallography or with methods similar to determination using Mosher’s esters. When this is complete, we hope to be able to report the relationship between the chirality of the ligand and the chirality of the *mono*-‘click’ product that is produced. Next, the reaction will be repeated, using the opposite enantiomer of the ligand to test if the opposite enantiomer of the product is observed.

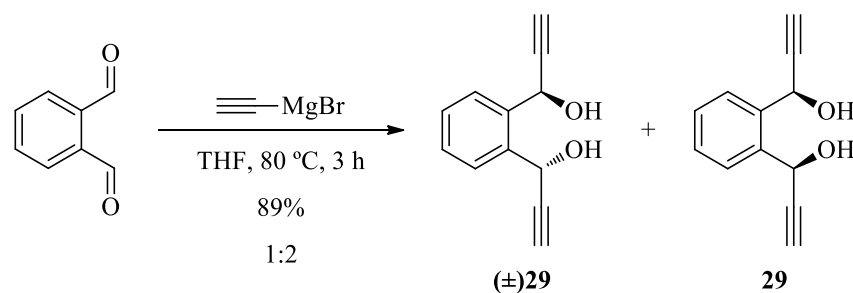
### 5.0 Conclusion

In conclusion, during this project we have successfully been able to provide a reliable new synthetic pathway for the production of 1,5-disubstituted triazoles, making use of the copper-catalysed ‘click’ reaction (Scheme 94). During this research we encountered an unusual rearrangement to get a 1,4,5-trisubstituted triazole, which although we have not successfully been able to repeat, we shall continue to look into its availability as a new pathway.



**Scheme 94:** New pathway for the synthesis of 1,5-triazoles using the CuAAC reaction

The synthesis of the *meso bis*-alkynes proved to be extremely difficult, with most needing further work. However, we had a great deal of success in synthesising *meso*-1,2-*bis*-(prop2-yn-1-ol)benzene **29**, and were further fortunate in the ability to separate and purify the *meso* compound using recrystallization (Scheme 95). This novel synthesis led to the production of more *meso bis*-alkynes by various transformations at the propargylic alcohol of **29** (Figure 15).



**Scheme 95:** Reaction of *o*-phthalaldehyde with ethynyl magnesium bromide

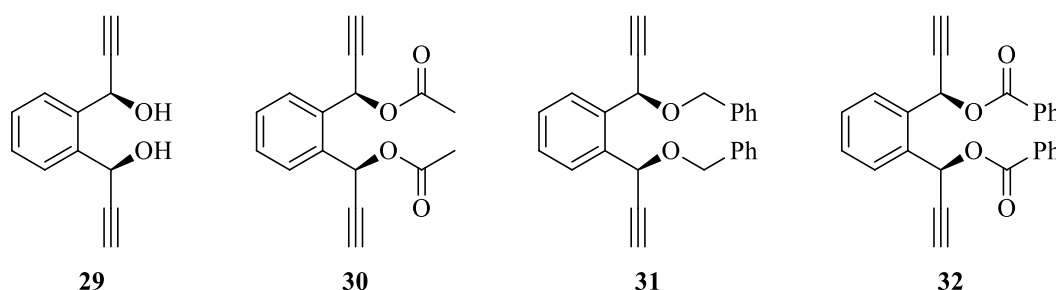


**Figure 15:** Synthesised *meso bis*-alkynes for testing

Finally, although we were not able to react any of *meso bis*-alkynes using the CuAAC reaction, we believe that this may be caused by strong intermolecular forces between the molecules, stopping the reaction from taking place.

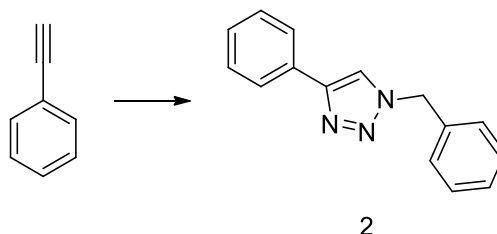
## **Chapter 3: Experimental**



## General Experimental

Unless otherwise stated, all starting materials were purchased from commercial suppliers and were used without further purification. If necessary, solvents were dried in the usual manner; THF and EtO<sub>2</sub> were distilled from the sodium benzophenone ketyl radical, and toluene, CH<sub>2</sub>Cl<sub>2</sub>, MeCN, pyridine and DMF were distilled from CaH<sub>2</sub>. Petroleum ether 40/60 was distilled in the lab prior to use. All non-aqueous reactions were carried out under an atmosphere of nitrogen or argon using flame-dried glassware, with liquid reagents and solvents being added to the reaction vessel by means of syringes through rubber septa.

TLC analysis was carried out on commercially available Kieselgel aluminium-backed plates. Visualization was accomplished by UV fluorescence, basic KMnO<sub>4</sub> solution and heat, phosphomolybdic acid and heat, acidic dinitrophenylhydrazine solution and heat, or acidic vanillin solution and heat. Column chromatography was carried out on Davisil® chromatographic silica media LC60Å 40-63 µm using standard methods. Melting points were obtained using a Büchi Melting Point B-545 apparatus and are uncorrected. IR spectra were recorded in the range 4000-400 cm<sup>-1</sup> on a Perkin-Elmer Spectrum 100 FT-IR spectrophotometer as thin films on KBr plates or as solid samples on diamond windows. NMR spectra were recorded on a Bruker Ascend™ 500 spectrometer at 500 MHz for <sup>1</sup>H NMR & 126 MHz for <sup>13</sup>C NMR, or a Bruker Ultrashield™ 400 plus spectrometer at 400 MHz for <sup>1</sup>H NMR & 101 MHz for <sup>13</sup>C NMR. Chemical shifts were recorded in parts per million (ppm) and are referenced to either tetramethylsilane or the residual protons (<sup>1</sup>H) or carbons (<sup>13</sup>C) of the deuterated solvents used. Mass spectra were determined at the EPSRC Mass Spectrometry Unit at the University of Wales, Swansea. Single crystal X-ray structures were determined at the School of Chemistry, University of St Andrews.

**1-Benzyl-4-phenyl-1*H*-1,2,3-triazole 2**<sup>107</sup>

Chemical Formula: C<sub>15</sub>H<sub>13</sub>N<sub>3</sub>

Molecular Weight: 235.28

**Original synthetic method:**

Benzyl azide (3.90 g, 29.32 mmol) was dissolved in a BuOH/H<sub>2</sub>O (1:1, 120 mL) mixture with stirring. Sodium ascorbate (0.582 g, 2.94 mmol), phenyl acetylene (3.46 mL, 31.57 mmol) and copper sulfate (0.469 g, 1.87 mmol) were added, and the solution stirred vigorously overnight. The solution was diluted with cold H<sub>2</sub>O; the solid that formed was collected using suction filtration and washed with cold H<sub>2</sub>O. The solid was dissolved in CH<sub>2</sub>Cl<sub>2</sub>, the solution dried with anhydrous MgSO<sub>4</sub>, and impurities removed with activated charcoal. The solution was filtered through Celite and the solvents removed under reduced pressure. The crude product was recrystallized from CH<sub>2</sub>Cl<sub>2</sub>/petroleum ether 40/60, yielding the titled compound as large colourless crystals (5.653 g, 82%).

**One-pot procedure:**

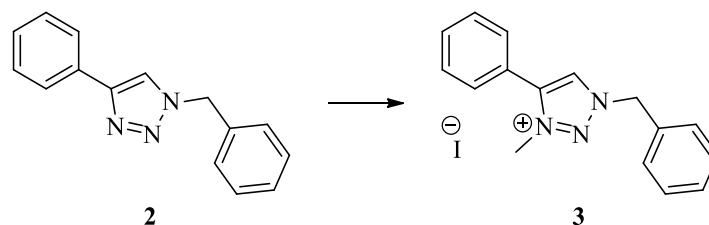
Sodium azide (2.14 g, 32.94 mmol) was dissolved in a BuOH/H<sub>2</sub>O (1:1, 120 mL) mixture with stirring. Benzyl bromide (3.6 mL, 30.27 mmol) was added and the mixture stirred for 10 min. Sodium ascorbate (0.78 g, 3.94 mmol), phenyl acetylene (3.3 mL, 30.08 mmol) and copper sulfate (0.99 g, 3.97 mmol) were added, and the solution stirred vigorously overnight. The solution was diluted with cold H<sub>2</sub>O; the solid that formed was collected using suction filtration and washed with cold H<sub>2</sub>O. The solid was dissolved in CH<sub>2</sub>Cl<sub>2</sub>, the solution dried with anhydrous MgSO<sub>4</sub>, and impurities removed with activated charcoal. The solution was filtered through Celite and the solvents

removed under reduced pressure. The crude product was recrystallized from CH<sub>2</sub>Cl<sub>2</sub>/petroleum ether 40/60, yielding the titled compound as large colourless crystals (6.06 g, 87%).

**Microwave-assisted one-pot method:**

Sodium azide (0.10 g, 1.53 mmol) was dissolved in a BuOH/H<sub>2</sub>O (1:1, 4 mL) mixture in a small microwave vial with stirring. Benzyl bromide (0.13 mL, 1.09 mmol), sodium ascorbate (0.019 g, 0.096 mmol), phenyl acetylene (0.11 mL, 1.0 mmol) and copper sulfate (0.021 g, 0.09 mmol) were added to the solution. The reaction was submitted to microwave irradiation for 10 min at 125 °C. The solution was diluted with cold H<sub>2</sub>O; the solid that formed was collected using suction filtration and washed with cold H<sub>2</sub>O. The solid was dissolved in CH<sub>2</sub>Cl<sub>2</sub>, the solution dried with anhydrous MgSO<sub>4</sub>, and impurities removed with activated charcoal. The solution was filtered through Celite and the solvents removed under reduced pressure. The crude product was recrystallized from CH<sub>2</sub>Cl<sub>2</sub>/petroleum ether 40/60, yielding the titled compound as large colourless crystals (0.22 g, 90%).

**1-Benzyl-4-phenyl-1*H*-1,2,3-triazole 2:** m.p. 130-131 °C, lit. 129-129.5 °C;<sup>107</sup> IR (neat): 3122, 1466, 1224, 1075, 1049, 766, 728, 693 cm<sup>-1</sup>; <sup>1</sup>H NMR (CDCl<sub>3</sub>, 400 MHz) δ: 7.80 (m, 2H), 7.66 (s, 1H), 7.46-7.35 (m, 5H), 7.35-7.28 (m, 3H), 5.58 (s, 2H); <sup>13</sup>C NMR (CDCl<sub>3</sub>, 126 MHz) δ: 134.9, 130.7, 129.3, 129.0, 128.9, 128.4, 128.2, 125.9, 119.7, 54.4.

**1-Benzyl-3-methyl-4-phenyl-1*H*-1,2,3-triazolium iodide 3<sup>108</sup>**

Chemical Formula: C<sub>16</sub>H<sub>16</sub>IN<sub>3</sub>

Molecular Weight: 377.22

**Original synthetic method:**

1-Benzyl-4-phenyl-1,2,3-triazole **2** (2.008 g, 8.5 mmol) was dissolved in MeCN (40 mL). Iodomethane (3.95 mL, 63.45 mmol) was added with vigorous stirring. The reaction mixture was heated at reflux for 24 h. The solvents were removed under reduced pressure to yield the desired product **3** as a light orange solid (2.52 g, 78%).

**Microwave-assisted method:**

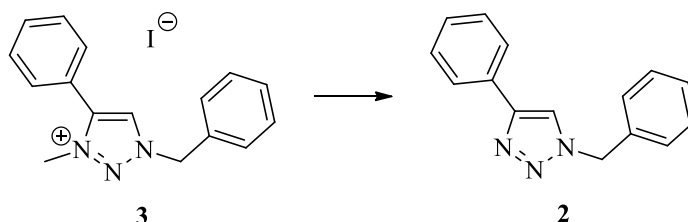
1-Benzyl-4-phenyl-1,2,3-triazole **2** (1.1795 g, 5.02 mmol) was dissolved in MeCN (12 mL) in a microwave vial. Iodomethane (0.31 mL, 0.71 mmol) was added. The reaction was submitted to microwave irradiation for 1 h at 60 °C. The solvents were removed under reduced pressure to yield the desired product **3** as a light yellow solid (1.60g, 85%).

**Optimised microwave-assisted method:**

1-Benzyl-4-phenyl-1,2,3-triazole **2** (1.66 g, 7.07 mmol) was dissolved in MeCN (12 mL) in a microwave vial. Iodomethane (1.73 mL, 35.10 mmol) was added. The reaction was submitted to microwave irradiation for 3 h at 100 °C. The solvents were removed under reduced pressure to yield the desired product **3** as a light yellow solid (2.79 g, 93%).

**1-Benzyl-3-methyl-4-phenyl-1*H*-1,2,3-triazolium iodide 3:** m.p. 133-135 °C, lit. 146-148 °C;<sup>108</sup> IR (neat): 3467, 3040, 1611, 1493, 1455, 1155, 768, 746, 699 cm<sup>-1</sup>; <sup>1</sup>H NMR

(CDCl<sub>3</sub>, 400 MHz)  $\delta$ : 9.33 (s, 1H), 7.69-7.60 (m, 4H), 7.54-7.40 (m, 3H), 7.37-7.33 (m, 3H), 5.97 (s, 2H), 4.26 (s, 3H); <sup>13</sup>C NMR (CDCl<sub>3</sub>, 126 MHz)  $\delta$ : 143.2, 132.2, 131.4, 130.1, 130.1, 129.8, 129.7, 129.6, 129.4, 121.7, 57.6, 39.6.

**1-Benzyl-3-methyl-4-phenyl-1*H*-1,2,3-triazolium iodide 3 with sodium alkoxide****With sodium methoxide:**

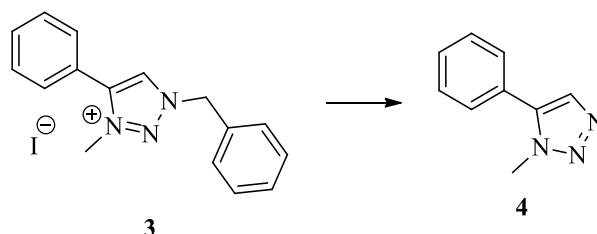
Sodium (3.12 g, 135.7 mmol) was slowly dissolved in absolute MeOH (50 mL), and the solution was cooled to 0 °C. Once all of the sodium was dissolved, 1-benzyl-3-methyl-4-phenyl-1*H*-1,2,3-triazolium iodide **3** (0.3193 g, 0.847 mmol) dissolved in absolute MeOH (15 mL) was added to the sodium methoxide solution, and the mixture was stirred overnight. The reaction was quenched with 1M HCl (25 mL) and the product was extracted from the aqueous layer using EtOAc (3x20 mL). The organic layers were combined and the solvents were removed under reduced pressure to yield compound **2** as colourless crystals (0.1811 g, 91%)

Data consistent with that reported for the original synthetic method of **2**.

**With sodium ethoxide:**

Sodium (3.03 g, 131.7 mmol) was slowly dissolved in absolute EtOH (50 mL), and the solution was cooled to 0 °C. Once all of the sodium was dissolved, 1-benzyl-3-methyl-4-phenyl-1*H*-1,2,3-triazolium iodide **3** (0.4213 g, 1.118 mmol) dissolved in absolute EtOH (15 mL) was added to the sodium ethoxide solution, and the mixture was stirred overnight. The reaction was quenched with 1M HCl (25 mL) and the product was extracted from the aqueous layer using EtOAc (3x20 mL). The organic layers were combined and the solvents were removed under reduced pressure to yield compound **2** as colourless crystals (0.252 g, 96%)

Data consistent with that reported for the original synthetic method of **2**.

**1-Methyl-5-phenyl-1*H*-1,2,3-triazole 4**<sup>109</sup>

Chemical Formula: C<sub>9</sub>H<sub>9</sub>N<sub>3</sub>

Molecular Weight: 159.19

**Reduction using LiAlH<sub>4</sub>:**

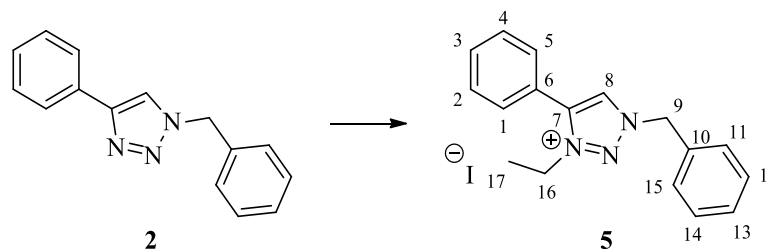
1-Benzyl-3-alkyl-4-phenyl triazolium iodide **3** (3.0145 g, 7.99 mmol) was dissolved in THF (30 mL) and the solution was cooled to 0 °C. LiAlH<sub>4</sub> (0.8776 g, 23.13 mmol) was added and the mixture was stirred overnight. The reaction was quenched with H<sub>2</sub>O (20 mL), stirred for a further 30 min, and the solution was filtered over Celite. The product was extracted from the aqueous layer using EtOAc (3x20 mL), the organic portions were combined, and the solvents removed under reduced pressure. The residue was purified using silica gel column chromatography, eluting with 1:1 EtOAc/ petroleum ether 40/60 to yield the desired compound **4** as a yellow oil (0.307 g, 24%).

**Reduction using *t*BuOK:**

1-Benzyl-3-alkyl-4-phenyl triazolium iodide **3** (0.78 g, 2.05 mmol) was dissolved in THF (45 mL) and the solution was cooled to 0 °C. *t*BuOK (0.61 g, 5.46 mmol) was added and the mixture stirred overnight. The reaction was quenched with H<sub>2</sub>O (30 mL), stirred for a further 30 min, and the solution was filtered over Celite. The product was extracted from the aqueous layer using EtOAc (3x20 mL), the organic portions were combined, and the solvents removed under reduced pressure. The residue was purified using silica gel column chromatography, eluting with 1:1 EtOAc/ petroleum ether 40/60 to yield the desired compound **4** as an orange oil (0.31 g, 93%).

**1-Methyl-5-phenyl-1*H*-1,2,3-triazole 4:** IR (neat): 3060, 3030, 2953, 1732, 1484, 1454, 1245, 767  $\text{cm}^{-1}$ ;  $^1\text{H}$  NMR ( $\text{CDCl}_3$ , 500 MHz)  $\delta$ : 7.73 (s, 1H), 7.57-7.45 (m, 3H), 7.45-7.35 (m, 2H), 4.08 (s, 3H);  $^{13}\text{C}$  NMR ( $\text{CDCl}_3$ , 126 MHz)  $\delta$ : 129.3, 128.7, 127.1, 35.7, 14.3.



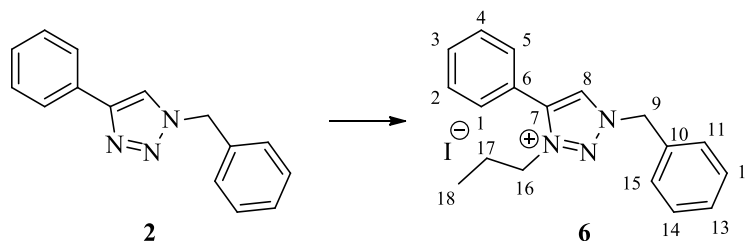
**1-Benzyl-3-ethyl-4-phenyl-1*H*-1,2,3-triazolium iodide 5**

Chemical Formula: C<sub>17</sub>H<sub>18</sub>IN<sub>3</sub>

Molecular Weight: 391.25

Prepared according to the procedure for the synthesis of 1-benzyl-3-methyl-4-phenyl-1*H*-1,2,3-triazolium iodide **3**, from **2** (1.65 g, 7.01 mmol) and iodoethane (2.8 mL, 35.00 mmol). The crude product was purified using silica gel column chromatography, eluting first with 1:1 EtOAc/petroleum ether 40/60, followed by 10% MeOH in CH<sub>2</sub>Cl<sub>2</sub> to yield the desired compound **5** as a light yellow solid (1.19 g, 86%).

m.p. 129-131 °C; IR (neat): 3467, 3041, 1610, 1492, 1456, 1153, 767, 739, 700 cm<sup>-1</sup>; <sup>1</sup>H NMR (CDCl<sub>3</sub>, 400 MHz) δ: 9.39 (s, 1H, H-8), 7.77-7.70 (m, 2H, H-1,5), 7.66-7.55 (m, 5H, H-2,3,4,11,15), 7.47-7.41 (m, 3H, H-12,13,14), 6.13 (s, 2H, H-9), 4.57 (q, *J*=7.3 Hz, 2H, H-16), 1.64 (t, *J*=7.3 Hz, 3H, H-17); <sup>13</sup>C NMR (CDCl<sub>3</sub>, 126 MHz) δ: 142.7 (C-7), 132.3, 131.5, 130.23, 130.17, 130.0, 129.9, 129.74, 129.69 (C-1-6,10-15), 121.9 (C-8), 57.9 (C-9), 47.8 (C-16), 14.8 (C-17); HRMS (NSI): *m/z* calcd for [C<sub>17</sub>H<sub>18</sub>N<sub>3</sub>]<sup>+</sup>: 264.1495; found for [M - I]<sup>+</sup>: 264.1493.

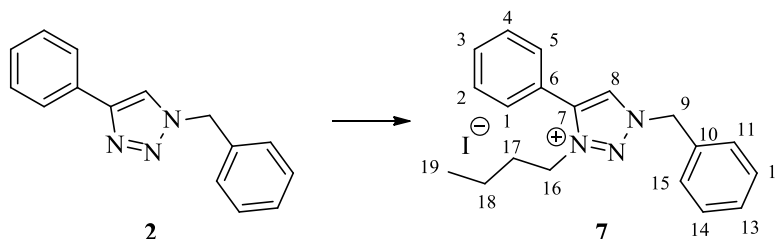
**1-Benzyl-3-*n*-propyl-4-phenyl-1*H*-1,2,3-triazolium iodide 6**

Chemical Formula: C<sub>18</sub>H<sub>20</sub>IN<sub>3</sub>

Molecular Weight: 405.28

Prepared according to the procedure for the synthesis of 1-benzyl-3-methyl-4-phenyl-1*H*-1,2,3-triazolium iodide **3**, from **2** (1.65 g, 7.01 mmol) and iodopropane (3.4 mL, 34.86 mmol). The crude product was purified using silica gel column chromatography, eluting first with 1:1 EtOAc/ petroleum ether 40/60, followed by 10% MeOH in CH<sub>2</sub>Cl<sub>2</sub> to yield the desired compound **6** as a pale yellow solid (0.62 g, 44%).

m.p. 120-122 °C; IR (neat): 3467, 3040, 1610, 1491, 1456, 1152, 768, 736, 700 cm<sup>-1</sup>; <sup>1</sup>H NMR (CDCl<sub>3</sub>, 500 MHz) δ: 9.45 (s, 1H, H-8), 7.75-7.69 (m, 2H, H-1,5), 7.65-7.53 (m, 5H, H-2,3,4,11,15), 7.46-7.40 (m, 3H, H-12,13,14), 6.14 (s, 2H, H-9), 4.46 (t, *J*=7.4 Hz, 2H, H-16), 2.04-1.96 (m, 2H, H-17), 0.96 (t, *J*=7.4 Hz, 3H, H-18); <sup>13</sup>C NMR (CDCl<sub>3</sub>, 126 MHz) δ: 142.8 (C-7), 132.2, 131.5, 130.2, 130.1, 130.0, 129.9, 129.7, 129.6 (C-1-6,10-15), 121.9 (C-8), 57.9 (C-9), 53.5 (C-16), 22.9 (C-17), 11.0 (C-18); HRMS (NSI): *m/z* calcd for [C<sub>18</sub>H<sub>20</sub>N<sub>3</sub>]<sup>+</sup>: 278.1652; found for [M - I]<sup>+</sup>: 278.1652.

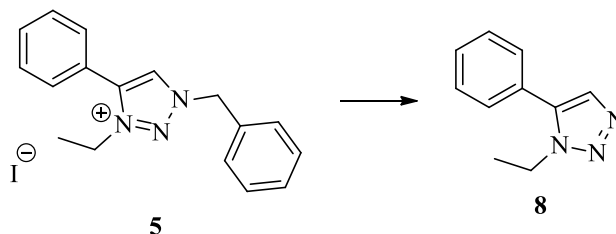
**1-Benzyl-3-*n*-butyl-4-phenyl-1*H*-1,2,3-triazolium iodide 7**

Chemical Formula: C<sub>19</sub>H<sub>22</sub>IN<sub>3</sub>

Molecular Weight: 419.30

**2** (0.94 g, 4.01 mmol) was dissolved in MeCN (12 mL) in a microwave vial and iodobutane (2.3 mL, 3.72 g, 20.20 mmol) was added. The reaction mixture was submitted to microwave irradiation for 3 h at 130 °C. The solvents were removed under reduced pressure and the residue purified using silica gel column chromatography, first with 1:1 EtOAc/ petroleum ether 40/60, followed by 10% MeOH in CH<sub>2</sub>Cl<sub>2</sub>. The fractions containing the product were combined and the solvents were removed. The residue was further purified using silica gel chromatography using 10% EtOH in CH<sub>2</sub>Cl<sub>2</sub> as the eluent to give product **7** as a yellow oil (0.67 g, 40%).

IR (neat): 3104, 2957, 1609, 1568, 1489, 1455, 1145, 764, 731, 696 cm<sup>-1</sup>; <sup>1</sup>H NMR (CDCl<sub>3</sub>, 500 MHz) δ: 9.48 (s, 1H, H-8), 7.77–7.68 (m, 2H, H-1,5), 7.65–7.50 (m, 5H, H-2,3,4,11,15), 7.48–7.38 (m, 3H, H-12,13,14), 6.15 (s, 2H, H-9), 4.52–4.44 (m, 2H, H-16), 1.99–1.87 (m, 2H, H-17), 1.40–1.29 (m, 2H, H-18), 0.90 (t, *J*=7.4 Hz, 3H, H-19); <sup>13</sup>C NMR (CDCl<sub>3</sub>, 126 MHz) δ: 132.1, 129.9, 129.7, 129.5, 57.7, 51.5, 31.0, 19.4, 13.1; HRMS (NSI): *m/z* calcd for [C<sub>19</sub>H<sub>22</sub>N<sub>3</sub>]<sup>+</sup>: 292.1808; found for [M - I]<sup>+</sup>: 292.1810.

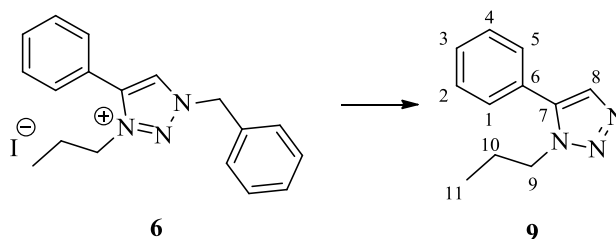
**1-Ethyl-5-phenyl-1*H*-1,2,3-triazole **8****<sup>109</sup>

Chemical Formula: C<sub>10</sub>H<sub>11</sub>N<sub>3</sub>

Molecular Weight: 173.21

Prepared according to the procedure for the synthesis of 1-methyl-5-phenyl-1*H*-1,2,3-triazole **4**, from **5** (1.18 g, 3.00 mmol) and *t*BuOK (0.86 g, 7.65 mmol) dissolved in THF (50 mL). The product did not need further purification and the desired compound **8** was obtained as a light yellow oil (0.61 g, 95%).

IR (neat): 3061, 2983, 2939, 1483, 1455, 1245, 766 cm<sup>-1</sup>; <sup>1</sup>H NMR (CDCl<sub>3</sub>, 500 MHz)  $\delta$ : 7.69 (s, 1H), 7.54-7.46 (m, 3H), 7.43-7.34 (m, 3H), 4.40 (q, *J*=7.3 Hz, 2H), 1.48 (t, *J*=7.3 Hz, 3H); <sup>13</sup>C NMR (CDCl<sub>3</sub>, 126 MHz)  $\delta$ : 133.3, 129.6, 129.3, 128.9, 127.4, 43.6, 15.8.

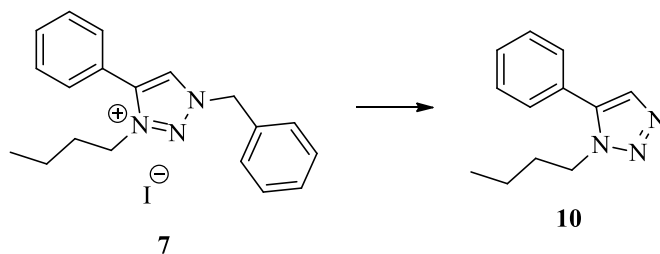
**1-*n*-propyl-5-phenyl-1*H*-1,2,3-triazole 9**

Chemical Formula: C<sub>11</sub>H<sub>13</sub>N<sub>3</sub>

Molecular Weight: 187.24

Prepared according to the procedure for the synthesis of 1-methyl-5-phenyl-1*H*-1,2,3-triazole **4**, from **6** (0.60 g, 1.48 mmol) and *t*BuOK (0.44 g, 3.89 mmol) dissolved in THF (50 mL). The product did not need further purification and the desired compound **9** was obtained as a light yellow oil (0.28 g, 90%).

IR (neat): 3061, 2967, 2935, 1483, 1456, 1241, 767 cm<sup>-1</sup>; <sup>1</sup>H NMR (CDCl<sub>3</sub>, 500 MHz) δ: 7.73 (s, 1H, H-8), 7.56-7.49 (m, 3H, H-2,3,4), 7.44-7.38 (m, 2H, H-1,5), 4.35 (t, *J*=7.3 Hz, 2H, H-9), 1.91-1.82 (m, 2H, H-10) 0.91 (t, *J*=7.3 Hz, 3H, H-11); <sup>13</sup>C NMR (CDCl<sub>3</sub>, 126 MHz) δ: 133.5, 129.2, 128.9 (C-1,2,3,4,5), 50.0 (C-9), 23.7 (C-10), 11.2 (C-11); HRMS (NSI): *m/z* [M + H]<sup>+</sup> calcd for : 188.1182; found: 188.1181.

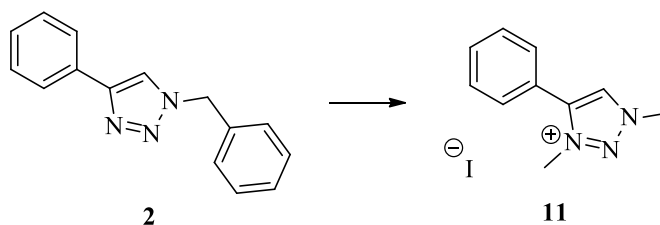
**1-*n*-Butyl-5-phenyl-1*H*-1,2,3-triazole 10**<sup>109</sup>

Chemical Formula: C<sub>12</sub>H<sub>15</sub>N<sub>3</sub>

Molecular Weight: 201.27

Prepared according to the procedure for the synthesis of 1-methyl-5-phenyl-1*H*-1,2,3-triazole **4**, from **7** (0.21 g, 0.51 mmol) and *t*BuOK (0.15 g, 1.30 mmol) dissolved in THF (50 mL). The residue was purified using silica gel column chromatography, eluting with 3:7 EtOAc/ petroleum ether 40/60 to give the desired compound **10** as a light yellow oil (0.10 g, 83%).

IR (neat): 3059, 2960, 2933, 1483, 1458, 767 cm<sup>-1</sup>; <sup>1</sup>H NMR (CDCl<sub>3</sub>, 500 MHz) δ: 7.69 (s, 1H), 7.55-7.44 (m, 3H), 7.43-7.33 (m, 3H), 4.35 (t, *J*=7.3 Hz, 2H), 1.87-1.73 (m, 2H), 1.34-1.22 (m, 2H), 0.86 (t, *J*=7.3 Hz, 3H); <sup>13</sup>C NMR (CDCl<sub>3</sub>, 126 MHz) δ: 133.1, 129.4, 129.1, 128.8, 127.4, 48.1, 32.2, 19.7, 13.4.

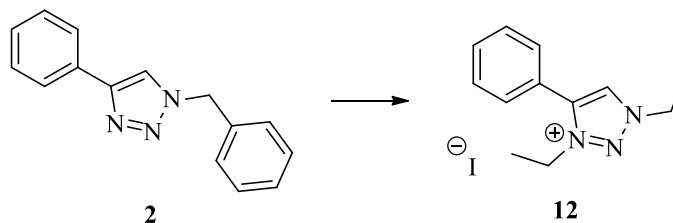
**1,3-Dimethyl-4-phenyl-1*H*-1,2,3-triazolium iodide **11****<sup>110</sup>

Chemical Formula: C<sub>10</sub>H<sub>12</sub>I<sub>3</sub>

Molecular Weight: 301.13

1-Benzyl-4-phenyl 1,2,3-triazole **2** (1.044 g, 4.44 mmol) was dissolved in MeCN (12 mL) in a microwave vial. Iodomethane (1.55 mL, 24.89 mmol) was then added to the solution. The reaction was submitted to microwave irradiation for 3 h at 160 °C. The solvents were removed under reduced pressure and the crude purified using silica gel column chromatography, first with 1:1 EtOAc/ petroleum ether 40/60, followed by 10% MeOH in CH<sub>2</sub>Cl<sub>2</sub> to yield the desired product **11** as a light yellow solid in good purity (1.24 g, 93%).

m.p. 168-170 °C; IR (neat): 3455, 3397, 3003, 1069 cm<sup>-1</sup>; <sup>1</sup>H NMR (CDCl<sub>3</sub>, 500 MHz) δ: 9.32 (s, 1H), 7.73 – 7.65 (m, 2H), 7.57 – 7.50 (m, 3H), 4.47 (s, 3H), 4.27 (s, 3H); <sup>13</sup>C NMR (CDCl<sub>3</sub>, 126 MHz) δ: 143.0, 131.9, 130.5, 129.7, 121.7, 41.4, 39.4.

**1,3-Diethyl-4-phenyl-1*H*-1,2,3-triazole 12**<sup>11</sup>

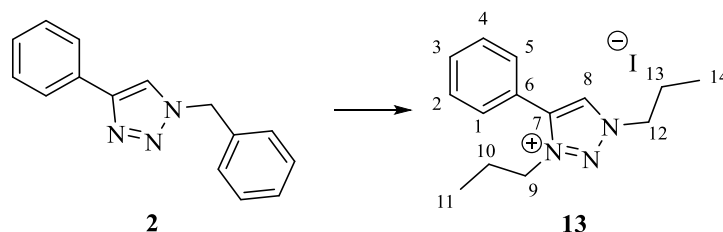
Chemical Formula: C<sub>12</sub>H<sub>16</sub>I<sub>N</sub><sub>3</sub>

Molecular Weight: 329.18

Prepared according to the procedure for the synthesis of 1,3-dimethyl-4-phenyl-1*H*-1,2,3-triazolium iodide **11**, from **2** (0.9989 g, 4.25 mmol) and iodoethane (1.70 mL, 21.25 mmol). The residue was purified using silica gel column chromatography, first with 1:1 EtOAc/ petroleum ether 40/60, followed by 10% MeOH in CH<sub>2</sub>Cl<sub>2</sub> to yield the desired product **12** as a light yellow oil (1.27 g, 91%).

IR (neat): 3444, 3048, 2983, 2940, 1612, 1448 cm<sup>-1</sup>; <sup>1</sup>H NMR (CDCl<sub>3</sub>, 500 MHz) δ: 9.52 (s, 1H), 7.73 – 7.66 (m, 2H), 7.62 – 7.54 (m, 3H), 4.93 (q, *J* = 7.4 Hz, 2H), 4.59 (q, *J* = 7.3 Hz, 2H), 1.74 (t, *J* = 7.4 Hz, 3H), 1.62 (t, *J* = 7.3 Hz, 3H); <sup>13</sup>C NMR (CDCl<sub>3</sub>, 126 MHz) δ: 142.6, 132.1, 130.0, 129.9, 129.7, 122.0, 50.4, 47.7, 14.8, 14.6.



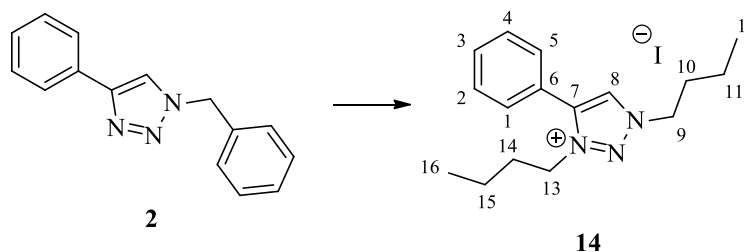
**1,3-Di-*n*-propyl-4-phenyl-1*H*-1,2,3-triazolium iodide 13**

Chemical Formula: C<sub>14</sub>H<sub>20</sub>I<sub>N</sub><sub>3</sub>

Molecular Weight: 357.23

Prepared according to the procedure for the synthesis of 1,3-dimethyl-4-phenyl-1*H*-1,2,3-triazolium iodide **11**, from **2** (0.9889 g, 4.20 mmol) and *n*-propyl iodide (2.05 mL, 21.05 mmol). The crude was purified using silica gel column chromatography, first with 1:1 EtOAc/ petroleum ether 40/60, followed by 10% MeOH in CH<sub>2</sub>Cl<sub>2</sub> to yield the desired product **13** as a light yellow oil (1.31 g, 87%).

IR (neat): 3458, 3279, 2967, 2935, 1654, 1458 cm<sup>-1</sup>; <sup>1</sup>H NMR (CDCl<sub>3</sub>, 500 MHz) δ: 9.63 (s, 1H, H-8), 7.70 – 7.66 (m, 2H, H-1,5), 7.63 – 7.55 (m, 3H, H-2,3,4), 4.89-4.69 (m, 2H, H-9), 4.56-4.38 (m, 2H, H-12), 2.20-2.11 (m, 2H, H-10), 2.02-1.97 (m, 2H, H-13), 1.05 (t, *J* = 7.4 Hz, 3H, H-11), 0.94 (t, *J* = 7.4 Hz, 3H, H-14); <sup>13</sup>C NMR (CDCl<sub>3</sub>, 500 MHz) δ: 142.6 (C-7), 132.0 (C-3), 130.2 (C-2,4), 129.9 (C-8), 129.7 (C-1,5), 121.9 (C-6), 56.1 (C-9), 53.5 (C-12), 23.1 (C-10), 22.6 (C-13), 10.9 (C-11), 10.8 (C-14).

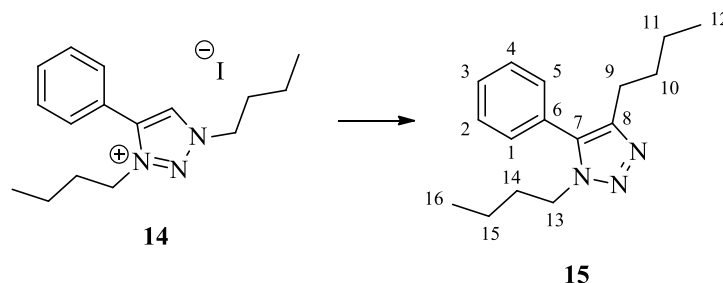
**1,3-Di-*n*-butyl-4-phenyl-1*H*-1,2,3-triazolium iodide **14****

Chemical Formula: C<sub>16</sub>H<sub>24</sub>IN<sub>3</sub>

Molecular Weight: 385.29

Prepared according to the procedure for the synthesis of 1,3-dimethyl-4-phenyl-1*H*-1,2,3-triazolium iodide **11**, from **2** (1.6558 g, 7.05 mmol) and *n*-butyl iodide (4.0 mL, 29.74 mmol). The residue was purified using silica gel column chromatography, first with 1:1 EtOAc/ petroleum ether 40/60, followed by 10% MeOH in CH<sub>2</sub>Cl<sub>2</sub> to yield the desired product **14** as a light brown oil (2.452 g, 90%).

IR (neat): 3453, 3266, 2959, 2872, 1652, 1455 cm<sup>-1</sup>; <sup>1</sup>H NMR (CDCl<sub>3</sub>, 500 MHz) δ: 9.29 (s, 1H, H-8), 7.77 – 7.70 (m, 2H, H-1,5), 7.65 – 7.60 (m, 3H, H-2,3,4), 4.93 (t, *J* = 7.4 Hz, 2H, H-13), 4.55 (t, *J* = 7.4 Hz, 2H, H-9), 2.19 – 2.10 (m, 2H, H-14), 2.02 – 1.92 (m, 2H, H-10), 1.56 – 1.45 (m, 2H, H-15), 1.44 – 1.32 (m, 2H, H-11), 1.04 (t, *J* = 7.4 Hz, 3H, H-16), 0.94 (t, *J* = 7.4 Hz, 3H, H-12); <sup>13</sup>C NMR (CDCl<sub>3</sub>, 126 MHz) δ: 142.9 (H-7), 132.1 (H-3), 129.9 (H-1,2,4,5), 129.9 (H-8), 121.9 (H-6), 54.9 (H-13), 51.9 (H-9), 31.4 (H-14), 31.2 (H-10), 19.7 (H-15,11), 13.6 (H-16,12); HRMS (NSI): *m/z* calcd for [C<sub>16</sub>H<sub>24</sub>N<sub>3</sub>]<sup>+</sup>: 258.1965; found for [M – I]<sup>+</sup>: 258.1959.

**1,4-Di-*n*-butyl-5-phenyl-1*H*-1,2,3-triazole **15**<sup>1</sup>**

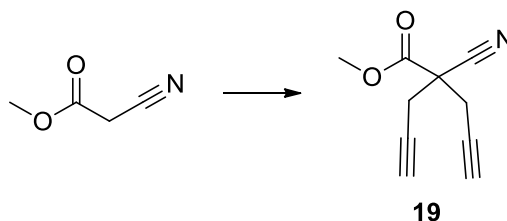
Chemical Formula: C<sub>16</sub>H<sub>23</sub>N<sub>3</sub>

Molecular Weight: 257.37

1,3-Di-*n*-butyl-4-phenyl triazolium iodide **14** (2.323 g, 5.54 mmol) was dissolved in THF (100 mL) and the solution was cooled to 0 °C. *t*BuOK (1.5545 g, 13.85 mmol) was added and the mixture stirred overnight at room temperature. The reaction was quenched with H<sub>2</sub>O (50 mL), stirred for a further 30 min, and the solution was filtered over Celite. The product was extracted from the aqueous layer using EtOAc (3x30 mL), the organic portions were combined, and the solvents were removed under reduced pressure. The residue was purified using silica gel column chromatography, eluting with 1:1 EtOAc/ petroleum ether 40/60 to yield the desired compound **15** as a light yellow oil (1.224 g, 86%).

IR (neat): 2959 2934, 2873 1637 cm<sup>-1</sup>; <sup>1</sup>H NMR (CDCl<sub>3</sub>, 500 MHz) δ: 7.62 – 7.53 (m, 2H, H-1,5), 7.48 – 7.41 (m, 2H, H-2,4), 7.38 – 7.31 (m, 1H, H-3), 4.28 (t, *J* = 7.3 Hz, 2H, H-13), 4.12 (t, *J* = 7.3 Hz, 2H, H-9), 1.90 – 1.83 (m, 2H, H-14), 1.83 – 1.75 (m, 2H, H-10), 1.48 – 1.38 (m, 2H, H-15), 1.36 – 1.27 (m, 2H, H-11), 0.97 (t, *J* = 7.4 Hz, 3H, H-16), 0.89 (t, *J* = 7.4 Hz, 3H, H-12); <sup>13</sup>C NMR (CDCl<sub>3</sub>, 126 MHz) δ: 129.0 (H-7), 128.3 (H-1,5), 128.2 (2,4), 127.5 (H-3), 51.4 (H-13), 44.5 (H-9), 31.1 (H-14), 30.9 (H-10), 20.0 (H-15), 19.7 (H-11), 13.8 (H-16), 13.5 (H-12).

<sup>1</sup> Since the first successful reaction, these results have not been repeatable

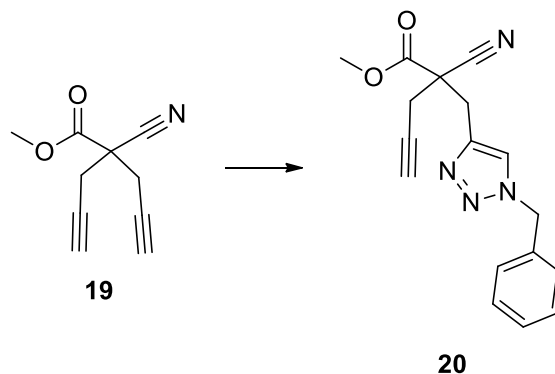
**Methyl 2-cyano-2-(prop-2-yn-1-yl)pent-4-ynoate **15**<sup>76</sup>**

Chemical Formula: C<sub>10</sub>H<sub>9</sub>NO<sub>2</sub>

Molecular Weight: 175.18

Methyl cyanoacetate (15 mL, 169.99 mmol) was dissolved in MeCN (300 mL) and K<sub>2</sub>CO<sub>3</sub> (62.43 g, 451.70 mmol) was added to the solution. The mixture was cooled to 0 °C and propargyl bromide (50 mL, 336.22 mmol) was slowly added over a period of 5 min. When the addition of the compound was complete, the reaction was heated at reflux for 12 h. The solution was cooled and diluted with H<sub>2</sub>O (100 mL). The product was extracted from the aqueous layer using EtOAc (3x30 mL). The organic layers were combined, washed with H<sub>2</sub>O (100 mL) and brine (100 mL), and then dried over anhydrous MgSO<sub>4</sub>. The solvents were removed under reduced pressure and the crude product was then purified by vacuum distillation at 115-125 °C to give the desired compound **19** as a colourless oil which solidified to a colourless solid (22.63 g, 76 %).

m.p. 47-49 °C; IR (neat): 3287, 2959, 2250, 2128, 1747 cm<sup>-1</sup>; <sup>1</sup>H NMR (CDCl<sub>3</sub>, 500 MHz) δ: 3.89 (3H, s), 2.94 (4H, d, *J* = 2.7 Hz), 2.23 (2H, t, *J* = 2.7 Hz); <sup>13</sup>C NMR (CDCl<sub>3</sub>, 126 MHz) δ: 166.6, 117.1, 76.2, 73.9, 54.3, 47.3, 25.9.

**Methyl 2-[(1-benzyl-1*H*-1,2,3-triazol-4-yl)methyl]-2-cyanopent-4-ynoate **20**<sup>76</sup>**

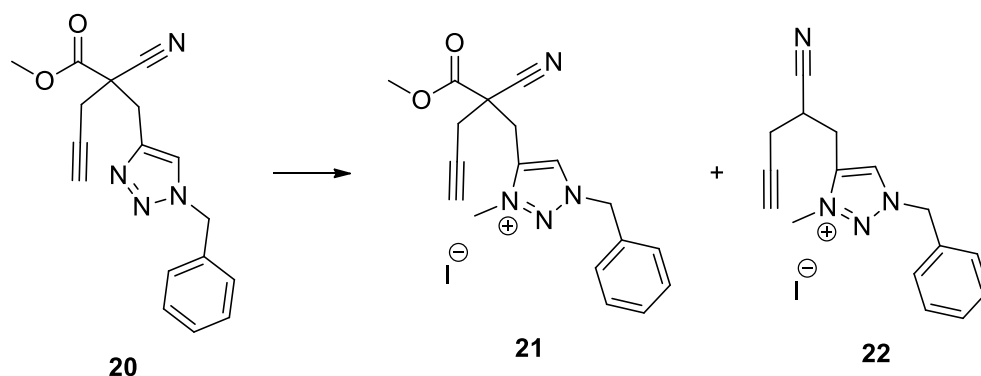
Chemical Formula: C<sub>17</sub>H<sub>16</sub>N<sub>4</sub>O<sub>2</sub>

Molecular Weight: 308.33

Methyl 2-cyano-2-(prop-2-yn-1-yl)pent-4-ynoate **19** (2.010 g, 11.47 mmol), copper (II) sulfate pentahydrate (2.970 g, 46.69 mmol) and benzyl azide (3 mL, 23.63 mmol) were dissolved in *t*BuOH/H<sub>2</sub>O (1:1, 50 mL) and the mixture was stirred overnight. The reaction was diluted with H<sub>2</sub>O (40 mL) and the product was extracted from the aqueous layer using EtOAc (3x25 mL). The organic layers were combined, dried using anhydrous MgSO<sub>4</sub> and then activated charcoal was added to remove any remaining copper. After filtering the solution over Celite the solvents were removed under reduced pressure and the crude product was purified using silica gel column chromatography, eluting with 1:1 EtOAc/petroleum ether 40/60 to yield the desired compound **20** as a colourless solid (1.626 g, 46%).

m.p. 70-72 °C; IR (neat): 3288, 3140, 2956, 1748 cm<sup>-1</sup>; <sup>1</sup>H NMR (CDCl<sub>3</sub>, 500 MHz) δ: 7.49 (1H, s), 7.40 – 7.32 (3H, m), 7.26 – 7.22 (2H, m), 5.52 (2H, s), 3.80 (3H, s), 3.39 (2H, s), 2.93 (1H, dd, *J* = 16.9, 2.6 Hz), 2.81 (1H, dd, *J* = 16.9, 2.6 Hz), 2.22 (1H, t, *J* = 2.6 Hz); <sup>13</sup>C NMR (CDCl<sub>3</sub>, 126 MHz) δ: 167.2, 140.7, 134.6, 129.1, 128.7, 127.9, 123.0, 117.7, 76.7, 73.5, 54.1, 53.9, 49.0, 32.1, 26.2.

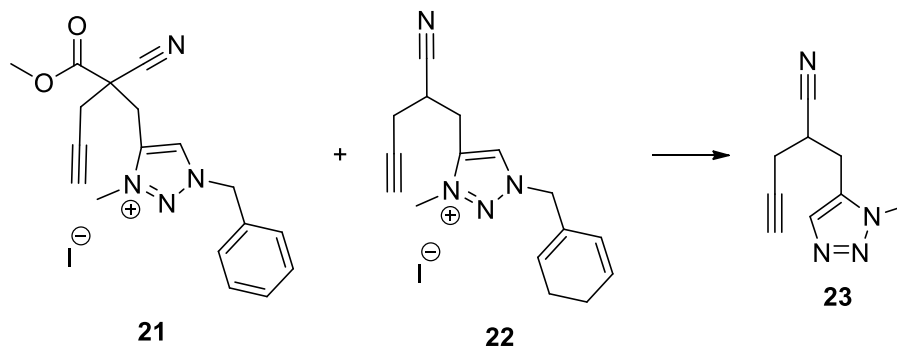
**Alkylation of methyl 3-(1-benzyl-1*H*-1,2,3-triazol-4-yl)-2-[(1-benzyl-1*H*-1,2,3-triazol-4-yl)methyl]-2-cyanopropanoate **20** with iodomethane**



Compound **20** (0.142 g, 0.462 mmol) was dissolved in MeCN (5 mL) in a microwave vial. Iodomethane (0.2 mL, 0.456 g, 3.23 mmol) was added. The reaction mixture was submitted to microwave irradiation for 3 h at 100 °C. The solvents were removed under reduced pressure and the residue purified using silica gel column chromatography, eluting with 10% MeOH in CH<sub>2</sub>Cl<sub>2</sub> to yield an inseparable mixture of products **21** and **22**.

**21-Benzyl-4-(2-cyano-2-(methoxycarbonyl)pent-4-yn-1-yl)-3-methyl-1*H*-1,2,3-triazolium iodide **21**:** <sup>1</sup>H NMR (CDCl<sub>3</sub>, 500 MHz) δ: 8.97 (s, 1H), 7.59–7.45 (m, 5H), 5.94 (s, 2H), 4.46 (s, 3H), 3.92 (dd, 2H, *J*=61.2, 15.9 Hz), 3.22–3.09 (m, 2H), 2.33 (t, 1H, *J*=2.6 Hz);

**1-Benzyl-4-(2-cyano-pent-4-yn-1-yl)-3-methyl-1*H*-1,2,3-triazolium iodide **22**:** <sup>1</sup>H NMR (CDCl<sub>3</sub>, 500 MHz) δ: 9.20 (s, 1H), 7.41–7.37 (m, 5H), 5.87–5.80 (m, 2H), 4.41 (s, 3H), 3.75 (td, 1H, *J*=11.2, 5.6 Hz), 3.59 (ddd, 2H, *J*=25.1, 15.7, 7.5 Hz), 2.86–2.75 (m, 4H), 2.20 (t, 2H, *J*=2.6 Hz).

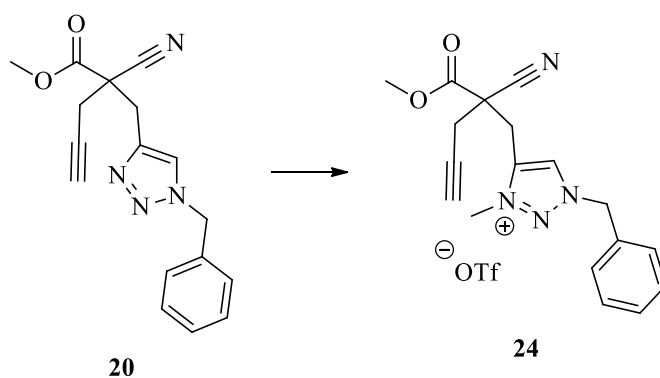
**2-((1-Methyl-1*H*-1,2,3-triazol-5-yl)methyl)pent-4-ynenitrile **23****

Chemical Formula: C<sub>9</sub>H<sub>10</sub>N<sub>4</sub>

Molecular Weight: 174.20

The mixture of compounds **21** and **22** was dissolved in THF (20 mL) and *t*BuOK (0.08 g, 0.71 mmol) was added. The reaction mixture was stirred at room temperature for 12 h. The reaction was quenched with 1M HCl (30 mL) and the product was extracted from the aqueous layer using EtOAc (3x20 mL). The organic layers were combined and the solvents were removed under reduced pressure. The crude product was purified using silica gel column chromatography, eluting with 1:1 EtOAc/petroleum ether 40/60, to yield the desired compound **23** as a brown oil (0.012 g, 15% over 2 steps).

IR (neat): 3287, 2923, 2852, 2250, 1722, 1450, 1242, 700 cm<sup>-1</sup>; <sup>1</sup>H NMR (CDCl<sub>3</sub>, 500 MHz) δ: 7.69 (s, 1H), 4.08 (s, 3H), 3.19 (d, 2H, *J*=6.6 Hz), 3.07–2.99 (m, 1H), 2.68–2.56 (m, 1H), 2.28 (t, 1H, *J*=2.6 Hz); <sup>13</sup>C NMR (CDCl<sub>3</sub>, 126 MHz) δ: 73.5, 30.3, 24.5, 21.5; HRMS (NSI): *m/z* calcd for [C<sub>9</sub>H<sub>11</sub>N<sub>4</sub>]<sup>+</sup>: 175.0978; found for [M + H]<sup>+</sup>: 175.0977.

**1-Benzyl-4-(2-cyano-2-(methoxycarbonyl)pent-4-yn-1-yl)-3-methyl-1*H*-1,2,3-triazol-3-ium triflate **24****

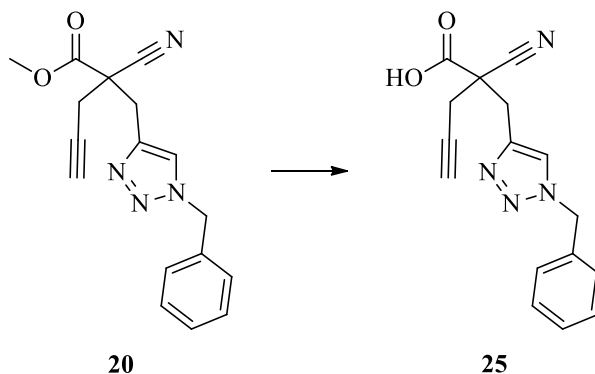
Chemical Formula: C<sub>19</sub>H<sub>19</sub>F<sub>3</sub>N<sub>4</sub>O<sub>5</sub>S

Molecular Weight: 472.44

Compound **20** (0.541 g, 1.758 mmol) was dissolved in CH<sub>2</sub>Cl<sub>2</sub> (15 mL) and methyl trifluoromethanesulfonate (1.5 mL, 2.244 g, 13.675 mmol) was added with stirring. After 20 min, the reaction was diluted with H<sub>2</sub>O (15 mL) and the product extracted from the aqueous layer using EtOAc (3x10 mL). The organic layers were combined and solvents were removed under reduced pressure to yield the desired compound **24** as a colourless oil (0.801 g, 96%).

IR (neat): 3289, 2253, 2126, 1751, 1440, 1254, 1166, 1030 cm<sup>-1</sup>; <sup>1</sup>H NMR (CDCl<sub>3</sub>, 500 MHz) δ: 8.45 (s, 1H), 7.54-7.39 (m, 5H), 5.75 (s, 2H), 4.39 (s, 3H), 3.82 (s, 3H), 3.71 (q, 2H, *J*=15.9 Hz), 3.02 (qd, 2H, *J*=15.9, 2.6 Hz), 2.30 (t, 1H, *J*=2.6 Hz); <sup>13</sup>C NMR (CDCl<sub>3</sub>, 126 MHz) δ: 166.1, 138.8, 130.5, 130.2, 129.8, 129.5, 75.5, 75.3, 60.6, 58.1, 55.0, 47.2, 38.8, 28.5, 27.3, 21.2, 20.6, 14.3; HRMS (NSI): *m/z* calcd for [C<sub>18</sub>H<sub>19</sub>N<sub>4</sub>O<sub>2</sub>]<sup>+</sup>: 323.1503; found for [M – CF<sub>3</sub>SO<sub>3</sub>]<sup>+</sup>: 323.1499.



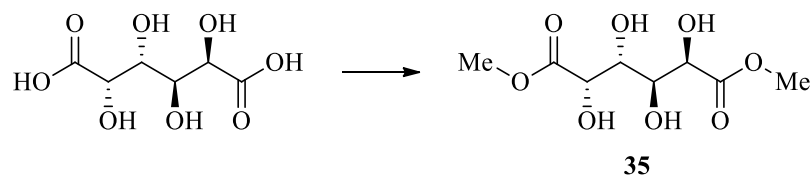
**Methyl 2-[(1-benzyl-1*H*-1,2,3-triazol-4-yl)methyl]-2-cyanopent-4-ynoic acid **25****

Chemical Formula: C<sub>16</sub>H<sub>14</sub>N<sub>4</sub>O<sub>2</sub>

Molecular Weight: 294.31

Compound **2** (0.3662 g, 1.18 mmol) was dissolved in H<sub>2</sub>O (100 mL) and MeOH (10 mL). LiOH (0.3265 g, 7.78 mmol) was added and the reaction mixture heated at reflux for 12 h. The reaction mixture was allowed to cool to room temperature and quenched with 1M HCl (50 mL). The product was extracted from the aqueous layer using EtOAc (3x25 mL) and the organic layer were combined, and dried over anhydrous MgSO<sub>4</sub>. The solvents were removed under reduced pressure to yield the desired compound **25** as a colourless oil (0.2288 g, 55%).

IR (neat): 3289, 2253, 2126, 1751, 1440, 1254, 1166, 1030 cm<sup>-1</sup>; <sup>1</sup>H NMR (CDCl<sub>3</sub>, 500 MHz) δ: 7.58 (s, 1H, H-8), 7.29 – 7.25 (m, 3H, H-1,3,5), 7.17 – 7.15 (m, 2H, H-2,4), 5.42 (dd, *J* = 32.8, 14.9 Hz, 2H, H-7), 3.42 (q, *J* = 14.6 Hz, 2H, H-10), 2.79 (ddd, *J* = 17.1, 2.6 Hz, 2H, H-15), 2.17 (t, *J* = 2.6 Hz, 1H, H-17); <sup>13</sup>C NMR (CDCl<sub>3</sub>, 126 MHz) δ: 167.9 (C-13), 140.7 (C-6), 133.9 (C-9), 129.4 (C-1,5), 129.2 (C-3), 128.3 (C-2,4), 124.1 (C-8), 118.1 (C-12), 77.3 (C-16), 73.8 (C-17), 54.9 (C-7), 31.5 (C-10), 31.1 (C-11), 26.1 (C-15).

**(2*R*,3*S*,4*R*,5*S*)-dimethyl 2,3,4,5-tetrahydroxyhexanedioate 35**<sup>112</sup>

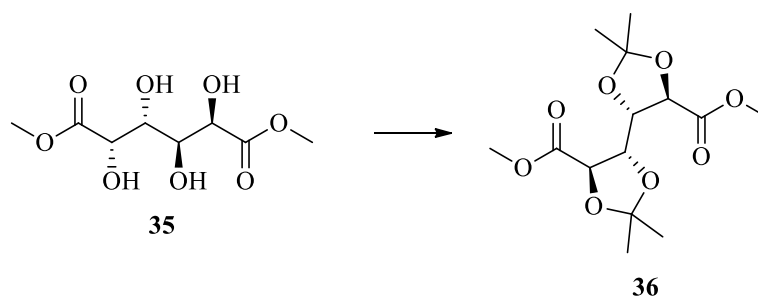
Chemical Formula: C<sub>8</sub>H<sub>14</sub>O<sub>8</sub>

Molecular Weight: 238.19

Galactaric acid (20.316 g, 96.68 mmol) was dissolved in MeOH (100 mL) and conc. H<sub>2</sub>SO<sub>4</sub> (1.5 mL, 26.733 mmol) was added slowly with vigorous stirring. The reaction mixture was heated at reflux for 12 h. The solution was allowed to cool to room temperature and the mixture was filtered using a Buchner funnel. The solid was washed with water and then dried to give the desired compound **35** as a white solid (22.410 g, 99%).

m.p. 189-190 °C, lit. 189 °C;<sup>112</sup> IR (neat): 3343, 3263, 2965, 1722, 1287 cm<sup>-1</sup>; <sup>1</sup>H NMR (DMSO, 400 MHz) δ: 4.92 (d, *J* = 8.0 Hz, 2H), 4.84 – 4.78 (m, 2H), 4.31 (d, *J* = 8.0 Hz, 2H), 3.82 – 3.75 (m, 2H), 3.64 (s, 6H); <sup>13</sup>C NMR (DMSO, 101 MHz) δ: 174.1, 71.2, 70.3, 51.4.

**(4*S*,4'*S*,5*R*,5'*R*)-Dimethyl-2,2,2',2'-tetramethyl-[4,4'-bi(1,3-dioxolane)]-5,5'-dicarboxylate **36**<sup>112</sup>**



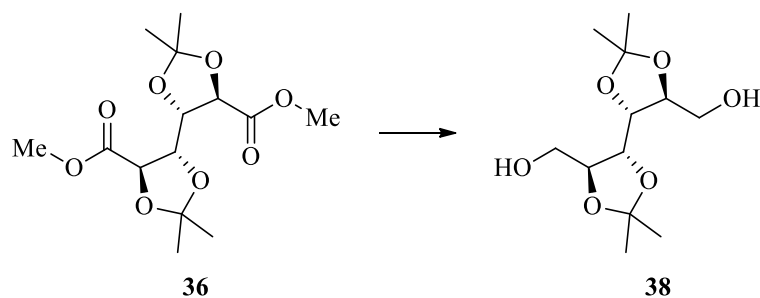
Chemical Formula: C<sub>14</sub>H<sub>22</sub>O<sub>8</sub>

Molecular Weight: 290.27

Compound **35** (15.096 g, 63.378 mmol) was suspended in acetone (250 mL), *p*TSA (0.076 g, 0.40 mmol) and DMP (17.5 mL, 14.84 g, 141.401 mmol) were then added to the solution with stirring. A Soxhlet extractor packed with 4Å molecular sieve was attached and the reaction was heated at reflux for 12 h. The reaction was allowed to cool to room temperature and then neutralised using a solution of Na<sub>2</sub>CO<sub>3</sub> (100 mL). The solution was filtered over Celite and solvents were removed under reduced pressure to give a light yellow solid. The solid was recrystallized from hot ethanol to give the desired compound **36** as a white solid (15.327 g, 76%).

m.p. 96-97 °C, lit. 98 °C;<sup>112</sup> IR (neat): 3278, 2987, 1758, 1727, 1219 cm<sup>-1</sup>; <sup>1</sup>H NMR (DMSO, 500 MHz) δ: 4.60 – 4.44 (m, 2H), 4.44 – 4.35 (m, 2H), 3.68 (s, 6H), 1.36 (s, 6H), 1.31 (s, 6H); <sup>13</sup>C NMR (DMSO, 126 MHz) δ: 171.3, 111.9, 78.8, 75.6, 52.7, 27.1, 26.0.

**((4*R*,4'*R*,5*S*,5'*S*)-2,2,2',2'-Tetramethyl-[4,4'-bi(1,3-dioxolane)]-5,5'-diyl)dimethanol**  
**38**<sup>113</sup>

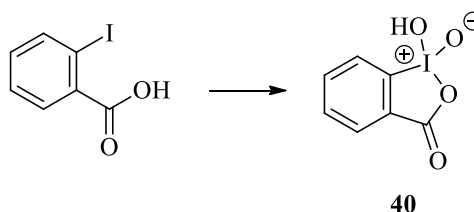


Chemical Formula: C<sub>12</sub>H<sub>22</sub>O<sub>6</sub>

Molecular Weight: 262.30

LiAlH<sub>4</sub> (0.416 g, 3.86 mmol) was suspended in Et<sub>2</sub>O (15 mL) and, a solution of **36** (1.010 g, 3.17 mmol) in Et<sub>2</sub>O (15 mL) was added. The grey suspension was heated at reflux for 12 h and then it was allowed to cool to room temperature. A spatula of anhydrous Na<sub>2</sub>SO<sub>4</sub> was added to the mixture and dropwise addition of H<sub>2</sub>O (3 mL) quenched the reaction. The solution was filtered over Celite and washed with Et<sub>2</sub>O (40 mL). The crude solid was recrystallized from isopropyl alcohol with petroleum ether 40/60 to give the desired compound **38** as a white solid (0.704 g, 85%).

m.p. 111-112 °C; IR (neat): 3323, 2990, 1738, 1381, 1216 cm<sup>-1</sup>; <sup>1</sup>H NMR (DMSO, 400 MHz) δ: 4.81 (t, *J* = 5.7 Hz, 2H), 4.06 – 3.89 (m, 2H), 3.84 – 3.69 (m, 2H), 3.61 (ddd, *J* = 11.7, 5.7, 3.1 Hz, 2H), 3.43 (dt, *J* = 11.7, 5.7 Hz, 2H), 1.32 (s, 6H), 1.30 (s, 6H); <sup>13</sup>C NMR (DMSO, 126 MHz) δ: 110.1, 81.4, 78.9, 62.6, 27.1, 26.9.

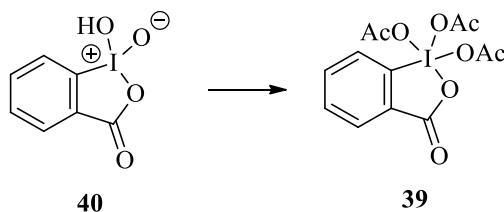
**2-Iodoxybenzoic acid (IBX) 40**<sup>114</sup>

Chemical Formula: C<sub>7</sub>H<sub>5</sub>IO<sub>4</sub>

Molecular Weight: 280.02

2-Iodobenzoic acid (10.1288 g, 251.33 mmol) was dissolved in H<sub>2</sub>SO<sub>4</sub> (10 mL, 178.22 mmol) and KBrO<sub>3</sub> (8.850 g, 52.99 mmol) was added. The reaction mixture was heated at reflux for 48 h. The solution was allowed to cool to room temperature and filtered. The collected solid was washed with H<sub>2</sub>O, followed by MeOH, and dried to give the desired compound **40** as a white solid (9.65 g, 84%).

m.p. 231-232 °C, lit. 232-233 °C;<sup>114</sup> IR (neat): 3428, 2255, 2128, 1651, 1026 cm<sup>-1</sup>; <sup>1</sup>H NMR (DMSO, 500 MHz) 8.14 (d, *J* = 7.7 Hz, 1H), 8.03 (dd, *J* = 7.7, 1.3 Hz, 1H), 8.00 (td, *J* = 7.7, 1.3 Hz, 1H), 7.84 (td, *J* = 7.7, 1.3 Hz, 1H); <sup>13</sup>C NMR (DMSO, 126 MHz) δ: 168.1, 146.8, 133.8, 133.4, 131.5, 130.5, 125.2.

**1,1,1-Triacetoxy-1,1-dihydro-1,2-benziodoxol-3(1H)-one (DMP) **39****<sup>114</sup>

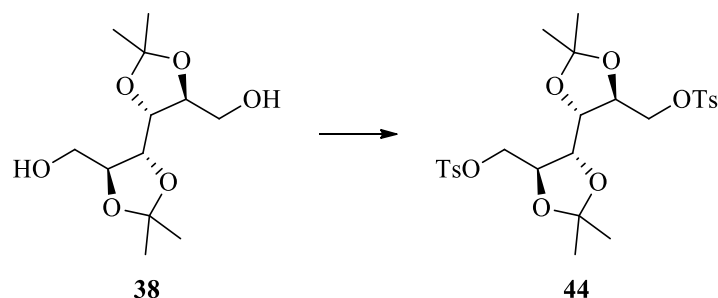
Chemical Formula: C<sub>13</sub>H<sub>13</sub>IO<sub>8</sub>

Molecular Weight: 424.14

IBX **40** (9.0682 g, 32.39 mmol) was suspended in acetic acid (45 mL) and acetic anhydride (2.9 mL, 30.61 mmol) was added. The reaction mixture was heated at reflux for 12 h. The reaction solution was allowed to cool to room temperature and concentrated by removal of solvent under reduced pressure. The precipitate formed was filtered using a Buchner funnel, washed with EtO<sub>2</sub> and dried to yield the desired compound **39** as a white solid (8.5615 g, 59%).

m.p. 133-134 °C, lit. 133-134 °C;<sup>114</sup> IR (neat): 3063, 2921, 1634, 1299 cm<sup>-1</sup>; <sup>1</sup>H NMR (CDCl<sub>3</sub>, 500 MHz) 8.27 (dd, *J* = 7.6, 1.4 Hz, 1H), 8.01 (dd, *J* = 8.3, 0.6 Hz, 1H), 7.95 – 7.91 (m, 1H), 7.72 (td, *J* = 7.5, 0.9 Hz, 1H), 2.26 (s, 3H), 2.23 (s, 3H), 2.17 (s, 3H); <sup>13</sup>C NMR (CDCl<sub>3</sub>, 126 MHz) δ: 175.7, 174.0, 166.0, 142.2, 135.8, 133.8, 131.9, 126.5, 126.4, 20.4, 20.3.

**((4*R*,4'*R*,5*S*,5'*S*)-2,2,2',2'-Tetramethyl-[4,4'-bi(1,3-dioxolane)]-5,5'-diyl)bis(methylene) bis(4-methylbenzenesulfonate) **44**<sup>115</sup>**

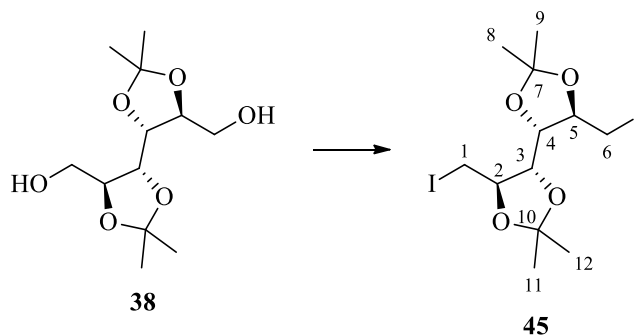


Chemical Formula: C<sub>26</sub>H<sub>34</sub>O<sub>10</sub>S<sub>2</sub>

Molecular Weight: 570.67

Compound **38** (0.9985 g, 3.8 mmol) was dissolved in CH<sub>2</sub>Cl<sub>2</sub> (30 mL) and *p*-toluenesulfonyl chloride (4.3964 g, 23.06 mmol) was added. Pyridine (1.2 mL, 79.1 mmol) was added and the reaction mixture stirred at room temperature for 12 h. The solvents were removed under reduced pressure and the crude dissolved in EtOAc (30 mL). The mixture was filtered over Celite and washed with 1M HCl (40 mL). The organic layer was separated, washed with aq. NaHCO<sub>3</sub> (30 mL), aq. CuSO<sub>4</sub> (30 mL), brine (30 mL) and then dried over anhydrous MgSO<sub>4</sub>. The solvents were removed under reduced pressure to yield the desired compound **44** as a white solid (1.04 g, 48%).

m.p. 164-166 °C, lit. 164-166 °C;<sup>115</sup> IR (neat): 3037, 2986, 2893, 1360, 1181 cm<sup>-1</sup>; <sup>1</sup>H NMR (DMSO, 500 MHz) δ: 7.78 (d, *J* = 8.0 Hz, 4H), 7.48 (d, *J* = 8.0 Hz, 4H), 4.14 (dd, *J* = 10.8, 2.0 Hz, 2H), 4.08 – 4.03 (m, 2H), 3.99 (dd, *J* = 10.8, 6.0 Hz, 2H), 3.70 (dd, *J* = 6.0, 2.0 Hz, 2H), 2.41 (s, 6H), 1.21 (s, 6H), 1.17 (s, 6H); <sup>13</sup>C NMR (DMSO, 126 MHz) δ: 145.2, 131.9, 130.2, 127.8, 110.1, 77.3, 76.5, 69.7, 26.6, 21.1.

**(4*S*,4'*S*,5*R*,5'*R*)-5,5'-Bis(iodomethyl)-2,2,2',2'-tetramethyl-4,4'-bi(1,3-dioxolane) 45**

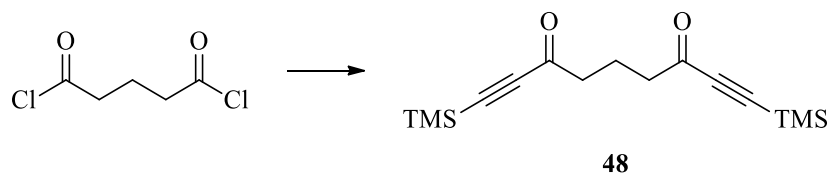
Chemical Formula: C<sub>12</sub>H<sub>20</sub>I<sub>2</sub>O<sub>4</sub>

Molecular Weight: 482.09

Triphenylphosphine (1.4001 g, 5.34 mmol) and imidazole (0.4144 g, 6.09 mmol) were dissolved in CH<sub>2</sub>Cl<sub>2</sub> (40 mL) and cooled to 0 °C. Iodine (1.2265 g, 4.83 mmol) and compound **38** (0.5032 g, 1.92 mmol) were added to the solution and it was allowed to reach room temperature. After stirring for 12 h, the solution was filtered over Celite and washed with EtOAc (3x25 mL). The solvents were removed under reduced pressure and the crude product was purified using silica gel column chromatography, eluting with 1:1 EtOAc/ petroleum ether 40/60, to yield the desired compound **45** as a white solid (0.8242 g, 89%)

m.p. 107-108 °C; IR (neat): 2984, 2895, 1380, 1161, 1061 cm<sup>-1</sup>; <sup>1</sup>H NMR (CDCl<sub>3</sub>, 500 MHz) δ: 3.89 – 3.79 (m, 2H, H-3,4), 3.78 – 3.65 (m, 2H, H-2,5), 3.52 (dd, *J* = 10.8, 3.4 Hz, 2H, H-6,1), 3.34 (dd, *J* = 10.8, 5.5 Hz, 2H, H-6,1), 1.48 (s, 6H, H-8,11), 1.40 (s, 6H, H-9,12); <sup>13</sup>C NMR (CDCl<sub>3</sub>, 126 MHz) δ: 110.5 (H-7,10), 81.5 (H-2,5), 79.4 (H-3,4), 27.5 (H-8,11), 27.5 (H-9,12), 7.3 (H-1,6).



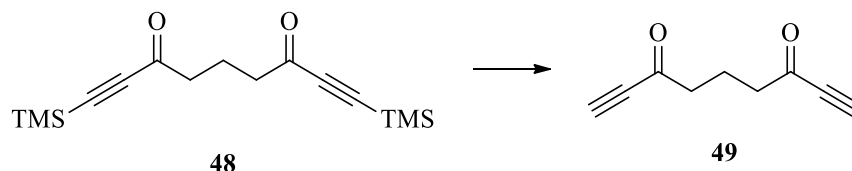
**1,9-Bis(trimethylsilyl)nona-1,8-diyne-3,7-dione **48****<sup>94</sup>

Chemical Formula: C<sub>26</sub>H<sub>34</sub>O<sub>2</sub>Si<sub>2</sub>

Molecular Weight: 292.52

Aluminium chloride (4.2710 g, 32.04 mmol) was dissolved in CH<sub>2</sub>Cl<sub>2</sub> (50 mL) and cooled to 0 °C. *Bis*-(trimethylsilyl)acetylene (6.5 mL, 29.5 mmol) and glutaryl dichloride (1.5 mL, 11.83 mmol) were added and the reaction solution stirred at 0 °C for 2.5 h. The reaction mixture was quenched with ice-cold H<sub>2</sub>O (100 mL) and the product extracted from the aqueous layer using CH<sub>2</sub>Cl<sub>2</sub> (3x30 mL). The organic layers were combined, washed with aq. NaHCO<sub>3</sub> (40 mL) and dried using anhydrous MgSO<sub>4</sub>. The solvent was removed under reduced pressure and the crude purified using bulb-to-bulb distillation to yield the desired compound **48** as a light yellow oil (3.45 g, 100%).

IR (neat): 2964, 2901, 2150, 1679, 1252, 1108 cm<sup>-1</sup>; <sup>1</sup>H NMR (CDCl<sub>3</sub>, 500 MHz) δ: 2.63 (t, *J* = 7.2 Hz, 4H), 1.99 (p, *J* = 7.2 Hz, 2H), 0.24 (s, 18H); <sup>13</sup>C NMR (CDCl<sub>3</sub>, 126 MHz) δ: 186.8, 101.9, 98.4, 44.0, 17.9, -0.7.

**Nona-1,8-diyne-3,7-dione 49<sup>94</sup>**

Chemical Formula: C<sub>9</sub>H<sub>8</sub>O<sub>2</sub>

Molecular Weight: 148.16

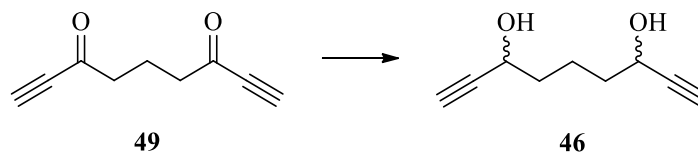
**Desilylation using potassium carbonate:**

**48** (1.0590 g, 3.62 mmol) was dissolved in a MeOH/H<sub>2</sub>O mixture (9:1, 30 mL). Potassium carbonate (2.1325 g, 15.43 mmol) was added and the solution stirred at room temperature for 12 h. The reaction mixture was quenched with 10% citric acid (30 mL) and the product extracted from the aqueous layer using EtOAc (3x20 mL). The organic layers were combined, washed with brine and dried using anhydrous MgSO<sub>4</sub>. The solvents were removed under reduced pressure and the residue purified using silica gel column chromatography, eluting with 3:2 EtO<sub>2</sub>/ petroleum ether 40/60, to yield the desired compound **49** as a yellow oil (0.032 g, 6%)

**Desilylation using sodium borate:**

**48** (2.79 g, 9.54 mmol) was dissolved in a MeOH/H<sub>2</sub>O mixture (9:1, 150 mL). Sodium borate (0.423 g, 0.164 mmol) was added and the solution stirred at room temperature for 12 h. The reaction mixture was quenched with 10% citric acid and the product extracted from the aqueous layer using EtOAc. The organic layers were combined, washed with brine and dried using anhydrous MgSO<sub>4</sub>. The solvents were removed under reduced pressure and the crude purified using silica gel column chromatography, eluting with 3:2 EtO<sub>2</sub>/ petroleum ether 40/60, to yield the desired compound **49** as a yellow oil (1.38 g, 98%)

**Nona-1,8-diyne-3,7-dione 49:** IR (neat): 3281, 1455, 1411, 1023, 1013 cm<sup>-1</sup>; <sup>1</sup>H NMR (CDCl<sub>3</sub>, 500 MHz) δ: 3.23 (s, 2H), 2.67 (t, *J* = 7.1 Hz, 4H), 2.05 – 1.99 (m, 2H); <sup>13</sup>C NMR (CDCl<sub>3</sub>, 126 MHz) δ: 186.3, 81.4, 78.9, 44.3, 18.6.

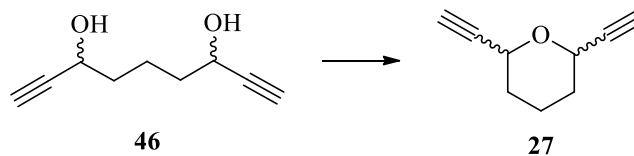
**Nona-2,8-diyne-3,5-diol 46 (mixture of diastereoisomers)**

Chemical Formula: C<sub>9</sub>H<sub>12</sub>O<sub>2</sub>

Molecular Weight: 152.19

**49** (0.5233 g, 3.54 mmol) was dissolved in THF (45 mL) and the solution was cooled to 0 °C. Sodium borohydride (0.5425 g, 14.35 mmol) was added and the reaction solution heated at reflux for 12 h. The reaction mixture was allowed to cool to room temperature, quenched with 1M HCl (40 mL) and the product was extracted from the aqueous layer using EtOAc (3x25 mL). The organic layers were combined, washed with brine and dried using anhydrous MgSO<sub>4</sub>. The solvents were removed under reduced pressure and the residue purified using silica gel column chromatography, eluting with 3:2 EtO<sub>2</sub>/ petroleum ether 40/60, to yield the desired compound **46** as a mixture of diastereoisomers as a light yellow oil (0.34 g, 63%).

IR (neat): 3282, 2940, 1702, 1604, 1417 cm<sup>-1</sup>; <sup>1</sup>H NMR (CDCl<sub>3</sub>, 500 MHz) δ: 5.01 – 4.87 (m, 2H), 3.73 – 3.54 (m, 2H), 2.17 – 2.11 (m, 2H), 1.61 – 1.56 (m, 4H); <sup>13</sup>C NMR (CDCl<sub>3</sub>, 126 MHz) δ: 77.3, 62.6, 32.7, 31.8, 23.8.

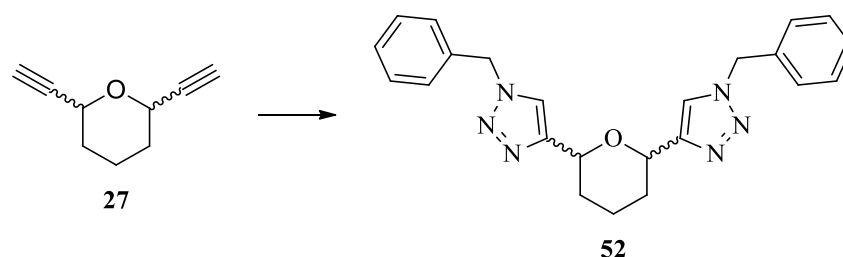
**2,6-Diethynyltetrahydro-2H-pyran 27 (mixture of diastereoisomers)**

Chemical Formula: C<sub>9</sub>H<sub>10</sub>O

Molecular Weight: 134.18

**46** (0.3211 g, 2.11 mmol) was dissolved in CH<sub>2</sub>Cl<sub>2</sub> (30 mL) and 4Å molecular sieve were added to the reaction flask. *p*-Toluenesulfonic acid (0.0573 g, 0.30 mmol) was added and the reaction solution stirred at room temperature for 12 h. The reaction mixture was filtered over Celite and washed with EtOAc (40 mL). The solvents were removed under reduced pressure to yield the desired compound **27** as a mixture of diastereoisomers as a yellow oil (0.207 g, 73%).

IR (neat): 3294, 2952, 2867, 1250 cm<sup>-1</sup>; <sup>1</sup>H NMR (CDCl<sub>3</sub>, 500 MHz) δ: 4.50 – 4.27 (m, 2H), 2.47 (d, *J* = 2.1 Hz, 2H), 1.87 – 1.57 (m, 8H); <sup>13</sup>C NMR (CDCl<sub>3</sub>, 126 MHz) δ: 84.8, 73.3, 62.8, 62.3, 37.2, 31.1, 20.8.

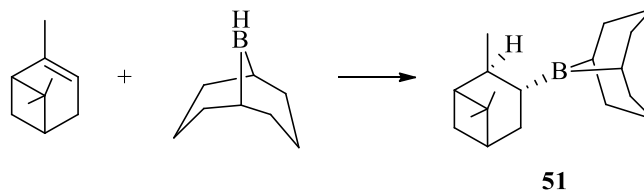
**2,6-Bis(1-benzyl-1H-1,2,3-triazol-4-yl)tetrahydro-2H-pyran 52 (mixture of diastereoisomers)**

Chemical Formula: C<sub>23</sub>H<sub>24</sub>N<sub>6</sub>O

Molecular Weight: 400.48

Sodium azide (0.5689 g, 8.75 mmol) was dissolved in a *t*BuOH/H<sub>2</sub>O (1:1, 50 mL) mixture with stirring. Benzyl bromide (1.0 mL, 8.51 mmol) was added and the mixture stirred for 10 min. Sodium ascorbate (0.1441 g, 0.73 mmol), compound **27** (0.5 g, 3.70 mmol) and copper sulfate (0.1995 g, 0.80 mmol) were added, and the solution stirred vigorously for 12 h. The solution was diluted with cold H<sub>2</sub>O (100 mL); the solid that formed was collected using suction filtration and washed with cold H<sub>2</sub>O. The solid was dissolved in CH<sub>2</sub>Cl<sub>2</sub> (40 mL), dried with anhydrous MgSO<sub>4</sub> and impurities removed with activated charcoal. The solution was filtered through Celite and the solvents removed under reduced pressure to yield the desired compound **52** as a light yellow oil (0.645 g, 63%).

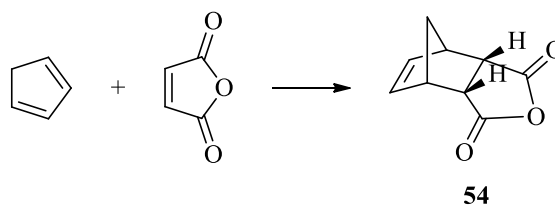
IR (neat): 3298, 2926, 1694, 1455 cm<sup>-1</sup>; <sup>1</sup>H NMR (CDCl<sub>3</sub>, 500 MHz) δ: 7.47 (s, 2H), 7.37 – 7.30 (m, 10H), 5.51 – 5.43 (m, 4H), 4.93 – 4.77 (m, 2H), 1.82 – 1.50 (m, 6H); <sup>13</sup>C NMR (CDCl<sub>3</sub>, 126 MHz) δ: 134.6, 129.3, 128.9, 128.3, 128.3, 128.3, 31.1, 29.8, 22.8, 21.3; HRMS (NSI): *m/z* [M + H]<sup>+</sup> calcd for : 401.2084; found: 401.2083.

**B-3-Pinanyl-9-borabicyclo[3.3.1]nonane (Alpine-borane) **51****<sup>97</sup>

Chemical Formula: C<sub>23</sub>H<sub>24</sub>N<sub>6</sub>O

Molecular Weight: 400.48

9-BBN (50 mL, 0.5 M in THF, 25 mmol) and  $\alpha$ -pinene (3.6 mL, 22.67 mmol) were heated at reflux for 3 h. The reaction mixture was allowed to cool to room temperature and the solution of **51** used immediately in the reduction reaction without isolation.

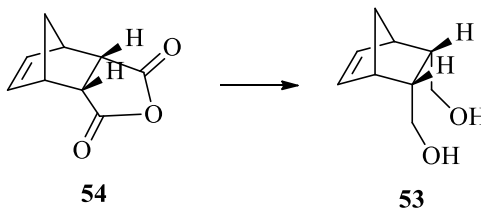
***endo*-Norbornene-5,6-dicarboxylic anhydride **54****<sup>116</sup>

Chemical Formula: C<sub>9</sub>H<sub>8</sub>O<sub>3</sub>

Molecular Weight: 164.16

Maleic anhydride (11.5072 g, 117.42 mmol) was dissolved in toluene (160 mL) and cooled to 0 °C. Cyclopentadiene (11.0 mL, 131.0 mmol) was added dropwise and the reaction mixture stirred at room temperature for 12 h. The solvents were removed under reduced pressure and the product recrystallized from hot MeOH to yield the desired compound **54** as colourless crystals (15.020 g, 78%).

m.p. 154-156 °C, lit. 164-165 °C;<sup>116</sup> IR (neat): 2980, 2954, 1772, 1705 cm<sup>-1</sup>; <sup>1</sup>H NMR (CDCl<sub>3</sub>, 500 MHz) δ: 6.29 (t, *J* = 1.7 Hz, 2H), 3.57 (dd, *J* = 2.9, 1.6 Hz, 2H), 3.52 – 3.43 (m, 2H), 1.84 – 1.49 (m, 2H); <sup>13</sup>C NMR (CDCl<sub>3</sub>, 126 MHz) δ: 171.5, 135.6, 52.8, 47.2, 46.2.

**endo-Norbornene-5,6-dimethanol 53**<sup>117</sup>

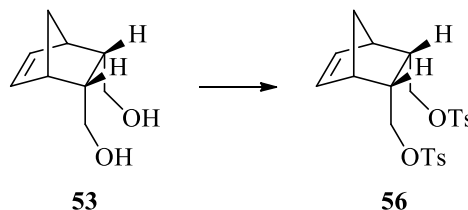
Chemical Formula: C<sub>9</sub>H<sub>14</sub>O<sub>2</sub>

Molecular Weight: 154.21

LiAlH<sub>4</sub> (0.9329 g, 24.55 mmol) was suspended in Et<sub>2</sub>O (20 mL) and the suspension cooled to 0 °C. A solution of **54** (2.0460 g, 12.48 mmol) in THF (20 mL) was added to the LiAlH<sub>4</sub> solution and the reaction mixture heated at reflux for 1 h. The reaction mixture was allowed to cool to room temperature and quenched with 10% H<sub>2</sub>SO<sub>4</sub> (10 mL). The product was extracted from the aqueous layer using EtOAc (3x20 mL), the organic layers were combined and dried using anhydrous MgSO<sub>4</sub>. The solvents were removed under reduced pressure to yield the desired compound **53** as a light yellow solid (1.443 g, 75%).

m.p. 80-82 °C, lit. 68.0-68.5 °C;<sup>117</sup> IR (neat): 3274, 2959, 2908, 2868, 1023 cm<sup>-1</sup>; <sup>1</sup>H NMR (CDCl<sub>3</sub>, 500 MHz) δ: 6.03 (t, *J* = 1.8 Hz, 2H), 3.64 (dd, *J* = 11.2, 3.6 Hz, 2H), 3.44 – 3.31 (m, 2H), 3.16 (s, 2H), 2.83 – 2.76 (m, 2H), 2.60 – 2.45 (m, 2H), 1.45 – 1.35 (m, 2H); <sup>13</sup>C NMR (CDCl<sub>3</sub>, 126 MHz) δ: 134.9, 63.7, 50.1, 46.7, 45.3.



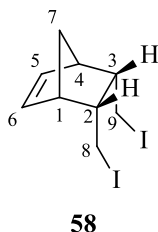
***endo*-Norbornene-5,6-diylbis(methylene)-bis(4-methylbenzenesulfonate) **56**<sup>117</sup>**

Chemical Formula: C<sub>23</sub>H<sub>26</sub>O<sub>6</sub>S<sub>2</sub>

Molecular Weight: 462.58

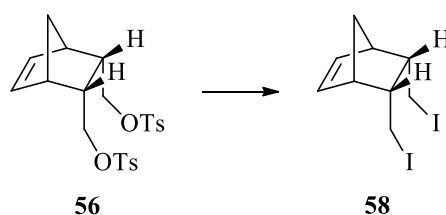
**53** (0.780 g, 5.06 mmol) was dissolved in pyridine (40 mL) and the solution was cooled to -5 °C. *p*-Toluenesulfonyl chloride (2.9083 g, 15.25 mmol) was added and the reaction mixture stirred at room temperature for 30 min. The reaction was quenched with H<sub>2</sub>O (40 mL) and the product extracted from the aqueous layer using EtOAc (3x20 mL). The organic layers were combined, washed with 1M HCl (40 mL), CuSO<sub>4</sub> solution (40 mL), brine (40 mL), and dried over anhydrous MgSO<sub>4</sub>. The solvents were removed under reduced pressure to yield the desired compound **56** as a white solid (3.6694 g, 52%).

m.p. 87-88 °C, lit. 87.5-88.0 °C;<sup>117</sup> IR (neat): 2978, 1597, 1361, 1176, 1096, 952 cm<sup>-1</sup>; <sup>1</sup>H NMR (CDCl<sub>3</sub>, 500 MHz) δ: 7.78 – 7.70 (m, 4H), 7.36 (dd, *J* = 8.5, 0.5 Hz, 4H), 5.91 (t, *J* = 1.8 Hz, 2H), 3.78 – 3.69 (m, 2H), 3.62 – 3.49 (m, 2H), 2.95 – 2.82 (m, 2H), 2.54 – 2.47 (m, 2H), 2.47 (s, 6H), 1.49-1.27 (dd, *J* = 8.7, 107.3 Hz, 2H); <sup>13</sup>C NMR (CDCl<sub>3</sub>, 126 MHz) δ: 145.1, 135.5, 132.9, 130.1, 128.0, 70.3, 48.9, 45.5, 40.9, 21.8.

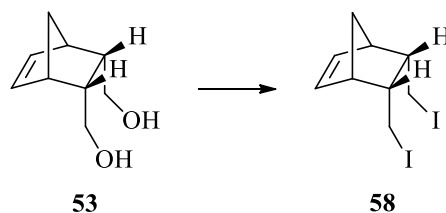
***endo*-Norbornene-5,6-dimethyl iodide **58****

Chemical Formula: C<sub>9</sub>H<sub>12</sub>I<sub>2</sub>

Molecular Weight: 374.00

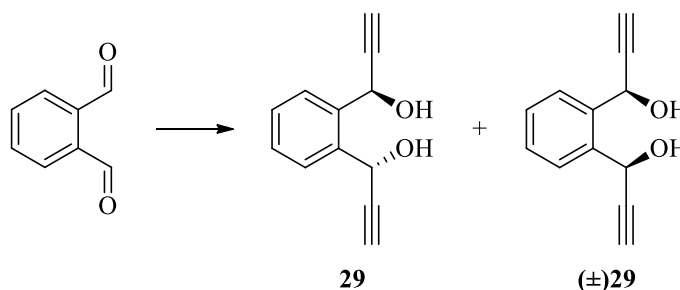
**From *bis*-tosyl **56**:**

**56** (0.2095 g, 0.45 mmol) was dissolved in acetone (25 mL) and sodium iodide (0.7339 g, 4.89 mmol) was added. The reaction mixture was heated at reflux for 24 h. The solution was allowed to cool to room temperature, filtered over Celite and washed with cold acetone. The solvent was removed at reduced pressure, keeping the temperature below 40 °C to prevent degradation. The oil was dissolved in Et<sub>2</sub>O (30 mL), washed with aqueous sodium thiosulfate (40 mL), and the combined organic layers dried over anhydrous MgSO<sub>4</sub>. The solvents were removed under reduced pressure. The residue was purified using silica gel column chromatography, eluting with 1:1 EtO<sub>2</sub>/ petroleum ether 40/60, to yield the desired compound **48** as a brown oil (0.1503 g, 87%).

**From diol 53:**

Triphenyl phosphine (4.2973 g, 16.40 mmol) and imidazole (1.1246 g, 16.54 mmol) were dissolved in  $\text{CH}_2\text{Cl}_2$  (40 mL), and the solution was cooled to 0 °C. Iodine (4.2504 g, 16.75 mmol) and **53** (1.0683 g, 6.94 mmol) were added, and the reaction mixture was stirred at room temperature for 12 h. The reaction solution was filtered over Celite and the solvents removed under reduced pressure. The residue was purified using silica gel column chromatography, eluting with 1:1  $\text{EtO}_2$ / petroleum ether 40/60, to yield the desired compound **58** as a brown oil (1.634 g, 63%).

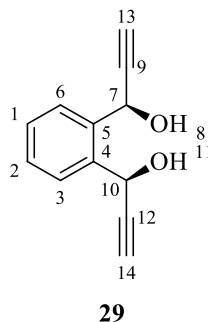
**endo-Norbornene-5,6-dimethyl iodide 58:** IR (neat): 3055, 2973, 1429, 1176  $\text{cm}^{-1}$ ;  $^1\text{H}$  NMR ( $\text{CDCl}_3$ , 500 MHz)  $\delta$ : 6.29 (t,  $J = 1.8$  Hz, 2H, H-5,6), 3.33 – 3.27 (m, 2H, H-1,4), 3.20 (dd,  $J = 8.9, 4.0$  Hz, 2H, H-8,9,2,3), 2.74 – 2.61 (m, 4H, H-8,9), 1.50 (dt,  $J = 8.6, 1.8$  Hz, 1H, H-7), 1.35 (dt,  $J = 8.6, 1.3$  Hz, 1H, H-7);  $^{13}\text{C}$  NMR ( $\text{CDCl}_3$ , 126 MHz)  $\delta$ : 135.5 (C-5,6), 49.9 (C-1,4), 47.9 (C-7), 47.8 (C-2,3), 7.6 (C-8,9).

**1,2-bis-(Prop-2-yn-1-ol)benzene 29**

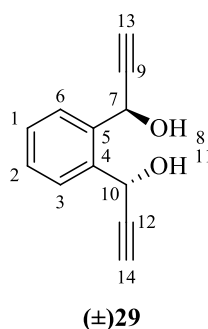
Chemical Formula: C<sub>12</sub>H<sub>10</sub>O<sub>2</sub>

Molecular Weight: 186.21

*o*-Phthalaldehyde (2.0025 g, 14.93 mmol) was dissolved in THF (75 mL) and ethynyl magnesium bromide solution (0.5 M in THF, 66 mL, 32.80 mmol) was added. The mixture was heated at reflux for 3 h, and allowed to cool to room temperature. The reaction was quenched with saturated aqueous NH<sub>4</sub>Cl (60 mL) and the product extracted from the aqueous layer using EtOAc (3x25 mL). The organic layers were combined and dried over anhydrous MgSO<sub>4</sub>. The solvents were removed under reduced pressure and the crude product was purified using silica gel column chromatography, eluting with 1:1 EtOAc/ petroleum ether 40/60 to yield the product as a mixture of diastereoisomers as a yellow oil (2.473 g, 89%). <sup>1</sup>H NMR spectrum analysis showed a mixture of isomers in a ratio of 2.1:1 *meso*/racemic. The *meso* isomer was precipitated from the product mixture using CH<sub>2</sub>Cl<sub>2</sub>/petroleum ether, and was separated by filtration of the crystalline *meso* isomer and washing with petroleum ether. The (±)-isomer remained in the filtrate. Several precipitations were required to achieve almost complete separation.

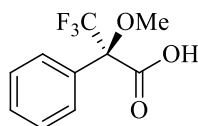
***meso*-(1*S*,1'*R*)-1,2-bis-(Prop-2-yn-1-ol)benzene 29:**

Large colourless crystals (1.67 g, 60%); m.p. 98-99 °C; IR (neat) 3276, 3264, 2116  $\text{cm}^{-1}$ ;  $^1\text{H}$  NMR ( $\text{CDCl}_3$ , 500 MHz)  $\delta$  7.92-7.77 (m, 2H, H-1,2,3,6), 7.49-7.35 (m, 2H, H-1,2,3,6), 5.91 (dd,  $J = 4.7, 2.2$  Hz, 2H, H-7,10), 2.95 (d,  $J = 4.7$  Hz, 2H, H-8,11), 2.75 (d,  $J = 2.2$  Hz, 2H, H-13,14);  $^{13}\text{C}$  NMR ( $\text{CDCl}_3$ , 126 MHz)  $\delta$  134.7 (C-4,5), 129.7 (C-1,2), 129.1 (C-3,6), 80.3 (C-9,12), 75.8 (C-13,14), 62.7 (C-7,10); Crystal data:  $\text{C}_{12}\text{H}_{10}\text{O}_2$ ,  $M = 186.21$ , triclinic,  $a = 9.7265(12)$ ,  $b = 10.6455(11)$ ,  $c = 11.2471(7)$  Å,  $V = 980.67(19)$  Å<sup>3</sup>,  $T = 173$  K, space group  $P-1$  (no. 2),  $Z = 4$ , 13495 reflections measured, 3562 unique ( $R_{\text{int}} = 0.0564$ ), which were used in all calculations. The final  $wR2$  was 0.1219 (all data).

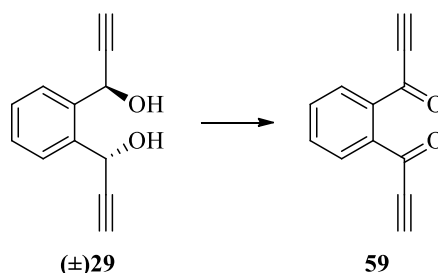
**(±)-1,2-bis-(Prop-2-yn-1-ol)benzene (±)29:**

Thick orange oil (0.79 g, 29%); IR (neat) 3414, 3287, 2117  $\text{cm}^{-1}$ ;  $^1\text{H}$  NMR ( $\text{CDCl}_3$ , 500 MHz)  $\delta$  7.73-7.63 (m, 2H), 7.41-7.37 (m, 2H), 6.03 (d,  $J = 2.3$  Hz, 2H), 2.73 (d,  $J = 2.3$  Hz, 2H);  $^{13}\text{C}$  NMR ( $\text{CDCl}_3$ , 126 MHz)  $\delta$  137.7 (C-4,5), 129.5 (C-1,2), 129.3 (C-3,6), 82.8 (C-9,12), 75.8 (C-13,14), 63.4 (C-7,10).

---

**General method for the esterification of compounds using Mosher's acid for the assessment of stereochemistry**

The compound, (*R*)-(+)- $\alpha$ -methoxy- $\alpha$ -trifluoromethylphenylacetic acid (3 Eq, 0.2 M in CH<sub>2</sub>Cl<sub>2</sub>), DCC (3 Eq) and DMAP (0.1 Eq, 0.06 M in CH<sub>2</sub>Cl<sub>2</sub>) were added, and stirred at room temperature for 20 min. H<sub>2</sub>O (5 mL) was added and the layers separated. The aqueous layer was extracted using CH<sub>2</sub>Cl<sub>2</sub> (5 mL). The organic layers were combined and dried over anhydrous MgSO<sub>4</sub>. The solvents were removed under reduced pressure to yield the desired Mosher's ester ready for <sup>1</sup>H NMR analysis.

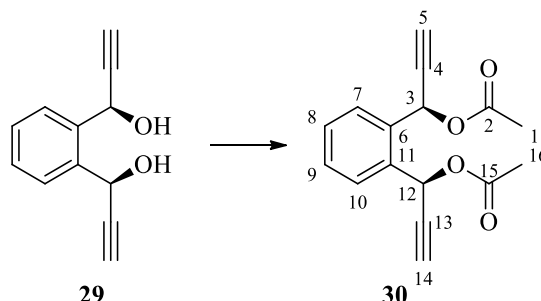
**1,1'-(1,2-Phenylene)-bis-(prop-2-yn-1-one) **59****<sup>118</sup>

Chemical Formula: C<sub>12</sub>H<sub>6</sub>O<sub>2</sub>

Molecular Weight: 182.17

**(±)29** (0.752 g, 4.04 mmol) was dissolved in acetone (15 mL) and Jones reagent (0.534 g CrO<sub>3</sub> dissolved in 0.46 mL conc. H<sub>2</sub>SO<sub>4</sub>, and diluted to 5 mL with H<sub>2</sub>O) was added. The reaction solution was stirred at room temperature for 12 h. The reaction mixture was quenched using *iso*-propanol (15 mL) and the product extracted from the aqueous layer using Et<sub>2</sub>O (3x10 mL). The organic layers were combined and washed with a solution of sodium bicarbonate (30 mL), brine (30 mL), and dried over anhydrous MgSO<sub>4</sub>. The solvents were removed under reduced pressure and the crude product was purified using silica gel column chromatography, eluting with 1:1 EtOAc/ petroleum ether 40/60 to yield the desired compound **59** as a light yellow oil (1.315 g, 93%).

IR (neat): 3215, 1635 cm<sup>-1</sup>; <sup>1</sup>H NMR (CDCl<sub>3</sub>, 500 MHz) δ: 7.87 (dd, *J* = 5.7, 3.3 Hz, 2H), 7.67 (dd, *J* = 5.7, 3.3 Hz, 2H), 3.44 (s, 2H);

**(1*S*,1'*R*)-1,2-bis-(1-(Acetyl)prop-2-yn-1-yl)benzene 30**

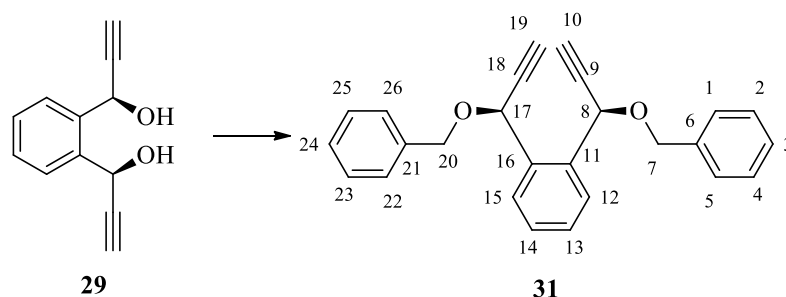
Chemical Formula: C<sub>16</sub>H<sub>14</sub>O<sub>4</sub>

Molecular Weight: 270.28

Compound **29** (0.5010 g, 2.68 mmol) was dissolved in CH<sub>2</sub>Cl<sub>2</sub> (6 mL) at 0 °C. DMAP (6.588 g, 54.0 mmol), triethylamine (1.1 mL, 8.06 mmol), and acetic anhydride (0.76 mL, 8.06 mmol) were added. The reaction mixture was stirred at room temperature for 2 h and quenched with H<sub>2</sub>O (25 mL). The product was extracted from the aqueous layer using CH<sub>2</sub>Cl<sub>2</sub> (3x10 mL) and the organic layers were combined, washed with brine (30 mL), and dried over anhydrous Na<sub>2</sub>SO<sub>4</sub>. The solvents were removed under reduced pressure and the crude product purified by precipitation from a CH<sub>2</sub>Cl<sub>2</sub>/petroleum ether 40/60 solvent system to yield the desired compound **30** as a colourless solid (0.63 g, 87%).

IR (neat) 3278, 3266, 2127, 1738, 1369, 1218 cm<sup>-1</sup>; <sup>1</sup>H NMR (CDCl<sub>3</sub>, 500 MHz) δ 7.70-7.62 (m, 2H, H-8,9), 7.46-7.37 (m, 2H, H-7,10), 6.75 (d, *J* = 2.3 Hz, 2H, H-3,12), 2.63 (d, *J* = 2.3 Hz, 2H, H-5,14), 2.12 (s, 6H, H-1,16); <sup>13</sup>C NMR (CDCl<sub>3</sub>, 126 MHz) δ 169.5 (C-2,15), 134.7 (C-6,11), 129.7 (C-8,9), 129.1 (C-7,10), 80.3 (C-4,13), 75.8 (C-5,14), 62.7 (C-3,12), 21.0 (C-1,16). *m/z* HRMS (NSI) calcd for [C<sub>16</sub>H<sub>18</sub>O<sub>4</sub>N]<sup>+</sup> 288.1230; Found for [M + NH<sub>4</sub>]<sup>+</sup> 288.1229.



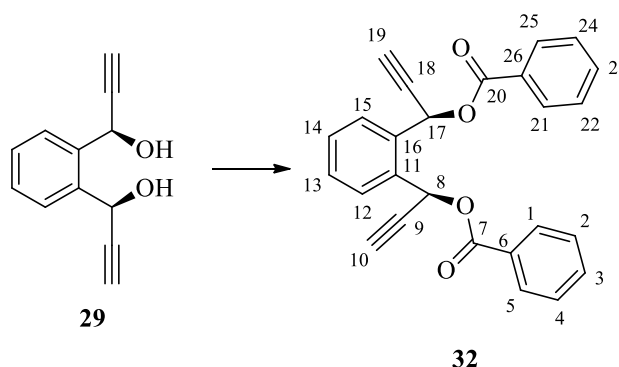
**(1*S*,1'*R*)-1,2-bis-(1-(Benzyloxy)prop-2-yn-1-yl)benzene 31**

Chemical Formula: C<sub>26</sub>H<sub>22</sub>O<sub>2</sub>

Molecular Weight: 366.45

**29** (2.0012 g, 12.3 mmol) was dissolved in a THF/DMF mixture (5:1, 60 mL) and the solution was cooled to 0 °C. NaH (0.89 g, 37.1 mmol) was added and the reaction mixture stirred for 30 min. Benzyl bromide (9.1 mL, 76.5 mmol) was added and the reaction mixture stirred at room temperature for a further 12 h. The reaction was quenched with H<sub>2</sub>O (50 mL) and the product extracted from the aqueous layer using EtOAc (3x20 mL). The organic layers were combined, washed with brine (40 mL), and dried over anhydrous Na<sub>2</sub>SO<sub>4</sub>. The solvents were removed under reduced pressure and the crude product was purified using silica gel column chromatography, eluting with 1:1 EtOAc/petroleum ether 40/60 to yield the desired compound **31** as a yellow oil (3.23 g, 82%).

IR (neat) 3287, 3064, 3031, 2866, 2112, 1496, 1454 cm<sup>-1</sup>; <sup>1</sup>H NMR (CDCl<sub>3</sub>, 500 MHz) δ 7.77-7.67 (m, 2H, H-13,14), 7.43-7.37 (m, 2H, H-12,15), 7.36-7.26 (m, 10H, H-1,2,3,4,5,22,23,24,25,26), 5.60 (d, *J* = 2.2 Hz, 2H, H-8,17), 4.70 (d, *J* = 11.6 Hz, 2H, H-7,20), 4.58 (d, *J* = 11.6 Hz, 2H, H-7,20), 2.60 (d, *J* = 2.2 Hz, 2H, H-10,19); <sup>13</sup>C NMR (CDCl<sub>3</sub>, 126 MHz) δ 137.6 (11,16), 136.2 (C-12,15), 129.0 (C-13,14), 128.5 (C-1,5,22,26), 128.3 (C-2,4,23,25), 127.9 (C-3,24), 81.6 (C-9,18), 75.9 (7,20), 70.6 (C-10,19), 67.6 (C-8,17). *m/z* HRMS (NSI) calcd for [C<sub>26</sub>H<sub>26</sub>O<sub>2</sub>N]<sup>+</sup> 384.1958; Found for [M + NH<sub>4</sub>]<sup>+</sup> 384.1957.

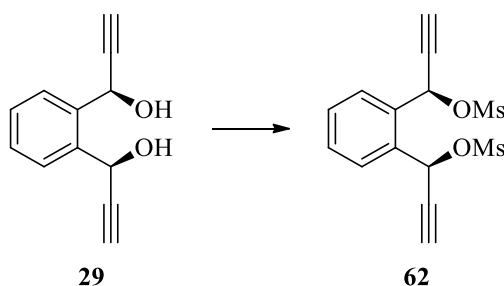
**(1*S*,1'*R*)-1,2-bis-(1-(Benzoyloxy)prop-2-yn-1-yl)benzene 32**

Chemical Formula: C<sub>26</sub>H<sub>18</sub>O<sub>4</sub>

Molecular Weight: 394.42

**29** (0.5032 g, 2.68 mmol) was dissolved in CH<sub>2</sub>Cl<sub>2</sub> (20 mL) and benzoyl chloride (0.5 mL, 4.02 mmol), triethylamine (0.75 mL, 5.36 mmol) and DMAP (0.0163 g, 0.13 mmol) were added. The reaction mixture was stirred at room temperature for 2 h. The product was extracted using CH<sub>2</sub>Cl<sub>2</sub> (3x20 mL) and the combined organic layers were dried over anhydrous MgSO<sub>4</sub>. The solvents were removed under reduced pressure and the crude product was purified using silica gel column chromatography, eluting with 1:1 EtOAc/petroleum ether 40/60 to yield the desired compound **32** as an orange oil (0.687 g, 64%).

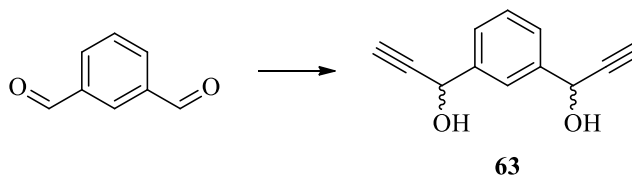
IR (neat) 3289, 3063, 2124, 1724, 1257 cm<sup>-1</sup>; <sup>1</sup>H NMR (CDCl<sub>3</sub>, 500 MHz) δ 8.11-7.99 (m, 2H, H-13,14), 7.86-7.77 (m, 2H, H-12,15), 7.56-7.50 (m, 2H, 3,23), 7.51-7.46 (m, 4H, H-2,4,22,24), 7.42-7.33 (m, 4H, H-1,5,21,25), 7.10 (d, *J* = 2.3 Hz, 2H, H-8,17), 2.61 (d, *J* = 2.3 Hz, 2H, H-10,19); <sup>13</sup>C NMR (CDCl<sub>3</sub>, 126 MHz) δ 165.1 (C-7,20), 134.9 (C-11,16), 133.4 (C-6,26), 130.1 (C-13,14), 129.9 (C-12,15), 129.5 (C-1,2,4,5,21,22,24,25), 128.5 (C-3,23), 80.3 (C-9,18), 76.2 (C-10,19), 63.5 (C-8,17). *m/z* HRMS (NSI) calcd for [C<sub>26</sub>H<sub>22</sub>O<sub>4</sub>N]<sup>+</sup> 412.1543; Found for [M + NH<sub>4</sub>]<sup>+</sup>412.1540.

**(1*S*,1'*R*)-1,2-bis-(1-((Methylsulfonyl)oxy)prop-2-yn-1-yl)benzene 62**

Chemical Formula: C<sub>14</sub>H<sub>14</sub>O<sub>6</sub>S<sub>2</sub>

Molecular Weight: 342.39

**29** (0.5013 g, 3.09 mmol) was dissolved in CH<sub>2</sub>Cl<sub>2</sub> (15 mL) and the solution was cooled to 0 °C. Triethylamine (1.25 mL, 9.02 mmol) was added, followed by methanesulfonyl chloride (0.8205 g, 7.20 mmol) and the reaction solution stirred for 30 min. The reaction solution was diluted with CH<sub>2</sub>Cl<sub>2</sub> (30 mL), washed with water (30 mL) and brine (30 mL), and dried over anhydrous MgSO<sub>4</sub>. The solvents were removed under reduced pressure to yield the desired compound **62** as a light yellow oil (1.0275 g, 97%). The isolated compound decomposed before spectral analysis could be performed.

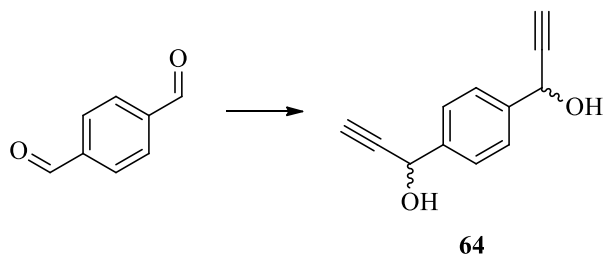
**1,3-bis-(Prop-2-yn-1-ol)benzene 63**

Chemical Formula: C<sub>12</sub>H<sub>10</sub>O<sub>2</sub>

Molecular Weight: 186.21

*m*-Phthalaldehyde (0.5022 g, 3.75 mmol) was dissolved in THF (20 mL). Ethynyl magnesium bromide solution (0.5 M in THF, 17 mL, 8.36 mmol) was added to the solution. The mixture was heated to reflux for 3 h, and allowed to cool to room temperature. The reaction was quenched with saturated aqueous NH<sub>4</sub>Cl (30 mL) and the product extracted from the aqueous layer using Et<sub>2</sub>O (3x20 mL). The organic layers were combined and dried over anhydrous MgSO<sub>4</sub>, filtered, and the solvents removed under reduced pressure. The crude product was purified using column chromatography, eluting with EtOAc/petroleum ether 40/60 (1:1) to give the desired product **63** as mixture of diastereoisomers as an orange oil (0.5293 g, 76%).

IR (neat): 3404, 3287, 2115, 1697, 1037 cm<sup>-1</sup>; <sup>1</sup>H NMR (CDCl<sub>3</sub>, 500 MHz) δ: 7.74 (d, *J* = 1.7 Hz, 1H), 7.54 (dd, *J* = 7.7, 1.7 Hz, 2H), 7.45 – 7.40 (m, 1H), 5.49 (d, *J* = 3.7 Hz, 2H), 2.68 (d, *J* = 2.2 Hz, 2H), 2.31 (d, *J* = 5.8 Hz, 2H); <sup>13</sup>C NMR (CDCl<sub>3</sub>, 126 MHz) δ: 140.7, 129.2, 126.9, 126.9, 125.0, 125.0, 83.5, 75.2, 64.3.

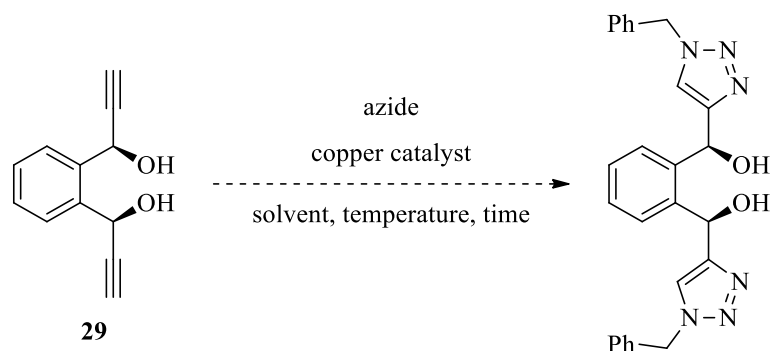
**1,4-bis-(Prop-2-yn-1-ol)benzene 64**

Chemical Formula: C<sub>12</sub>H<sub>10</sub>O<sub>2</sub>

Molecular Weight: 186.21

*p*-Phthalaldehyde (2.0335 g, 15.18 mmol) was dissolved in THF (75 mL). Ethynyl magnesium bromide solution (0.5 M in THF, 66 mL, 32.80 mmol) was added to the solution. The mixture was heated to reflux for 3 h, and allowed to cool to room temperature. The reaction was quenched with saturated aqueous NH<sub>4</sub>Cl (50 mL) and the product extracted from the aqueous layer using Et<sub>2</sub>O (3x30 mL). The organic layers were combined and dried over anhydrous MgSO<sub>4</sub>, filtered, and the solvents removed under reduced pressure. The crude product was purified using column chromatography, eluting with EtOAc/petroleum ether 40/60 (1:1) to give the desired product **64** as mixture of diastereoisomers as an orange solid (1.9156 g, 67%).

m.p. 101-106 °C; IR (neat): 3342, 3281, 2118, 1411, 1023, 1013 cm<sup>-1</sup>; <sup>1</sup>H NMR (DMSO, 500 MHz) δ: 7.44 (s, 2H), 6.03 (d, *J* = 5.9 Hz, 1H), 5.34 (dd, *J* = 5.9, 2.3 Hz, 1H), 3.48 (d, *J* = 2.3 Hz, 2H); <sup>13</sup>C NMR (DMSO, 126 MHz) δ: 141.31, 126.22, 85.51, 75.79, 62.10.

**General method used for the attempted ‘click’ reaction of 29 shown in Table 5**

Compound **29** (1.1 Eq, 0.2M in solvent), the copper source (0.1 Eq) and the azide source (2 Eq) were stirred for the desired time at the desired temperature. The reaction was quenched with 1M HCl. The product was extracted from the aqueous layer using EtOAc and the organic layer were combined, and dried over anhydrous  $\text{MgSO}_4$ . The solvents were removed under reduced pressure to yield the reaction product.

## References

---

- 1 W. Nugent, *J. Am. Chem. Soc.*, 1992, **114**, 2768–2769.
- 2 L. E. Martinez, J. L. Leighton, D. H. Carsten and E. N. Jacobsen, *J. Am. Chem. Soc.*, 1995, **117**, 5897–5898.
- 3 D. M. Murphy, I. A. Fallis, E. Carter, D. J. Willock, J. Landon, S. Van Doorslaer and E. Vinck, *Phys. Chem. Chem. Phys.*, 2009, **11**, 6757–6769.
- 4 Z. Li, M. Fernández and E. N. Jacobsen, *Org. Lett.*, 1999, **1**, 1611–1613.
- 5 K. Arai, S. Lucarini, M. M. Salter, K. Ohta, Y. Yamashita and S. Kobayashi, *J. Am. Chem. Soc.*, 2007, **129**, 8103–8111.
- 6 S. Nakamura, M. Hayashi, Y. Kamada, R. Sasaki, Y. Hiramatsu, N. Shibata and T. Toru, *Tetrahedron Lett.*, 2010, **51**, 3820–3823.
- 7 C. Schneider, *Angew. Chem. Int. Ed.*, 2009, **48**, 2082–2084.
- 8 P. Wang, *Beilstein J. Org. Chem.*, 2013, **9**, 1677–1695.
- 9 M. Senatore, A. Lattanzi, S. Santoro, C. Santi and G. Della Sala, *Org. Biomol. Chem.*, 2011, **9**, 6205–6207.
- 10 E. B. Rowland, G. B. Rowland, E. Rivera-Otero and J. C. Antilla, *J. Am. Chem. Soc.*, 2007, **129**, 12084–12085.
- 11 R. F. Heck and J. P. Nolley, *J. Org. Chem.*, 1972, **37**, 2320–2322.
- 12 M. Mori, K. Chiba and Y. Ban, *Tetrahedron Lett.*, 1977, **18**, 1037–1040.
- 13 F. Ozawa and T. Hayashi, *J. Organomet. Chem.*, 1992, **428**, 267–277.
- 14 N. E. Carpenter, D. J. Kucera and L. E. Overman, *J. Org. Chem.*, 1989, **54**, 5846–5848.
- 15 S. Liu and J. S. Zhou, *Chem. Commun.*, 2013, **49**, 11758–60.
- 16 F. Ozawa, a Kubo, Y. Matsumoto, T. Hayashi, E. Nishioka, K. Yanagi and K. Moriguchi, *Organometallics*, 1993, **12**, 4188–4196.
- 17 M. Lautens, K. Fagnou and T. Rovis, *J. Am. Chem. Soc.*, 2000, **122**, 5650–5651.
- 18 M. Lautens and K. Fagnou, *Proc. Natl. Acad. Sci. U. S. A.*, 2004, **101**, 5455–5460.

- 19 G. C. Fu, J. C. Ruble and J. Tweddell, *J. Org. Chem.*, 1998, **63**, 2794–2795.
- 20 H. Schedel, K. Kan, Y. Ueda, K. Mishiro, K. Yoshida, T. Furuta and T. Kawabata, *Beilstein J. Org. Chem.*, 2012, **8**, 1778–1787.
- 21 T. Oriyama, H. Taguchi, D. Terakado and T. Sano, *Chem. Lett.*, 2002, 26–26.
- 22 B. M. Trost and T. Mino, *J. Am. Chem. Soc.*, 2003, **125**, 2410–2411.
- 23 E. T. Michalson and J. Szmuszkowicz, *Prog. Drug Res.*, 1989, **33**, 135–149.
- 24 O. Kitagawa, K. Yotsumoto, M. Kohriyama, Y. Dobashi and T. Taguchi, *Org. Lett.*, 2004, **6**, 3605–3607.
- 25 O. Kitagawa, S. Matsuo, K. Yotsumoto and T. Taguchi, *J. Org. Chem.*, 2006, **71**, 2524–2527.
- 26 Y. Zhao, J. Rodrigo, A. H. Hoveyda and M. L. Snapper, *Nature*, 2006, **443**, 67–70.
- 27 J. Kang, J. W. Lee, J. I. Kim and C. Pyun, *Tetrahedron Lett.*, 1995, **36**, 4265–4268.
- 28 K. Matsuki, H. Inoue, A. Ishida, M. Takeda, M. Nakagawa and T. Hino, *Chem. Pharm. Bull.*, 1994, **42**, 9–18.
- 29 B. J. Marsh, H. Adams, M. D. Barker, I. U. Kutama and S. Jones, *Org. Lett.*, 2014, **16**, 3780–3783.
- 30 238 US PAT. 2, 489, 1949.
- 31 F. Xiong, X. X. Chen and F. E. Chen, *Tetrahedron Asymmetry*, 2010, **21**, 665–669.
- 32 M. Jia and S. You, *Chem. Commun.*, 2012, **48**, 6363.
- 33 D. Perdicchia and K. A. Jørgensen, *J. Org. Chem.*, 2007, **72**, 3565–3568.
- 34 N. Maezaki, N. Kojima, A. Sakamoto, H. Tominaga, C. Iwata, T. Tanaka, M. Monden, B. Damdinsuren and S. Nakamori, *Chem. Eur. J.*, 2003, **9**, 389–399.
- 35 F. Q. Alali, X. X. Liu and J. L. McLaughlin, *J. Nat. Prod.*, 1999, **62**, 504–540.
- 36 N. Maezaki, A. Sakamoto, N. Nagahashi, M. Soejima, Y. X. Li, T. Imamura, N. Kojima, H. Ohishi, K. I. Sakaguchi, C. Iwata and T. Tanaka, *J. Org. Chem.*, 2000, **65**, 3284–3291.
- 37 H. C. Kolb, M. G. Finn and K. B. Sharpless, *Angew. Chem. Int. Ed.*, 2001, **40**, 2004–2021.



- 38 H. C. Kolb, M. S. VanNieuwenhze and K. B. Sharpless, *Chem. Rev.*, 1994, **94**, 2483–2547.
- 39 A. B. Lowe, *Polymer Chem.*, 2010, **1**, 17.
- 40 A. R. Kannurpatti, J. W. Anseth and C. N. Bowman, *Polymer*, 1998, **39**, 2507–2513.
- 41 G. Kavadias and R. Droghini, *Can. J. Chem.*, 1979, **57**, 1870–1876.
- 42 E. Vogel, F. Kuebart, J. a. Marco, R. Andree, H. Guenther and R. Aydin, *J. Am. Chem. Soc.*, 1983, **105**, 6982–6983.
- 43 P. Lin, K. Bellos, H. Stamm and A. Onistschenko, *Tetrahedron*, 1992, **48**, 2359–2372.
- 44 S. Biswas, R. J. Knipp, L. E. Gordon, S. R. Nandula, S. U. Gorr, G. J. Clark and M. H. Nantz, *ChemMedChem*, 2011, **6**, 2063–2069.
- 45 J. Spiegel, C. Mas-Moruno, H. Kessler and W. D. Lubell, *J. Org. Chem.*, 2012, **77**, 5271–5278.
- 46 T. D. Penning, J. J. Talley, S. R. Bertenshaw, J. S. Carter, P. W. Collins, S. Docter, M. J. Graneto, L. F. Lee, J. W. Malecha, J. M. Miyashiro, R. S. Rogers, D. J. Rogier, S. S. Yu, G. D. Anderson, E. G. Burton, J. N. Cogburn, S. A. Gregory, C. M. Koboldt, W. E. Perkins, K. Seibert, A. W. Veenhuizen, Y. Y. Zhang and P. C. Isakson, *J. Med. Chem.*, 1997, **40**, 1347–1365.
- 47 Y. Kobuke, T. Sugimoto, J. Furukawa and T. Fueno, *J. Am. Chem. Soc.*, 1972, **94**, 3633–3635.
- 48 S. Löber, P. Rodriguez-Loaiza and P. Gmeiner, *Org. Lett.*, 2003, **5**, 1753–1755.
- 49 H. C. Kolb and K. B. Sharpless, *Drug Discovery Today*, 2003, **8**, 1128–1137.
- 50 V. V. Rostovtsev, L. G. Green, V. V. Fokin and K. B. Sharpless, *Angew. Chem. Int. Ed.*, 2002, **41**, 2596–2599.
- 51 C. W. Tornøe, C. Christensen and M. Meldal, *J. Org. Chem.*, 2002, **67**, 3057–3064.
- 52 M. Meldal and C. W. Tomøe, *Chem. Rev.*, 2008, **108**, 2952–3015.
- 53 V. D. Bock, H. Hiemstra and J. H. Van Maarseveen, *European J. Org. Chem.*, 2006, **2006**, 51–68.
- 54 B. T. Worrell, J. a Malik and V. V Fokin, *Science*, 2013, **340**, 457–460.

- 55 J. D. Ochocki, D. G. Mullen, E. V. Wattenberg and M. D. Distefano, *Bioorg. Med. Chem. Lett.*, 2011, **21**, 4998–5001.
- 56 L. Jia, Z. Cheng, L. Shi, J. Li, C. Wang, D. Jiang, W. Zhou, H. Meng, Y. Qi, D. Cheng and L. Zhang, *Appl. Radiat. Isotopes*, 2013, **75**, 64–70.
- 57 R. Franke, C. Doll and J. Eichler, *Tetrahedron Lett.*, 2005, **46**, 4479–4482.
- 58 X. L. Sun, C. L. Stabler, C. S. Cazalis and E. L. Chaikof, *Bioconjugate Chem.*, 2006, **17**, 52–57.
- 59 Q. Wang, T. R. Chan, R. Hilgraf, V. V. Fokin, K. B. Sharpless and M. G. Finn, *J. Am. Chem. Soc.*, 2003, **125**, 3192–3193.
- 60 J. Gierlich, G. a. Burley, P. M. E. Gramlich, D. M. Hammond and T. Carell, *Org. Lett.*, 2006, **8**, 3639–3642.
- 61 P. Wu, A. K. Feldman, A. K. Nugent, C. J. Hawker, A. Scheel, B. Voit, J. Pyun, J. M. J. Fréchet, K. B. Sharpless and V. V. Fokin, *Angew. Chem. Int. Ed.*, 2004, **43**, 3928–3932.
- 62 P. Wu, M. Malkoch, J. N. Hunt, R. Vestberg, E. Kaltgrad, M. G. Finn, V. V Fokin, K. B. Sharpless and C. J. Hawker, *Chem. Commun.* , 2005, 5775–5777.
- 63 V. Ladmiral, G. Mantovani, G. J. Clarkson, S. Cauet, J. L. Irwin and D. M. Haddleton, *J. Am. Chem. Soc.*, 2006, **128**, 4823–4830.
- 64 E.-H. Ryu and Y. Zhao, *Org. Lett.*, 2005, **7**, 1035–1037.
- 65 W. G. Lewis, L. G. Green, F. Grynszpan, Z. Radić, P. R. Carlier, P. Taylor, M. G. Finn and K. B. Sharpless, *Angew. Chem. Int. Ed.*, 2002, **41**, 1053–1057.
- 66 V. P. Mocharla, B. Colasson, L. V. Lee, S. Röper, K. B. Sharpless, C. H. Wong and H. C. Kolb, *Angew. Chem. Int. Ed.*, 2004, **44**, 116–120.
- 67 M. Whiting, J. Muldoon, Y.-C. Lin, S. M. Silverman, W. Lindstrom, A. J. Olson, H. C. Kolb, M. G. Finn, K. B. Sharpless, J. H. Elder and V. V Fokin, *Angew. Chem. Int. Ed.* , 2006, **45**, 1435–1439.
- 68 L. V Lee, M. L. Mitchell, S.-J. Huang, V. V Fokin, K. B. Sharpless and C.-H. Wong, *J. Am. Chem. Soc.*, 2003, **125**, 9588–9589.
- 69 M. Nahrwold, T. Bogner, S. Eissler, S. Verma and N. Sewald, *Org. Lett.*, 2010, **12**, 1064–1067.
- 70 J. Zhang, J. Kemmink, D. T. S. Rijkers and R. M. J. Liskamp, *Org. Lett.*, 2011, **13**, 3438–3441.

- 71 L. Zhang, X. Chen, P. Xue, H. H. Y. Sun, I. D. Williams, K. B. Sharpless, V. V. Fokin and G. Jia, *J. Am. Chem. Soc.*, 2005, **127**, 15998–15999.
- 72 B. C. Boren, S. Narayan, L. K. Rasmussen, L. Zhang, H. Zhao, Z. Lin, G. Jia and V. V. Fokin, *J. Am. Chem. Soc.*, 2008, **130**, 8923–8930.
- 73 V. O. Rodionov, V. V. Fokin and M. G. Finn, *Angew. Chem. Int. Ed.*, 2005, **44**, 2210–2215.
- 74 J. C. Meng, V. V. Fokin and M. G. Finn, *Tetrahedron Lett.*, 2005, **46**, 4543–4546.
- 75 F. Zhou, C. Tan, J. Tang, Y. Y. Zhang, W. M. Gao, H. H. Wu, Y. H. Yu and J. Zhou, *J. Am. Chem. Soc.*, 2013, **135**, 10994–10997.
- 76 G. R. Stephenson, J. P. Buttress, D. Deschamps, M. Lancelot, J. P. Martin, A. I. G. Sheldon, C. Alayrac, A. C. Gaumont and P. C. B. Page, *Synlett*, 2013, **24**, 2723–2729.
- 77 J. N. Brantley, K. M. Wiggins and C. W. Bielawski, *Science*, 2011, **333**, 1606–1609.
- 78 M. M. Caruso, D. a. Davis, Q. Shen, S. a. Odom, N. R. Sottos, S. R. White and J. S. Moore, *Chem. Rev.*, 2009, **109**, 5755–5798.
- 79 K. Kacprzak, *Synlett*, 2005, 943–946.
- 80 P. Appukkuttan, W. Dehaen, V. V Fokin and E. Van Der Eycken, *Org. Lett.*, 2004, **6**, 4223–4225.
- 81 S. Hanelt and J. Liebscher, *Synlett*, 2008, **2008**, 1058–1060.
- 82 S. Kozima, T. Itano, N. Mihara, K. Sisido and T. Isida, *J. Organomet. Chem.*, 1972, **44**, 117–126.
- 83 S. Koguchi and K. Izawa, *Synth.*, 2012, **44**, 3603–3608.
- 84 B. C. Boren, S. Narayan, L. K. Rasmussen, L. Zhang, H. Zhao, Z. Lin, G. Jia and V. V Fokin, *J. Am. Chem. Soc.*, 2008, **130**, 8923–8930.
- 85 S.-G. Hu, T.-S. Hu and Y.-L. Wu, *Org. Biomol. Chem.*, 2004, **2**, 2305–2310.
- 86 K. Omura and D. Swern, *Tetrahedron*, 1978, **34**, 1651–1660.
- 87 J. R. Parikh and W. V. E. Doering, *J. Am. Chem. Soc.*, 1967, **89**, 5505–5507.
- 88 D. B. Dess and J. C. Martin, *J. Org. Chem.*, 1983, **48**, 4155–4156.

- 89 *Work Conducted by Ali Mouawia as part of an ISCE-Chem Interreg Exchange Project.*
- 90 R. Appel, *Angew. Chem. Int. Ed.*, 1975, **14**, 801–811.
- 91 P. J. Garegg, R. Johansson, C. Ortega and B. Samuelsson, *J. Chem. Soc. Perkin Trans. 1*, 1982, 681.
- 92 J. K. De Brabander, B. Liu and M. Qian, *Org. Lett.*, 2008, **10**, 2533–2536.
- 93 S. Caddick, V. M. Delisser, V. E. Doyle, S. Khan, A. G. Avent and S. Vile, *Tetrahedron*, 1999, **55**, 2737–2754.
- 94 K. A. Parker and M. W. Ledebor, *J. Org. Chem.*, 1996, **61**, 3214–3217.
- 95 B. Grant and C. Djerassi, *J. Org. Chem.*, 1974, **39**, 968–970.
- 96 W. T. Borden, *J. Am. Chem. Soc.*, 1970, **92**, 4898–4901.
- 97 M. Mark midland, A. Tramontano, A. Kazubski, R. S. Graham, D. J. S. Tsai and D. B. Cardin, *Tetrahedron*, 1984, **40**, 1371–1380.
- 98 J. A. Dale, D. L. Dull and H. S. Mosher, *J. Org. Chem.*, 1969, **34**, 2543–2549.
- 99 E. P. Kündig and A. Enriquez-Garcia, *Beilstein J. Org. Chem.*, 2008, **4**, 3–7.
- 100 S. H. Lee, I. S. Kim, Q. R. Li, G. R. Dong, L. S. Jeong and Y. H. Jung, *J. Org. Chem.*, 2011, **76**, 10011–10019.
- 101 A. Murali, M. Puppala, B. Varghese and S. Baskaran, *European J. Org. Chem.*, 2011, 5297–5302.
- 102 D. Zhang, X. Zhang, J. Ai, Y. Zhai, Z. Liang, Y. Wang, Y. Chen, C. Li, F. Zhao, H. Jiang, M. Geng, C. Luo and H. Liu, *Bioorganic Med. Chem.*, 2013, **21**, 6804–6820.
- 103 P. V. Ramachandran, G. M. Chen and H. C. Brown, *Tetrahedron Lett.*, 1997, **38**, 2417–2420.
- 104 K. Soai, Y. Inoue, T. Takahashi and T. Shibata, *Tetrahedron*, 1996, **52**, 13355–13362.
- 105 L. Jin, D. R. Tolentino, M. Melaimi and G. Bertrand, *Sci. Adv.*, 2015, **1**, e1500304–e1500304.
- 106 M. C. Marcotullio, V. Campagna, S. Sternativo, F. Costantino and M. Curini, *Synthesis*, 2006, 2760–2766.

- 107 H. Sharghi, R. Khalifeh and M. M. Doroodmand, *Adv. Synth. Catal.*, 2009, **351**, 207–218.
- 108 P. Mathew, A. Neels and M. Albrecht, *J. Am. Chem. Soc.*, 2008, **130**, 13534–13535.
- 109 S. Koguchi and K. Izawa, *Synth.*, 2012, **44**, 3603–3608.
- 110 D. Canseco-Gonzalez, A. Gniewek, M. Szulmanowicz, H. Müller-Bunz, A. M. Trzeciak and M. Albrecht, *Chem. Eur. J.*, 2012, **18**, 6055–6062.
- 111 D. Canseco-Gonzalez and M. Albrecht, *Dalt. Trans.*, 2013, **42**, 7424–32.
- 112 S. Amslinger, A. Hirsch and F. Hampel, *Tetrahedron*, 2004, **60**, 11565–11569.
- 113 D. D. Long, R. J. E. Stetz, R. J. Nash, D. G. Marquess, J. D. Lloyd, A. L. Winters, N. Asano and G. W. J. Fleet, *J. Chem. Soc. Perkin Trans. 1*, 1999, 901–908.
- 114 D. B. Dess and J. C. Martin, *J. Am. Chem. Soc.*, 1991, **113**, 7277–7287.
- 115 United States Patent, US 4438260 A, 1984, 4438260.
- 116 J. M. Goll and E. Fillion, *Organometallics*, 2008, **27**, 3622–3625.
- 117 Y. Nagao, T. Inoue, E. Fujita, S. Terada and M. Shiro, *Tetrahedron*, 1984, **40**, 1215–1223.
- 118 W. Winter and E. Muller, *Synthesis*, 1974, **1974**, 709–710.